Function and Regulation of Polycystin-2 and Epithelial Sodium Channel

by

Qian Wang

A thesis submitted in partial fulfillment of the requirements for the degree of

Doctor of Philosophy

Department of Physiology
University of Alberta

ABSTRACT

Polycystin-2, encoded by the *PKD2* gene, is mutated in ~15% of autosomal dominant polycystic kidney disease, and functions as a Ca^{2+} permeable non-selective cation channel. It is mainly localized on the endoplasmic reticulum membrane, and is also present on the plasma membrane and primary cilium. Polycystin-2 is critical for cellular homeostasis and thus a tight regulation of its expression and function is needed.

In Chapter 2, filamin-A, a large cytoskeletal actin-binding protein, was identified as a novel polycystin-2 binding partner. Their physical interaction was confirmed by different molecular biology techniques, e.g., yeast two-hybrid, GST pull-down, and co-immunoprecipitation. Filamin-A C terminal fragment (FLNAC) mediates the interaction with both N- and C- termini of polycystin-2. Functional study in lipid bilayer reconstitution system showed that filamin substantially inhibits polycystin-2 channel activity. This study indicates that filamin is an important regulator of polycystin-2 channel function, and further links actin cytoskeletal dynamics to the regulation of this channel.

In Chapter 3, further effect of filamin on polycystin-2 stability was studied using filamin-deficient and filamin-A replete human melanoma cells, as well other human cell lines together with filamin-A siRNA/shRNA knockdown. Filamin-A was found to repress polycystin-2 degradation and enhance its total expression and plasma membrane targeting. FLNAC overexpression reduced the physical binding between full-length filamin-A and polycystin-2, as well as the expression level of polycystin-2, presumably by competing with filamin-A for binding polycystin-2. Further, filamin-A mediated polycystin-2 binding with actin by forming complex polycystin-2–filamin-A–actin. Finally, the physical interaction of polycystin-2 and filamin-A was found to be Ca^{2+}-dependent, i.e., Ca^{2+} depletion weakened

their binding strength. Taken together, this study indicates that filamin anchors polycystin-2 to the actin cytoskeleton through the polycystin-2–filamin-A–actin complex to reduce degradation and increase stability, and possibly regulates polycystin-2 function in a Ca^{2+}-dependent manner.

The dynamic regulation and the net effect of filamin on polycystin-2 were explored in Chapter 4. First, we found that the Ca^{2+}-dependent binding of filamin-A with polycystin-2 N- differs from that with C- terminus. In addition, lipid bilayer experiment showed that filamin does not exhibit an inhibitory effect on polycystin-2 channel activity in the absence of Ca^{2+}. These data indicate that filamin regulates/inhibits polycystin-2 activity in a Ca^{2+}-dependent manner, which is probably through adjusting their physical interaction. The net effect and physiological relevance of polycystin-2-filamin binding were tested by live cell Ca^{2+} imaging. We found that filamin-A has a net inhibitory effect on polycystin-2 channel function through a combination of expression and functional regulations that are both important in maintaining intracellular Ca^{2+} homeostasis. The physiological role of filamin-A on regulating polycystin-2 channel function will be further investigated in animal models such as zebrafish and mice in the future study.

Epithelial sodium channel (ENaC) in the kidneys mediates Na reabsorption across the epithelium, which is critical for Na^{+} balance, extracellular volume, and blood pressure. Abnormal ENaC function is associated with pseudohypoaldosteronism type 1, and Liddle syndrome. The channel function of ENaC is regulated by many factors, such as hormones, chemicals and binding partners. Chapter 5 is about the structural interaction and functional regulation of ENaC by filamin. In this study, ENaC-filamin binding was detected by different *in vitro* and *in vivo* methods. Biotinylation and co-immunoprecipitation combined assays

together revealed the presence of the ENaC-filamin complex on the cell surface. Functional study using *Xenopus* oocyte expression system and the two-electrode voltage clamp electrophysiology showed that co-expression of an ENaC-binding domain of filamin FLNAC dramatically reduces ENaC channel function. Lipid bilayer electrophysiology further confirmed the inhibition by showing that FLNAC reduces ENaC single channel open probability. This study demonstrated that filamin reduces ENaC channel function through direct interaction on the cell surface.

In summary, the studies described in this thesis demonstrated that several properties of channel proteins polycystin-2 and ENaC are regulated by cytoskeleton protein filamin.

PREFACE

This thesis is an original work of Qian Wang.

Chapter 2 of this thesis has been published in the journal of PLoS One in 2012 as 'Structural interaction and functional regulation of polycystin-2 by filamin' by **Qian Wang**, Xiao-Qing Dai, Qiang Li, Zuocheng Wang, Maria del Rocio Cantero, Shu Li, Ji Shen, Jian-Cheng Tu, Horacio Cantiello and Xing-Zhen Chen (Conceived and designed the experiments: QW XQD QL JCT HC XZC; Performed the experiments: QW XQD QL ZW MRC SL JS HC; Analyzed the data: QW XQD QL ZW HC XZC; Contributed reagents/materials/analysis tools: JCT HC XZC; Wrote the paper: QW QL ZW HC XZC).

Chapter 3 of this thesis has been published in the journal of PLoS One in 2015 as 'Filamin-A increases the stability and plasma membrane expression of polycystin-2' by **Qian Wang**, Wang Zheng, Zuocheng Wang, JungWoo Yang, Shaimaa Hussein, Jingfeng Tang and Xing-Zhen Chen (Conceived and designed the experiments: QW JFT XZC; Performed the experiments: QW WZ ZCW JWY; Analyzed the data: QW SH JFT; Wrote the paper: QW ZCW JFT XZC).

Chapter 4 of this thesis forms part of an international research collaboration project with Dr. Richard Zimmermman from University of Saarland in Germany. The Ca^{2+} imaging experiments were conducted and analyzed by QW under the help of Dr. Zimmermman and his fellows. Dr. Horacio Cantiello from Universidad de Buenos Aires, Argentina, conducted the lipid bilayer experiments.

Chapter 5 of this thesis has been published in Journal of Biological Chemistry in 2013 as 'Filamin interacts with ENaC and inhibits its channel function' by **Qian Wang**, Xiao-Qing Dai,

Qiang Li, Jagdeep Tuli, Genqing Liang, Shayla S.Li, and Xing-Zhen Chen (Conceived and designed the experiments: QW XZC; Performed the experiments: QW XQD QL JT GL SL; Analyzed the data: QW XQD; Wrote the paper: QW QL XZC).

Chapter 1 and **Chapter 6** are originally written by QW.

ACKNOWLEDGEMENTS

My 5 years' PhD study is very rich and plentiful. I sincerely appreciated the attentive training and generous support from my supervisor Dr. Xing-Zhen Chen. Thank you for your careful and patient supervision on conducting research on all aspects and providing me a lot of opportunities to learn. Also, I want to express my deepest gratitude to my supervisory committees Dr. Yves Sauve and Dr. Ted Alllison, who have provided pertinent and valuable suggestions toward my PhD project and dissertation completion. Dr. Yves Sauve also taught me electroretinography to conduct research on retina and guide me in scientific writing. I would like to thank our Germany partner Dr. Richard Zimmerman for allowing me to study in his lab for 5 month and learn the Ca^{2+} imaging technique. I would also like to thank Dr. Klaus Ballanyi for spending time on discussion of a variety of questions.

I want to say thank you to the previous lab members Jungwoo Yang, Zuocheng Wang, and current lab members Wang Zheng, Shaimaa Hussein for happy collaboration and knowledge sharing.

My family has offered me strong support during my PhD study. I want to express my deep love to my husband, my mother and father. In particular, I would like to thank my uncle, who aroused my passion in biology, inspired me to learn, built my philosophy, and was always there with me facing all kinds of difficulties. Finally I want give a big kiss to my son who will be born in Feburary 2016 and has accompanied me to complete this thesis.

Table of content

CHAPTER 1 1
INTRODUCTION 1
1.1 Kidney physiology 2
1.2 ADPKD 3
1.2.1 Clinical features 3
1.2.2 Molecular mechanism 4
1.2.3 PKD1 (PC1) 5
1.2.4 PKD2 (PC2) 6
1.2.4.1 Molecular composition and structure 6
1.2.4.2 Oligomerization 9
1.2.4.3 Channel property and subcellular localization 10
1.2.4.4 Tissue distribution and physiological significance 12
1.2.5 Cellular abnormality and pathways that are involved in ADPKD 13
1.2.6 Models used to study ADPKD and relevant genes 14
1.2.6.1 Cultured cell model 14
1.2.6.2 Primary cell culture 16
1.2.6.3 Zebrafish model 17
1.2.6.4 Mouse model 18
1.3 ENaC (Epithelial sodium channel) 19
1.3.1 Molecular composition and structure 19
1.3.2 Biophysical characteristics 23
1.3.3 Tissue distribution and physiological function 24
1.3.4 Regulation 26
1.3.5 Interaction with cytoskeleton protein 27
1.4 Filamin 28
1.4.1 Gene and protein structure 28
1.4.2 Subcellular localization and function 33
1.4.3 Modification (cleavage and phosphorylation) 34
1.4.4 Physiological function and defects 35

1.5 Thesis objectives and rationale 36

CHAPTER 2 38
RESULT #1 Structural interaction and functional regulation of polycystin-2 by filamin 38
2.1 ABSTRACT 39
2.2 INTRODUCTION 40
2.3 MATERIALS AND METHODS 43
2.4 RESULTS 48
2.4.1 Association of PC2 with filamins revealed by yeast two-hybrid assay 48
2.4.2 Interaction of PC2 with filamins revealed by GST pull-down and co-IP 50
2.4.3 Co-localization of PC2 with FLNAA and calnexin revealed by IF 57
2.4.4 Effect of filamin on the channel function of PC2 in lipid bilayer system 59
2.5 DISCUSSION 62

CHAPTER 3 65
RESULT #2 FLNA increases the stability and plasma membrane expression of PC2 65
3.1 ABSTRACT 66
3.2 INTRODUCTION 67
3.3 MATERIALS AND METHODS 70
3.4 RESULTS 75
3.4.1 Effect of FLNA on the steady-state level of PC2 75
3.4.2 Effect of FLNA on PC2 degradation 78
3.4.3 Effect of FLNA on the plasma membrane (PM) PC2 expression 80
3.4.4 Effects of FLNAC on the FLNA-PC2 interaction and PC2 expression 82
3.4.5 Role of the PC2-FLNA-actin complex in surface PC2 stabilization 87
3.4.6 Roles of Ca 91
3.5 DISCUSSION 93

CHAPTER 4 97
RESULT #3 Dynamic regulation and the net effect of filamin on PC2 channel activity 97
4.1 INTRODUCTION 98
4.2 MATERIALS AND METHODS 101

4.3 RESULTS 103
4.3.1 Roles of Ca^{2+} on the physical and functional interaction of PC2 and FLNA 103
4.3.2 Effect of PC2 silencing on ER Ca^{2+} leakage and ER Ca^{2+} content in intact cells . 106
4.3.3 Effect of PC2 knockout in ER Ca^{2+} leakage and ER Ca^{2+} content in intact cells.. 111
4.3.4 The net effect of FLNA on PC2 channel function 113
4.4 DISCUSSION 114

CHAPTER 5 117
RESULT #4 Filamin interacts with ENaC and inhibits its channel function 117
5.1 ABSTRACT 118
5.2 INTRODUCTION 119
5.3 MATERIALS AND METHODS 121
5.4 RESULTS 128
5.4.1 Physical interaction between ENaC and filamins 128
5.4.2 Modulation of ENaC channel function by FLNA in *Xenopus* oocytes 136
5.4.3 Modulation of ENaC expression and distribution by FLNA 139
5.4.4 Modulation of α-ENaC channel function by FLNAC in planar lipid bilayer 143
5.5 DISCUSSION 148

CHAPTER 6 152
GENERAL DISCUSSION 152
6.1 Transient Receptor Potential Polycystins (TRPPs) and diseases 153
6.1.1 Polycystins and ADPKD 153
6.1.2 Polycystins and cancer 156
6.2 Regulation of PC2 by FLNA 158
6.2.1 Expression 158
6.2.2 Localization 160
6.2.3 Functional regulation 161
6.2.4 Physiological importance of PC2-FLNA interaction 163
6.3 Regulation of PC2 by the cytoskeleton 164
6.4 ENaC channel function and regulation by filamin 166
6.5 REFERENCES 168

LIST OF FIGURES

Chapter 1

Figure 1-1. Structure of the nephron …….....2
Figure 1-2. Membrane topology of PC2 …….....6
Figure 1-3. Structure of chicken ASIC and human α-ENaC ….....20
Figure 1-4. Predicted structure of oligomerized human ENaC…….....22
Figure 1-5. Structure of amiloride and guanidine ….....23
Figure 1-6. Transepithelial ion transport in a principal cell of the cortical collecting duct.....25
Figure 1-7. A schematic structure of filamin-A molecule and the F-actin crosslink.....29
Figure 1-8. Model of ABD opening….....31

Chapter 2

Figure 2-1. Structural domains and sequence of filamins and PC2, and their interaction identified by yeast two-hybrid assay….....49
Figure 2-2. Interaction between PC2 and filamins by GST pull-down....….....52
Figure 2-3. Interaction between PC2 and filamin by co-IP....….....55
Figure 2-4. Cellular localization of PC2…….....58
Figure 2-5. Effect of FLNA on purified PC2 channel activity in a lipid bilayer system……..60
Figure 2-6. Regulation of hST PC2 channel function by FLNA.....….....61

Chapter 3

Figure 3-1. Effects of FLNA on PC2 protein expression and PC2 synthesis...….....76
Figure 3-2. Effect of FLNA on PC2 degradation...….....79
Figure 3-3. Effect of FLNA on PC2 PM expression.....….....81
Figure 3-4. Effect of FLNAC on the FLNA-PC2 interaction.....83
Figure 3-5. Effect of FLNAC on the surface and total PC2 expression.....85
Figure 3-6. Role of FLNA in, and effect of FLNAC on, the interaction of PC2 with actin.....89
Figure 3-7. Ca^{2+} dependence of the physical interaction between PC2 and FLNA.....92

Chapter 4

Figure 4-1. Schematic overview of the major regulators in ER Ca^{2+} homeostasis.....100
Figure 4-2. Ca^{2+} dependent physical binding and functional regulation of PC2-filamin.....104
Figure 4-3. Effect of PC2 silencing by siRNA on Tg-induced ER Ca^{2+} leakage and ER luminal Ca^{2+} content.....108
Figure 4-4. Effect of 3'UTR siRNA resistant PC2 plasmid on recuing the phenotype of PC2 silencing.....110
Figure 4-5. Effects of PC2 on Tg-induced ER Ca^{2+} leakage and ER luminal Ca^{2+} content in MCD cells.....112
Figure 4-6. Effect of FLNA on PC2 silencing-induced ER Ca^{2+} leak.....113

Chapter 5

Figure 5-1. Physical interaction between ENaC and filamins.....129
Figure 5-2. Interaction between ENaC and filamin A by co-IP.....132
Figure 5-3. Interaction between endogenous ENaC and filamin A by co-IP.....134
Figure 5-4. Effect of filamin on whole-cell transport mediated by αβγ-ENaC or α-ENaC overexpressed in *Xenopus* oocytes.....137
Figure 5-5. Effect of FLNAC on expression and subcellular distribution of α-ENaC.....141
Figure 5-6. Tandem affinity purification of human α-, β-, and γ-ENaC from MDCK stable cell lines and channel function of α-ENaC reconstituted in lipid bilayer.....145
Figure 5-7. Regulation of α-ENaC channels by FLNAC in a lipid bilayer system.....146

LIST OF ABBREVIATIONS

aa	Amino acid
ABD	Actin binding domain
ABS	Acting-binding sites
ADPKD	Autosomal dominant polycystic kidney disease
AFM	Atomic force microscopy
AIDS	Acquired immune deficiency syndrome
ARPKD	Autosomal recessive polycystic kidney disease
ASIC	Acid sensing ion channel
bp	Base pair
BSA	Bovine serum albumin
CaM	Calmodulin
CC	Coiled-coil
CFTR	Cystic fibrosis transmembrane conductance regulator
CH	Calponin homology
CHX	Cycloheximide
Co-IP	Co-immunoprecipitation
CRC	Colorectal cancer
Ctrl	Control
DMEM	Dulbecco's modified Eagle's medium
DMSO	Dimethyl sulphoxide

dpf	Day post-fertilization
ENaC	Epithelial sodium channel
ER	Endoplasmic reticulum
F-actin	Filamentous actin
FBS	Fetal bovine serum
FLNA	Filamin-A
FLNAC	Filamin-A Carboxyl terminus
GFP	Green fluorescent protein
GPS	G-protein-coupled receptor proteolytic site
HEK293	Human embryonic kidney 293
Hr	Hour(s)
hST	Human syncytiotrophoblast
IB	Immuno blotting
Ig	immunoglobulin
IHC	Immunohistochemistry
IMCD	Inner medullary collecting duct
IP3R	Inositol trisphosphate receptor
kb	kilobase
KD	Knockdown
KDa	Kilodalton
MCD	Mouse collecting duct
MDCK	Madin-Darby canine kidney
Min	Minutes

MO	Morpholino
MOT	Mean open time
mTOR	Mammalian target of rapamycin
PACS	Phosphofurin acidic cluster sorting
PAGE	Polyacrylamide gel electrophoresis
PBS	Phosphate-buffered saline
PC1	Polycystin-1
PC2	Polycystin-2
PC2C	Polycystin-2 Carboxyl terminus
PC2N	Polycystin-2 Nitrogen terminus
PCL	Polycystin-2-like-1
PERK	Pancreatic ER-resident eIF2α kinase
PM	Plasma membrane
RyR	Rynodine receptor
SCNN1	Sodium channel nonvoltage-gated 1
SDS	Dodecyl sulfate,sodium salt
SEM	Standard error of the mean
SERCA	Sarco(endo) plasmic reticulum calcium ATPase
siRNA/shRNA	Small interfering RNA/Small hairpin RNA
Tg	Thapsigargin
TM	Transmembrane
TRPP2	Transient receptor potential polycystic 2

CHAPTER 1

INTRODUCTION

1.1 Kidney physiology

The kidneys, with bean-like structure as big as an adult fist, are the major organs of the excretory systems of humans and vertebrates. The main functions of the kidneys are to remove waste products of metabolism from the blood and to reabsorb nutrients back to the blood. They also serve as a homeostatic regulator that maintains acid-base balance, salt-water balance and electrolyte balance.

The basic structure and functional unit of the kidney is the nephron, which is composed of a corpuscle and a tubule. The corpuscle represents the initial filtering component; it contains a glomerulus consisting of a capillary ball (providing blood supply and pressure), and the Bowman's capsule surrounding the glomerulus that absorbs the filtrate. The renal tubule contains three components, proximal convoluted tubule, loop of Henle and distal convoluted tubule, with highly specialized functions for each segment. The proximal tubule reabsorbs 2/3 of the filtered salt and water, and all filtered organic solutes including glucose, protein, vitamins, urea and uric acid, etc. The loop of Henle is a hairpin like U-shaped loop with a descending limb and an ascending limb. The descending limb is permeable to water but less permeable to salt and thus it mainly contributes to concentrate the filtrate. Reversely, the ascending limb works to actively pump salt out with no permeability to water. The distal tubule mainly functions by active transport, such as the absorption of H^+, Na^+, Ca^{2+}, and the secretion of K^+ and biocarbonate. The collecting ducts combine filtrate from multiple initial collecting

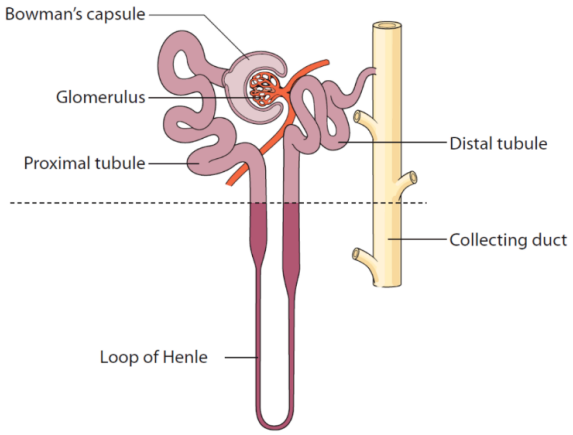

Figure 1-1. Structure of the nephron. (1)

tubules. Reabsorption of H_2O and Na^+ continues in the collecting duct to further concentrate the urea. This process is tightly regulated by different hormones. (1)

1.2 ADPKD

1.2.1 Clinical features

Autosomal Dominant Polycystic Kidney Disease (ADPKD) is an inherited systemic disorder that affects ~0.2% of the adult population (2). The major clinical feature is defined by the formation of bilateral fluid-filled cysts in the kidney, with systemic complications affecting other organs including the liver, heart, pancreas, brain and the arteries. Enlargement of kidney cysts gradually destroys the functioning renal parenchyma leading to renal insufficiency and ultimately to end-stage renal failure, over about six decades. Liver cyst, left ventricular hypertrophy, intracranial aneurysms and hypertension are also common manifestations seen in ADPKD cases (3). However, end-stage renal failure and cardiovascular complications are the two leading causes of death in patients with ADPKD (4). Up to now, kidney transplantation and dialysis are the only effective therapies of ADPKD, as limited medications have been shown promising in clinical trials. In early 2014, tolvaptan, a vasopressin receptor 2 antagonist, has been approved as the first drug for treatment of ADPKD patients in Japan and Canada (http://www.businesswire.com/news/home/20140323005043/en/Otsuka-Pharmaceuticals-Samsca%C2%AE-Approved-Japan-Worlds-Drug#.VSb6Yk1_mUl), however it is not recommend by the US Food and Drug Administration due to unclear risk-benefit ratio. Thus, deeper understanding of the molecular mechanism of ADPKD is urgently needed for discovery of novel potential therapies.

ADPKD is caused by mutations of two genes, *PKD1* and *PKD2*, which account for 85%

and 15%, respectively. Phenotypes caused by *PKD1* deficiency are more severe than those caused by *PKD2*. Notably, the onset time of end-stage renal failure in *PKD1* type ADPKD manifects 20 years earlier than that in *PKD2* type (5). In addition, ADPKD reveals vast phenotype variability independent of genetic effects. First, no genotype/phenotype correlation has been found for either *PKD1* or *PKD2* type ADPKD (6) (7). Second, patients with identical mutations displayed different disease severity (8). What's more convincing is that in monozygotic twins who carry the same genetic information, the onset time to end stage renal disease is largely variable (9). This is highly consistent with the hypothesis that non-genetic factors have played critical roles in the progression of ADPKD (details see Section 1.2.2.Two hit model), indicating that ADPKD is a complex multi-factorial disease.

1.2.2 Molecular mechanism

So far, there are two models proposed to implicate the molecular mechanism of ADPKD. The ‘two hit’ model suggests that ADPKD is caused by mutations of either *PKD1* or *PKD2* gene in one allele (heterozygous) followed by a second hit which results in dysfunction of the second allele. Complete loss of the second *PKD1* or *PKD2* allele initiates cyst formation. Thus, at the molecular level, ADPKD is recessively, rather than dominantly inherited. This ‘two hit’ model is supported by the finding that cyst formation is focal and sporadic even though all the kidney cells have the same germline mutation, and that cystic cells lose heterozygosity compared to the noncystic cells (10,11). Thus, factors other than the germline mutation are required to produce a ‘second hit’ for cyst formation. The time at which the second hit happens determines the onset of cyst formation and explains the phenotypic variability of clinical features in ADPKD patients. However, recently a ‘dosage/threshold’ model was proposed

based on the finding that both reduced (12) and gain-of (13-15) function of polycystins cause ADPKD in mice. However, as no clinical cases of ADPKD are found caused by polycystins over-sufficiency, the physiological importance of this model needs further validation. Additionally, the features of ADPKD caused by mutations of *PKD1* or *PKD2* are indistinguishable, suggesting that their gene products may work through a common pathway and/or as a complex.

1.2.3 PKD1 (PC1)

The *PKD1* gene is located on the short arm of chromosome 16 (16p13.3), and spans ~52 kb of genomic sequence. *PKD1* has 46 exons, which produce a 14.5 kb transcript with two different isoforms due to alternative splicing. Isoform I (NM_001009944), with one amino acid (aa) longer than isoform II (NM_000293), has a 12909 bp open reading frame that encodes the predominant form of *PKD1* protein, polycystin-1 (PC1). PC1 is a large integral membrane glycoprotein with 4302 aa, and ~465 KDa in size. It contains a large extracellular N terminus (~3000 aa), 11 putative transmembrane (TM) regions, and a short cytosolic C tail (16). The N terminus contains a number of well-recognized repeats and domains, notably the G-protein-coupled receptor proteolytic site (GPS). PC1 undergoes *cis*-autoproteolytic cleavage at the GPS site, which is critical for PC1 proper targeting and function (17-19). Cleavage of PC1 C-tail has also been reported, with the released fragment migrating to the nucleus and initiating signaling processes (20). The PC1 C terminus contains a coiled-coil domain (See PKD2 section for detail) that mediates the interaction with polycystin-2 (21). Overall, PC1 has a structure of a receptor or adhesion molecule (3).

PC1 is expressed in various tissues and subcellular compartments (22). In the kidney, PC1

is found in most nephron segments and is localized to the plasma membrane (PM), primary cilium, and the cell-cell junctions of epithelial cells (22-24). Based on its structure and localization, PC1 is postulated to act as a PM receptor involved in cell-cell/matrix interactions and a mechanosensor of flow on the primary cilia of kidney cells (25).

1.2.4 PKD2 (PC2)

The *PKD2* gene is located on the long arm of chromosome 4 (4q22.1) and encodes a 5.3 kb mRNA transcript containing 15 exons. The gene product, polycystin-2 (PC2), also called transient receptor potential polycystic 2 (TRPP2), belongs to the TRP superfamily and functions as a Ca^{2+}-permeable non-selective cation channel (26).

1.2.4.1 Molecular composition and structure

PC2 is a 968 aa, ~110 KDa integral membrane protein with 6 TMs and intracellular N- and C- termini (Figure 1-2), which shares significant homology to the voltage-activated Ca^{2+} channels (27). The TM domains form channel pores and the N-/C- tails contain many regulatory sites and motifs. The major role of PC2 N terminus (PC2N, aa 1-244) is to regulate PC2 trafficking. E.g., the RVxP motif of PC2N (aa 6-9) and serines 76 phosphorylation are found to be essential for PC2 cilia (28) and PM (29) targeting,

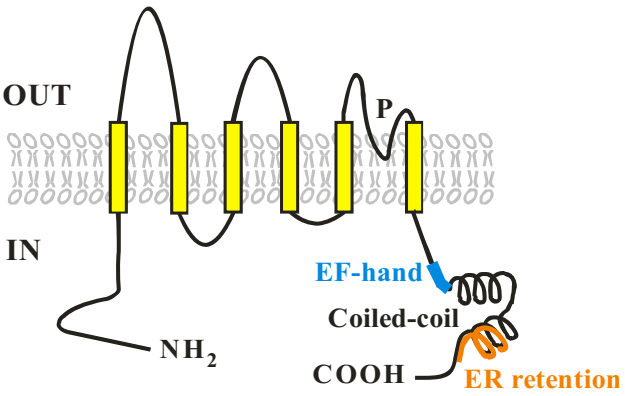

Figure 1-2. Membrane topology of PC2.
Pore region (P), EF-hand Ca^{2+}-binding motif, coiled-coil and ER-retention domains are indicated.

respectively. In addition, PC2N mediates the self-dimerization through aa 199-207 (30) and the interaction with ryanodine receptor (RyR) via aa 130-220 (31). PC2 C-tail (PC2C, aa 704-968) mediates many aspects of PC2 function, mostly through protein-protein interactions. In the current model, PC2C contains an EF-hand domain (aa 720-797) and a coiled-coil domain (aa 833-895, known as CC2) connected by a flexible acidic linker (32).

EF-hand

The EF hand is a well-characterized Ca^{2+} binding motif with a helix-loop-helix structure. The canonical EF hand domain contains a pair of EF-hand motifs and two Ca^{2+}-binding sites while only one Ca^{2+} binding site was found in the PC2 EF hand. Further sequence alignment and biophysical structure analysis revealed that PC2 contains two EF hand motifs; however the first lacks essential aa for Ca^{2+} binding. Loss of the second Ca^{2+} binding site is likely a result of evolution because PC2 orthologs in the eailier invertebrate organisms still maintain it (33). And adding back the lost aa to human PC2 did retrieve its second Ca^{2+} binding capacity (34). The PC2 EF hand binds Ca^{2+} with very low affinity (Kd = 214 μM) and non-cooperatively (32) because of its single Ca^{2+}-binding site and the monomeric status of EF hand. However, PC2C does bind Ca^{2+} with higher affinity (Kd = 22 μM) and cooperatively with the multimeric structure formed by the coiled-coil domain (35). Several studies using various biochemical and biophysical analyses showed that both EF hand and the whole PC2C tail undergo Ca^{2+} -dependent conformational changes (32,33,36), which are essential to mediate channel gating/activation of PC2 (34,37). These together could explain the 'bell-shaped Ca^{2+} -dependence of PC2 channel activation' (38): Ca^{2+}-sensing by EF hand changes the protein conformation and facilitates cooperatively Ca^{2+} binding, then activates PC2 channel function;

but once the available Ca^{2+} binding sites are saturated, the channel will undergo inactivation. In terms of polycystin-2-like-1 (PCL), a homolog protein of PC2, the EF hand removal retains and even increases channel function (39). In this case, the EF hand at the C terminus of PCL may function to prevent channel from over stimulation.

Linker

In the linker region, phosphorylation of single residue serines 812 by casein kinase II was found to modulate PC2 channel sensitivity to Ca^{2+} stimulation (38). In addition, serine 812 phosphorylation enabled PC2 to be recognized by two adaptor proteins, phosphofurin acidic cluster sorting (PACS) protein-1 and -2, which in turn mediate the retrieval of PC2 from the PM to the Golgi and from the Golgi to the endoplasmic reticulum (ER), respectively, eventually leading to an ER retention of PC2 (38,40).

Coiled-coil domain

Coiled-coil (CC) domain is an alpha-helical structural motif known to mediate interactions of a wide array of proteins, and usually presents as dimer or trimer. Structure prediction suggests two putative CC domains in PC2C, named CC1 (aa 769-796) (21) and CC2 (aa 833-895) (32). CC2 domain was reported to form both dimer (41) and trimer (35,42), which contributes to the homomeric structure of PC2C and the full length PC2. In addition to self-association, CC2 domain also mediates the interactions with PC1 (43) and other partners such as the ER membrane ion channel RyR (31), receptor like protein fibrocystin (44), and cytoskeletal protein α-actinin (45) and troponin-I (46). On the other hand, CC1 domain was predicted to be unfavorable in a coiled-coil interface. Indeed, CC1 was found to be monomeric

(41) and not essential to mediate the interactions with several proteins, including I inositol 1,4,5-triphosphate receptor (IP3R), TRPC1, tropomyosin-1, and PC1.

1.2.4.2 Oligomerization

The TRP superfamily is a group of channels that mediate numerous sensory transduction processes and are assumed to assemble as tetramers based on their structural similarity with the tetrameric Shaker K^+ channels (47). Indeed, many of the TRP channels such as TRPC1 (48), TRPV1 (49), TRPV5/6 (50) and TRPM2 (51) have been shown to be tetramers by a variety of structural and functional studies such as atomic force microscopy (AFM), Blue Native-PAGE and the lipid bilayer electrophysiology. In addition, the CC domain has been found to be essential for the formation of tetramer of TRPM8 (52) and TRPV1 (53), however not for TRPP2 (PC2) oligomerization (41). Interestingly, heterotetramer formation between TRPs was also reported, e.g., TRPP2-TRPP1 (42), TRPP2-TRPC1(43,54) and TRPV5-TRPV6 (50).

However, the oligomerization state of PC2 has been controversial. Current reports support two models. One model suggests that PC2 assembles as homotetramers and heterotetramers with a 2:2 ratio, e.g., 2PC2-2TRPC1 complex (55,56). This is supported by both the structure review by AFM and the functional lipid bilayer study. Another model suggests that PC2 forms homotrimers or heterotetramers with a 3:1 ratio, e.g., 3PC2-1PC1 complex (42). This is supported by methods of Blue Native-PAGE (cell line), live cell photobleaching (*Xenopus* oocytes), and crystal structure of the CC domains. Both N- and C- termini are involved in PC2 oligomerization. PC2N possesses a dimerization domain (30) while PC2C is present in different status, such as dimer, trimer and tetramer (35,37). Thus, the oligomerization state of PC2 is relatively complicated.

1.2.4.3 Channel property and subcellular localization

PC2 is a Ca^{2+}-regulated, non-voltage gated, non-selective cation channel permeable to Na^{+}, Ca^{2+} and K^{+}. The ion permeability differs from different reports. Two studies, by using endogenous PC2 in IMCD cells and exogenous PC2 expressed in *Xenopus* oocytes showed that PC2 is more selective for K^{+} over Ca^{2+} and Na^{+}, with a ratio of 1:0.21:0.19 (57,58). While human placental PC2 and *in vitro* translated PC2 shows a slightly higher Ca^{2+} permeability compared to Na^{+} and K^{+}, with a ratio of 1.3:1:1 (26). This discrepancy remains to be solved. In addition, elevated intracellular Ca^{2+} transiently activates PC2 channel by increasing its open probability, while high concentration of Ca^{2+} (50 mM) has an inhibitory effect (58). This Ca^{2+}-dependent channel activation is believed to be mediated by the EF-hand domain located at the C terminus of PC2 (34,37). Further, no voltage dependence was observed within the physiological voltage range from -100 mV to -50 mV (57,58).

PC2 is mainly localized on the ER membrane (59), and also present on PM (57) and epithelial primary cilia (25). Subcellular localization of PC2 varies in difference cell types. E.g., PC2 has been reported to be present on the ER of LLC-PK1 (59,60), Chinese hamster ovary (61), and *Xenopus* oocyte (62), on the PM of MDCK (63), IMCD (57) and Sf9 insect cells (26), and on the primary cilia of many renal epithelial cell types (28,64,65).

ER-PC2

The primary ER-localization of PC2 is determined by its C terminus, which contains an ER retention region (aa 787-820) (60). PC2 pathogenic truncation mutant R742X missing the ER retention domain is predominantly expressed on the PM of *Xenopus* oocytes while wild type remains in the intracellular compartments (62). Further study revealed that PACS proteins, which recognize an acidic cluster (aa 810-821) within the ER retention region, direct the ER

localization of PC2 (40). As a non-selective cation channel, ER localized PC2 was found to enhance IP3R mediated Ca^{2+} release (66) and itself functions as an independent Ca^{2+}-activated Ca^{2+} release channel (58,59). In contract, Wegierski *et al* reported that PC2 reduces ER Ca^{2+} release by increasing ER Ca^{2+} permeability and reducing the ER Ca^{2+} content (67). Thus, it remains controversial whether PC2 exhibits basal Ca^{2+} permeability or functions as a Ca^{2+}-activated Ca^{2+} release channel that requires an increase in cytosolic Ca^{2+}, to confer Ca^{2+} permeability of the ER.

PM-PC2

PC2 PM targeting has been reported to be regulated by many factors including PC1 (61), PACS proteins (40), intracellular Ca^{2+} (68), chemical chaperons and proteasome modulators (58). PC1 functions as a chaperon that brings PC2 together to the PM and the PC1/PC2 complex shows a non-selective cation channel property. However, PC2 has also been found to traffic to the PM independent of PC1 (28,69,70). Blocking the binding of PACS to the acidic sequence of PC2C relocates PC2 to the PM (40). Increased intracellular Ca^{2+} also facilitates PC2 trafficking to the PM (68). Treatment of chemical reagents such as lactacysin or glycerol has been shown to successfully translocate ER-PC2 to the PM (58).

Cilia-PC2

PC2 co-localized with PC1 on the renal primary cilia, where the PC1-PC2 complex functions to mediate mechanotransduction and subsequent rise of intracellular Ca^{2+} (25). The physical interaction of PC1-PC2 was deemed to be essential for cilia targeting and PC2 function, whereas other study revealed that PC2 possesses a cilial trafficking motif RVxP at it N terminus, which is required and sufficient for PC2 cilia targeting independent of PC1 (28). In

addition, PC1-independent function of ciliary PC2 was also reported to be critical in the left-right axis formation during moues embryo development (71). The mechanism of cilia trafficking by RVxP motif is unknown but it is likely that the RVxP is part of a protein interaction domain and mediates the interaction of PC2 with other cilia trafficking partners (28).

1.2.4.4 Tissue distribution and physiological significance

PC2 is widely expressed in numerous tissues, including the kidney, liver, pancreas, heart, lung, brain, intestine, and reproductive organs. In mouse embryo, PC2 is developmentally regulated and detectable in the embryonic ectoderm and endoderm at E6 and in the metanephric ureteric bud at E12.5 (72). Embryonic deficiency of PC2 results in lethality mainly due to cardiac defects and hemorrhages (73). In adults, the expression pattern of PC2 is more constant. In the kidney, PC2 together with PC1, is localized to the primary cilia of the renal tubule and mediates the fluid-flow sensation (60). Deficiency of either PC2 or PC1 results in renal cyst formation, which is the major characteristic of ADPKD. Liver and pancreatic cysts are also strongly associated with PC2 and PC1. In the heart, PC2 is localized to the ER membrane of cardiomyocytes and regulates Ca^{2+} signaling and cardiac contractility (31,74). Mice expressing mutant PC2 develop dilated cardiomyopathy and heart failure (75). In the lung, PC2 is present on the apical surface of bronchial epithelial, possibly invovled in cell locomotion and fluid movement (76). In addition, both PC1 and PC2 are detected in the vascular smooth muscle cells of the major vessels in associated with dense plaques, suggesting a role in the maintenance of myoelastic wall of arteries (77). This is consistent with the manifestation of ADPKD patients who developed vascular abnormalities such as intracranial

aneurysms and hypertension.

1.2.5 Cellular abnormality and pathways that are involved in ADPKD

At the cellular level, ADPKD is associated with 1) increased cell proliferation and apoptosis; 2) enhanced fluid secretion; 3) abnormal cell-matrix interactions and 4) alterations in cell polarity. (78) Increased proliferative activity was found to be associated with abnormal intracellular Ca^{2+} regulation (41), and overexpression of oncogenes or growth factors (79). Increased apoptosis is due to cellular defect in apoptotic regulation because polycystins have been reported to protect cells from apoptosis through regulating the Ca^{2+} dependent pathways (67,80). Fluid secretion from tubular epithelium is primarily mediated by transepithelial NaCl secretion with water movement. This process is associated with over active Cl^- transporters cystic fibrosis transmembrane conductance regulator (CFTR) (81), and dislocated Na^+/K^+ ATPase (82). In addition, ADPKD cyst epithelia show abnormal membrane components such as laminin, fibronectin, and type IV collagen. Cell polarity change is mainly reflected by mislocation of membrane proteins such as Na^+/K^+ ATPase (82), E-cadherin and EGF receptors (83).

1.2.6 Models used to study ADPKD and relevant genes

1.2.6.1 Cultured cell model

Cell lines are derived from the primary culture and modified to be immortal by different ways such as virus transformation. Below is the detailed introduction of HeLa, HEK293, IMCD, MDCK, LLC-PK1, MEF, and MCD cell lines used in this thesis.

HeLa

HeLa is a human epithelial carcinoma cell line derived from the cervical cancer cells of a patient named Henrietta Lacks. It is the first human cell line established in culture (84) and since 1951 has been widely used in scientific research including virus infection, cancer, AIDS, products testing, and signaling transduction. Because of human papillomavirus integration, HeLa genome is different from human genome, particularly in terms of its chromosome numbers. The complete genome of the HeLa cells was sequenced and published on March 11th 2013. HeLa cells have a modal chromosome number of 82, with four copies of chromosome 12 and three copies of chromosomes 6, 8, and 17 (85). Nowadays, HeLa cell line is an excellent model for gene overexpression or knockdown due to its superior easy and efficient transfection property and thus used in studying protein-protein interaction and regulation in this thesis.

HEK293

HEK293 is a human embryonic kidney cell line derived from human embryonic kidney cells of a legally aborted healthy fetus and the cell line was generated by transformation with sheared adenovirus 5 DNA. The number 293 is just the scientist's habit of numbering his experiments. HEK293 has a modal chromosome number of 64 including a total of three copies

of the X chromosome and four copies of chromosome 17 and 22. Searched in PubMed, HEK293 is the second only to HeLa cells in the frequency of use in cell biology research (86). While for a long time, HEK293 was misinterpreted as a typical kidney epithelial cell line until some evidences emerged to show its neuronal property (87,88). A recently study by whole genome sequencing and transcriptomes analysis clearly showed that the pattern of HEK293 stains most closely resembles that in adrenal cells, which has many neuronal properties (86), suggesting an embryonic adrenal precursor origin of HEK293 line. Given the location of the adrenal gland (next to the kidney), it is possible that adrenal cells are found in an embryonic kidney derived cultures. Thus, HEK293 is not a good *in vitro* model of a typical kidney cell line. However, because of easy culture, extreme transfectability and expression efficiency, HEK293 is as popular as HeLa cells in the studies of ADPKD.

MDCK

MDCK is Madin-Darby canine kidney epithelial cells derived in 1958 by S.H Madin and N.B. Darby from the kidney of a normal adult female cocker spaniel. MDCK cell line resembles the cortical collecting duct cells however consists of two subpopulations, the intercalated cells and principle cells with the chromosome number around 79 and 83, respectively (89,90). Technically, because of low transfection efficiency, MDCK stable cell lines are often established to study ADPKD.

LLC-PK1

LLC-PK1 is a porcine kidney epithelial cell line derived in 1976 from a 3-4 weeks male Hampshire pig kidney (91). LLC-PK1 processes the characteristics of the polarized renal

proximal tubule cells (92) and is an excellent *in vitro* model to study the transcellular transport mechanism of the proximal tubule. The chromosome counts are between 36 to 40 range (normal pig contains 38 chromosomes), with a X and Y (91).

IMCD

IMCD is a mouse inner medullary collecting duct cell line derived in 1999 from an individual tubule of the terminal inner medullary collecting duct of a SV40 transgenic mouse (90,93). The SV40 T antigen is oncogenic and used to induce the establishment of immortalized cell line. IMCD is polarized kidney epithelial cells that retain many differentiated characteristics of the original nephron segment including extreme osmotic tolerance (93), which makes it highly suitable for studies of osmotic stress. The IMCD chromosome number counts around 58 (94).

MCD (D3 and B2)

MCD D3 (*Pkd*2$^{+/-}$) is a mouse collecting duct cell line derived from an 8 week SV40: *Pkd2*$^{f3/-}$ transgenic mouse. The *Pkd2*^{f3} allele, in which *Pkd2*-exon-3 is flanked by two *loxP* sites, can be conditionally inactivated using a *Cre*-loxP system. B2 (*Pkd*2$^{-/-}$) is a daughter cell line of D3 generated by infection of *Cre*-expressing adenovirus to induce *Pkd*2 exon 3 deletion and result in two null-*Pkd2* alleles (*Pkd2*$^{d3/-}$) (95).

1.2.6.2 Primary cell culture

Due to the convenience of the established cell lines and the importance of *in vivo* animal models, primary cultured cells are not widely used. However, primary culture has its own

advantages against cell lines. Without being immortalized, primary cultured cells are more closer to the *in vivo* tissues in terms of histology and functional activity, and skipping the selection step also enables less phenotypic variability resulted from different operations between investigators and isolations. In the ADPKD field, primary cultured mouse embryonic renal epithelial cells were used to study the flow-sensing mechanosensation of polycystins. In that study, PC1/PC2 complex was found to form a mechanosensor of the fluid-flow in renal epithelium (25). Human kidney epithelial primary culture was also used to study shear stress induced Ca^{2+} response and cell proliferation, from where ADPKD cystic epithelial cells are found to be lacking of Ca^{2+} signalling (96) and show over proliferation (97).

1.2.6.3 Zebrafish model

Zebrafish has offered a convenient and attractive model for studying ADPKD. First, zebrafish pronephric kidney is a relatively simple organ consisting of two nephrons with fused glomeruli and paired, bilateral pronephric ducts. Many aspects of its kidney development and function are similar to that of higher vertebrates. Morpholino (MO) injection is a widely used technique to knockdown (KD) genes in zebrafish, and the phenotype is visible during 2-5 days post-fertilization (dpf). Several studies have demonstrated that MO KD of zebrafish ortholog of *pkd2*, results in kidney cysts and tail curvature from 2-3 dpf (98,99). Since zebrafish has transparent embryos and larvae, which develop outside the mother, it would be easy for direct visualization of kidney cysts. Transgenic zebrafish line with a targeted mutation in *pkd2* is also commercially available (http://zfin.org/action/fish/search, cat # sa18283).

1.2.6.4 Mouse model

Mouse has been recognized as the best physiologically relevance model for studying of human ADPKD. A variety of gene knockout/KD and transgenic mice have been put in use. *Pkd1*$^{+/-}$ and *Pkd*2$^{+/-}$ mice are the initial mouse model used to study ADPKD. The heterozygotes are normal at birth but gradually develop kidney cysts at older ages (100,101). Bilineal mice (*Pkd1*$^{+/-}$*Pkd2*$^{+/-}$) develop more severe renal cysts at an even earlier onset time (102,103). However, this heterozygous model develops severe liver cysts as well. *Pkd1*$^{-/-}$ and *Pkd2*$^{-/-}$ mice are embryonic lethal (73,104). Thus, in order to study the full spectrum of *PKD* gene function, many inducible knockout mice have been produced. Mouse model with hypermutable allele for *Pkd2* (*Pkd2WS25*) helped confirm the 'two hit' model that loss of heterozygosis is the molecular mechanism of cystogenesis in ADPKD (101). Based on the *Cre*-loxP system, *Pkd2* conditional knockout mice *Pkd2*$^{f3/-}$ were generated, which have provided a powerful tool for studying of the tissue-specific function of PC2 during embryogenesis and organogenesis (95). Notably, the *Pkd2* conditional knockout mouse is the origin of the mouse collecting duct D3 (*Pkd2*$^{+/-)}$ and B2 (*Pkd2*$^{-/-}$) cell lines. Interestingly, study of transgenic mice with enhanced *Pkd1* or *Pkd2* expression demonstrated that gain of function of polycystins is also cystogenic (13,15), supporting a dosage threshold model.

1.3 ENaC (Epithelial sodium channel)

1.3.1 Molecular composition and structure

Epithelial sodium channel (ENaC) belongs to the degenerin/epithelial sodium channel superfamily, which encodes a variety of functionally distinct sodium channels. ENaC is sodium-selective, voltage-independent and amiloride sensitive, and therefore also known as SCNN1 (sodium channel nonvoltage-gated 1) or amiloride sensitive sodium channel.

ENaC is composed of three subunits, ENaC-alpha (α-ENaC) cloned in 1993 (105), -beta (β-ENaC) and -gamma (γ-ENaC) cloned in 1994 (106). *a-ENaC* gene is located at the end of chromosome 12 short arm (12p13), with 14 exons and three splicing variants. Transcript variant 1 encodes the predominant form of α-ENaC with 669 aa. *β-ENaC* and *γ-ENaC* genes are closely localized to each other on chromosome 16 within the 16p12 region, and have 15 and 13 exons, respectively. Without transcript variants, the gene products of *β-ENaC* and *γ-ENaC* subunits are 640 aa and 649 aa, respectively. The three ENaC subunits share 30-35% sequence identity and are predicted to have the same membrane topology, with two TM domains (TM1 and TM2), a large extracellular loop (comprising 80% of the protein) and intracellular N- and C- termini. Though no crystal structure of ENaC is available, mapping ENaC to the published chicken acid sensing ion channel (ASIC) structure (107) has provided insights toward understanding the structure of ENaC (108). In the homology mapping model (Figure 1-3), ENaC subunits contain many of the secondary structures and higher ordered domains as identified in the chicken ASIC. E.g., the extracellular loop of α-ENaC contains the palm domain, β-ball domain, finger domain, thumb domain and knuckle domain as shown in ASIC though significant differences were also observed. One of the most obvious differences is in the finger domain where sequences are so variable between the two molecules. Another

difference is in the β-ball domain where ENaC lacks two of the β strands, β4 and β5, but other than that, the sequences are quite conserved. Given the proposed role of ASIC β-ball domain in sensing acid, this difference may explain the inability of ENaC to sense acid.

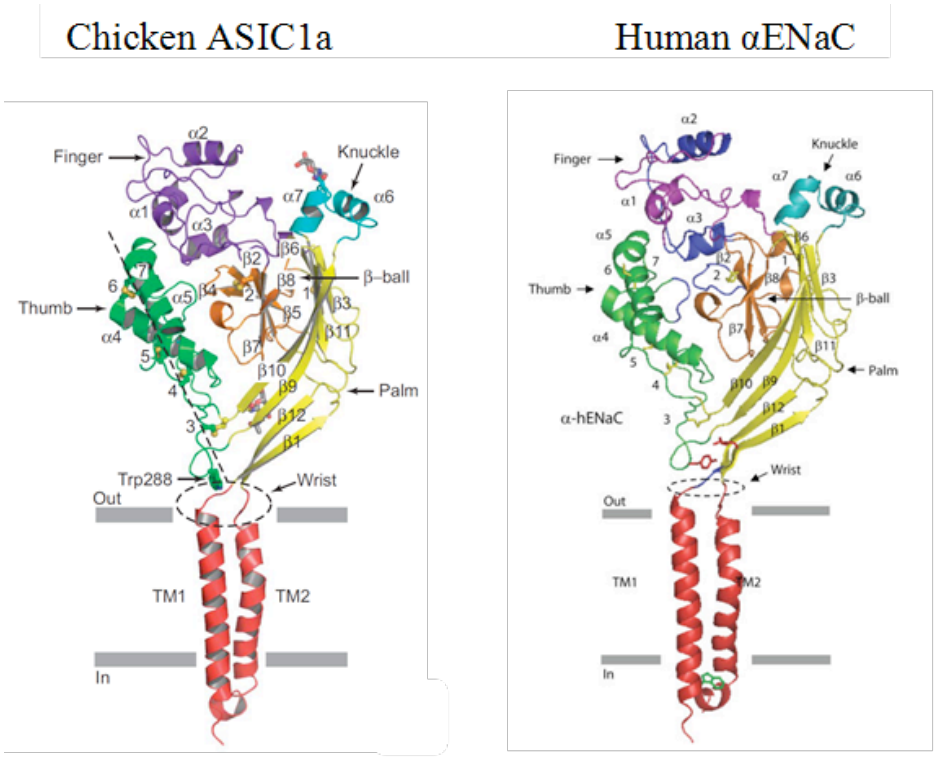

Figure 1-3. Structure of chicken ASIC and human α-ENaC. A, Domain organization of chicken ASIC1a single subunit from X-ray crystal structure. Locations of disulphide bridges (labeled 1-7), glycosylation sites and conserved tryptophan residue (Trp288) are indicated. (107) B, Predicted domain organization of human αENaC subunit modeled on the chicken ASIC1a monomer using 2QTS coordinates. Putative disulfide bridges are labeled 1-7 and shown as yellow sticks. The conserved Trp87 (green side chain) at the beginning of TM1 and Tyr391 (red side chain) within the putative coupling loop are shown. Transmembrane domains TM1 and TM2 and linker regions red, palm yellow, β-ball orange, knuckle cyan, thumb green, and finger magenta. Blue areas of human α-ENaC indicate possible differences compared to chicken ASIC1. (108)

ENaC channel is a heteromultimer composed of all three subunits. α-ENaC is the pore forming unit, which is sufficient to induce channel activity, while β- and γ-subunits allow a maximal activation of the channel (106). The stoichiometry of ENaC complex is controversial. Some studies proposed that ENaC functions as a tetramer with a 2α:1β:1γ stoichiometry (109,110) , while others suggested a higher number of subunits in the complex (111). However, the crystal structure of chicken ASIC, a close orthologous relative to ENaC in the degenerin/epithelial sodium channel superfamily, strongly supports a trimer architecture of ENaC (108), which afterwards was also confirmed by other groups using AFM (112). The ENaC trimeric structure is predicted in a chalice-like shape (Figure 1-4) as same as chicken ASIC (108): a large funnel-like extracellular domain, a slender TM domain and a broadened base formed by the cytoplasmic tails. Three TM2s form the channel pore with TM1s surrounding around. The gating mechanism is still unknown. But it was suggested that the ENaC finger domain which contains two peptidase cleavages sites may function as an autoligand which upon cleavage allows the conserved tyrosine residue at the base of the thumb to pass the information to the pore (108).

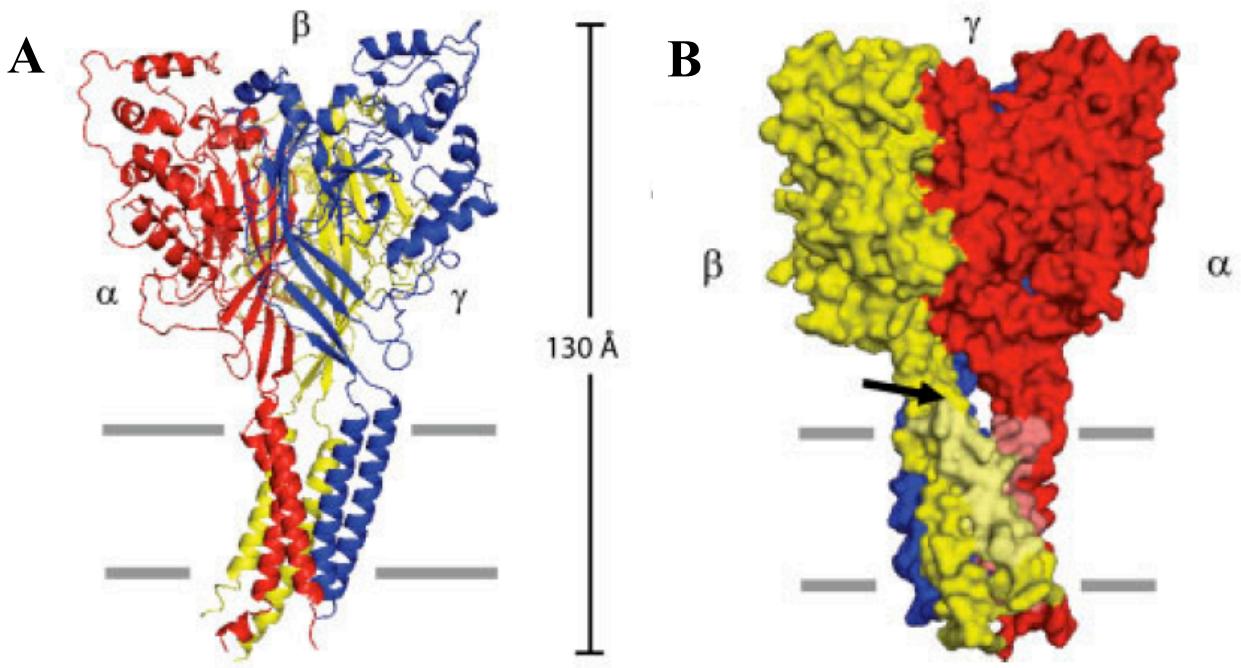

Figure 1-4. Predicted structure of oligomerized human ENaC. A, ribbon structure of the predicted heterotrimeric human ENaC. B, Predicted human ENaC heterotrimer with filled surfaces to the molecular threefold axis highlighting fenestration between TM1 (pale yellow) and TM2 (pale red) of adjacent monomers, and the numerous cavities and crevices formed by the subunits. Adapted human α- (red), β- (yellow), and γ- (blue) ENaC modeled using the 2QTS structural coordinates for the α-, β-, and γ- subunits of the chicken ASIC1 homotrimer. (108)

1.3.2 Biophysical characteristics

Before cloning, ENaC was functionally characterized as an amiloride-sensitive Na^+ channel. Though amiloride blocks a wide range of Na^+ channels in the ENaC/degenerin family such as ASIC, ENaC shows the highest affinity by amiloride inhibition, with an IC_{50} in the submicromolar range (113). Amiloride (3,5-diamino-6-chloropyrazinoylguanidine) consists of a substituted pyrazine ring and a guanidine group (Figure 1-5) (114). Biochemical analysis with structural analogues of amiloride suggested that the guanidine group is essential for the inhibitory effect while pyrazine ring greatly increases the molecular activity (114). The mechanism of amiloride inhibition remains elusive. One model proposed that amiloride does not block the channel pore but interacts with the extracellular loop (115-117) while other data suggested that amiloride physically occludes the channel pore (118,119). Crystal structure of ASIC revealed that the ASIC glycine 439, which position is equivalent to human α-ENaC serines 583, represents the amiloride binding site as it enters the pore but adjacent amino acids in the pore region also contribute to the binding (119).

ENaC is highly Na^+/Li^+ selective over K^+. This ion selectivity is defined by the '(Glycine/Serine)-X-Serine' tripeptide in TM2, known as the 'GAS' motif (120,121). Crystal structure of ASIC also supports GAS motif as an ion selectivity definer (122).

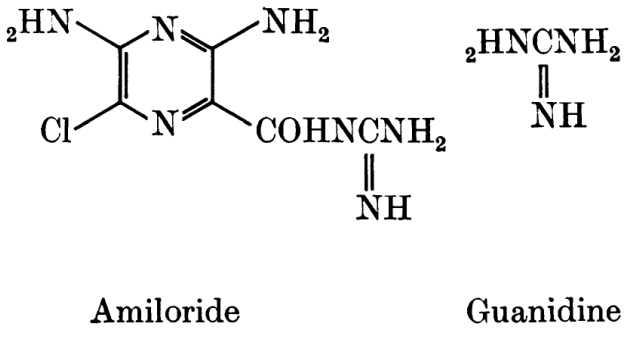

Figure 1-5. Structure of amiloride and guanidine. (114)

1.3.3 Tissue distribution and physiological function

ENaC is widely expressed in the absorptive epithelia of the kidney, colon, lung, intestine, and secretory glands, to mediate Na^+ transport/reabsorption. Na^+ transport through epithelia is a two-step process (Figure 1-6) (123). At the apical membrane, ENaC mediates Na^+ entry down its electrochemical gradient and at the basolateral membrane, Na^+ is pumped out by the Na^+/K^+ ATPase. As a result, Na^+ is reabsorbed from the lumen into the blood. In the kidney, ENaC is located on the apical membrane of the distal tubule and ENaC-mediated Na^+ reabsorption is crucial in maintenance of Na^+ and fluid homeostasis thus controlling blood pressure and volume. Gain of function of ENaC results in excessive Na^+ reabsorption and causes severe hypertension, known as Liddle Sydrome (124). While channel function loss/reduction causes salt losing nephropathy and hypotension found in pseudohypoaldosteronism type-1 (125). In the lung, ENaC mediated Na^+ absorption is crucial at birth for liquid clearance during the lung conversion from liquid to air environment (126), and after birth to maintain the airway surface fluid and anti-bacterial (low Na^+) environment (127). Abnormal function of lung ENaC is associated with the pathogenesis of cystic fibrosis (128). In the urinary bladder and distal colon, ENaC mediated Na^+ reabsorption is observed as well. In addition, ENaC is detected in the taste cells of the tongue and has been strongly suggested as a salt taste receptor (129,130). β-ENaC and γ-ENaC are expressed in non-epithelial cells such as neurons, and probably function in mechanosensation (131).

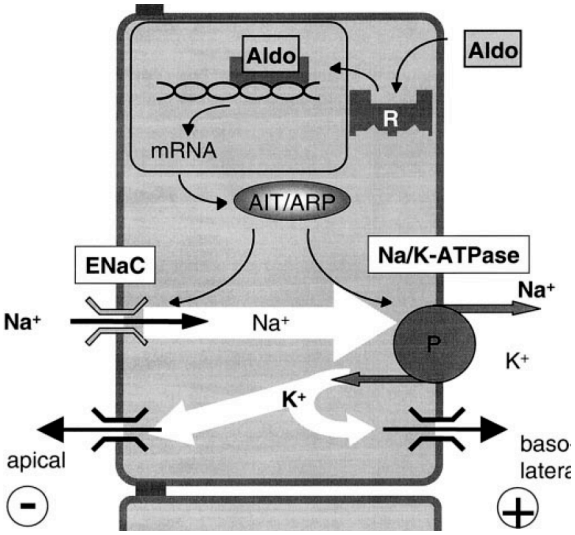

Figure 1-6. Transepithelial ion transport in a principal cell of the cortical collecting duct. ENaC mediates Na^+ entry from the tubule lumen at the apical membrane, and Na^+/K^+-ATPase extrudes Na^+ at the basolateral side. K^+ channels at the apical membrane mediate K^+ secretion into the tubular lumen. Aldosterone (Aldo) which binds to intracellular receptors that are translocated to the nucleus and affect the expression and subcellular localization of ENaC and the Na^+/K^+-ATPase as well as other targets. (123)

1.3.4 Regulation

The ENaC channel activity is regulated by a number of factors including hormones, proteases, growth factors, and cations. Two of the major hormones are vasopressin and aldosterone, both of which function to augment ENaC mediated Na^+ permeability (132). The effect of aldosterone shows two phases, the early phase and the late phase. In the early phase, aldosterone directly activates ENaC channel (133), and induces ENaC translocation to the PM through a few of potential mediators, such as the glucocorticoid-regulated kinase (134) and K-Ras2 (135). In the late phase, aldosterone increases *α-ENaC* gene transcription through re-programming promoter methylation (136) thus increasing protein synthesis. Another important hormone vasopressin increases ENaC surface expression and channel open probability through the adenylate cyclase-cAMP pathway (137,138). Furin, a protease that cleaves the extracellular loop of α- and r-ENaCs (139,140), activates ENaC channel by increasing its channel open probability. ENaC surface expression is decreased by the E3 ubiquitin-protein ligase Nedd4 (141) and growth factor TGF-β (142) through promoting endocytosis. In addition, the channel activity of ENaC is regulated by both extracellular and intracellular Na^+ (132). The inhibitory effect of high extracellular Na^+ on ENaC is referred to as Na^+ self-inhibition (143). The mechanism of Na^+ self-inhibition is unknown but it has been shown to be a process of rapid reduction in channel open probability (144). Extracellular histidine residues and half of the cysteine residues are found crucial for the Na^+ mediated self-inhibition (145), and are possibly involved in the conformational change of ENaC in response to Na^+ stimuli. The inhibition by intracellular Na^+ is a feedback regulation partially due to reduced channel density at the PM regulated by Nedd4 (146) and the conserved internalization motif 'PPPxYxxL' located at the C terminus of all three ENaCs (147).

1.3.5 Interaction with cytoskeleton protein

Cytoskeletal proteins have been reported to play critical roles in regulating ENaC channel activity. Actin, the major component of cytoskeleton, directly interacts with ENaC (148) and regulates its channel activity both *in vitro* (149) and *in vivo* (150). Ankyrin and alpha-spectrin have been also reported to associate with ENaC (151). The C terminal domain of ENaC was found to mediate these interactions. Disruption of actin microfilaments with cytochalasin D or addition of the actin filaments alters ENaC activity in A6 cells (152) and impairs its regulation in frog skin (153). Disruption of the cytoskeletal network also affects the population of apical membrane ENaC channels (154). Taken together, the cytoskeleton is important regulator of ENaC channels.

1.4 Filamin

Filamin, previously known as actin-binding protein 280, belongs to a superfamily of actin-binding proteins that cross-link the actin filament into a dynamic network and play critical roles in the cytoskeleton organization. This superfamily contains many subfamilies such as α-actinin, β-spectrin, dystrophin and fimbrin. Filamin is a member of the spectrin subfamily which is characterized by the presence of the spectrin repeat (antiparallel triple-helical coiled-coil structure), actin binding domain and EF hand (155). Filamin serves as scaffolds for over 90 binding partners including channels, receptors, intracellular signaling molecules and transcription factors (156). There are three isoforms of filamin, filamin-A, -B, and -C. They are highly similar in amino acid sequence and structure but with different expression pattern. Filamin-A and -B are universally expressed in the whole body while -C is more specifically expressed in the smooth muscle and heart.

1.4.1 Gene and protein structure

Filamin-A (FLNA) is encoded by *FLNA* gene residing in the long arm of X chromosome at Xq28, with a genomic sequence size of 26,115 bases (Genecards). *FLNA* has two transcripts: transcript 1 contains 47 exons with a total of 8533 bases, and transcripts 2 is slight longer with 48 exons and a total of 8557 bases. The predominant form of FLNA is encoded by transcript 1 which produces a 2639 aa cytoskeletal protein, corresponding to ~280 KDa in size. FLNA is the first non-muscle actin filament cross-linking protein identified in 1975. It functions as a dimer in a V-shaped structure and each monomer contains a N terminal actin binding domain (ABD) and 24 β-sheet repeats with 2 hinge regions (H1 and H2) in between (Figure 1-7) (156).

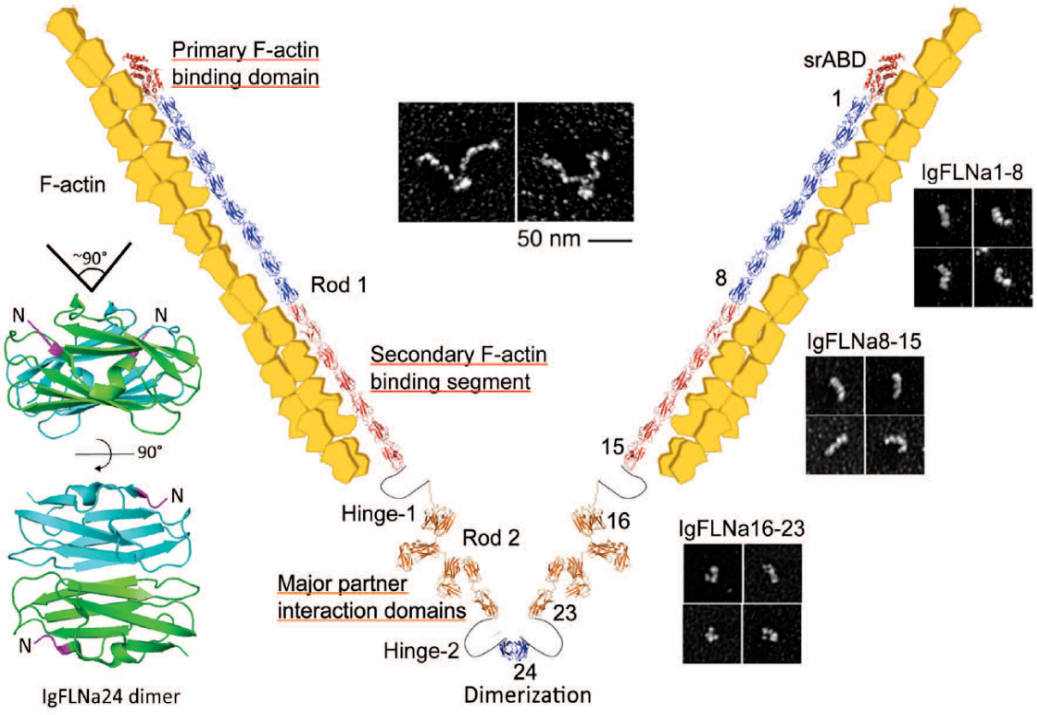

Figure 1-7. A schematic structure of FLNA molecule and the F-actin crosslink. This model was generated on PyMOL (www.pymol.org) by assembling Ig domains uploaded on protein data bank and by fitting them within rotary shadowed images of FLNA molecules. Structures were modeled using the Swiss model database (http://swissmodel.expasy.org). The atomic structure of IgFLN a24 was generated on PyMOL (PD B accession number: 3CNK). (156)

Actin binding domain (ABD)

The FLNA ABD (278 aa) contains two calponin homology domains (CH1 and CH2) separated by a linker (157). Notably calponin is a family of proteins that interact with actin filaments and are involved in the regulation of smooth muscle contraction (158). The CH domain (~100 aa), is an α-helical secondary structure that mediates actin binding and is shared by all the actin binding proteins (159). It is predicted that the CH1 domain (isoleucine 44-tyrosine 148) contains two putative acting binding sites (ABS) while CH2 (proline 168-phenylalanine 264) has only one. This is supported by the fact that the CH1 domain binds to actin filament stronger than the binding of CH2 (160). Further, CH1 is more conserved than CH2 and is involved in both direct binding with filamentous actin (F-actin) and the regulation of F-actin binding by Ca^{2+}-activated calmodulin while CH2 is only associated with the regulation of F-actin binding (160,161). The linker in between CHs is an acidic region full of aspartate and glutamic acid. Though not available for FLNA, the three-dimensional structures of ABD have been reported for actin binding proteins a-actinin (162), plectin (163) and fimbrin (164). All three reported ABDs are in the closed conformation under native condition that CH1 and CH2 are in an extensive contact, while conformation changes occur upon actin binding (Figure 1-8).

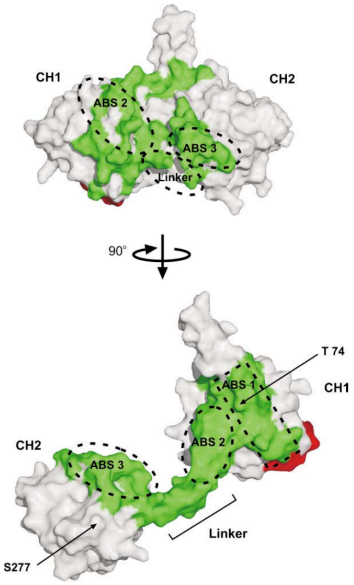

Figure 1-8. Model of ABD opening. Surface representation of plectin ABD in the closed conformation observed in the crystal structure (upper panel) and a hypothetical conformational change upon F-actin binding (lower panel). CH1 is rotated 90° around a vertical axis to expose all three ABS. Residues potentially interact with F-actin are colored in green. ABS and linker region are indicated. (163)

Repeated β-sheets

The 24 repeats are separated by two hinges (H1 and H2) into Rod 1 (repeats 1-15), Rod 2 (repeat 16-23) and the self-association domain (repeat 24). Each repeat contains ~96 aa in average and is arranged in the immunoglobulin-like (Ig) fold (165). Of note, the Ig domain is composed of two β-sheets with a total of 7-9 β-strands and forms a sandwich structure. The majority of the repeats are 7-stranded Ig like structure, and together with the short linker between repeats revealed an extended confirmation. However, repeats 18 and 20 are in a 6-stranded structure. Missing one strand induces more compact arrangement and produces a zigzag conformation of repeats 17-19 and 19-21 (161). In repeats 9-15, a secondary F-actin binding domain was found though with lower binding affinity compared with the ABD (166). Other than that, the majority of partner binding occurs in Rod 2. The most C terminal repeat 24, mediates FLNA self-dimerization and bestows a V-shape to the dimeric molecules (166). A compensatory dimerization activity of the fragment containing H1 and repeats 16-23 was observed when repeat 24 is deficient to form dimer (167).

Hinges

The two hinges (H1 and H2) in between repeats account for the flexibility of filamin molecules. In addition, both hinges contain a calpain-cleavage site and phosphorylation consensus sequences. H1 contains 25 residues with a calpain cleavage site at tyrosine 1761-threonine 1762 (168). H2 is a 35 residues insertion with the calpain cleavage site not defined yet. The physiological importance of the protease cleavage and phosphorylation will be discussed in Section 1.4.3.

1.4.2 Subcellular localization and function

Filamin is a large cytosolic protein, cross links the actin filament and provides scaffolds for a variety of proteins, including transmembrane receptors and channels, signaling proteins, cytoskeletal and other cytoplasmic proteins (156,169). Representative transmembrane proteins are dopamine receptor, furin receptor, platelet glycoprotein Ibα, β-integrin, presenilin and Kv4.2 potassium channel. Filamin interacting signaling proteins involve a variety of GTPase, like RalA, Rab22B, RhoA, Rac1, and Cdc42. Examples of cytoplasmic proteins are myotilin, calmodulin, and granzyme B. Filamin binds, mostly via their C-terminal Rod 2 repeats, to their partners with diverse functions. For example, FLNA directly binds furin receptor to reduce internalization and increase protein synthesis (170). FLNA decreases the proteasomal/lysosomal degradation of the platelet glycoprotein subunit GpIbα though physical binding (171). The presence of FLNA is the prerequisite for the proper function of several proteins, such as GTPase RalA and Cdc42 (172), and the TNF receptor superfamily (173).

In addition to its classic role in scaffolding, filamin also plays other roles, notably regulating gene expression. One of the mechanisms is that cytoplasmic filamin binds some of the transcriptional regulators and prevents their entry to the nucleus, where they carry out functions. Examples of these transcriptional regulators are PEBP2/CBF (174) and p73α (175). On the other hand, filamin regulates gene expression directly in the nucleus. Both the C terminal fragments produced by proteolytic cleavage and the full length FLNA were found present in the nucleus. The C terminal repeats 16-23 translocate to the nucleus together with the transcriptional factor androgen receptor (176), resulting in repression of its transactivation activity (177). Furthermore, the importance of this FLNA C fragment in regulating androgen receptor dependent pathway was implicated in prostate cancer (178,179). Full length FLNA

protein is present in the nucleolus where it functions to suppress ribosome RNA transcription through interacting with the RNA polymerase I (180). Further investigation revealed that a putative nuclear localizing signal (RRRR) is present in FLNA repeat 20 (aa 2146–2149), however it remains to be known how the full-length filamin translocates to the nuclear. In addition, filamin has been found to participate in the DNA damage repair process by interacting with BRCA1 (181) and BRCA2 (182), the products of breast and ovarian cancer susceptibility genes that control the efficiency of homologous recombination during DNA double stranded breaks repair.

1.4.3 Modification (cleavage and phosphorylation)

The major regulation/modification of filamin is through proteolysis and phosphorylation. Filamin contains two proteolysis sites in the hinge domains that both H1 and H2 can be cleaved by calpains and caspases (183). Cleavage at H1 occurs between aa 1761 and 1762 (168), resulting in a ~170 kDa fragment containing the ABD and repeats 1-15, and a ~110 kDa protein containing repeats 16-24. The 110 kDa protein fragment will be further cleaved at H2 to yield a ~90 kDa fragment (169). The proteolysis cleavage site at H2 remains to be determined. It is believed that the cleaved C terminal fragment of filamin is capable of nucleus translocation where it functions to regulate gene expression as mentioned in Section 1.4.2. On the other hand, filamin is strongly phosphorylated in cells by a variety of kinases including cyclin-dependent kinase 1 (Cdk1)/cyclin B1 (184), p21-activated kinase 1 (185), p90 ribosomal S6 protein kinase (186), and cAMP-dependent protein kinase (187). The phosphorylation state of filamin affects its interaction with other protein partners such as GTPase (188) and actin (189). Phosphorylation affects cleavage as well, e.g., phosphorylation of filamin serines 2152

increases its resistance to calpain proteolysis (168,187,190,191). Also, it is worth mentioning that the phosphorylation state of filamin changes in response to various cell signals. E.g., the phosphorylation of FLNA serine residues 1084, 1459 and 1533 by Cdk1 occurs in mitotic cells rather than cells in the interphase, and thus is important for cell division (184).

1.4.4 Physiological function and defects

Filamin is essential for mammalian development and change of its expression/function leads to diverse congenital anomalies. First, filamin is necessary for cell-cell contact/intercellular junctions during vascular development and cardiac morphogenesis (192). Mutations with decreased activity of FLNA cause genetic heart vascular disorder and familiar cardiac valvular dystrophy in human (193). Cardiac malformation was also observed in mice with FLNA mutations (194). Complete loss of FLNA causes embryonic lethality in mice, mainly due to severe defects in blood vessel and cardiovascular formation (192,194). Second, filamin is required for cell migration, especially in the nervous system. Mutations of FLNA have been found to cause a X-linked hereditary disease called periventricular heterotopia (PH) in which neurons fail to migrate properly to the cerebral cortex but remain as nodules lining the ventricular surface (195). Interestingly, duplication of *FLNA* gene also causes PH, indicating that the dosage of filamin matters. Further, the functional implication of filamin in cancers was stated in several studies. Filamin was mutated at a significant frequency in human breast and colon cancers (196). Moreover in colon cancers, FLNA expression level was in high correlation with the incidence and development of colorectal cancer, and thus considered as an indicator of prognosis (197). In addition, the nuclear filamin fragments show different abundance in benign prostate than that in metastatic prostate cancers (179).

1.5 Thesis objectives and rationale

Objectives

It is known that ADPKD is caused by mutations of *PKD1* or *PKD2* gene, and several pathways have been proposed to contribute to the disease pathogenesis, e.g., renal primary cilia, Ca^{2+} signaling, mammalian target of rapamycin (mTOR), MAPK/ERK, Wnt signaling and vasopressin receptor (3). However, clinical trials targeting to these pathways have been proved to be disappointing (198-200). The main objective of this thesis is to explore novel targets and alternative pathways in the *PKD2* gene induced ADPKD. We hypothesized that PC2 functions in a protein complex and the activity is largely regulated by its binding partners. The strategy is to screen for new binding partners of PC2 and analyze the physiological significance of their interaction, which are illustrated in Aims 1, 2, and 3. This thesis also includes a study of the epithelial sodium channel (ENaC) as discussed in Aim 4, following the same strategy used in the PC2 study. The specific aims are as follows:

Aim 1: To examine the physical interaction of PC2 and filamin and their functional regulation

Aim 2: To study how filamin stabilizes PC2 plasma membrane and total expression

Aim 3: To study the net effect of filamin-PC2 interaction

Aim 4: To examine the physical and functional interaction between ENaC and filamin

Rationale

In ADPKD cases, a series of downstream pathways have been found to be abnormal and thus drugs targeting to a certain pathway may not significantly or fully correct/rescue the entire phenotype. Direct targeting to the disease-causing molecule, PC2 in this thesis, would be the most effective and efficient way for further therapeutic strategies. Either gain or loss of PC2

function results in cystogenesis, no matter due to mutations or wild type dosage changes. Thus, the channel function of PC2 needs to be maintained in a narrow range. The PC2 channal function is determined by its protein expression, subcellular localization and single molecular activity, and all three parameters have been shown to be regulated by its binding partners. Thus in my study, I am looking at new PC2 binding partners and the regulatory effect on all three aspects of PC2. Cultured cell line is the major model used in this study because it is easy to manipulate (For details see Section 1.2.6). For functional study, planar lipid bilayer, a well-established *in vitro* method, was employed. Live cell Ca^{2+} imaging was used to study the *in vivo* function of and the net effect of filamin on PC2. At the end, zebrafish model was explored to investigate the physiological relevance of PC2-filamin interaction.

The strategy used in the ENaC study is basically the same as that in PC2. One different is that *Xenopus* oocyte model in combination with two-electrode voltage clamp electrophysiology was used to study the channel function of ENaC. This is due to the advantage that abundant ENaC molecules are targeted to the plasma membrane of *Xenopus* oocyte, compared to PC2.

CHAPTER 2

RESULT #1 Structural interaction and functional regulation of polycystin-2 by filamin

A version of this chapter has been published in 2012
Qian Wang, Xiao-Qing Dai, Qiang Li, Zuocheng Wang, Maria del Rocio Cantero, Shu Li, Ji Shen, Jian-Cheng Tu, Horacio Cantiello and Xing-Zhen Chen.
PLoS One. 2012;7(7):e40448

2.1 ABSTRACT

Filamins are important actin cross-linking proteins implicated in scaffolding, membrane stabilization and signal transduction, through interacting with ion channels, receptors and signaling proteins. Here we reported a physical and functional interaction between filamins and polycystin-2 (PC2), a TRP-type cation channel mutated in 10–15% patients with autosomal dominant polycystic kidney disease. Yeast two-hybrid and GST pull-down experiments demonstrated that the C termini of filamin isoforms A, B and C directly bind to both the intracellular N- and C- termini of PC2. Reciprocal coimmunoprecipitation experiments showed that endogenous PC2 and filamins are in the same complex in renal epithelial cells and human melanoma A7 cells. We then examined the effect of filamin on PC2 channel function by electrophysiology studies in a lipid bilayer reconstitution system and found that filamin-A substantially inhibits PC2 channel activity. Our study indicates that filamins are important regulators of PC2, and further links actin cytoskeletal dynamics to the regulation of this channel protein.

2.2 INTRODUCTION

Mammalian filamin was first isolated from rabbit macrophages in 1975 as an actin-binding protein (201). The mammalian filamin family consists of three ~280 kDa isoforms, filamin-A (FLNA), -B (FLNB) and -C (FLNC), sharing 60-80% sequence homology, of which FLNA is the most abundant and widely distributed (202). Filamins contain a N terminal actin-binding domain (ABD) that shares sequence similarity with other actin-binding proteins, and a rod domain consisting of 24 repeated anti-parallel β-sheets with one or two short 'hinges' inserted before repeats 16 and 24 (Fig. 1A). Filamins self-associate within a C terminal 7 kDa domain, to form homodimers with flexible V-shaped structure acting as 'a molecular leaf spring' to facilitate cross-linking of actin filaments (168).

By cross-linking actin filaments at wide angles, filamins act as important actin cytoskeleton organizers implicated in sol-gel transformations and membrane stabilization as anchors of many transmembrane proteins, and as scaffolding proteins for various signaling molecules (169). Indeed, as versatile scaffolding proteins, filamins physically interact with, and regulate the activity of, many proteins with diverse functions (202). Mutations in the *FLNA* and *FLNB* genes are known to cause a variety of developmental disorders in humans, including bone anomalies, periventricular heterotopia, aortic dissection and aneurysm (203-205).

Polycystin-2 (PC2), also known as TRPP2, is a member of the transient receptor potential polycystin (TRPP) subfamily of TRP channels. PC2, encoded by the *PKD2* gene, is a 968 amino acid (aa) integral membrane protein with six transmembrane domains and intracellularly localized N- and C- termini. PC2 bears similar membrane topology with other TRP channels and voltage-gated cation channels (27). PC2 is localized to different subcellular compartments such as the endoplasmic reticulum (ER) membrane (60), the primary cilium (65,206) and the

plasma membrane (PM) (207). Mutations in *PKD2* account for 10-15% of autosomal dominant polycystic kidney disease (ADPKD), a common genetic disorder with a population prevalence of ~1:1000 that is characterized by formation of cysts in various organs, including the kidneys, liver and pancreas (208). Non-cystic manifestations of the disease include mitral valve prolapse, aortic dissection and vascular aneurysm (209,210). Despite the fact that cystic cells are associated with cell over-proliferation, de-differentiation and apoptosis, the underlying mechanisms of cyst formation remain ill defined. We found that PC2 inhibits cell proliferation by up-regulating the activity of the translation inhibitor eIF2α (211). Mice with either loss- or gain-of-function of PC2 are cystogenic (15,101). Thus, it seems critical for cells to control the PC2 cellular expression level within a narrow range. We recently found that PC2 degradation is regulated by the ER-associated degradation (ERAD) pathway through the ubiquitin-proteasome system, demonstrating that PC2 is a novel ERAD substrate (212).

There are important connections between PC2 and the actin cytoskeleton. About half of PC2 interacting partners identified to date are cytoskeleton or cytoskeleton-associated proteins (213). PC2 interacts with α-actinin, an actin-bundling protein important in cytoskeletal organization, cell adhesion, proliferation and migration. Interestingly, both intracellular N- and C- termini of PC2 associate with this actin-binding protein. Their interaction substantially increases PC2 channel activity by increasing the channel open probability, but not the single channel conductance (45). Thus, α-actinin binds to PC2 to regulate the channel gating rather than affecting its physical channel pore. Dynamic changes in actin filament organization also modulate the channel function PC2 in the apical membrane of human syncytiotrophoblast (hST), a preparation that contains abundant endogenous PC2 (26). Either addition of G-actin, treatment with the actin filament disrupter cytochalasin D, or addition of the actin-severing

protein gelsolin to the apical membrane of the hST dramatically increases PC2 channel activity (214). Thus, the actin cytoskeleton anchors PC2 to the PM not only for structural purposes, but also to regulate its channel function. It was reported that both hydrostatic and osmotic pressures stimulate PC2 channel activity in hST, a phenomenon in which the effect of both physical factors was abolished by pre-treatment with the cytoskeletal disrupter cytochalasin D (215). Thus, PC2 and actin structures together, but not the channel alone, confer PC2 sensitivity to these physical factors. This suggests that the actin cytoskeleton associated with PC2 acts as an integral part of a sensing complex responsive to hydrostatic and osmotic changes.

In the present study, we first examined and documented by various *in vitro* and *in vivo* approaches, the physical interaction between PC2 and the actin cross-linking proteins filamins. We then examined the effect of FLNA on PC2 channel function.

2.3 MATERIALS AND METHODS

Antibodies

Three anti-PC2 antibodies were used in this study, including mouse 1A11 (44,45), goat G-20 (45) and rabbit H-280 (Santa Cruz Biotech, Santa Cruz, CA). The antibodies used to label filamins included mouse FIL-2, raised using chicken gizzard filamin antigen (Sigma-Aldrich Canada, Oakville, ON), mouse anti-FLNA E-3 and rabbit H-300 (Santa Cruz Biotech). Affinity purified goat anti-GFP EU4 (Eusera, Edmonton, AB) was utilized for immunoprecipitation (IP) and mouse anti-GFP B-2 (Santa Cruz Biotech) for immunoblotting (IB). Mouse anti-His Tag 27E8 (New England Biolabs, Pickering, ON) was employed to detect His-tagged filamins C termini in GST pull-down. Rabbit anti-calnexin C4731 (Sigma-Aldrich Canada) was used for immunofluorescence (IF). Either rabbit A2066 (Sigma-Aldrich Canada) or mouse anti-β-actin C4 (Santa Cruz Biotech), and mouse anti-HSP60 H-1 (Santa Cruz Biotech) antibodies were used as loading controls. Secondary antibodies were purchased from GE Healthcare (Baie d'Urfe, Quebec) or Santa Cruz Biotech.

Plasmid construction

The FLNAC and FLNBC cDNAs were isolated by PCR from either a human kidney cDNA library or HEK293 cells. The cDNA encoding the C terminus of FLNC (FLNCC, aa 2144-2725) was cut from the pACT2-FLNCC plasmid. The cDNAs were subcloned into pGADT7 and pET28a (Novagen, EMD Chemicals, Gibbstown, NJ) for yeast and bacterial expression, respectively. Mammalian expression plasmids pEGFP-PC2, pEGFP-PC2ΔC (aa 1-688, lacking the C terminus) and pEGFP-PC2ΔN (aa 209-968, lacking the N terminus), in which GFP is fused to the N terminal end of PC2, were constructed based on a method

previously described (45). All plasmid constructs were verified by sequencing.

Yeast two-hybrid analysis

cDNA fragments encoding either the N terminus (PC2N, aa 1-215) or C terminus (PC2C, aa 682-968) of human PC2 were subcloned in frame into the GAL4 DNA binding domain of the pGBKT7 vector (Clontech, Palo Alto, CA) by a PCR-based approach. Either PC2N or PC2C was used as a bait in a yeast two-hybrid screen using human heart library (Clontech) constructed in the pGADT7 vector in the yeast strain AH109 containing Ade2, His3 and LacZ reporter genes under the control of the GAL4 upstream activating sequences as described (45). A pair bait-prey was then co-transformed in the yeast strain Y187. The β-GAL activity was determined based on the time it takes for colonies to turn blue in X-gal filter lift assays performed at 30ºC.

GST pull-down

The cDNA fragments encoding PC2N or PC2C were subcloned into the pGEX5X vector (Pharmacia, Piscataway, NJ, USA). Expression of GST-PC2C, GST-PC2N or GST alone was conducted in the protease-deficient bacterial strain *E. coli* BL21 (DE3). Protein expression was allowed for 5 hrs at 28ºC after inducing with IPTG (1 mM). The bacterial pellet was obtained and lysed by grinding with Alumina type A-5 (Sigma-Aldrich, Canada) in an extraction buffer, containing 140 mM NaCl, 10 mM Na_2HPO_4, and 1.8 mM KH_2PO_4, pH 7.5. The supernatant was either used for GST purification with a commercial kit (Clontech, Polo Alto, CA), or used directly in GST pull-down experiments. The cDNA fragments encoding either, FLNAC, FLNBC, or FLNCC were cloned into the pET28a vector containing a poly His epitope on its 5'

end (Novagen). Proteins were similarly expressed and purified by a His Bind® kit (Novagen) according to manufacturer's protocol. Either pre-cleared bacterial protein extracts (250 µl) containing GST-tagged PC2N, PC2C or GST alone, or purified GST fusion proteins (2 µg), were incubated with purified His-FLNAC, -FLNBC or -FLNCC fusion protein (2 µg), in the binding buffer, containing 150 mM NaCl, 1.0 mM $CaCl_2$, and 50 mM Tris, pH 7.5. The mixture was incubated at room temperature (RT) for 1 hr with gentle shaking, followed by another hour of incubation after addition of 100 µl glutathione-agarose beads (Sigma-Aldrich Canada). The beads were then washed 4-5 times with 140 mM NaCl, 10 mM Na_2HPO_4, and 1.8 mM KH_2PO_4, pH 7.5. The remaining proteins are eluted using elution buffer containing 10 mM glutathione, 50 mM Tris, and pH 8.0. The protein samples were then prepared for IB.

Cell culture and transfection

Renal cell lines, including HEK293, MDCK, IMCD, and porcine kidney cells LLC-PK1 were cultured in Dulbecco's modified Eagle's medium (DMEM) supplemented with L-glutamine, penicillin-streptomycin, and 10% fetal bovine serum (FBS). MDCK cells stably expressing either GFP-PC2 or GFP alone were selected as previously described (216) and maintained in the presence of 300 µg/ml G418 (Invitrogen Canada Inc., Burlington, ON). The human melanoma cell lines M2 and A7 were maintained in minimal essential medium supplemented with 8% newborn calf serum and 2% fetal calf serum. Transfection of cDNAs was performed using Lipofectamine 2000 (Invitrogen Canada Inc.) according to the manufacturer's protocol.

Human melanoma cell lines

Human melanoma M2 cells, grown as previously described (217), is deficient of filamins. Transfection of FLNA into M2 cells generated A7 cells. To generate M2 and A7 PC2 stable cell lines, 600 mg/ml of hygromycin and 300 μg/ml G418 were added to select viable clones one day following transfection, and then maintained using 100 μg/ml hygromycin or hygromycin plus 300 μg/ml G418, respectively. M2 cells display impaired motility and dysfunctional actin organization. FLNA-replete A7 cells that exhibit both normal motility and actin cytoskeletal organization (217).

Immunofluorescent microscopy

MDCK, M2 and A7 human melanoma cells stably expressing PC2 were grown on coverslips, fixed for 10 min at RT with 2% paraformaldehyde, and washed twice with PBS. Cells were then permeabilized for 3 min at RT with PBS containing 0.05% Triton X-100, blocked in PBS with 3% skim milk powder for 1 hr, and incubated with either anti-FLNA E3 or anti-calnexin overnight at 4ºC, followed by 1 hr incubation with the secondary antibody. Cells were finally washed with PBS containing 0.1% Tween 20. Vectashield mounting medium with DAPI (Vector Laboratories, Burlingame, CA) was used to protect IF signals from fading. Pictures were captured with a fluorescence microscope with Colibri LED (Carl Zeiss Canada Ltd., Toronto, ON). The final composite images were created using AxioVision 4.8 (Carl Zeiss Canada Ltd.).

Protein preparation and lipid bilayer electrophysiology

Commercial chicken gizzard filamin (FLNA, Cell Sciences, Canton, MA) was used as a modulator of PC2 channel function. Purified PC2 protein was obtained either by *in vitro*

translation (Applied Biosystems) or by our modified tandem affinity purification method from PC2 stably expressing MDCK cells (45,216). PC2-containing hST apical membrane vesicles were prepared and reconstituted in a lipid bilayer system for electrophysiology studies, as previously described (216,218). Briefly, a lipid bilayer membrane was formed with a mixture of 1-palmitoyl-2-oleoyl phosphatidyl-choline and phosphatidyl-ethanolamine (Avanti Polar Lipids, Birmingham, AL, USA) at a 7:3 ratio in a Deldrin cup inserted in an acrylic chamber (Harvard Apparatus, Montreal, QC, Canada). The *cis* (intracellular) compartment contains 10 mM MOPS, 150 mM KCl and 15 μM Ca^{2+} (by 1 mM EGTA and 1.01 mM/L $CaCl_2$), pH 7.4. The *trans* (extracellular) chamber contains 10 mM MOPS and 15 mM KCl, pH 7.4. The PC2 preparation was either added to the *cis* chamber in the proximity of the bilayer, or was 'painted' directly into the membrane. Filamin was added to the *trans* chamber of the bilayer cuvette, to a final concentration of approximately 25 nM. Negative controls were also conducted by addition of either a similar volume of saline without filamin, or addition of the same concentration of denatured filamin obtained by boiling the protein for 5-10 min. Voltage clamping of single channel currents was performed using Clampex 9 (Molecular Devices, Union City, CA, USA).

Data analysis

IB signals were quantified by ImageJ (National Institute of Health, Bethesda, MD), analyzed and plotted using SigmaPlot 11 (Systat Software Inc., San Jose, CA). Data were expressed as mean ± SEM (*n*), where *n* indicates the number of experimental repeats. Statistical analysis was conducted by Student's *t*-test, and a probability value (*p*) of less than 0.05 was considered significant (*).

2.4 RESULTS

2.4.1 Association of PC2 with filamins revealed by yeast two-hybrid assay

To identify novel proteins interacting with PC2 *in vivo*, we screened a human heart yeast two-hybrid library (Clontech) with the PC2 N terminus (PC2N, aa 1-215) and C terminus (PC2C, aa 682-968), as previously described (45,219). One plasmid isolated from the library represented a splicing variant of FLNC (Accession Number: AF146692, 9044 bp coding for 2691 aa). The identified FLNC cDNA was the 3' fragment starting at nucleotide 6331, encoding a polypeptide that corresponds to FLNC aa 2111-2691 and comprises both the 20-24 repeats and the second hinge. This region interacted with both PC2N and PC2C (Figure 2-1). Given that the three mammalian filamin isoforms share high sequence similarities, we further explored whether FLNA and FLNB, which are more abundantly and universally expressed than FLNC, also bound PC2. Indeed, the C terminus of human FLNA (FLNAC, aa 2150-2647), FLNB (FLNBC, aa 2105-2602) and FLNC (FLNCC, aa 2144-2725) associated with both PC2N and PC2C (Figure 2-1 C).

A

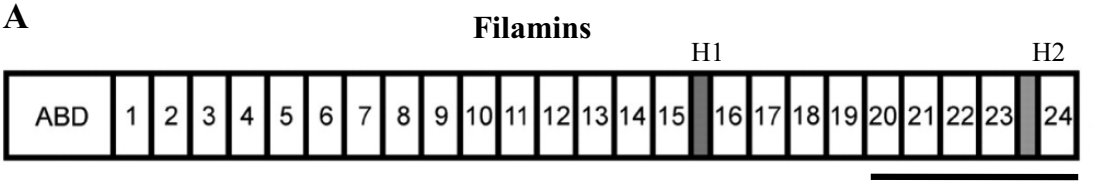


```
FLNA 2150 APSVANVGSHCDLSLKIP------------------------------------------------------------
FLNB 2105 APSVATVGSICDLNLKIP------------------------------------------------------------
FLNC 2144 APSIATIGSTCDLNLKIPGNWFQMVSAQERLTRTFTRSSHTYTRTERTEISKTRGGETKREVRVEESTQVGGDPFPAVFG

FLNA 2168 --------------------EISIQDMTAQVTSPSGKTHEAEIVEGENHTYCIRFVPAEMGTHTVSVKYKGQHVPGSPFQ
FLNB 2123 --------------------ELNSSDMSAHVTSPSGRVTEAEIVPMGKNSHCVRFVPQEMGVHTVSVKYRGQHVTGSPFQ
FLNC 2224 DFLGRERLGSFGSITRQQEGEASSQDMTAQVTSPSGKVEAAEIVEGELSAVSVRFVPQEMGPHTVAVKYRGQHVPGSPFQ

FLNA 2228 FTVGPLGEGGAHKVRAGGPGLERAEAGVPAEFSIWTREAGAGGLAIAVEGPSKAEISFEDKKDGSCGVAYVVQEPGDYEV
FLNB 2183 FTVGPLGEGGAHKVRAGGPGLERGEAGVPAEFSIWTREAGAGGLSIAVEGPSKAEIIFDDHKNGSCGVSYIAQEPGNYEV
FLNC 2304 FTVGPLGEGGAHKVRAGGTGLERGVAGVPAEFSIWTREAGAGGLSIAVEGPSKAEIAFEDKKDGSCGVSYVVQEPGDYEV

FLNA 2308 SVKFNEEHIPDSPFVVPVASPSGDARRLTVSSLQESGLKVNQPASFAVSLNGAKGAIDAKVHSPSGALEECYVTEIDQDK
FLNB 2263 SIKFNDEHIPESPYLVPVIAPSDDARRLTVMSLQESGLKVNQPASFAIRLNGAKGKIDAKVHSPSGAVEECHVSELEPDK
FLNC 2384 SIKFNDEHIPDSPFVVPVASLSDDARRLTVTSLQETGLKVNQPASFAVQLNGARGVIDARVHTPSGAVEECYVSELDSDK

FLNA 2388 YAVRFIPRENGVYLIDVKFNGTHIPGSPFKIRVGEPGHGGDPGLVSAYGAGLEGGVTGNPAEFVVNTSNAGAGALSVTID
FLNB 2343 YAVRFIPHENGVHTIDVKFNGSHVVGSPFKVRVGEPGQAGNPALVSAYGTGLEGGTTGIQSEFFINTIRAGPGTLSVTIE
FLNC 2464 HTIRFIPHENGVHSIDVKFNGAHIPGSPFKIRVGEQSQAGDPGLVSAYGPGLEGGTTGVSSEFTVNTLNAGSGALSVTID

FLNA 2468 GPSKVKMDCQECPEGYRVTYTPMAPGSYLISIKYGGPYHIGGSPFKAKVTGPRLVSNHSLHETSSVFVDSLTKATCA--P
FLNB 2423 GPSKVKMDCQETPEGYKVMYTPMAPGNYLISVKYGGPNHIVGSPFKAKVTGQRLVSPGSANETSSILVESVTRSSTE--T
FLNC 2544 GPSKVQLDCRECPEGHVVTYTPMAPGNYLIAIKYGGPQHIVGSPFKAKVTGPRISGGHSLHETSTVLVETVTKSSSSRGS

FLNA 2546 QHGAPGPGPADASKVVAKGLGLSKAYVGQKSSFTVDCSKAGNNMLLVGVHGPRTPCEEILVKHVGSRLYSVSYLLKDKGE
FLNB 2501 CYSAIPKASSDASKVTSKGAGLSKAFVGQKSSFLVDCSKAGSNMLLIGVHGPTTPCEEVSMKHVGNQQYNVTYVVKERGD
FLNC 2624 SYSSIPKFSSDASKVVTRGPGLSQAFVGQKNSFTVDCSKAGINMMMVGVHGPKTPCEEVYVKHMGNRVYNVTYTVKEKGD

FLNA 2626 YTLVVKWGHEHIPGSPYRVVVP 2647
FLNB 2581 YVLAVKWGEEHIPGSPFEVTVP 2602
FLNC 2704 YILIVKWGDESVPGSPFKVKVP 2725
```

B

Polycystin-2

C

prey (PGADT7) / bait (PGBKT7)	FLNAC (2150-2647)	FLNBC (2105-2602)	FLNCC (2144-2725)	Vector
PC2N (1-215)	++	++	+++	-
PC2C (682-968)	++	++	+++	-
PC1C (4088-4302)	-	-	-	-
Vector	-	-	-	-

Figure 2-1. Structural domains and sequence of filamins and PC2, and their interaction identified by yeast two-hybrid assay. (**A**) *Upper panel*, domain structure of human filamins, FLNA, FLNB and FLNC, and sequence alignment. Filamins share common features such as the N terminal ABD and a semi-rigid rod composed of 24 Ig-like repeats (~96 aa each) interrupted by two short flexible hinges (H1 and H2). The PC2 binding domain is indicated. *Lower panel*, sequence alignment of three filamin C termini, which share 70-75% sequence similarity. (**B**) Structural domain of PC2 is shown, indicating both the intracellular N- and C- termini (PC2N and PC2C, filamin-interacting domains) and transmembrane spans (TMs). (**C**) Interaction data revealed by β-GAL induction assay in the yeast two-hybrid screen system. PC2N, PC2C, the C terminus of polycystin-1 (PC1C) and the empty vector were used as bait. The C termini of filamins and the empty vector were used as prey. '+++', '++', '+' and '-' indicate development of blue color within 1, 3 and 24 hours, and no development of blue color within 24 hours, respectively, in X-gal filter lift assays.

2.4.2 Interaction of PC2 with filamins revealed by GST pull-down and co-IP

We employed an *in vitro* GST fusion protein affinity binding assay to further characterize the interaction between PC2 and filamins. Both PC2N and PC2C were fused in frame with a GST epitope, expressed in the bacterial strain BL21 and purified (Figure 2-2 A). His-tagged FLNAC, FLNBC and FLNCC were similarly expressed and purified (Figure 2-2 A). PC2N and PC2C present in the cell lysates were found to interact with purified FLNAC, FLNBC and FLNCC (Figure 2-2 B). Purified PC2N and PC2C also interacted with all three filamin C termini (Figure 2-2 C). These data together demonstrated that PC2 directly binds the C termini of filamins through its N- and C- termini. The amounts of PC2N detected by GST antibody were much lower than that of PC2C (Figure 2-2 B, GST bands, lower panels) whenever cell lysates were used. However, their binding to filamins was comparable (Figure 2-2 B, His bands, *upper panels*), indicating a stronger PC2N-filamin interaction than the PC2C-filamin interaction. Consistently, after taking into account the different amounts of purified PC2N and PC2C that were pulled down by GST antibody (Figure 2-2 C, GST bands, *lower panels*), it can be seen that the PC2N-filamin binding was stronger than the PC2C-filamin binding (Figure 2-2 C, His bands, *upper panels*). Thus, these data together indicated that binding of PC2N to the filamin C terminus is stronger than that of PC2C to the filamin C terminus.

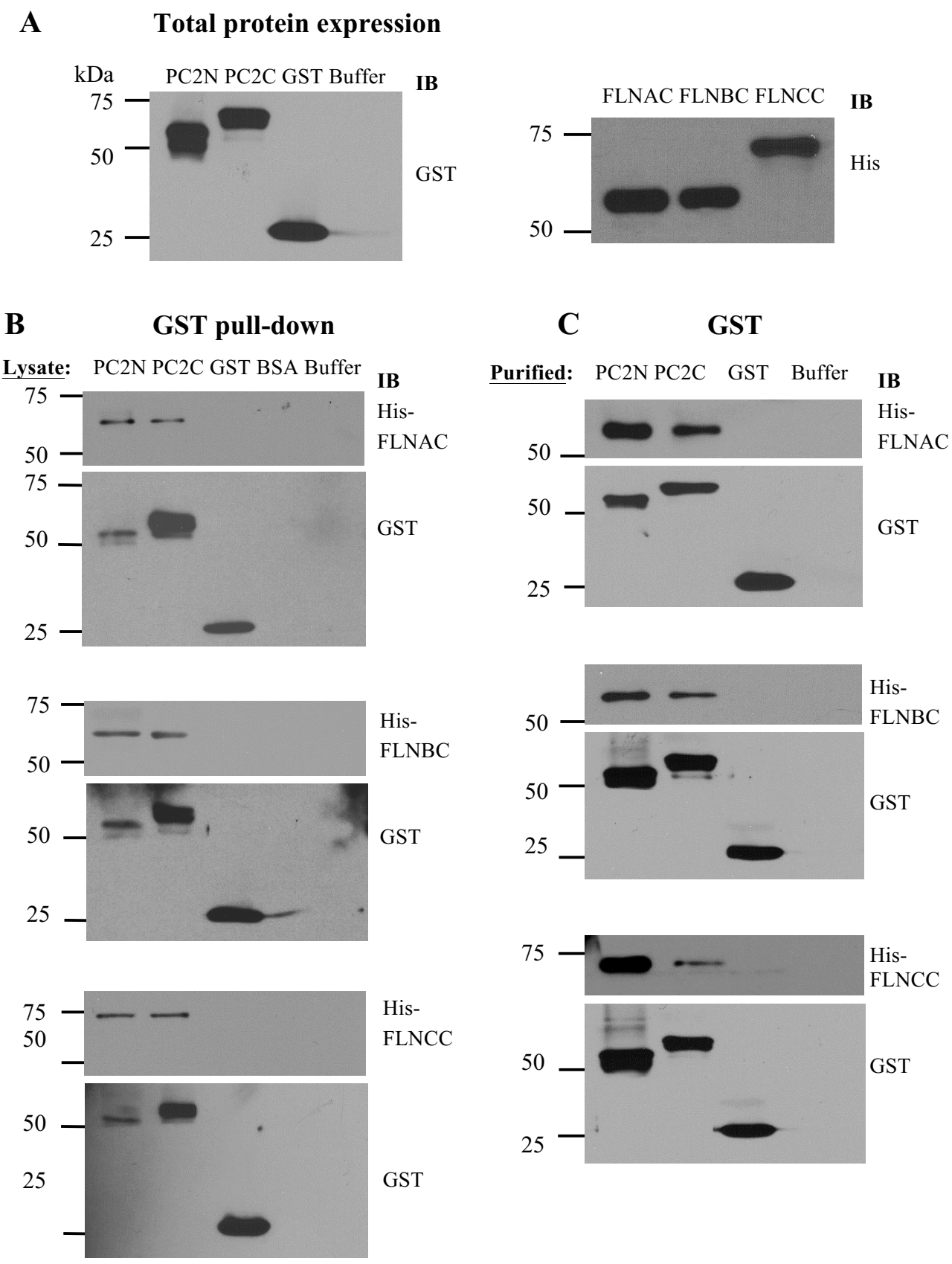
A
Total protein expression
kDa
PC2N PC2C GST Buffer
IB
75
50
25
GST
FLNAC FLNBC FLNCC
IB
75
50
His
B
GST pull-down
Lysate:
PC2N PC2C GST BSA Buffer
IB
His-FLNAC
GST
His-FLNBC
GST
His-FLNCC
GST
C
GST
Purified:
PC2N PC2C GST Buffer
IB
His-FLNAC
GST
His-FLNBC
GST
His-FLNCC
GST

Figure 2-2. Interaction between PC2 and filamins by GST pull-down. (**A**) Total expression of purified GST- or His-tagged proteins. *Left panel*, representative data obtained with an anti-GST antibody showing purified GST fusion proteins and buffer from *E. coli*. *Right panel*, IB imaging obtained with an anti-His antibody showing purified His-tagged FLNAC, FLNBC and FLNCC from *E. coli*. (**B**) *E. coli* lysates from cells expressing GST-PC2N, GST-PC2C, GST alone, BSA or binding buffer alone, were incubated with purified His-tagged FLNAC, FLNBC or FLNCC. Glutathione-agarose beads were used to pull down GST epitope binding proteins. The resultant (Bound) protein samples were immunoblotted with an anti-His antibody or an anti-GST antibody to indicate the effective GST fusion proteins participated in interaction with His-tagged proteins. (**C**) Data were obtained under similar conditions as in panel B, except that we utilized purified GST-PC2N, GST-PC2C, GST alone, or the binding buffer alone, incubated with purified His-tagged FLNAC, FLNBC or FLNCC. All data are representative of six experiments.

.

To further explore whether endogenous PC2 interacts with filamins in mammalian cells, we performed co-IP experiments using IMCD and MDCK epithelial cells. FLNA was detected in the precipitated lysates using a PC2 antibody, but not in the control immunoprecipitates using non-immune serum (Figure 2-3 A). Reciprocally, PC2 was detected in the FLNA precipitated lysates (Figure 2-3 A). The endogenous PC2-FLNA interaction was confirmed by co-IP in LLC-PK1 and HEK293 cells (Figure 2-3 B). Taken together, these results demonstrated that PC2 not only directly binds FLNA *in vitro* but also forms protein complexes with FLNA *in vivo*. Further, by over-expressing PC2N and PC2C in human melanoma A7 cells we found by co-IP that both PC2N and PC2C interact with endogenous FLNA and that the PC2N-FLNA interaction is stronger than the PC2C-FLNA interaction (Figure 2-3 C), in agreement with our results obtained from *in vitro* binding data (Figures 2-1 and 2-2).

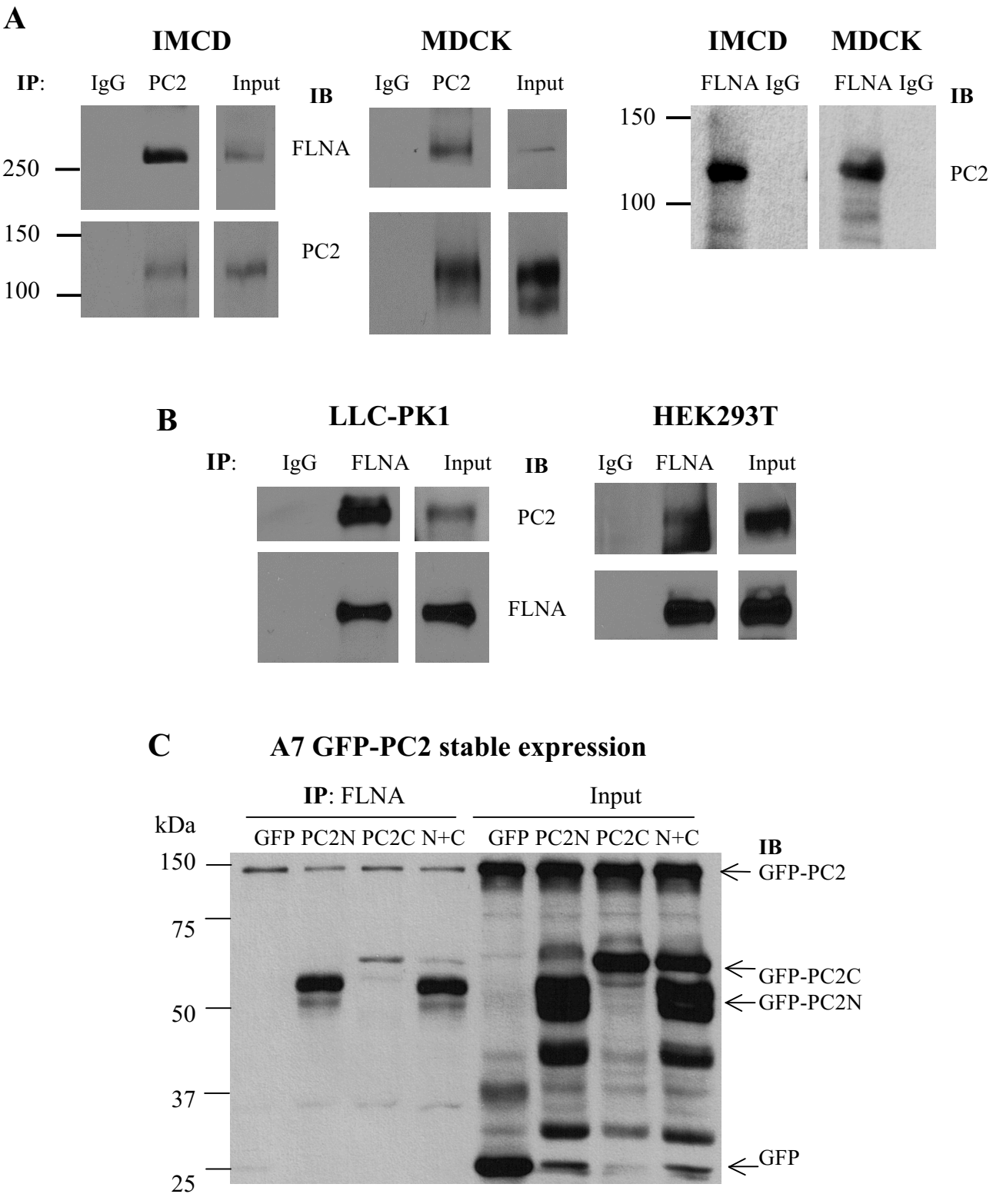
A
IMCD
MDCK
IMCD
MDCK
IP:
IgG
PC2
Input
IB
IgG
PC2
Input
FLNA IgG
FLNA IgG
IB
250
150
100
FLNA
PC2
150
100
PC2
B
LLC-PK1
HEK293T
IP:
IgG
FLNA
Input
IB
IgG
FLNA
Input
PC2
FLNA
C
A7 GFP-PC2 stable expression
IP: FLNA
Input
kDa
GFP PC2N PC2C N+C
GFP PC2N PC2C N+C
IB
150
75
50
37
25
GFP-PC2
GFP-PC2C
GFP-PC2N
GFP

Figure 2-3. Interaction between PC2 and filamin by co-IP. Data are representative of three experiments. (A) Interaction between endogenous PC2 and FLNA in IMCD and MDCK cells was determined by co-IP. Total proteins were precipitated with either anti-PC2 H-280 or non-immune rabbit IgG, and detected with the anti-FLNA antibody H-300 or anti-PC2 antibody 1A11 (Bound). Input indicates the protein expression of FLNA and PC2 (Total). Reciprocally, total proteins were precipitated with either anti-FLNA H-300 or non-immune rabbit IgG, and probed with anti-PC2 antibody 1A11. (B) Interaction between endogenous PC2 and FLNA in LLC-PK1 and HEK293 cells by co-IP. Total proteins were precipitated with either H-300 or non-immune rabbit IgG, and probed with anti-PC2 antibody 1A11 or H-300 (Bound). Input indicates the protein expression of PC2 and FLNA (Total). (C) Interaction of endogenous FLNA with over-expressed PC2 in A7 cells stably expressing GFP-PC2 and transiently expressing GFP-PC2N, GFP-PC2C, GFP-PC2N+GFP-PC2C (N+C), or GFP. After 48 hr of transient transfection, cells were collected for IP with anti-FLNA antibody (H-300) and the subsequent precipitates were subject to SDS-PAGE and immunoblotting with anti-GFP antibody B-2 to detect the signals of GFP-PC2, GFP-PC2N, GFP-PC2C and GFP.

2.4.3 Co-localization of PC2 with FLNAA and calnexin revealed by IF

We stably expressed GFP-tagged human PC2 in FLNA-deficient M2 human melanoma cells, and A7 cells genetically rescued by expression of FLNA. The subcellular distribution of both PC2 and FLNA was examined, and as expected, GFP signals were detected in both M2 and A7 cells, while FLNA was only observed in A7 cells (Figure 2-4). We found that GFP-PC2 and FLNA partially colocalized in the perinuclear region of A7 cells (Figure 2-4 A). Using an antibody against the ER membrane marker calnexin, we also found that a significant fraction of intracellular PC2 localizes to the ER (Figure 2-4 B).

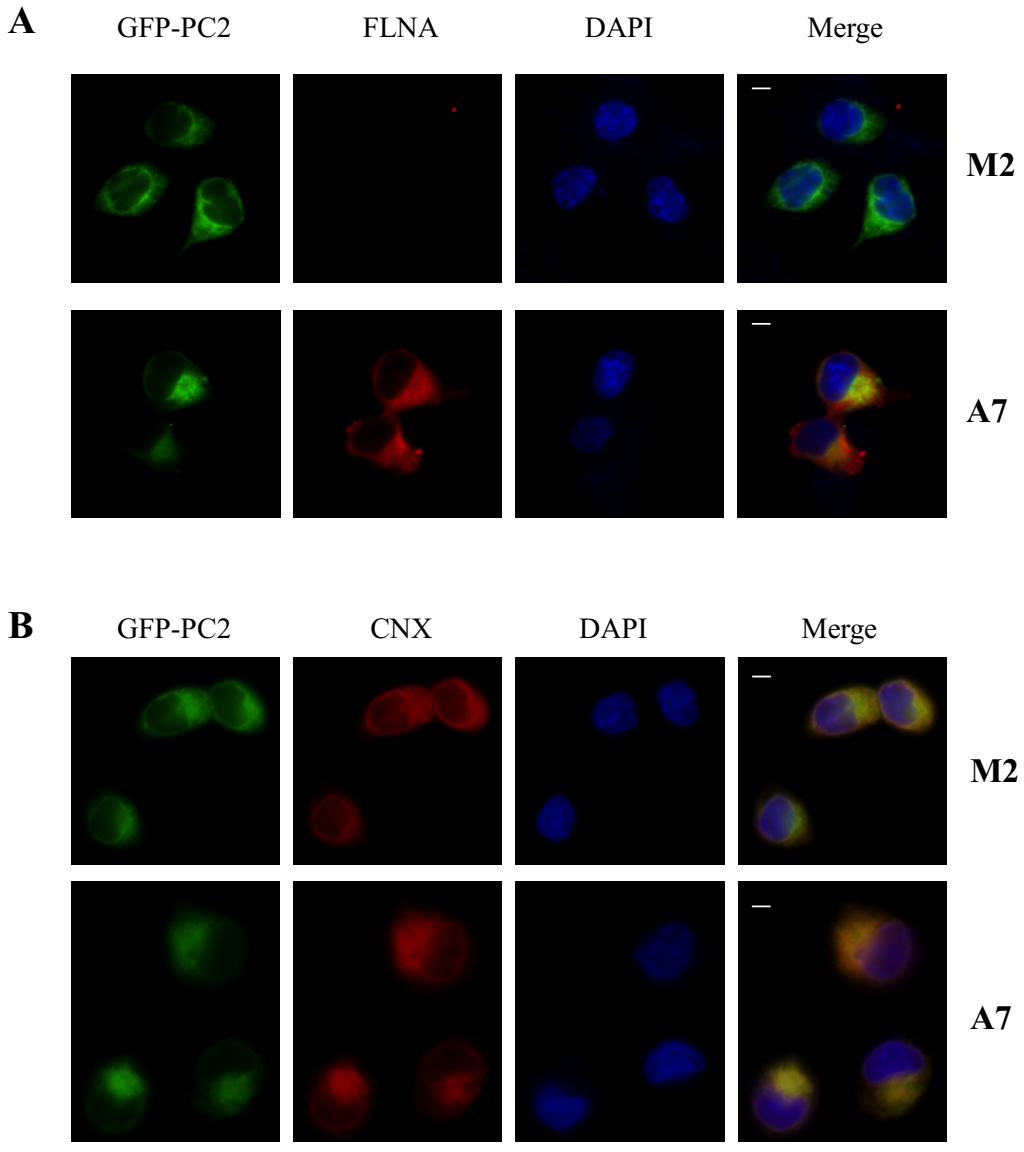

Figure 2-4. Cellular localization of PC2. M2 and A7 human melanoma cells over-expressing GFP-PC2 were grown on coverslips and incubated at 4°C overnight after fixation, with either anti-FLNA E-3 or anti-calnexin primary antibodies. The length of the white bar is 20 µm. Data are representative of three experiments. (A) Subcellular colocalization of PC2 and FLNA. (B) Subcellular co-localization of PC2 and the ER marker calnexin (CNX).

2.4.4 Effect of filamin on the channel function of PC2 in lipid bilayer system

Among the various interactions between the actin cytoskeleton and PC2, previous studies have shown that both actin-binding proteins and actin cytoskeletal dynamics control PC2 channel function. Thus, we next explored the possibility that FLNA exerts a direct effect on the cation channel activity of PC2. For this, we used either PC2 protein obtained by *in vitro* translation, which should be devoid of associated proteins, or obtained from MDCK cells stably expressing PC2 by our modified tandem affinity purification method (216) (data not shown). PC2 was reconstituted in a lipid bilayer system for electrophysiology studies. We observed that addition of commercial chicken gizzard FLNA (25 nM) to the *cis* side of the lipid bilayer chamber abolished PC2 channel activity (n = 4, Figure 2-5). In control experiments, addition of either the same saline solution containing no FLNA or denatured (boiled for 7 min) FLNA (25 nM) did not significantly affect PC2 channel activity (n = 4, data not shown), indicating the specific inhibitory effect of FLNA on PC2 channel. To provide further evidence of the inhibitory effect of filamins on PC2 channel function, we also used hST apical membrane vesicles expressing abundant endogenous PC2, as previously described (215), in a lipid bilayer reconstitution system. We observed that commercial chicken gizzard FLNA, but not the denatured one, also reduces PC2 channel activity in hST vesicles (Figure 2-6).

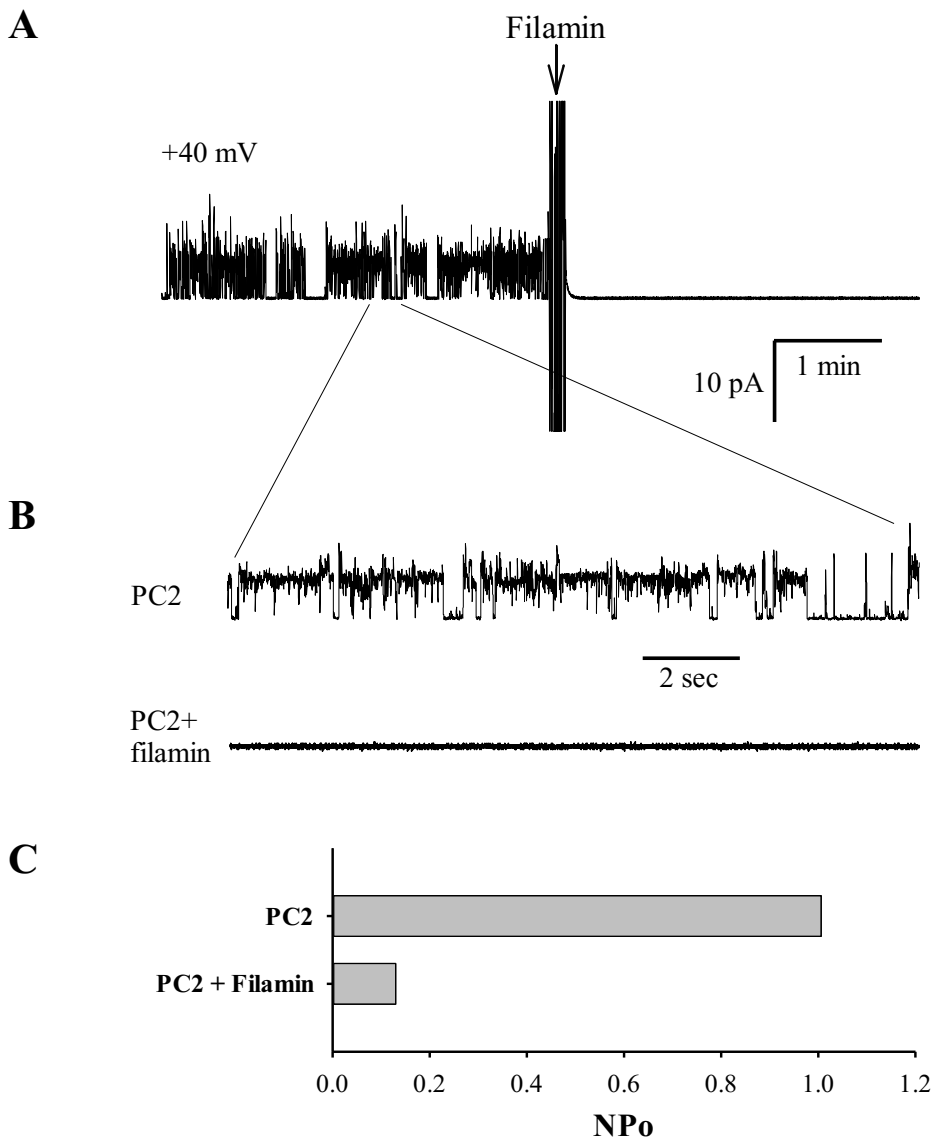

Figure 2-5. Effect of FLNA on purified PC2 channel activity in a lipid bilayer system. The PC2 protein was prepared by *in vitro* translation and reconstituted in a lipid bilayer system. (**A**) Representative tracings of reconstituted PC2 at +40 mV before and after addition of commercial chicken gizzard FLNA (25 nM), to the *cis* chamber. (**B**) Expanded tracings from panel A, recorded before and after FLNA addition (n = 3). (**C**) Averaged open probability recorded at +40 mV before and after addition of FLNA (n = 4; $p < 0.01$, by paired t-test).

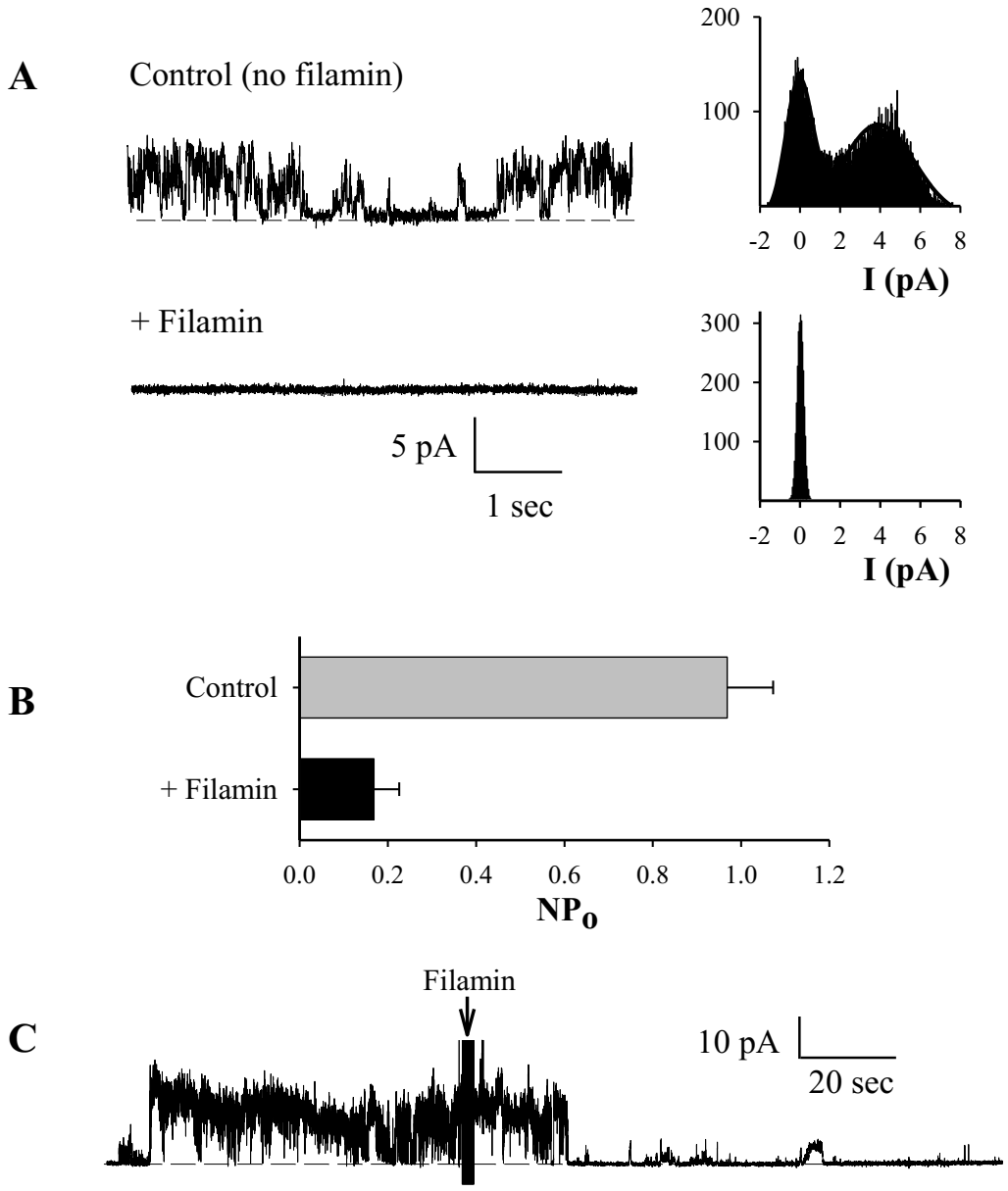

Figure 2-6. Regulation of hST PC2 channel function by FLNA. Apical hST membranes, containing endogenous PC2 were reconstituted in a lipid bilayer electrophysiology system, as in Figure 2-5. (A) Representative recordings of PC2 channel activity in the absence and presence of commercial FLNA (25 nM) added to the *cis* chamber. All-point histograms are shown on the right of each tracing, to indicate current amplitude (n = 7). (B) Averaged open probability in the presence and absence of FLNA (n = 7; $p < 0.05$). (C) Representative recording showing real-time inhibition of PC2 activity by addition of FLNA to the cis chamber (n = 7).

2.5 DISCUSSION

In this study we have demonstrated, by various protein-protein interaction methods including yeast two-hybrid screen, GST pull-down and co-IP, that PC2 physically interacts with the actin cross-linking protein filamin. We also determined by a lipid bilayer electrophysiology reconstitution system that filamin functionally interacts with, and inhibits the channel function of PC2.

PC2 has been shown to interact with a number of components of both actin-based and microtubular cytoskeleton, including Hax-1 (220), CD2-associated protein (221,222), tropomyosin-1 (219), troponin-I (46), α-actinin (45) and the kinesin-2 motor subunits KIF3A and KIF3B (44,223). Some of these interactions are not only structural, i.e., helping anchorage of the channel protein to the cytoskeletal network, but also functional, enabling the regulation of PC2 channel activity. KIF3B, e.g., was shown to mediate not only the physical interaction between PC2 and fibrocystin, the single transmembrane receptor-like protein mutated in human autosomal recessive PKD, but also the stimulation of the PC2 channel activity by fibrocystin (44). On the other hand, KIF3A only binds PC2 but not fibrocystin, and directly stimulates PC2 channel activity (223). An important interaction between the actin cytoskeleton and PC2 is observed by actin-binding proteins such as α-actinin. α -actinin not only binds PC2 but up-regulates its channel function as well. This may imply a more general regulatory mechanism in the control of ionic membrane permeability, because α-actinin also regulates the activity of a number of other ion channels, including the K^+ channel Kv1.5 (224), the L-type Ca^{2+} channel (225) and NMDA receptors through direct binding (226,227). Here we have shown that filamin, an actin cross-linking protein that helps creating and regulating actin three-dimensional gels, binds directly to PC2N and PC2C, and represses PC2 channel activity.

In this study, we employed several approaches to demonstrate structural and functional interactions between PC2 and the three isoforms of filamins. We also investigated the protein fragments of both PC2 and filamin that are involved in this interaction.

Interestingly, it was recently observed that PC2 expression inhibits stretch activated channels (SACs) activity in smooth muscle cells, while polycystin-1, a membrane receptor-like protein mutated in about 80% of ADPKD, reverses the inhibition by forming a protein complex with PC2 (228). This study, which is believed to be important for understanding myogenic regulation, also seems to have revealed a potential physical interaction between PC2 and FLNA. Sharif-Naeini *et al*. demonstrated that in the mouse VSMC line MOVAS, the actin cytoskeleton is indeed implicated in SAC inhibition by PC2, as this effect was abolished by F-actin disruption in the absence of FLNA (228). SAC non-selective channel activity was reduced in the presence of FLNA, and the inhibitory effect of PC2 expression was abolished when FLNA was absent. The study employed co-IP to show that PC2 and FLNA are in the same complex, since FLNA precipitated PC2 from COS cells over-expressing both PC2 and FLNA. It remained undetermined, however, not only as to whether the two proteins would bind each other directly, but also as to which domains were involved in the interaction and whether endogenous PC2 and FLNA would interact with each other *in vivo*. Our present study specifically answered these questions by using various *in vitro* and *in vivo* protein-protein interaction approaches (Figures 2-1, 2-2, 2-3).

Filamins directly bind, mostly via their C termini, to more than 30 protein partners with diverse functions, showing their great versatility as signalling scaffolds (202). In particular, studies have demonstrated that filamin binding is important for the synthesis, surface membrane retention, and/or degradation of partner proteins. E.g., FLNA directly binds furin to

reduce its internalization and increase its protein synthesis (170). Through physical binding, FLNA decreases the proteasomal/lysosomal degradation of the platelet glycoprotein subunit GpIbα, the G protein-coupled calcitonin receptor, and the class I IgG receptor FcγRI. FLNA increases the degradation of epidermal growth factor receptor, and possibly of prostate-specific membrane antigen PSMA (171,229-232). Finally, FLNA also stabilizes FcγRI and PSMA in the PM (170,230,232).

Although ADPKD is mainly associated with cyst formation in the kidneys and liver, ADPKD and mutations in filamins are associated with comparable manifestations in the vascular system, such as dissection, aneurysm and fragility (203-205,209,210). It is thus important to determine the contribution of the PC2-filamin interaction to these vascular abnormalities, e.g., through the use of animals with mutations in both PC2 and filamins. In summary, our data indicated that the actin cross-linking protein filamin is an interacting partner of PC2, and an important regulator of PC2 function, which may be relevant to the pathogenesis associated with mutations in either PC2 or filamins.

CHAPTER 3

RESULT #2 Filamin-A increases the stability and plasma membrane expression of polycystin-2

A version of this chapter has been published in 2015
Qian Wang, Wang Zheng, Zuocheng Wang, JungWoo Yang, Shaimaa Hussein, Jingfeng Tang and Xing-Zhen Chen. PLoS One. 2015 Apr 10;10(4):e0123018

3.1 ABSTRACT

Polycystin-2 (PC2), encoded by the *PKD2* gene, is mutated in ~15% of autosomal dominant polycystic kidney disease. Filamins are actin-binding proteins implicated in scaffolding and membrane stabilization. Here we studied the effects of filamin on PC2 stability using filamin-deficient human melanoma M2, filamin-A (FLNA)-replete A7, HEK293 and IMCD cells together with FLNA siRNA/shRNA knockdown. We found that the presence of FLNA is associated with higher total and plasma membrane PC2 protein expression. Western blotting analysis in combination with FLNA knockdown showed that FLNA in A7 cells represses PC2 degradation, prolonging the half-life from 2.3 to 4.4 hours. By co-immunoprecipitation and Far Western blotting we found that the FLNA C terminus (FLNAC) reduces the FLNA-PC2 binding and PC2 expression, presumably through competing with FLNA for binding PC2. We further found that FLNA mediates PC2 binding with actin through forming complex PC2-FLNA-actin. FLNAC acted as a blocking peptide and disrupted the link of PC2 with actin through disrupting the PC2-FLNA-actin complex. Finally, we demonstrated that the physical interaction of PC2-FLNA is Ca^{2+}-dependent. Taken together, our current study indicates that FLNA anchors PC2 to the actin cytoskeleton through complex PC2-FLNA-actin to reduce degradation and increase stability, and possibly regulate PC2 function in a Ca^{2+}-dependent manner.

3.2 INTRODUCTION

Polycystin-2 (PC2 or TRPP2) belongs to the transient receptor potential polycystin (TRPP) subfamily of TRP channels. PC2 is a 968 aa integral membrane protein with six transmembrane domains and intracellularly localized N- and C- termini. Encoded by the *PKD2* gene, PC2 is a Ca^{2+}-permeable cation channel (27) mainly located in the endoplasmic reticulum (ER) membrane (60), but is also present in the primary cilium (65,206) and plasma membrane (PM) (207). PC2 membrane targeting is regulated by several factors, such as PC1, phosphofurin acidic cluster sorting proteins and intracellular calcium release (25,40,68,233). Mutations in *PKD2* account for 10-15% of the autosomal dominant polycystic kidney disease (ADPKD) (27), a prominent inherited disorder that affects 12.5 million people worldwide. ADPKD is characterized by formation of cysts in the kidneys, and to a less extent in the liver and pancreas. At the cellular level, ADPKD is associated with elevated cell proliferation, apoptosis, and de-differentiation (234-236). Until now, the underlying mechanisms of cyst formation have remained ill defined and no effective therapy has been developed. Previously, we found that PC2 down-regulates cell proliferation via promoting PERK-dependent phosphorylation of eukaryotic initiation factor eIF2α (211). Mice with either loss- or gain-of-function of PC2 are cystogenic (15,101). Therefore, PC2 cellular level has to be regulated within a narrow range.

Filamin, the first non-muscle actin filament cross-linking protein, was identified in 1975 (201). The filamin family comprises three members, filamin-A (FLNA), -B (FLNB) and -C (FLNC) which share 60-80% sequence homology, of which FLNA is the most abundant and widely distributed (202). Filamins contain a spectrin-related domain in the N terminus that directly binds actin and is followed by 24 β-sheet repeats (169,202). The most C terminal

repeat 24 mediates formation of a homodimer of a flexible V-shaped structure that acts as 'a molecular leaf spring' to facilitate cross-linking of actin filaments (168). By cross-linking cortical actin, filamins give cells a dynamic three-dimensional structure. They also interact with a large number of proteins of great functional diversity, indicating that they are versatile scaffolding proteins. Over 90 filamin interacting partners have so far been identified, including channels, receptors, intracellular signaling molecules, and even transcription factors (180). Recently, we reported that filamins interact with the epithelial sodium channel on the surface membrane for both structural purposes and functional regulation (237). The presence of this extensive array of associated proteins may account in part for the fact that mutations in human filamin genes result in a wide range of cell and tissue anomalies, including bone anomalies, periventricular heterotopias, aortic dissection and aneurysm (203-205).

Connections between PC2 and cytoskeleton proteins have been established by several studies. Among PC2 interacting partners identified so far, half are cytoskeleton or cytoskeleton-associated proteins (213). In 2005, we found that α-actinin, an actin-binding protein important in cytoskeleton organization, cell adhesion, proliferation and migration, interacts with both the intracellular N- and C- termini of PC2 and substantially stimulated its channel function (45). PC2 channel function is modulated by dynamic changes in actin filament organization in the apical membrane of human syncytiotrophoblast, which is the most apical epithelial barrier that covers the villous tree of human placenta (26). Further studies suggested that cytoskeleton proteins are likely to mediate the regulation of PC2 channel function by physical forces such as hydrostatic and osmotic pressure in human syncytiotrophoblast (215). In mitotic spindles of dividing cells PC2 interacts and co-localizes with mDia1, a member of the RhoA GTPase-binding formin homology protein family that

participates in cytoskeletal organization (233). Recently, we demonstrated that C terminus of filamins directly bind to both the intracellular N- and C- termini of PC2, and that FLNA substantially inhibits PC2 channel activity in a lipid bilayer reconstitution system (237).

In the present study, we explored the role of FLNA in regulating PC2 stability and degradation, using mammalian cultured cells in combination with ^{35}S pulse labeling, Western blotting (WB), co-immunoprecipitation (co-IP), cell surface biotinylation, and gene over-expression/knockdown (KD). We also examined the Ca^{2+}-dependence of the PC2-FLNA binding.

3.3 MATERIALS AND METHODS

Antibodies

PC2 (H-280), GFP (B-2), FLNA (E-3), FLNA (H-300), β-actin (C4), Na^+/K^+ ATPase (H-300) and HSP60 (H-1) antibodies were purchased from Santa Cruz Biotech (Santa Cruz, Dallas, TX, USA). PC2 (1A11) mouse polyclonal antibody (44,45) and PC2 (H-280) was used to detect native PC2. Antibody E-3 against the N terminus of FLNA was used to detect full length FLNA while antibody H-300 was used to detect both the full length and C terminus of FLNA (FLNAC, aa 2150-2647). Goat anti-GFP (EU4) was purchased from Eusera (Eusera, Edmonton, AB, Canada). Secondary antibodies were purchased from GE Healthcare (Baie d'Urfe, QC, Canada).

Cell lines and transfection

M2 and A7 PC2 stable cell lines, as previously described (237), were maintained with hygromycin (100 μg/ml) (M2) or hygromycin plus G418 (300 μg/ml) (A7) (Invitrogen Canada, Burlington, ON, Canada). Full length human FLNA plasmid pcDNA3-myc-FLNA (ID 8982) was purchased from Addgene (Addgene, Cambridge, MA, USA). FLNA shRNA and the corresponding empty vector p/PUR/U6 as a negative control were generous gifts of Dr. Z. Shen (Cancer Institute of New Jersey, New Brunswick, NJ, USA). Briefly, HeLa and A7 cells were transfected with either the empty vector or FLNA shRNA using the Lipofectamine 2000 reagent (Invitrogen Canada) according to the manufacturer's instructions. After 48 hr of transfection, 5 μg/ml of puromycin (Invitrogen Canada) was added to the medium for selection of FLNA stable KD cells. FLNA siRNA pairs 5601 (5'-CCCAUGGAGUAGUGAACAATT-3' and 5'-UUGUUCACUACUCCAUGGGTG-3'),

7116 (5'-CAGAAAUUGACCAAGAUAATT-3' and 5'-UUAUCUUGGUCAAUUUCUGTG-3'), and 371 (5'-GGAAGAAGAUCCAGCAGAATT-3' and 5'UUCUGCUGGAUCUUCUUCCAC-3'), were ordered from GenePharma (GenePharma, Shanghai, China). FLNA siRNA, or control siRNA were transfected into HeLa, HEK293 and IMCD cells using HiPerFect Reagent (Qiagen, Hilden, Germany) according to the manufacturer's instructions (siRNA final concentration: 20 nM). Cells were transfected for a second time after 24 hr. The efficiency of shRNA and siRNA KD was assessed by immunoblotting (IB). Transient transfection with previously described pEGFPC2 plasmids (with GFP tag) harboring PC2, the C terminus of PC2 (PC2C, aa 682-968), the N terminus of PC2 (PC2N, aa 1-215) or His-FLNAC (237) was performed using Lipofectamine 2000 and the expression was assessed 48 hr after transfection. For IMCD and M2 cells, a second transfection was performed 24 hr after the first transfection to increase transfection efficiency. Cells were harvested 72 hr after the first transfection.

^{35}S pulse labeling

^{35}S pulse labeling assay was carried out to study the effect of FLNA on PC2 synthesis. Equal number of M2 and A7 cells either stably or transiently expressing GFP-tagged PC2 were plated in 60 mm dishes for 1 hr starvation in the pre-labeling medium L-methionine and L-cysteine free DMEM with 10% FBS and penicillin/streptomycin. This was followed by pulse-labeling with 250 μCi of [^{35}S] methionine/cysteine EXPRE^{35}S Protein Labeling Mix (PerkinElmer, Woodbridge, ON, Canada) for 30 min. Cells were harvested in ice-cold CelLyticTM-M lysis buffer (Sigma-Aldrich Canada, Oakville, ON, Canada) supplemented with protease inhibitor cocktail (Sigma-Aldrich Canada and 500 μg total protein was used for

IP with anti-GFP (EU4) and magnetic Dynabeads (Invitrogen Canada). The resulting precipitates were subject to SDS-PAGE and autoradiography.

Cell surface biotinylation

Cells were grown to 90% confluency in 100 mm dishes, washed with ice-cold PBS and borate buffer (10 mM boric acid, 154 mM NaCl, 7.2 mM KCl, and 1.8 mM $CaCl_2$, pH 9.0), and then incubated with 0.5 mg/ml Pierce EZ-LinkTM Sulfo-NHS-SS-Biotin (Fisher Scientific Canada, Toronto, ON, Canada) at 4° C with agitation for 30 min. After washing with quenching buffer (192 mM glycine, 25 mM Tris, pH 8.3), cells were lysed in ice-cold CelLyticTM-M reagent supplemented with protease inhibitor cocktail to make 2-5 μg/μl total protein lysate. The biotinylated and flow-through intracellular proteins were separated using 50 μl of Pierce Avidin Agarose (Fisher Scientific Canada, Markham, ON, Canada) by incubation overnight at 4ºC and subsequent centrifugation. After intensive washing in the NP40 buffer (50 mM Tris pH 7.5, 150 mM NaCl, and 1% NP40) with protease inhibitor cocktail, biotinylated proteins were resuspended in the SDS sample buffer and eluted from beads by heating at 65ºC for 5 min. An equal amount of biotinylated proteins and 20 μg of total and intracellular proteins were separated on 8% SDS-PAGE for IB.

Degradation analysis

Degradation assays were based on the use of protein synthesis inhibitor cycloheximide (CHX) and proteasome inhibitor MG132 (Sigma-Aldrich Canada). Equal numbers of cells were plated into 6-well plates, treated with CHX (50 μM in DMSO) or MG132 (10μM in DMSO). DMSO was used in the control treatment. For CHX treatment, cells were lysed at different time points (0, 2, 4 and 8 hr). For MG132 treatment, cells were lysed at the same time

points. Cells were harvested into samples with equal volume (equal cell number). The lysates were loaded for WB and signal density was measured by ImageJ.

Co-immunoprecipitation (co-IP)

Cells growing on 100 mm dish were harvested in 1 ml ice-cold CelLyticTM-M lysis buffer according to the manufacturer's instructions. 500 μg total proteins from postnuclear supernatant were incubated with 2 μg primary antibodies at 4ºC for 4 hr, followed by overnight incubation with gentle shaking upon the addition of 50 μl protein G sepharose (Thermo Fisher Scientific, Rockford, USA). The precipitates absorbed to protein G sepharose were resuspended in SDS sample buffer and subjected to SDS-PAGE followed by IB. For Ca^{2+} dependent co-IP experiments, 1 mM Ca^{2+} and 1 mM EGTA were added to the lysis and washing buffers.

Far Western blotting (WB)

Far WB was performed as previously described (238). Briefly, 50 μg protein lysates from M2 and A7 cells stably expressing PC2 were separated by SDS-PAGE. After transfered onto nitrocellulose membranes, proteins were denatured, renatured and incubated with *E.coli* purfied GST-PC2C with or without His-FLNAC, as previously used (237). After washing, proteins were detected with FLNA and PC2 antibody. FLNA-deficient M2 cells served as a negative control.

Data analysis

IB signals were quantified by ImageJ and data were analyzed and plotted using SigmaPlot 12 (Systat Software, San Jose, CA, USA), and expressed as mean ± SEM (*n*), where SEM

represents the standard error of the mean and *n* indicates the number of experimental repeats. Paired or unpaired *t*-test was used to compare two sets of data. Probability values (*p*) of less than 0.05 and 0.01 were considered significant (*) and very significant (**), respectively.

3.4 RESULTS

3.4.1 Effect of FLNA on the steady-state level of PC2

We recently reported that FLNA reduces PC2 channel activity through direct binding with both the N- and C- termini of PC2 (237). Here we found by WB analysis that in HeLa and HEK293 cells the endogenous PC2 expression level substantially decreases in the presence of FLNA KD by three different siRNA pairs (Figure 3-1 A). These data show a clear association between the PC2 and FLNA levels. A similar effect of FLNA KD was also observed in IMCD cells (data not shown). The use of the three effective FLNA siRNA pairs strongly indicates a specific effect of FLNA KD on PC2 expression. We next used human melanoma M2 cells deficient of filamins and FLNA-replete A7 cells for similar experiments. We found that the steady-state level of stably and transiently expressed GFP-PC2 in A7 cells is 64 ± 10% (n = 5; $p < 0.001$) and 41 ± 10% (n = 3; $p < 0.001$), respectively, more than that in M2 cells (Figure 3-1 B). These data let us think that the presence of FLNA may lead to higher PC2 protein synthesis or lower PC2 protein degradation. For this we performed ^{35}S pulse labeling in combination of co-IP with GFP antibody and magnetic Dynabeads to measure the synthesis of GFP-PC2. WB analysis did not reveal an increased GFP-PC2 protein synthesis (for 30 min) in FLNA-containing A7 cells compared with M2 cells (Figure 3-1 C), suggesting that PC2 in A7 cells may have a lower degradation rate than in M2 cells. These data together let us reason that FLNA may have inhibited cellular PC2 degradation.

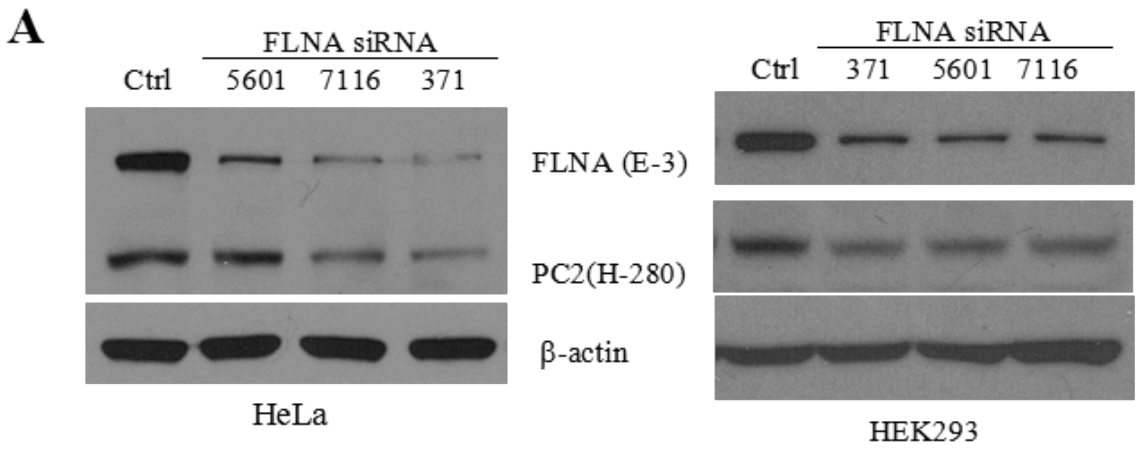
A
FLNA siRNA
Ctrl
5601
7116
371
FLNA (E-3)
PC2(H-280)
β-actin
HeLa
FLNA siRNA
Ctrl
371
5601
7116
HEK293

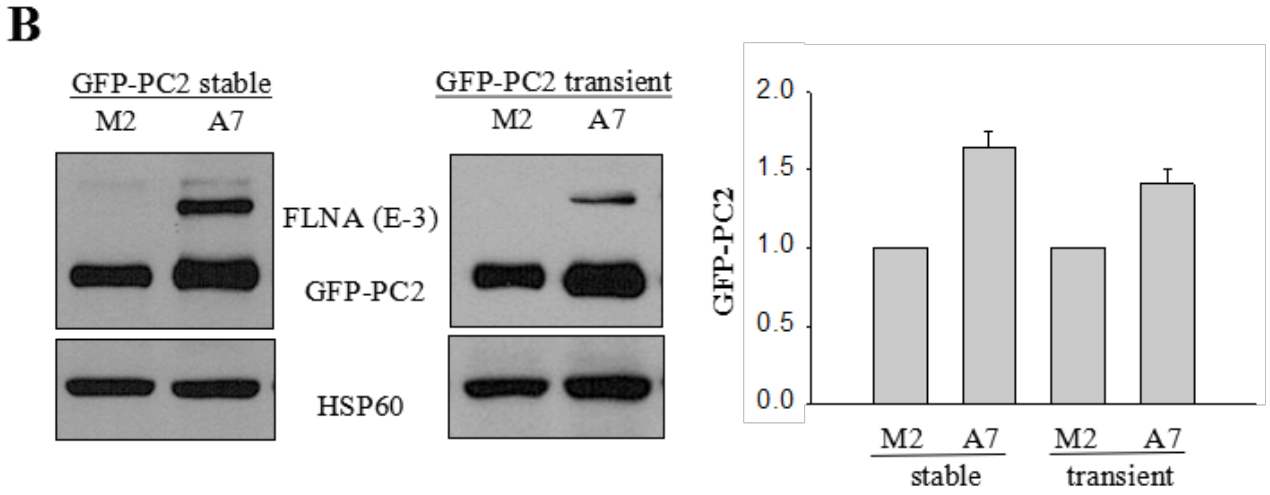
B
GFP-PC2 stable
M2
A7
GFP-PC2 transient
M2
A7
FLNA (E-3)
GFP-PC2
HSP60
GFP-PC2
2.0
1.5
1.0
0.5
0.0
M2
A7
M2
A7
stable
transient

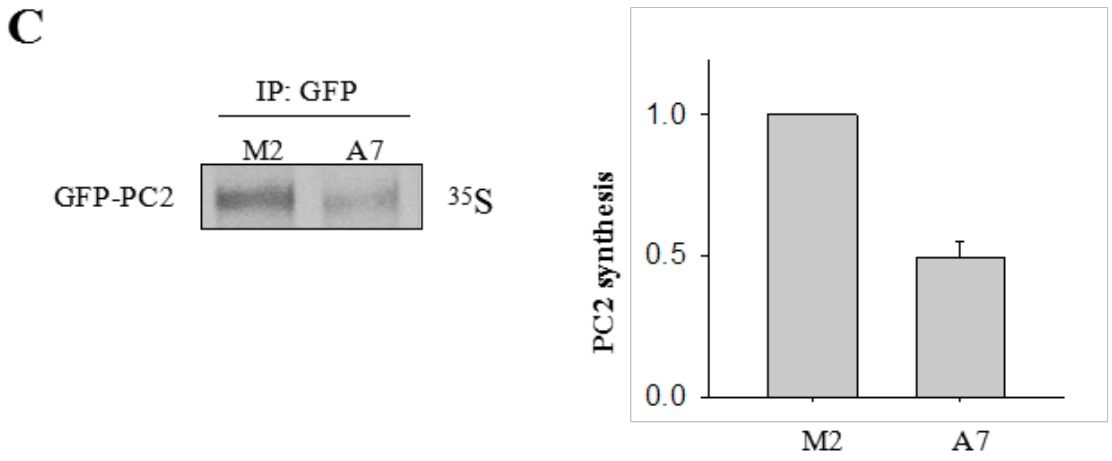
C
IP: GFP
M2
A7
GFP-PC2
35S
PC2 synthesis
1.0
0.5
0.0
M2
A7

Figure 3-1. Effects of FLNA on PC2 protein expression and PC2 synthesis. A, WB showing endogenous PC2 level in HeLa (*Left panel*) and HEK293 (*Right panel*) cells with FLNA KD by siRNA 5601, 7116 and 371, respectively. Ctrl means scramble siRNA. The numbers indicate the nucleotide positions in the *FLNA* mRNA open reading frame where the siRNA sequence starts. β-actin was used as a loading control (n = 3). B, *left panel*, data from WB showing the expression of PC2 in M2 and A7 cells stably expressing GFP-PC2. GFP (B-2) antibody was used to detect GFP-PC2. *Middle panel*, PC2 expression in M2 and A7 cells transiently expressing GFP-PC2. *Right panel*, comparison between averaged GFP-PC2 levels normalized by HSP60 in M2 and A7 cells under stable and transient expression conditions (n = 3). C, *left panel,* representative data from M2 and A7 cells showing GFP-PC2 synthesis assessed by ^{35}S pulse labeling. Anti-GFP (EU4) was used to precipitate GFP-PC2. *Right panel*, comparison between averaged GFP-PC2 syntheses in M2 and A7 cells (n = 4; p = 0.004).

3.4.2 Effect of FLNA on PC2 degradation

We next examined the effect of FLNA on degradation of GFP-PC2 in A7 and M2 stable cell lines. For this, we used CHX to stop the biosynthesis and chased the PC2 expression at different time points by WB. We found that PC2 degradation is significantly slower in FLNA-containing A7 cells than in M2 cells (Figure 3-2 A). In average, the half-life of PC2 protein in A7 cells was 4.4 $\pm$ 0.2 hr (n = 4) while that in M2 cells was only 2.3 $\pm$ 0.5 hr (n = 4). Similar results were obtained for transiently expressed GFP-PC2 in A7 cells with or without FLNA KD, i.e., FLNA KD in A7 cells speeded up PC2 degradation (Figure 3-2 B, *upper panel*). Interestingly, although both PC2C and PC2N bind filamins, we found that FLNA only reduces the degradation of PC2C (Figure 3-2 B, *middle panel*), but not PC2N (Figure 3-2 B, *lower panel*) in A7 cells. Our data together indicated that FLNA represses PC2 degradation through interaction with its C terminus. We and other researchers previously found that PC2 undergoes proteasome degradation (212,239). To determine whether FLNA affects the pathway through which PC2 is degraded, we utilized proteasome inhibitor MG-132 and found that incubation with MG-132 for 4 hr substantially blocks PC2 degradation in both A7 and M2 cells (Figure 3-2 C), demonstrating that PC2 degradation is still proteasome dependent in the absence of filamin.

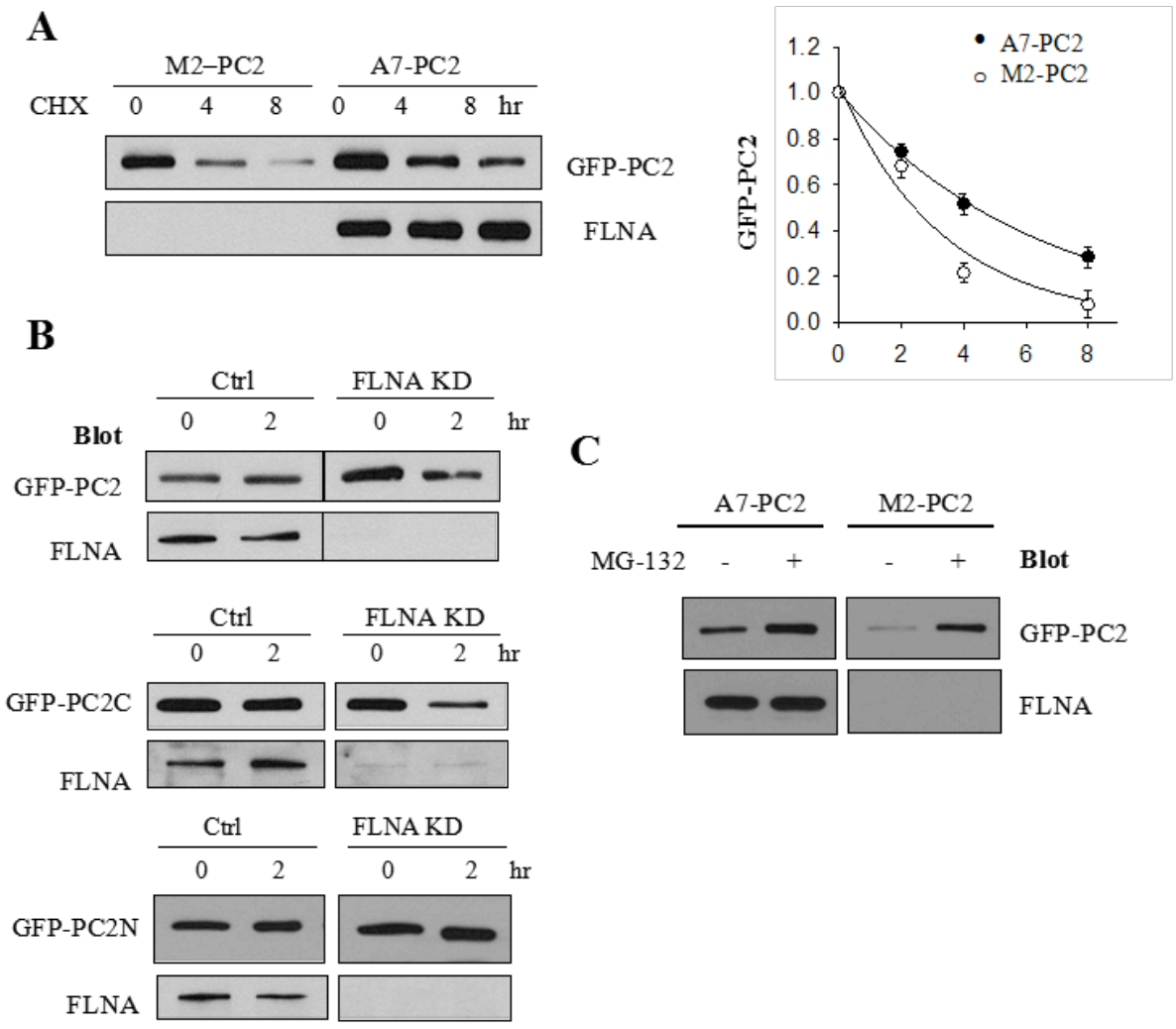

Figure 3-2. Effect of FLNA on PC2 degradation. A, *left panel*, representative data from WB showing PC2 degradation in M2 and A7 cells using CHX to block protein synthesis for various time (in hr). *Right panel*, data of PC2 degradation were normalized, averaged and fitted with exponential decay curves $Y(t) = 2^{-t/\tau}$, where τ represents the protein half-life (n = 4). B, representative data showing degradation of GFP-PC2 (*upper panel),* GFP-PC2C (*middle panel*) and GFP-PC2N (*lower panel*) transiently expressed in A7 cells with FLNA KD or control (Ctrl) (n = 3). C, representative data showing proteasome-dependent inhibition of degradation of GFP-PC2 stably expressed in A7 and M2 cells by MG-132. Cells were treated with MG-132(10 μM) or DMSO (negative control) for 4 hr before proceeding to WB with FLNA and PC2 antibodies (n = 3).

3.4.3 Effect of FLNA on the plasma membrane (PM) PC2 expression

By use of surface biotinylation, we found that more PC2 is present on the PM of A7 cells compared to M2 cells (Figure 3-3 A). In average, surface PC2 in A7 cells increased by 1.6 ± 0.5 fold ($n = 3$; $p = 0.01$) of that in M2 cells. Because the total PC2 expression in A7 cells was only increased by 0.6 fold of that in M2 cells (Figure 3-1 A), this result suggests that FLNA has a stronger stabilizing effect on PM PC2 than intracellular PC2. Interestingly, we detected much more FLNA in the biotinylated A7 cell lysate with PC2 over-expression than in control lysates (Figure 3-3B), indicating that more FLNA molecules bound with PM PC2 were pulled down under this condition. In fact, we recently reported a similar phenomenon for the scaffolding protein, receptor for activated C kinase RACK1, that interacts with surface membrane TRPP3 channel, a homolog of PC2 (240). We next examined whether M2 cells transiently transfected with wild type FLNA mimics A7 cells in terms of regulating PM PC2. By using WB and biotinylation assays, we found that PM PC2 was increased in the presence of FLNA though the signal is very weak, while the flow-through PC2 remained unaffected (Figure 3-3 C). No signals of FLNA and actin were detected from the surface protein lysate, possibly because FLNA over-expression is rather modest due to its large size and low expression efficiency.

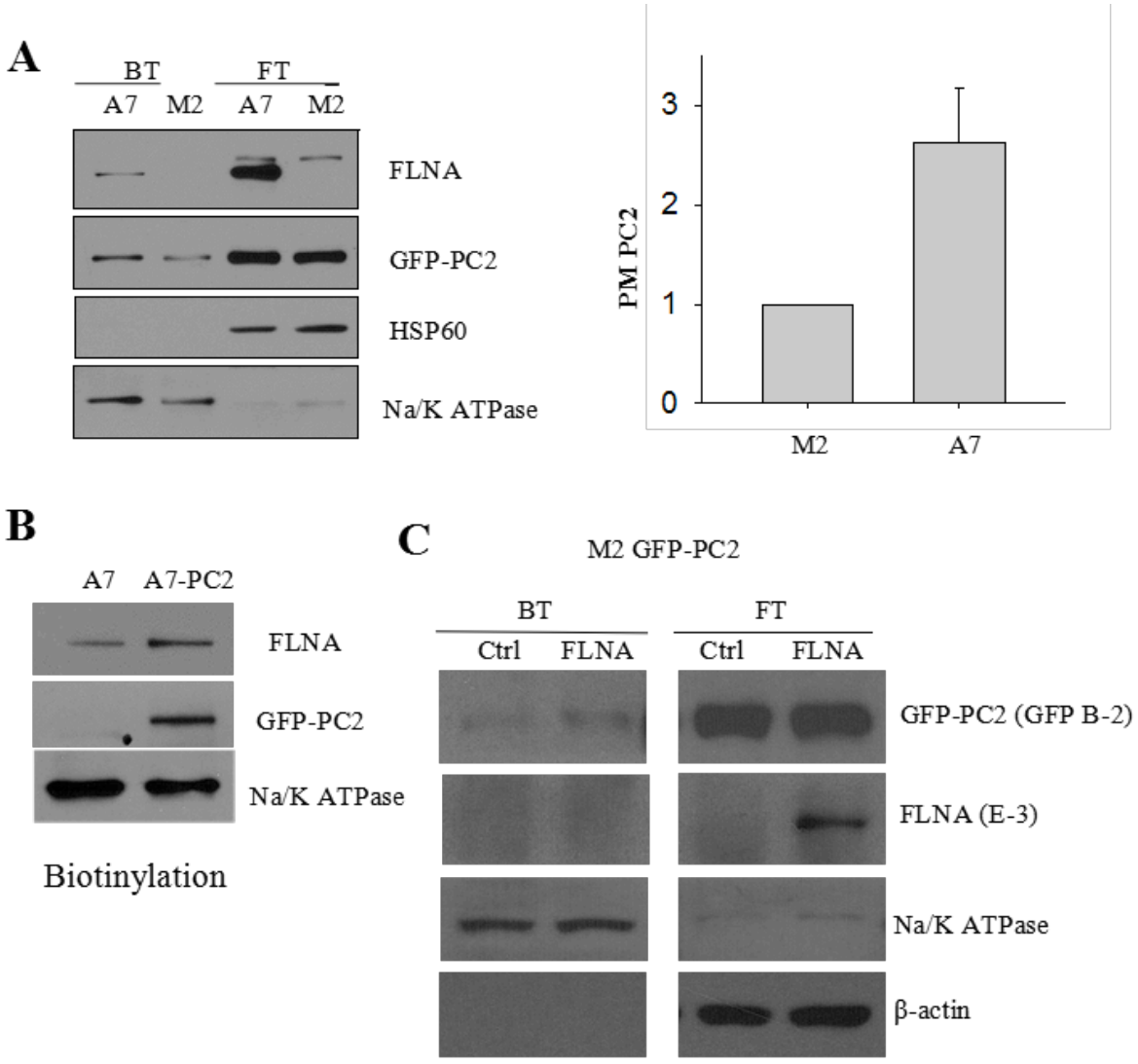

Figure 3-3. Effect of FLNA on PC2 PM expression. A, *left panel*, cell surface biotinylation to assess GFP-PC2 PM expression in A7 and M2 cells. Shown are data from biotinylated (BT) and flow-through (FT) lysates. *Right panel*, comparison between averaged GFP-PC2 surface membrane expression normalized by Na^+/K^+ ATPase in M2 and A7 cells (n = 3; p = 0.01). B, biotinylation assays using native A7 (Ctrl) and A7 PC2 stable cells to determine the effect of surface PC2 on the recruitment of FLNA to the PM (n = 3). C, biotinylation assays using M2 cells with and without transient wild type FLNA transient expression to determine the rescue effect of FLNA on M2 cells (n = 3).

3.4.4 Effects of FLNAC on the FLNA-PC2 interaction and PC2 expression

Because PC2 binds FLNA through FLNA C terminus aa 2150-2647 (FLNAC) (237), we next utilized FLNAC as a potential blocking peptide to explore how FLNA regulates surface membrane expression of PC2. For this we transiently transfected FLNAC into M2 and A7 cells stably expressing GFP-PC2 and performed co-IP with GFP antibody. The interaction of FLNAC with PC2 was detected in M2 and A7 cells, as expected (Figure 3-4 A). Overexpression of FLNAC reduces the PC2-FLNA interaction in A7 cells (Figure 3-4 B), indicating that FLNAC effectively acts as a blocking peptide. Interestingly, we also observed an interaction between FLNA and FLNAC (Figure 3-4 B), consistent with the fact that FLNA molecules form dimers through their C terminus (168), which together suggests the presence of complex nPC2-FLNA-FLNAC, where n indicates the number of PC2 molecules in the complex. To further document the role of FLNAC as a blocking peptide in the PC2-FLNA interaction, we performed Far WB assays using A7 and M2 cells. PC2C signal was detected on the membrane at the position/size of FLNA in A7, but not in M2 cell lysate after incubating with GST-PC2C protein purified from *E. coli* (Figure 3-4 C, *left panel*), indicating direct binding between PC2C and FLNA. Then, co-incubation of *E. coli* purified His-FLNAC and purified GST-PC2C reduced the PC2C signal (Figure 3-4 C, *right panel*), indicating that FLNAC competed with PC2C for binding with FLNA.

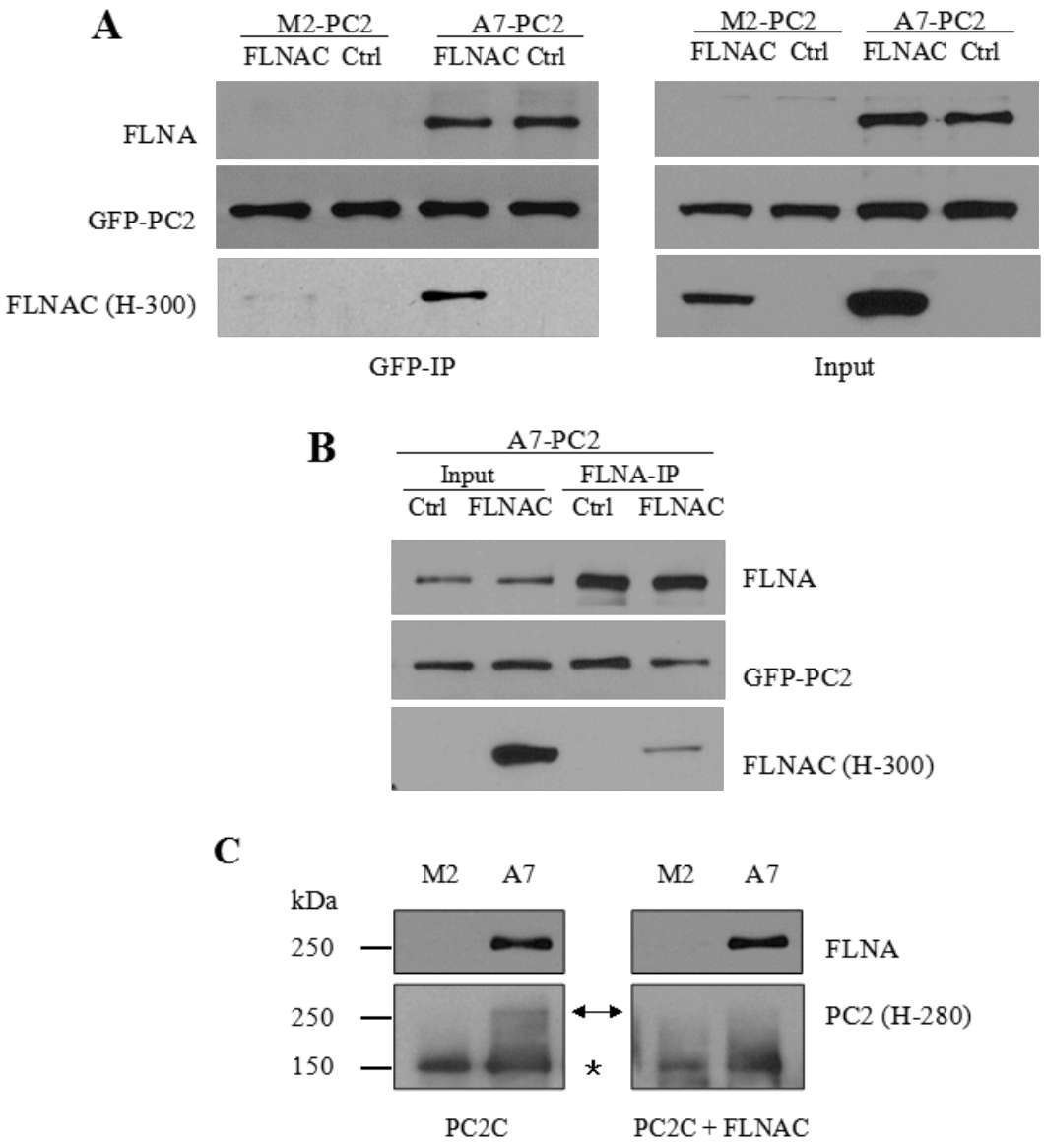

Figure 3-4. Effect of FLNAC on the FLNA-PC2 interaction. All data are from three independent experiments. A, co-IP showing the interaction of GFP-PC2 with FLNA and FLNAC in M2 and A7 cells. B, the effect of FLNAC on FLNA-PC2 interaction in A7 cells. C, Far WB showing the competition of FLNAC with PC2C for binding to FLNA. Lysates of M2 and A7 cells stably expressing GFP-PC2 were separated by SDS-PAGE and transferred to nitrocellulose membrane. Proteins were renatured and incubated with purified GST-PC2C and none (*left panel*) or His-FLNAC (*right panel*). Bound protein was detected by PC2 (H-280) antibody. The arrow (←) indicates PC2C signal detected at the site of FLNA. The star (*) indicates stably expressed GFP-PC2 signal, as a control.

We reasoned that if the binding domain of FLNA (FLNAC) is sufficient to prevent PC2 degradation, FLNAC over-expression would prolong PC2 half life in M2 cells. On the other hand, if full length FLNA is required to maintain the stability of PC2, then through disrupting the PC2-FLNA interaction FLNAC should destabilize PC2 in A7 cells but not in M2 cells. To test this hypothesis, we overexpressed FLNAC in A7 and M2 cells and measured the steady-state level of the PM and total PC2. FLNAC significantly reduced the PM level of PC2 (Figure 3-5 A and B) in A7 cells while it had no or a very modest effect on the flow-through or total PC2 (Figure 3-5 A, *right panel*, and 5C, *left panel*), and indeed had no effect on either the PM or total PC2 in M2 cells (Figure 3-5 A and C, *right panel*). Further, over-expression of FLNAC in HeLa, HEK293 and IMCD cells also resulted in a decreased endogenous PC2 level (Figure 3-5 D). These data together indicated that while full length FLNA maintains the stability of PC2, FLNAC decreases PC2 stability through interfering with the FLNA-PC2 binding.

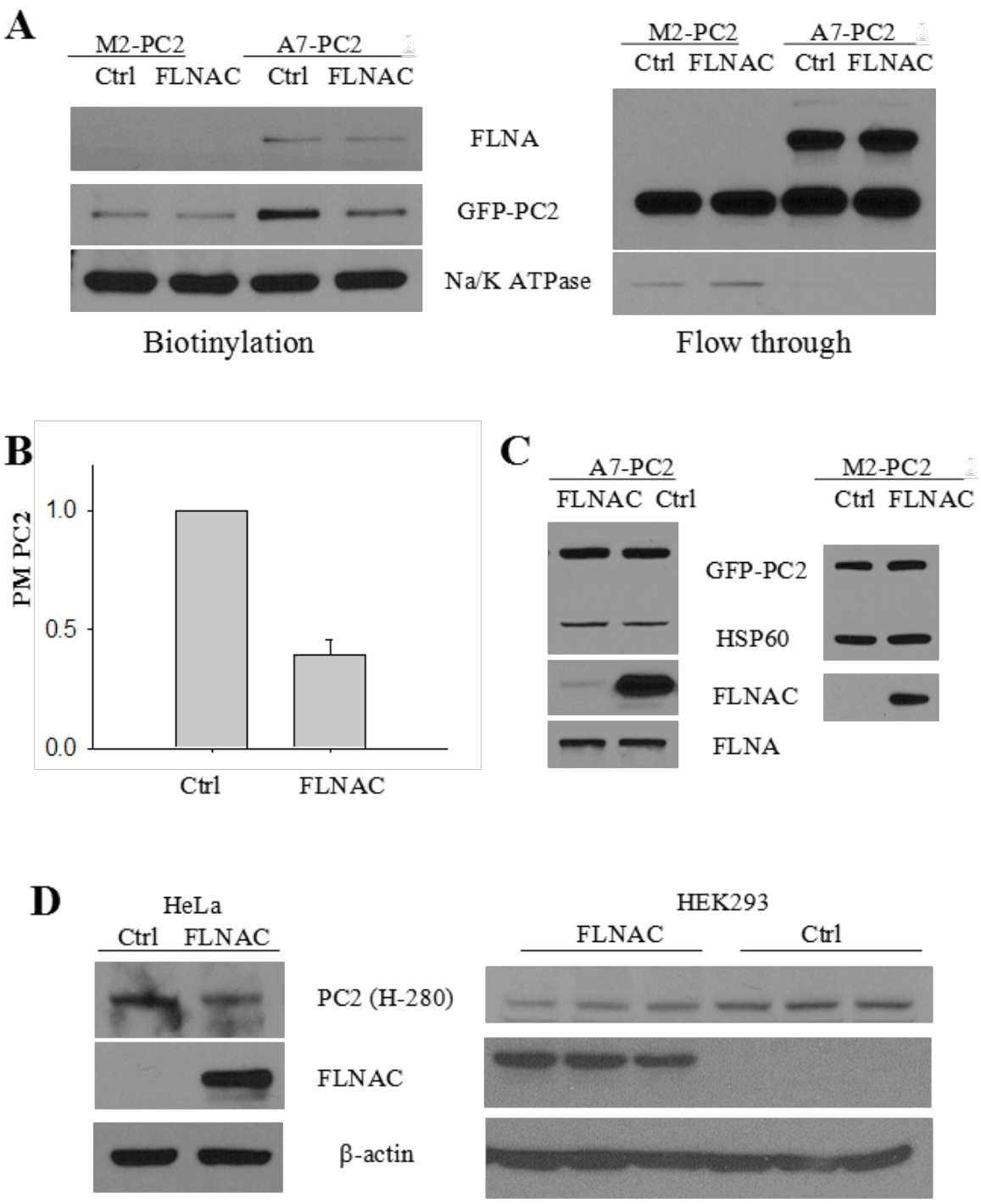
A
M2-PC2
A7-PC2
Ctrl FLNAC Ctrl FLNAC
FLNA
GFP-PC2
Na/K ATPase
Biotinylation
M2-PC2
A7-PC2
Ctrl FLNAC Ctrl FLNAC
Flow through
B
PM PC2
1.0
0.5
0.0
Ctrl
FLNAC
C
A7-PC2
FLNAC Ctrl
M2-PC2
Ctrl FLNAC
GFP-PC2
HSP60
FLNAC
FLNA
D
HeLa
Ctrl FLNAC
PC2 (H-280)
FLNAC
β-actin
HEK293
FLNAC
Ctrl

Figure 3-5. Effect of FLNAC on the surface and total PC2 expression. A, representative biotinylation data showing the effect of FLNAC on the PM (biotinylation) and intracellular (FT) GFP-PC2 expression in M2 and A7 cells. B, averaged PC2 PM expression in A7 cells showing the effect of FLNAC over-expression. FLNAC reduced PC2 PM expression to 46% ± 12% (n = 3; p < 0.001) of the control level. C, representative data showing the effect of FLNAC on the total PC2 expression in GFP-PC2 stably expressing A7 (*left panel*) (n = 3; p = 0.01) and M2 cells (*right panel*) (n = 3; p = 0.16). HSP60 was used as a loading control. D, WB data showing the effect of FLNAC on the endogenous PC2 level in HeLa (*left panel*), HEK293 (*middle panel*) and IMCD (*right pane*l) cells detect by antibody H-280. β-actin was used as a loading control (n = 3).

3.4.5 Role of the PC2-FLNA-actin complex in surface PC2 stabilization

Since FLNAC decreased the interaction of PC2 with full length FLNA and seemed to have destabilized surface PC2 in A7 cells, and FLNA is a well-known actin binding protein, we reasoned that FLNA stabilizes PC2 on the cell surface through anchoring to actin filaments. To test this, we first performed co-IP assays to prove the presence of the PC2-FLNA-actin complex. We utilized A7 GFP-PC2 stable cells, with either control (Ctrl) or FLNA KD. We found that both FLNA and β-actin were precipitated by GFP antibody (Figure 3-6A). FLNA KD dramatically decreased the binding strength of β-actin with PC2, indicating that FLNA is an important mediator for the PC2-β-actin interaction. Furthermore, similar results were obtained using endogenous PC2 in HeLa cells with or without FLNA KD, i.e., FLNA KD much reduced the interaction strength between endogenous PC2 and β-actin (Figure 3-6 B). Given the fact that FLNA binds directly with actin (241), our data together strongly show that PC2, FLNA and β-actin are in the same protein complex, presumably in the form of PC2-FLNA-actin. We also performed immunofluorescence assays with A7 and IMCD cells over-expressing GFP-PC2 to show the relative localization of PC2, FLNA and actin (Figure 3-6 C*, upper and lower panels*). The PM expression of PC2 in A7 cells was also demonstrated by its colocalization with Na^+/K^+ ATPase (Figure 3-6 C, *middle panel*).

Next, we performed biotinylation assay to check the PC2-FLNA-β-actin complex on the cell surface. We found that in A7 cells, a larger proportion of PC2 is expressed on the cell surface compared to M2 cells (Figure 3-5 A). And correspondingly, more β-actin was detected in the biotinylation lysate of A7 cells than M2 cells (Figure 3-6 D), presumably due to the presence of FLNA in A7 cells. However, in M2 cells, PC2 was also able to bind β-actin at a lower strength, possibly through other interacting partners (Figure 3-6 D). These data suggest

that FLNA tethers the PM PC2 to the actin network to prevent rapid internalization as seen in M2 cells. Interestingly, FLNAC overexpression in A7 cells substantially reduced the PM localized PC2-FLNA-β-actin complex (Figures 3-5 A and 3-6 D), presumably because the competition between FLNAC and FLNA for binding PC2 resulted in destabilization of the complex. Thus, because FLNAC does not bind with actin (241), our data indicate that, by reducing the PC2-FLNA interaction, FLNAC prevents PC2 from anchoring to the actin filament, thereby destabilizing PM PC2 and decreasing its PM expression. In summary, these data demonstrate that FLNA stabilizes PC2 on the PM by forming PC2-FLNA-actin complex to anchor it to the actin filament.

The stabilizing effect of actin may also contribute to a higher amount of FLNAC detected in the PM PC2 precipitate in A7 cells than in M2 cells (Figure 3-6 D). As filamin mainly exists as dimers in cells, complex nPC2-FLNAC-FLNAC would be present in M2 cells. However, as this complex is unable to bind to actin due to the absence of the actin-binding domain localized on the FLNA N terminus, it should be less stable than complex nPC2-FLNA-FLNAC in A7 cells that is able to bind to actin. Further, the fact that both the PM PC2 and total FLNAC levels in A7 cells are much higher than those in M2 cells (Figures 3-3 A and 3-4 A) should be another contributing factor for a higher amount of FLNAC bound to the PM PC2 in A7 cells.

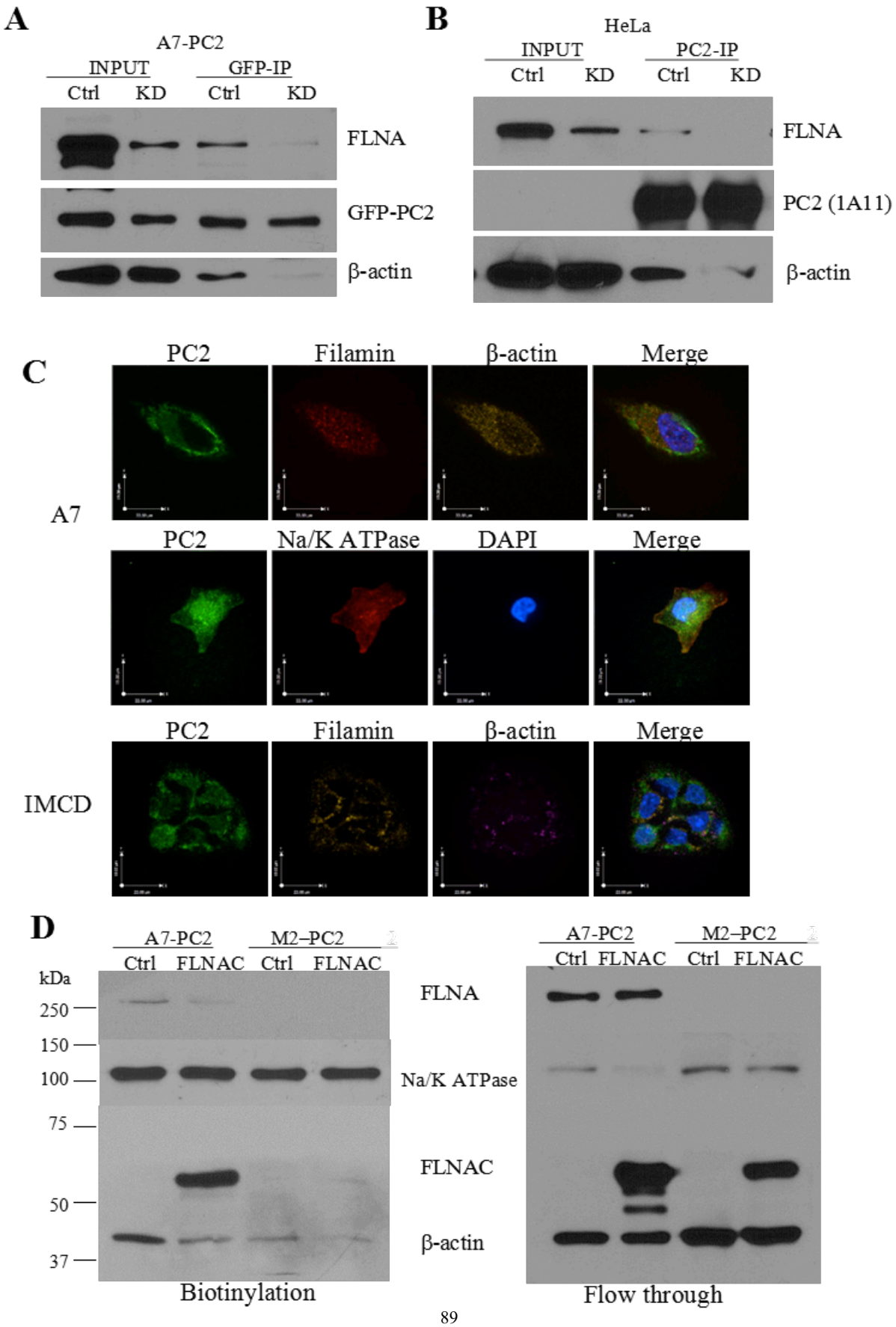
A
A7-PC2
INPUT
GFP-IP
Ctrl
KD
Ctrl
KD
FLNA
GFP-PC2
β-actin
B
HeLa
INPUT
PC2-IP
Ctrl
KD
Ctrl
KD
FLNA
PC2 (1A11)
β-actin
C
PC2
Filamin
β-actin
Merge
A7
PC2
Na/K ATPase
DAPI
Merge
PC2
Filamin
β-actin
Merge
IMCD
D
A7-PC2
M2–PC2
Ctrl
FLNAC
Ctrl
FLNAC
kDa
250
150
100
75
50
37
FLNA
Na/K ATPase
FLNAC
β-actin
Biotinylation
A7-PC2
M2–PC2
Ctrl
FLNAC
Ctrl
FLNAC
Flow through

Figure 3-6. Role of FLNA in, and effect of FLNAC on, the interaction of PC2 with actin. A, effect of FLNA KD on the PC2-actin interaction revealed by co-IP with anti-GFP (EU4) antibody in A7 PC2 stable cells. B, effect of FLNA KD on the PC2-actin interaction revealed by co-IP with PC2 (H-280) antibody in HeLa cells. C, localization of PC2, FLNA and actin in A7 (*upper panel*) and IMCD *(lower panel)* cells, and co-localization of PC2 and Na^+/K^+ ATPase in A7 cells were determined by IF assay. GFP-PC2 is stably expressed in A7 and IMCD cell lines. Primary antibodies against FLNA (H-300), β-actin (C-4), and Na^+/K^+ ATPase (H-300) were used. Rabbit Cy3- and mouse Cy5-conjugated secondary antibodies were used to detect FLNA (or Na^+/K^+ ATPase) and actin, respectively. Images were acquired using AIVI spinning disc confocal microscopy with x60 objective. D, effect of FLNAC on the FLNA-mediated PC2-actin interaction using A7 and M2 cells revealed by biotinylation assays that showed recruitment of actin to the PM.

3.4.6 Roles of Ca^{2+} on the physical interaction of PC2 and FLNA

While our current study showed a stabilizer effect of FLNA on PC2 protein expression, we previously reported that FLNA inhibits PC2 cation channel activity that shows high permeability to Ca^{2+} (237). We reasoned that their physical binding should be for the purpose of (channel) functional regulation. Thus, it is possible that the FLNA-PC2 binding is to regulate the Ca^{2+} entry through PC2. If this is the case, their binding may be Ca^{2+}-dependent. For this we performed co-IP assays between FLNA and PC2 using HeLa cells and added a final concentration of 1 mM EGTA (to chelate Ca^{2+}), 1 mM Ca^{2+}, or none to the lysates. Indeed, we found that Ca^{2+} chelation by EGTA substantially decreases the FLNA-PC2 binding (Figure 3-7 A), indicating a strong Ca^{2+}-dependent binding between the two proteins. No significant effect was observed for addition of 1 mM Ca^{2+}, presumably because the Ca^{2+} concentration in the cell lysate is already saturated for the binding between PC2 and FLNA that normally should face only submicromolar cytoplasmic Ca^{2+} in living cells. Similar Ca^{2+} dependence of the PC2-FLNA binding was observed in HEK293 and IMCD cells, but not in the presence of FLNA KD by siRNA (Figure 3-7 B and C). This Ca^{2+}-dependent PC2-FLNA interaction is possibly for the purpose of functional regulation of PC2 by FLNA in response to Ca^{2+}, that increased intracellular Ca^{2+} promotes the binding of FLNA with PC2 and regulates PC2 conducted ion permeability.

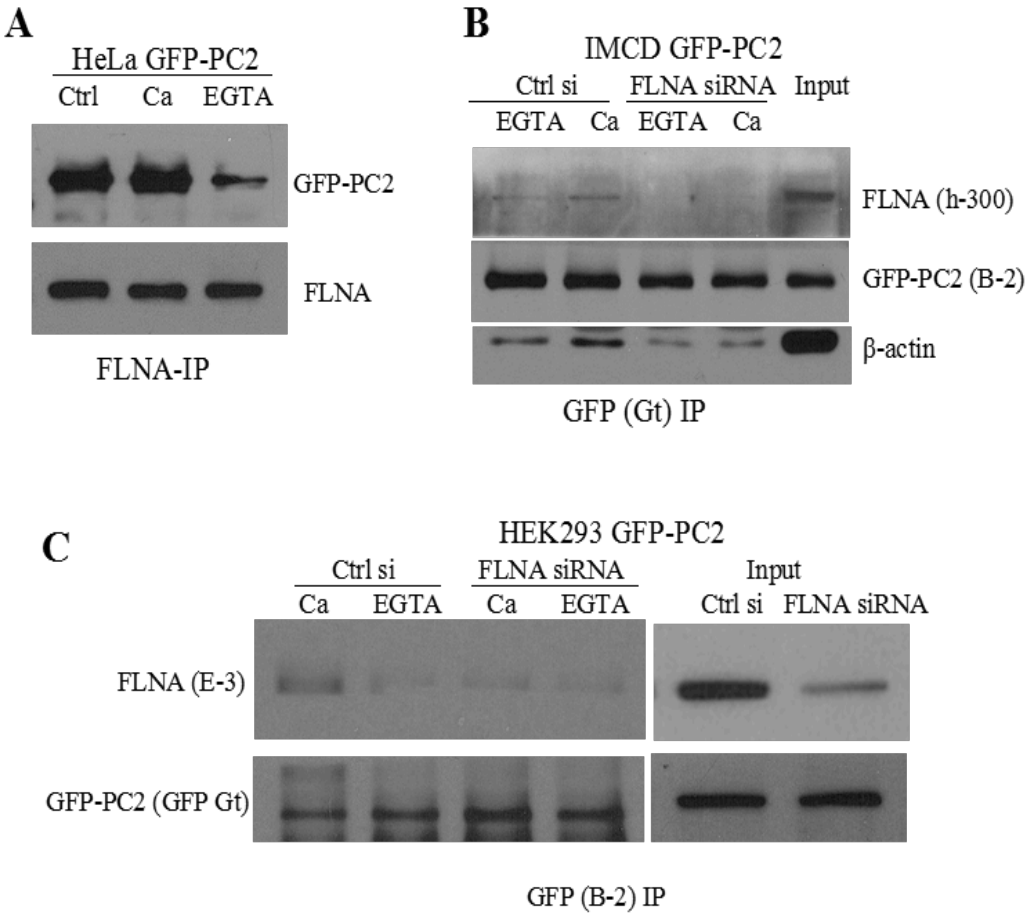

Figure 3-7. **Ca^{2+} dependence of the physical interaction between PC2 and FLNA.** A, co-IP experiments showing Ca-dependent binding between FLNA and PC2 in HeLa cells. HeLa cell lysate with GFP-PC2 transient overexpression was equally split into three samples and added with none (Ctrl), 1 mM Ca^{2+} or 1 mM EGTA (all final concentrations). FLNA (E-3) and GFP (EU4) antibodies were used for IP and IB detection, respectively. B and C, co-IP experiments showing the effect of Ca^{2+} on the FLNA-PC2 binding in GFP-PC2 stably expressing IMCD (B) and HEK293 (C) cells with and without FLNA KD.(n = 3)

3.5 DISCUSSION

Because too much or too little of PC2 is pathogenic (15,101), understanding how PC2 is regulated by cellular factors is of great importance. Recently we reported protein-protein interaction between filamin and polycystin-2 (PC2), through which filamin inhibited PC2 channel function (237). In the current study we have demonstrated how FLNA regulates the stability and surface membrane expression of PC2 protein in human cultured cells, and how FLNA interacts with PC2 in a Ca^{2+}-dependent manner. In particular, we have found that FLNA stabilizes PC2 on the cell surface by forming a protein triplex PC2-FLNA-actin, and the physical interaction of PC2-FLNA are Ca^{2+}-dependent.

Filamins are well known structural proteins that act as actin organizers, membrane stabilizers and scaffolds (242). It was reported that FLNA stabilizes the surface membrane localization and/or inhibit degradation of several target proteins such as the Ca^{2+}-sensing receptor, calcitonin receptor, chloride channel CFTR, ENaC, dopamine receptor, inwardly rectifying potassium channel Kir2.1, and pacemaker channel HCN (229,242-247). For example, FLNA interacts with Ca^{2+}-sensing receptors in M2 and HEK293 cells to increase its PM and cellular levels by preventing degradation (247). FLNA inhibits the degradation of calcitonin receptor and is critical in maintaining its normal recycling from endosomes to the surface membrane in HEK293 cells (229). FLNA also stabilizes the PM localization of dopamine D2 receptors and potassium channel Kir2.1 but has no effect on the total expression of the receptors (244,245). Further, FLNA is critical for podosome stabilization for macrophage mesenchymal migration (248). FLNC may also play important roles in protein stabilization and degradation as mutations in FLNC can cause myofibrillar myopathy characterized by disintegration of myofibrils, massive formation of protein aggregates, and altered degradation pathways within skeletal muscle fibers (249). Thus, our current study allows adding PC2 as a

novel regulation target of FLNA, in terms of PM localization and protein degradation. On the other hand, in view of similar effects of FLNA on PC2 and other membrane proteins listed above, our finding that protein complex PC2-FLNA-actin is critical for PC2 stability and prevention of degradation suggests that the 'membrane protein-FLNA-actin' link may be a general way by which many membrane proteins are anchored to actin filaments and stabilized.

It has been reported that filamin links several membrane proteins to the actin cytoskeleton, such as dopamine receptors, platelet glycoprotein Ibα, β-integrin and FcγRI (230,244,250,251), but there has never been direct and firm demonstration as to how filamin mediates the link. In fact, most evidence came from co-IP assays showing interactions between pairs of two proteins among membrane protein, filamin and actin. However, showing interactions between all three possible pairs does not guarantee the existence of a membrane protein-filamin-actin triplex. Because of this, we carried out co-IP assays between PC2 and actin by altering the level of FLNA in A7 and HeLa cells via FLNA shRNA, and found that FLNA is critical in the complexing between PC2 and actin (Figure 3-6 A and B), which demonstrated the presence of a protein triplex in the form of PC2-FLNA-actin. This was further supported by increased recruitment of actin molecules to the surface membrane when FLNA is present and is not interfered by blocking peptide FLNAC (Figure 3-6 D).

Several studies indicated that the protein level of PC2 is critical for cell function and needs to be strictly regulated within a narrow range. Immunohistochemistry studies using staged mouse embryos indicated that PC2 expression is developmentally regulated and that this regulation is important for embryo development (72). In adult mice, PC2 was also reported to be markedly up regulated by renal ischaemic injury (252-254), indicating the importance of PC2 for the recovery from ischaemia. Studies of PC2-dependent ADPKD in mouse model also

showed that both PC2 knockout and knockin mice develop typical renal cysts and an increase in cell proliferation and apoptosis, which are reflective of human ADPKD phenotypes (15,101). However, mechanisms of how PC2 protein level is regulated are still not well understood. Generally, the steady-state protein level is defined by both synthesis and degradation. Although some transcription factors such as E2F, EGRF and SP1 were predicted by computational analyses to bind with the *PKD2* promoter, little experimental data on *PKD2* transcriptional regulation have been published (255). On the translation level, it was reported that microRNA miR-17 down regulates PC2 by binding with its 3' untranslated region (256) and that this binding site is also recognized by the RNA-binding cystic protein bicaudal C, which antagonizes the repressive activity of miR-17 (99). Previously, we reported that PC2 is regulated by endoplasmic reticulum associated degradation (ERAD) through the ubiquitin-proteasome system by interacting with Herp, an ubiquitin-like protein implicated in regulation of ERAD (212). Our current study revealed a novel mechanism by which a membrane protein can be stabilized, namely through forming protein complex PC2-FLNA-actin for anchorage to the actin filaments.

We also examined whether FLNA affects the mRNA level of *PKD2* in HeLa, HEK293, A7 and M2 cells by reverse transcript (RT)-PCR and real-time RT-PCR, and found that the *PKD2* mRNA level (the mRNA of β-actin as an internal control) is much lower in the presence of FLNA, e.g., the mRNA level in A7 cells represented only 41 ± 5% ($n = 5$; $p < 0.001$) of that in M2 cells, which roughly accounted for the observed lower synthesis (Figure 3-1 C). The mechanism of how FLNA regulates the mRNA level of *PKD2* remained to be determined by future studies. However, it was previously reported that cytoplasmic FLNA through binding with transcription factors such as PEBP2/CBF and p73α regulates the transcription of several

genes including interlukin-3, T cell receptors, and cell cycle inhibitor p21 Waf1/Cip1 (174,175,257). Therefore, it is possible that *PKD2* gene is a downstream target of a FLNA-regulated transcription factor.

In summary, our present study found that FLNA is an important regulator of PC2 that it prevents PC2 degradation and stabilizes surface membrane PC2 through forming protein triplex PC2-FLNA-actin for anchoring to the cytoskeleton. This mechanism of stabilization may be important for cystogenesis of ADPKD. However, ADPKD renal cysts arise from different nephron segments (proximal and distal tubules) with different characteristics (258) which can't be modeled by cultured cell lines. This should be considered when interpreting the data obtained in the present study. Our finding of PC2 stabilized by filamin and actin may also be applicable to other membrane proteins of which the stability and degradation are similarly regulated by filamin. On the other hand, FLNA binds PC2 and inhibits its channel function through direct binding (237), and the PC2-FLNA binding was found to be Ca^{2+}-dependent (Figure 3-7). With regard to what is the net effect of FLNA, we think that when the cytoplasmic Ca^{2+} concentration is high, FLNA through direct binding shuts down PC2-mediated Ca^{2+} entry (from the extracellular space or ER) to avoid Ca^{2+} overloading; Conversely, when Ca^{2+} is low, FLNA dissociates from PC2 thereby removing the inhibition to allow Ca^{2+} entry via PC2. Because the intracellular Ca^{2+} concentration would frequently change in time and space filamins may still be able to maintain PC2 stability on the membrane while accomplishing its Ca^{2+}-dependent binding with and functional regulation of PC2.

CHAPTER 4

RESULT #3 Dynamic regulation and the net effect of filamin on polycysin-2 channel activity

In this part, the Ca^{2+} imaging experiments are in collaboration with Dr. Richard Zimmermann from Saarland University in Germany.

4.1 INTRODUCTION

Polycystin-2 (PC2), also called TRPP2 (transient receptor potential polycystin-2), is a 968 aa integral membrane protein and functions as a cation channel permeable to Ca^{2+}, Na^{+} and K^{+} (26). PC2 is widely distributed in various tissues and cell types, though the subcellular localization is somewhat controversial and seems to be cell-type and organelle dependent. PC2 contains an ER retention domain at its intracellular C terminus (60), which traps a large population of PC2 in the ER membrane.

ER is the main intracellular Ca^{2+} store and plays significant roles in maintaining cellular Ca^{2+} homeostasis. The ER contains three types of Ca^{2+}-handling proteins: sarco- and endoplasmic-reticulum Ca^{2+}-ATPase (SERCA) allowing active Ca^{2+} uptake, Ca^{2+}-binding proteins allowing the storage of significant amounts of Ca^{2+} in the lumen, and Ca^{2+} channels allowing the release/leak of Ca^{2+} into the cytosol. Inositol 1,4,5-trisphosphate receptor (IP3R) and rynodine receptor (RyR) are two well-known Ca^{2+} channels responsible for a controlled release of Ca^{2+} in response to stimuli (259). In addition to this, it was found since 1993 that ER displays an inherent 'basal' Ca^{2+} leak which can be unmasked by the inhibition of Ca^{2+} pumps SERCA by either ATP depletion or inhibitor thapsigargin (Tg) (260,261). The leakage was found to be unrelated to SERCA, IP3R or RyR (262-265). Several possible Ca^{2+} leak channel candidates have been proposed, including Bcl-2 (266), presenilins (267), translocon (Sec 61 complex) (265) and PC2 (67). PC2 is characterized as a Ca^{2+} permeable cation channel mainly localized on the ER, but it is still controversial as to whether PC2 exhibits basal Ca^{2+} leakage or requires an increase in intracellular Ca^{2+} to confer permeability of Ca^{2+} from the ER, known as Ca^{2+} activiated Ca^{2+} release channel (59,66,67).

In Chapter 2, we reported that filamin inhibits the channel function of PC2 in the presence of high Ca^{2+} through direct interaction. In Chapter 3, we found that filamin increases the stability of PC2 by anchoring it to the actin filaments. With further discovery that the physical binding of PC2-FLNA is Ca^{2+}-dependent, we proposed that filamin may efficiently control PC2 mediated Ca^{2+} permeability through a dynamic regulation of PC2 channel activity. In this chapter, we further tested the dynamic regulation (with and without Ca^{2+}) of filamin on PC2 in the lipid bilayer system, and used GST pull-down to investigate the Ca^{2+} dependent binding of FLNA with PC2N-/C- fragments. In addition, we employed live cell Ca^{2+} imaging technique to explore the function of PC2, and the net effect of filamin on PC2 channel activity in intact cells.

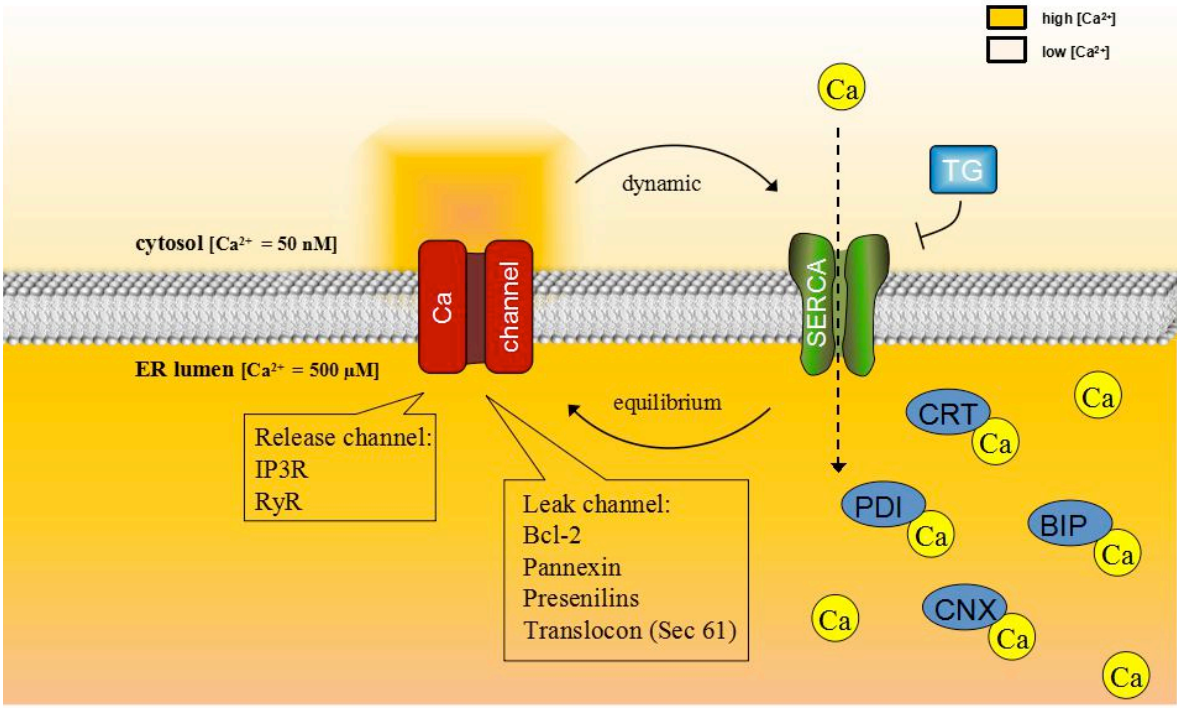

Figure 4-1. Schematic overview of the major regulators in ER Ca^{2+} homeostasis.

1. SERCA, sarco (endo) plasmic reticulum Ca^{2+} ATPase, allowing active Ca^{2+} uptake;

2. Ca^{2+} binding proteins (CRT, PDI, BIP, CNX) allowing the storage of significant amounts of Ca^{2+} in the ER lumen. CRT, calreticulin. CNX, calnexin;

3. Ca^{2+} channels allowing release of Ca^{2+} into the cytosol. IP3R and RyR are two well-known Ca^{2+} release channels. Several Ca^{2+} leak channels have been proposed as shown. IP3R, inositol trisphosphate receptor; RyR, rynodine receptor. Tg, thapsigargin, inreversible SERCA inhibitor to unmask passive Ca^{2+} leakage from the ER.

4.2 MATERIALS AND METHODS

Lipid bilayer electrophysiology

The experimental procedure is as described in Chapter 2.3 MATERIALS AND METHODS protein preparation and lipid bilayer electrophysiology. PC2-containing human syncytiotrophoblast (hST) apical membrane was reconstituted in the lipid bilayer. The *cis* (intracellular) chamber was bathed with a solution containing 150 mM KCl and 10 mM HEPES at pH 7.4. The *trans* side contained a similar solution with 15 mM KCl to create a KCl chemical gradient. 'Ca^{2+} free condition' was obtained by adding 1 mM EGTA. 10 μM 'Ca^{2+} containing condition' was obtained by adding 1 mM EGTA and 1.004 mM Ca^{2+} (http://web.stanford.edu/~cpatton/webmaxcS.htm). Commercial filamin (FLNA) was added to the *cis* chamber to a final concentration of 25 nM. PC2 from hST was identified by a large conductance K^+-conducting channel in the presence of a KCl chemical gradient, which was inhibited by *trans* (extracellular) amiloride (100 mM) and *cis* (cytoplasmic) anti-PC2 antibody, properties that also ensured identification of its orientation in the reconstituted membrane.

GST pull-down

The experimental procedure is as described in Chapter 2.3 MATERIALS AND METHODS GST pull-down. The binding buffer contains 150 mM NaCl, 50 mM Tris, pH 7.5 with 1.0 mM EGTA (Ca^{2+} free) or 1.0 mM $CaCl_2$ (Ca^{2+} containing). The washing buffer contains 140 mM NaCl, 10 mM Na_2HPO_4, 1.8 mM KH_2PO_4, pH 7.5 with 1.0 mM EGTA (Ca^{2+} free) or 1.0 mM $CaCl_2$ (Ca^{2+} containing).

Cell culture and gene silencing/overexpression

HeLa, HEK293, and MCD cells (ATCC no. CCL-2) were cultivated at 37°C in DMEM with 10% FBS and 1% penicillin/streptomycin in a humidified environment with 5% CO2. For live cell Ca^{2+} imaging, cells were grown on cover slips pre-treated with poly-L-lysine (1 mg/ml) for 1 hr. For gene silencing, cells were transfected with targeting siRNA or control scramble siRNA (with a final concentration of 20 nM) using HiPerFect Reagent (Qiagen) according to the manufacturer's instructions. PC2 siRNA pairs are 1477 (5'-GGAAAUUCGCAUUCACAAATT-3' and 5'-UUUGUGAAUGCGAAUUUCCAA-3') 1565 (5'-GGAAUUAACAUAUACAGAATT-3' and 5'-UUCUGUAUAUGUUAAUUCCTA-3') and 1888 (5'-AGAGUGUAUCUUCACUCAATT-3' and 5'-UUGAGUGAAGAUACACUCUTG-3'). FLNA siRNA pairs are 5601 (5'-CCCAUGGAGUAGUGAACAATT-3' and 5'-UUGUUCACUACUCCAUGGGTG-3'). After 24 hr, medium was changed and cells were transfected for a second time. Overexpression was conducted after 48 hr with Fugene HD (Promega). Silencing and overexpression efficiencies were evaluated by WB analysis.

Live cell Ca^{2+} imaging

Live cell Ca^{2+} imaging was carried out as described by Lang *et al* (268). Briefly, cells were loaded with ratio-metric dye Fura-2 AM and imaging of cytosolic Ca^{2+} was carried out in Ca^{2+}-free buffer. Fura-2 signals were recorded as the changes of the F340/F380 ratio before and after the addition of Tg or Ca^{2+} ionophore ionomycin, with F340 and F380 corresponding to the background-subtracted fluorescence intensity at 340 and 380 nm, respectively. Cytosolic Ca^{2+} concentration in HeLa cells was estimated from ratio measurements using an established calibration method (269). Data were analyzed using Excel 2007.

4.3 RESULTS

4.3.1 Roles of Ca^{2+} on the physical and functional interaction of PC2 and FLNA

In Chapter 2, we reported that filamin reduces PC2 channel activity (in the presence of Ca^{2+}) in the lipid bilayer system through direct binding with both the N- and C- termini of PC2. In Chapter 3, we found a Ca^{2+}-dependent physical binding of PC2-FLNA. Here we further checked the binding of PC2 N-/C- fragments with FLNA under different Ca^{2+} conditions. GST pull-down revealed that both PC2N and PC2C bind FLNA in a Ca^{2+}-dependent manner. However the two termini of PC2 respond to Ca^{2+} differently, i.e., presence of Ca^{2+} enhances the binding of FLNA with PC2N, but weakens the binding with PC2C (Figure 4-2 A), suggesting different roles of the two PC2 fragmentsin responding to Ca^{2+} regulation. In addition, in order to check if the Ca^{2+}-dependent PC2-FLNA binding is for the purpose of channel functional regulation, we performed further lipid bilayer electrophysiology and showed that filamin inhibits hST PC2 channel activity only in the presence of 10 μM Ca^{2+} (Figure 4-2 B). Recently it was reported that 10 μM Ca^{2+} was without effect in regulating the channel activity of *in vitro* translated PC2 (270), suggesting that the Ca^{2+}-dependent inhibitory effect of PC2 is filamin dependent. These data together suggest a dynamic regulation of PC2 mediated Ca^{2+} flux by filamin, namely, increased intracellular Ca^{2+} concentration promotes the binding of filamin to PC2 to reduce Ca^{2+} flux from the channel to avoid further intracellular Ca^{2+} increase.

A

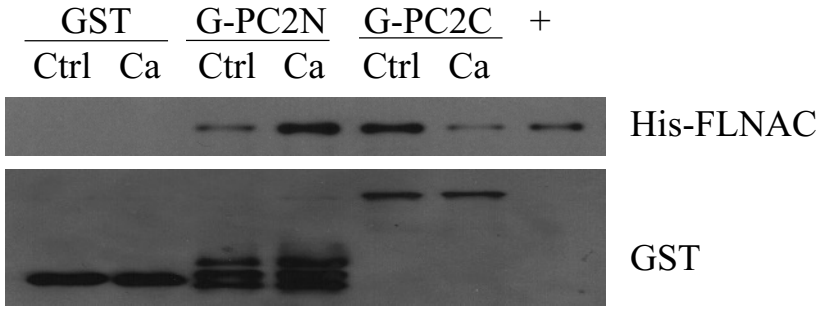
GST
G-PC2N
G-PC2C
+
Ctrl
Ca
Ctrl
Ca
Ctrl
Ca
His-FLNAC
GST

B

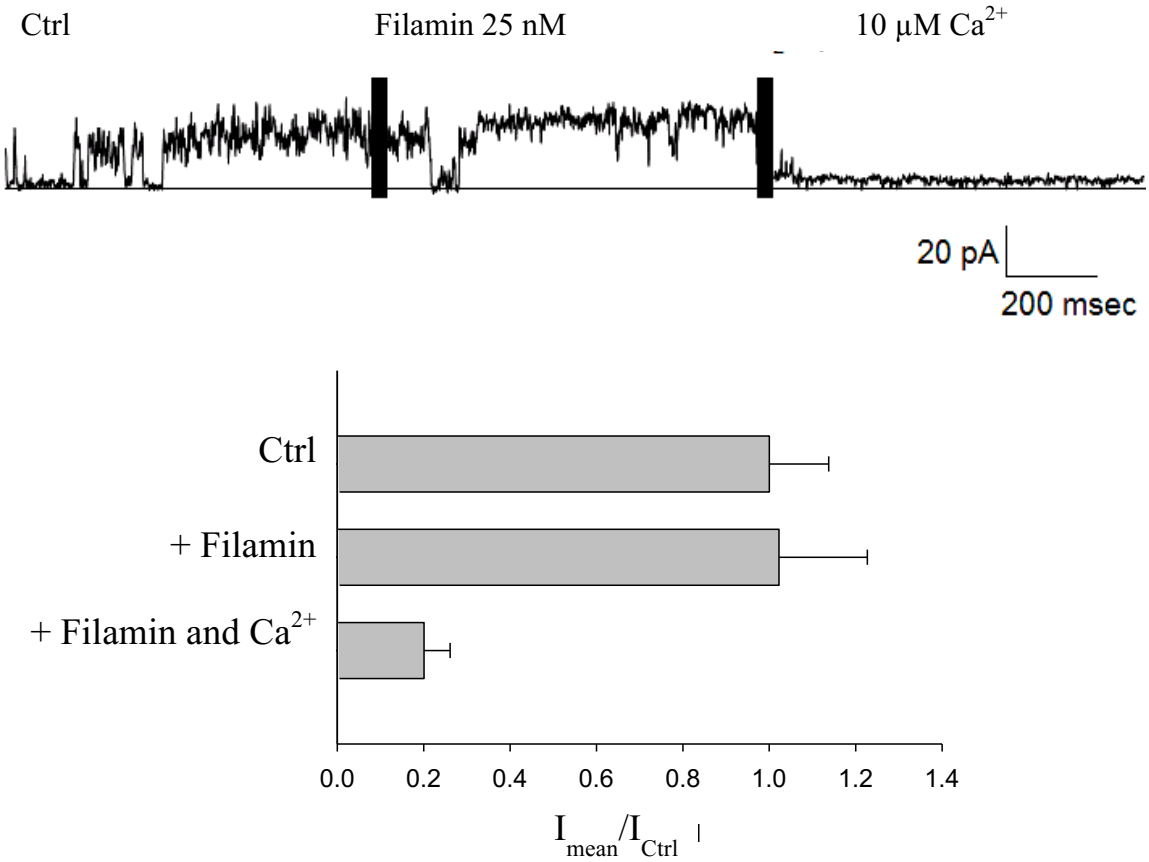
Ctrl
Filamin 25 nM
10 µM Ca2+
20 pA
200 msec
Ctrl
+ Filamin
+ Filamin and Ca2+
0.0
0.2
0.4
0.6
0.8
1.0
1.2
1.4
Imean/ICtrl

Figure 4-2. Ca^{2+} dependent physical binding and functional regulation of PC2-FLNA. A, GST pull-down with purified GST, GST-PC2N, GST-PC2C and His-FLNAC protein under the condition of none (Ctrl) and 1 mM Ca^{2+} (final concentrations). + lane a is positive control loaded with purified His-FLNAC protein (n = 3). B, *upper panel,* representative recordings at +40 mV showing hST PC2 channel activity in the absence and presence of 10 μM Ca^{2+} and commercial filamin (25 nM) added to the *cis* chamber. *Lower panel*, averaged mean current recorded at +40 mV after addition of filamin and Ca^{2+}, normalized by control current (n = 4). Experiments were conducted by Dr. Horacio Cantiello from Universidad de Buenos Aires, Argentina.

4.3.2 Effect of PC2 silencing on ER Ca^{2+} leakage and ER Ca^{2+} content in intact cells

In order to check the function of ER localized PC2 in intact cells, we performed live cell Ca^{2+} imaging experiment with PC2 silencing or overexpression. Using the Ca^{2+} indicator Fura-2 in the absence of extracellular Ca^{2+} enables the measuring of ER Ca^{2+} leakage in response to the irreversible SERCA inhibitor thapsigargin (Tg), and the ER luminal total Ca^{2+} content in response to the Ca^{2+} ionophere ionomycin, through visualization increased cytosolic Ca^{2+} concentration in intact cells. HeLa cells were treated with three different PC2 siRNA pairs for 72 hr and subjected to Ca^{2+} imaging experiments. In contract with the control siRNA, PC2 siRNA silencing significantly increases the Tg-induced ER Ca^{2+} leakage (Figure 4-3 A) as well the steady-state ER total Ca^{2+} (Figure 4-3 B). WB analysis showed that the silencing efficiency is more than 85% off (Figure 4-3 A *lower panel*). HeLa cells with PC2 transient overexpression showed no significant difference in Tg-induced ER Ca^{2+} leakage and ER total Ca^{2+} content compared to the empty vector control (data not shown). These contrast with Wegierski's report in which both the ER Ca^{2+} leakage and ER Ca^{2+} content decreased with PC2 stably expressed in HeLa cells (67). Thus, this controversy is possibly due to low efficiency of transient overexpression.

In order to confirm the specificity of siRNA silencing, we performed a rescue experiment by silencing endogenous PC2 with siRNA targeting to its 3' untranslated region (UTR), and express cDNA containing the coding sequence of PC2 (Figure 4-4 A). We observed a rescue of PC2 silencing phenotype in the form of restoration of the basal Ca^{2+} leakage and the ER luminal Ca^{2+} content (Figure 4-4 B and C).

In summary, PC2 silencing stimulates Tg-induced ER Ca^{2+} leakage. However, as the ER luminal Ca^{2+} content, which serves as a driving force of the leakage, also increased by PC2

silencing, it is hard to direct assess the function of PC2 in terms of its contribution to Ca^{2+} leakage. However, given the steady-state level of ER Ca^{2+} is increased, there must be a process of ER Ca^{2+} accumulation after PC2 level decreases, suggesting that PC2 may function as a ER Ca^{2+} leak channel.

A Ca^{2+} leak assessed by Tg-induced cytosolic Ca^{2+} increase

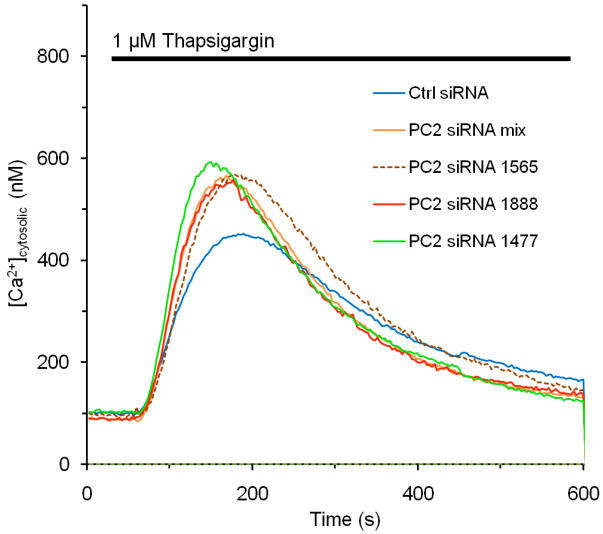

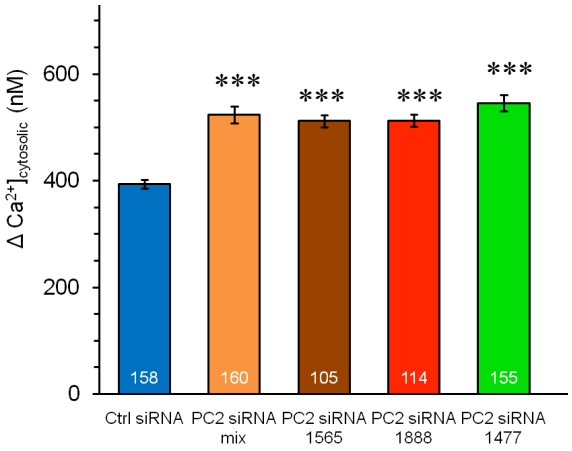

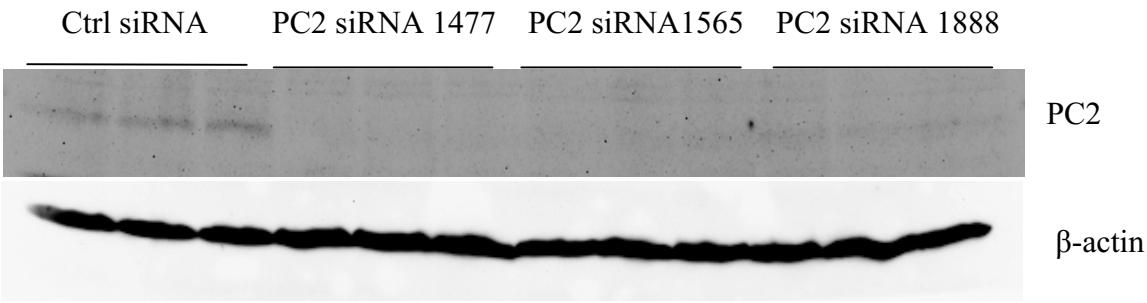

B ER Ca^{2+} content assessed by ionomycin-induced depletion

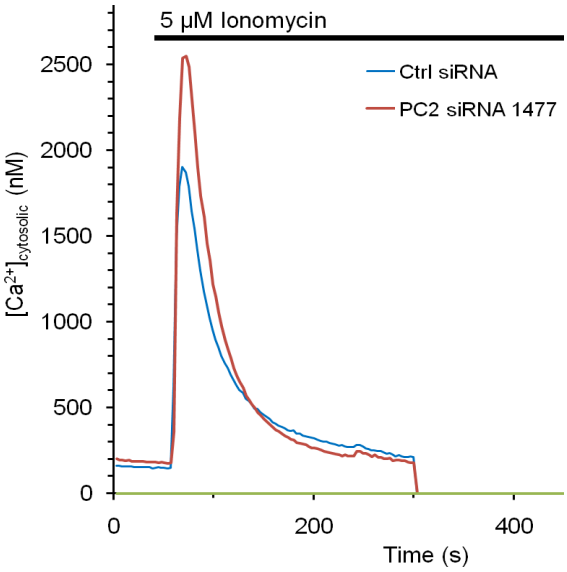

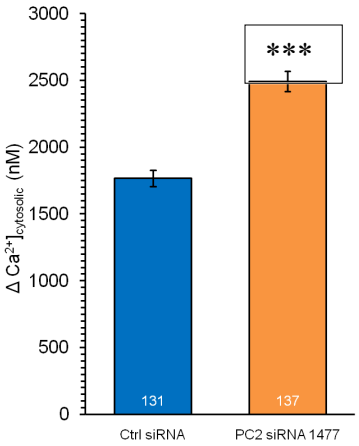

Figure 4-3. **Effect of PC2 silencing by siRNA on Tg-induced ER Ca^{2+} leakage and ER luminal Ca^{2+} content.** HeLa cells were transfected with PC2 siRNA for 72 hr and Ca^{2+} imaging experiments were performed with Fura-2 AM cytosolic Ca^{2+} dye in a Ca^{2+}-free EGTA buffer. Fluorescence was measured by 340/380 ratio and converted to Ca^{2+} concentration after calibration. A, *left panel*, Tg-induced changes in cytosolic Ca^{2+} was measured to assess ER Ca^{2+} leak. *Right panel*, statistical analysis of the changes in the cytosolic Ca^{2+} concentration after addition of Tg. *Lower panel*, WB analysis of PC2 siRNA silencing efficiency. B, *left panel,* ER total Ca^{2+} was assessed by measuring cytosolic Ca^{2+} change following ionomycin (5 μM) treatment to deplete ER Ca^{2+}. *Right panel*, statistical analysis of the changes in the cytosolic Ca^{2+} concentration after addition of ionomycin. Experiments are from 3 independent batches of cells and 9 measurements with analyzed cell numbers indicated. The error bars represent the standard error of the mean (SEM). Triple asterisk (***) indicate a *p* value of <0.001 from unpaired t-test.

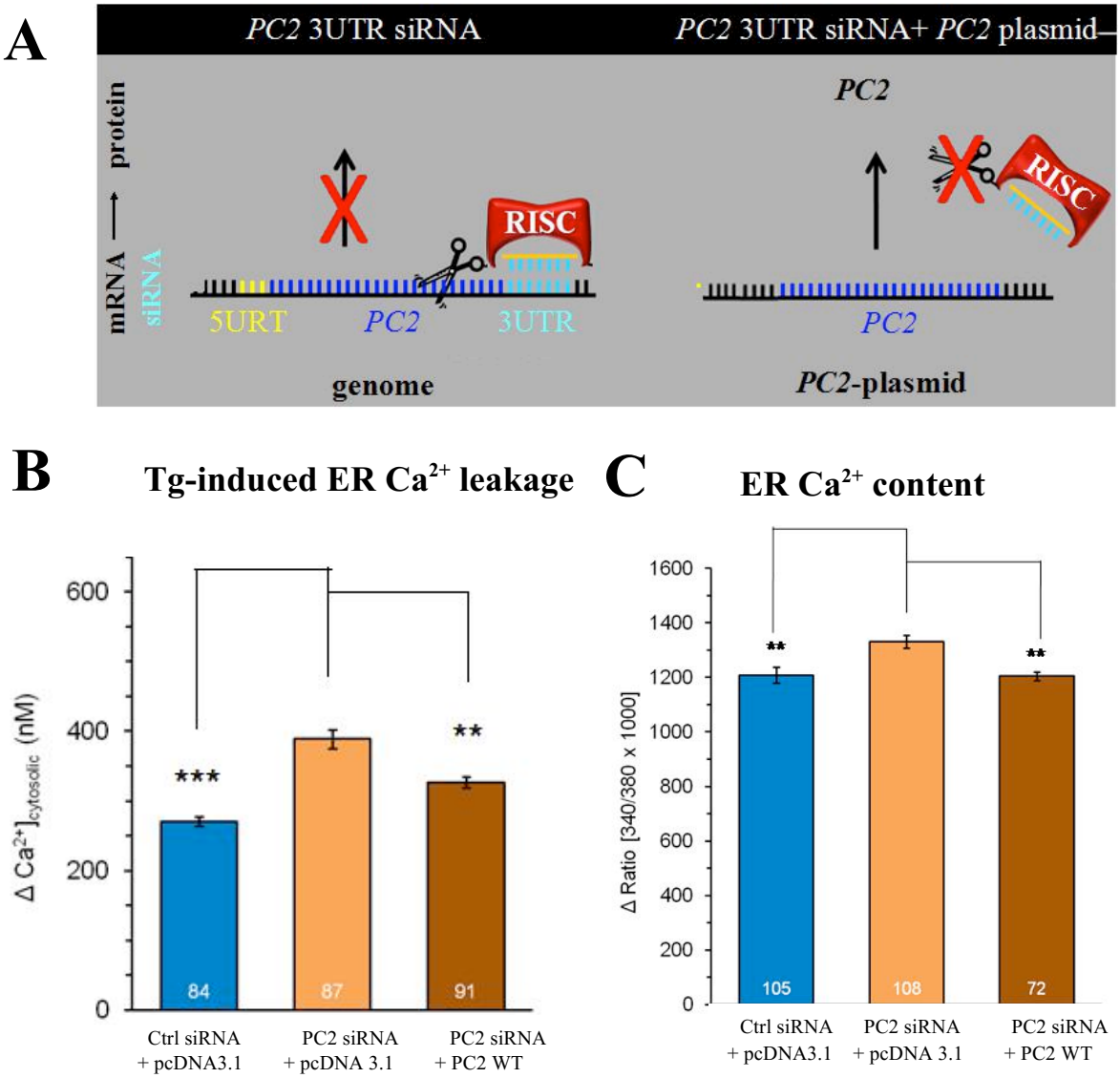

Figure 4-4. Effect of 3'UTR siRNA resistant PC2 plasmid on recuing the phenotype of PC2 silencing. A, diagram showing the strategy of PC2 siRNA targeting to the 3' untranslated region (3'UTR) and rescue with PC2 WT cDNA. B and C, statistical analysis of Tg-induced Ca^{2+} leakage (B) and ER luminal Ca^{2+} content (C) by PC2 3'UTR siRNA silencing with control plasmid or PC2 WT cDNA plasmid overexpression. HeLa cells were treated with PC2 3'UTR siRNA for 48 hr followed by over-expressing of UTR siRNA resistant plasmids for 36 hr, then subjected to Ca^{2+} imaging. Experiments are from 3 independent batches of cells and 9 measurements. Double asterisk (**) indicate a *p* value of <0.01 from unpaired t-test.

4.3.3 Effect of PC2 knockout in ER Ca^{2+} leakage and ER Ca^{2+} content in intact cells

After transient silencing of genes, cells undergo a series of changes and feedback regulation and finally reach an equilibration after a certain time period. At the time point when experiments are conducted, cells may not be in the equilibrated state and thus the results may not reflect a balanced situation. Given that it is hard to conclude from the transient silencing data (Figure 4-3), we next employed PC2 stable knockout mouse collecting duct (MCD) cell line B2 (*Pkd2*$^{-/-}$) extracted from *Pkd2*$^{-/-}$ mouse embryonic kidneys and its control cell line D3 (*Pkd2*$^{+/+}$). We found that Tg-induced ER Ca^{2+} leakage significantly decreases in *Pkd2*$^{-/-}$ cells (Figure 4-5 A) even though the steady-state ER Ca^{2+} content, which serves as the driving force, is much higher than that in the control MCD *Pkd2*$^{+/+}$ cells (Figure 4-5 B). This data strongly indicates that PC2 functions as an ER Ca^{2+} leak channel that the absence of PC2 decreased Ca^{2+} leakage thus resulting in an accumulation of ER luminal Ca^{2+} level.

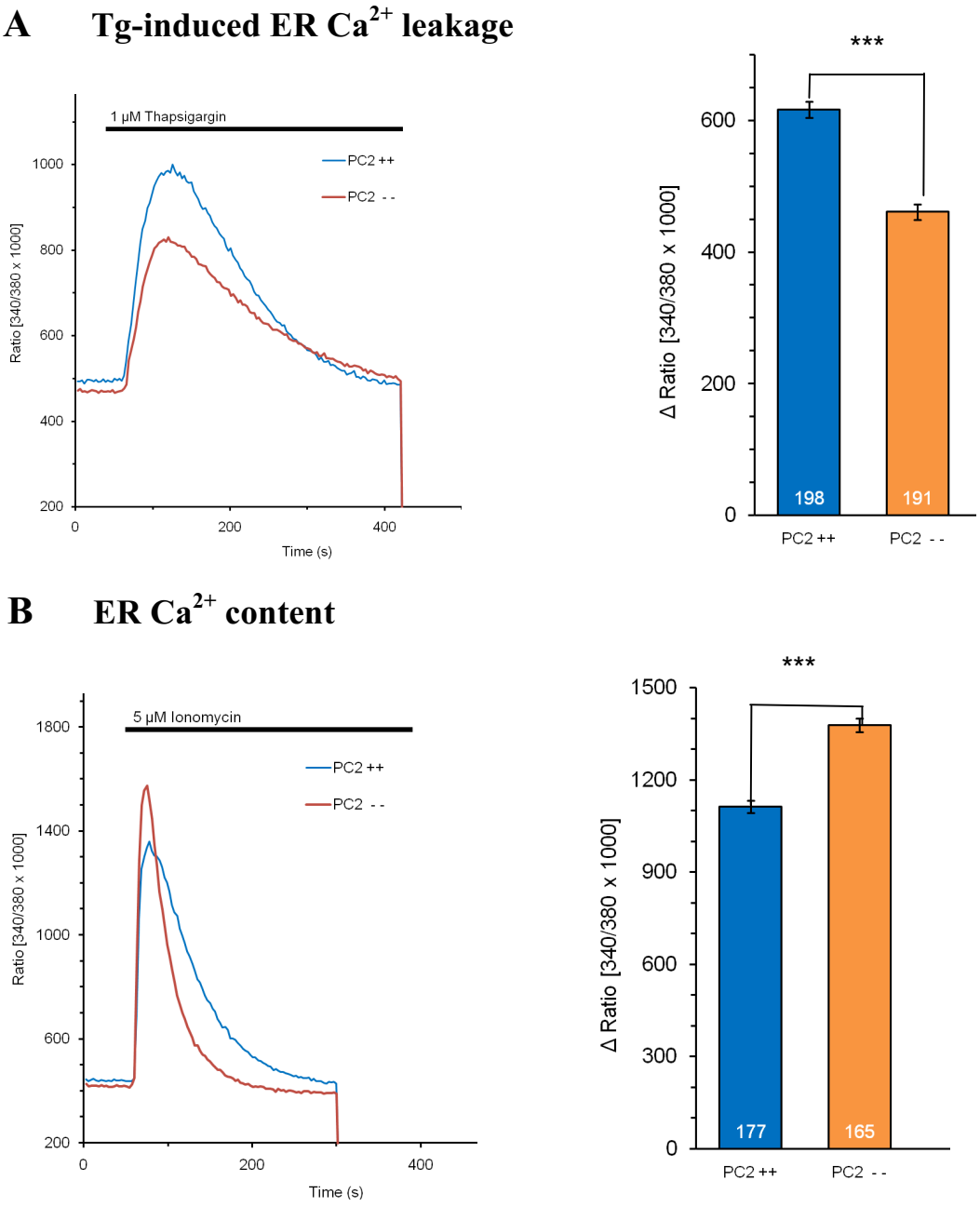

Figure 4-5. Effects of PC2 on Tg-induced ER Ca^{2+} leakage and ER Ca^{2+} content in MCD cells. A, *left panel*, Tg-induced ER Ca^{2+} leakage in D3 *Pkd2*$^{+/+}$ ($PC2^{+/+}$) and B2 *Pkd2*$^{-/-}$ ($PC2^{-/-}$) MCD cells. B, *left panel*, ER total Ca^{2+} content in $PC2^{+/+}$ and $PC2^{-/-}$ MCD cells. *Right panel,* statistical analysis. Experiments are from 3 independent batches of cells and 9 measurements with analyzed cell numbers indicated. The error bars represent the SEM. Triple asterisk (***) indicate *p* value <0.001 from unpaired *t*-test.

4.3.4 The net effect of FLNA on PC2 channel function

In order to investigate the net effect of FLNA (a combination of expression and functional regulation) on PC2 channel function in intact cells, we performed PC2 and FLNA double siRNA silencing and checked Tg-induced ER Ca^{2+} leakage as a read out of PC2 channel function in live cell Ca^{2+} imaging with non-ratio metric cytosolic Ca^{2+} dye Fluo-8. Even though no direct conclusion was obtained on whether PC2 functions as an ER Ca^{2+} leak channel from PC2 transient silencing Ca^{2+} imaging, Tg-induced ER Ca^{2+} leakage can still serve as a read out of PC2 channel function, to study its regulation by other factors. We observed that FLNA siRNA silencing decreases Tg-induced ER Ca^{2+} leakage, which is in opposite of PC2 siRNA silencing. Double silencing of PC2 and FLNA restores Ca^{2+} leak to the control level. This suggests that FLNA has a net inhibitory effect on PC2 channel function that KD of FLNA releases the inhibition and results in an effect in opposite to PC2 KD.

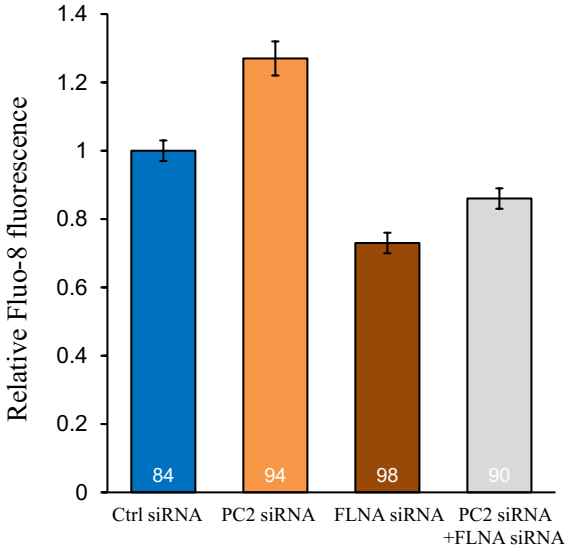

Figure 4-6. Effect of FLNA on PC2 silencing-induced ER Ca^{2+} leakage. HeLa cells transfected with the indicated siRNA(s) for 72 hr before Ca^{2+} imaging experiments with non-ratio metric cytosolic dye Fluo-8 measuring Tg-induced ER Ca^{2+} leak. Shown are statistical analysis of the relative peak fluorescence change from the indicated numbers of cells. Experiments are from 1 batch of cells and 3 measurements.

4.4 DISCUSSION

Ca^{2+}-dependent physical interaction of PC2 and FLNA was reported in Chapter 3 that Ca^{2+} enhances the binding strength of PC2-FLNA. In this chapter, we further investigated the Ca^{2+}-dependent binding of FLNA with PC2 N- and C- terminal fragments. GST pull-down revealed an enhanced PC2N-FLNA interaction but weakened PC2C-FLNA binding in the presence of Ca^{2+}, indicating that PC2 N- and C- tails may play different roles in responding to Ca^{2+}-dependent filamin regulation. Further lipid bilayer experiment showed that FLNA inhibits PC2 channel activity only in the presence of high Ca^{2+}, which taken together supports a Ca^{2+} dependent filamin inhibitory role on the channel. In addition, by employing Ca^{2+} imaging technique, we found that ER-localized PC2 functions as an ER passive Ca^{2+} leak channel, and FLNA has a net inhibitory effect on PC2 channel function in intact cells (which means the stabilizing effect of FLNA as described in Chapter 3 is overwhelmed by its inhibitory effect on PC2 channel activity shown in Chapter 2). Thus, it is proposed that there is a dynamic regulation of PC2-mediated ER Ca^{2+} flux by filamin; namely, increased intracellular Ca^{2+} concentration promotes the binding of FLNA to PC2 to reduce Ca^{2+} leak from the ER thereby preventing further intracellular Ca^{2+} increase.

To study the channel function of ER localized PC2 by live cell Ca^{2+} imaging, we have utilized three pairs of PC2 siRNA as well conducted the rescue experiment, which further confirmed the specificity of PC2 silencing. In addition, we employed MCD PC2 stable knockout kidney epithelial cell lines, which directly revealed the function of PC2 as an ER Ca^{2+} leak channel in intact cells. Previous study showed that *in vitro*, PC2 functions a non-selective cation channel and shows Ca^{2+}-activated Ca^{2+} permeability (58). However, it remains controversial in terms of the function of ER resident PC2 *in vivo,* that whether PC2

exhibits basal Ca^{2+} leakage or functions as a Ca^{2+}-activated Ca^{2+} release channel that requires an increase in cytosolic Ca^{2+} to confer permeability of Ca^{2+} of the ER. It appears that the function of ER resident PC2 is quite cell type dependent. Koulen *et al* found that PC2 functions as a Ca^{2+}-activated Ca^{2+} release channel in LLC-PK1 cells (59). Whereas, Wegierski *et al* reported that PC2 functions as an ER Ca^{2+} leak channel which decreases ER Ca^{2+} content and results in decreased Ca^{2+} release in HEK293 and MDCK cells (67). Another group even reported that PC2 does not significantly contribute to the ER Ca^{2+} homeostasis in the proximal tubule epithelial cells extracted from human urine (271). Our results from HeLa and MCD cells are more in consistent with Wegierski's study which supports PC2 as an ER Ca^{2+} leak channel. The discrepancy obtained from different cell lines is possibly due to distinguished environment where PC2 is residing. Due to different properties of each cell line, PC2 is in the protein complex with different binding partners, which confer different regulatory mechanism and entitle PC2 with either basal channel function or ligand stimulated channel activity.

In terms of the regulation of PC2 by FLNA, though FLNA silencing shows an opposite effect in Tg-induced Ca^{2+} leakage compared to PC2 silencing, the use of FLNA siRNA is not sufficient to specifically target to the channel function of PC2 as FLNA has been shown as a regulator of a number of targeting proteins. Fortunately, no other ER Ca^{2+} channels have been reported as downstream targets of FLNA. However it is more convincing to use blocking peptides, which will specifically disrupt PC2-FLNA interaction and examine PC2 mediated ER Ca^{2+} leakage to reveal the importance of PC2-FLNA complex.

The physiological importance of PC2-FLNA interaction was tested in zebrafish model as well by performing double silencing of PC2 and FLNA (Data not shown). *Pkd2* MO KD in zebrafish causes tail-curling phenotype which is often used as a read out of PC2 activity (272).

With *flna* and *Pkd2* double MO KD, we expected to see a rescue of PC2 channel function and alleviation of *Pkd2* KD caused phenotype. However, KD of *flna* alone shows even severe defect/abnormality in zebrafish, which makes the double KD results un-interpretative. This is understandable as FLNA plays fundamental roles in the cell and has a number of downstream target proteins, in addition of PC2. Thus, in order to specifically study the significance of PC2-FLNA binding, a similar strategy as discussed in Ca^{2+} imaging experiment is to use blocking peptides to specifically break down their interaction and check the tail curling phenotype to estimate the net effect of FLNA on PC2 and the importance of their interaction.

CHAPTER 5

RESULT #4 Filamin interacts with ENaC and inhibits its channel function

A version of this chapter has been published in 2013
Qian Wang, Xiao-Qing Dai, Qiang Li, Jagdeep Tuli, Genqing Liang, Shayla S.Li, and Xing-Zhen Chen.
J Biol Chem. 2013 Jan 4; 288(1): 264–273

5.1 ABSTRACT

Epithelial sodium channel (ENaC) in the kidneys is critical for Na^+ balance, extracellular volume and blood pressure. Altered ENaC function is associated with respiratory disorders, pseudohypoaldosteronism type 1 and Liddle syndrome. ENaC is known to interact with components of the cytoskeleton, but the functional roles remain largely unclear. Here, we examined the interaction of ENaC and filamins, important actin filament components. We first discovered by yeast two-hybrid screening that the C termini of ENaC α and β subunits bind filamin A, B and C, and we then confirmed the binding by *in vitro* biochemical assays. We demonstrated by co-immunoprecipitation that ENaC, either overexpressed in HEK293, HeLa, and melanoma A7 cells or natively expressed in LLC-PK1 and IMCD cells, is in the same complex with native filamin. Furthermore, biotinylation and co-immunoprecipitation combined assays showed the ENaC-filamin interaction on the cell surface. Using *Xenopus* oocyte expression and two-electrode voltage clamp electrophysiology, we found that co-expression of an ENaC-binding domain of filamin substantially reduces ENaC channel function. Western blotting and immunohistochemistry experiments revealed that filamin A C terminus (FLNAC) modestly reduces the expression of ENaC α subunit in oocytes and A7 cells. After normalizing the current by plasma membrane expression, we found that FLNAC results in 50% reduction in ENaC channel activity. The inhibitory effect of FLNAC was confirmed by lipid bilayer electrophysiology using purified ENaC and FLNAC, which showed that FLNAC substantially reduces ENaC single channel open probability. Taken together, our study demonstrated that filamin reduces ENaC channel function through direct interaction on the cell surface.

5.2 INTRODUCTION

The epithelial sodium channel (ENaC)/degenerin (DEG) family represents a class of ion channels discovered in the early 1990s (106). Members of this family are involved in Na^+ and H_2O reabsorption, taste, touch, acid-base homeostasis, and are divided into four main subfamilies as follows: ENaC, FMRF (Phe-Met-Arg-Phe)-amide-gated channels, acid-sensing ion channels, and mechanosensory channel proteins of nematode degenerins. This family includes more than 20 members that all possess two transmembrane domains plus intracellular N- and C- termini, and are Na^+ selective and amiloride inhibitable (123,273-275).

ENaC has small conductance (~5 pS) and is putatively composed of two α subunits (α-ENaC, 669 aa), one regulatory β subunit (β-ENaC, 640 aa) and one regulatory γ subunit (γ-ENaC, 649 aa) (2α1β1γ) arranged pseudosymmetrically around the channel pore. It is known that actin filament is an important regulator of ENaC channel and that ENaC directly binds α-spectrin, ankyrin and F-actin (148,276). ENaC is sensitive to membrane stretch, hydrostatic pressure and shear stress, as showed in *Xenopus* oocytes, mammalian cultured cells, artificial lipid bilayers, and native tissues (277,278). In the kidneys, ENaC plays a critical role in Na^+ balance, extracellular volume and blood pressure. In the lung, ENaC has a distinct role in controlling the ionic content of the air-liquid interface thereby determining the rate of mucociliary transport. In human and animal models, abnormal ENaC activity leads to a number of pathologies, e.g. hypertension, altered mucociliary transport, respiratory distress, and high-altitude pulmonary edema. Loss-of-function mutations in α-ENaC cause salt-wasting syndrome in pseudohypoaldosteronism type 1, while gain-of-function mutations in β- and γ-ENaC cause Liddle's syndrome, a form of salt-sensitive hypertension (123,273,279-281).

Filamins are large cytoplasmic proteins that cross-link cortical actin into a dynamic

three-dimensional structure and were discovered as the first family of non-muscle actin-binding proteins. Mammalian filamins consist of three actin-binding homologs (A, B, and C), each of ~280 kDa and containing an N terminal actin-binding domain (~300 aa), followed by a long rod-like domain made of 24 repeats of anti-parallel β-sheets (~96 aa each) and two 'hinge' regions. Two filamin molecules self-associate to form a homodimer through the last C terminal repeat, which allows the formation of a V-shaped flexible structure that is essential for the function (169,204). Current data suggest that filamins are involved in the organization of cytoskeleton, which is important for cell adhesion and motility, interacts with and regulates several membrane proteins (ion channels, receptors, β-integrins and glycoprotein Ibα) and cytoplasmic signaling proteins (Rho GTPases, TRAF2, Smads and SEK-1) (152,169,202,204,237,242,282,283). Nevertheless, a clear mechanistic explanation for their importance is still lacking. Genetic evidence indicates that filamins are essential for human development, and mutations in either filamin-A (*FLNA*) or -B (*FLNB*) are associated with abnormal development of brain, bone, cardiovascular system and many other organs. Although different filamin isoforms seem to have distinct roles in development, they may also be functionally similar and confer genetic redundancies that lead, upon mutations, to a wide degree of variances in the genetic syndromes.

The C terminus of α-ENaC has been shown to be important for channel modulation by the actin cytoskeleton (284). However, whether and how the actin-binding protein influences the function of ENaC remains poorly understood. In the present study, we employed various approaches of molecular biology and electrophysiology to investigate physical and functional interactions between ENaC and filamins, with an emphasis on the pore-forming α-ENaC and the predominant FLNA isoform.

5.3 MATERIALS AND METHODS

Antibodies

Four rabbit polyclonal antibodies, anti-α-ENaC 324870 (Calbiochem), anti-α-ENaC ENACA11-A (Alpha Diagnostic Inc., San Antonio, TX), anti-α-ENaC PA1-920A (Peirce), and anti-α-ENaC C-20 (Santa Cruz Biotech, Santa Cruz, CA) were used in this study. Anti-β-ENaC H-190 and anti-γ-ENaC F-20 were purchased from Santa Cruz Biotechnology. Anti-FLNA antibodies were mouse monoclonal FIL2 antibodies raised using the filamin antigen purified from chicken gizzard (Sigma), mouse monoclonal anti-FLNA E-3 and rabbit polyclonal anti-FLNA H-300 (Santa Cruz Biotechnology). Anti-GST B-14 (Santa Cruz Biotechnology) and anti-His 27E8 (Cell Signaling, Danvers, MA) antibodies were used in the GST pull-down assay. Mouse anti-GFP B-2 (Santa Cruz Biotechnology) was used in immunoblotting (IB) of GFP-tagged proteins. Anti-β-actin antibody C-4 (Santa Cruz Biotechnology) was used in Western blotting (WB) for loading controls.

Human melanoma cell lines

Human melanoma M2 cells are deficient of filamins. Transfection of FLNA into M2 cells generated A7 cells. To generate M2 and A7 ENaC stable cell lines, 600 mg/ml of hygromycin and G418 (Invitrogen) were added to select viable clones one recovery day following transfection and then maintained using hygromycin (100 μg/ml) (M2) or hygromycin plus G418 (300 μg/ml) (A7).

Cell culture and Transfection

HEK293, HeLa, IMCD, MDCK, porcine kidney cells LLC-PK1, M2 and A7 cells were

cultured in DMEM supplemented with L-glutamine, penicillin-streptomycin, and 10% FBS. Transfection of ENaC was performed on HEK293, HeLa and MDCK cells cultured to 90% confluency using Lipofectamine 2000 (Invitrogen) according to the manufacturer's protocol.

Plasmid construction

The C termini of human *FLNA* (NM_001456, FLNAC, aa 2150-2647) and *FLNB* (NM_001457, FLNBC, aa 2105-2602) were isolated from either human kidney cDNA library or HEK293 cells. The C terminus of *FLNC* (NM_001458, FLNCC, aa 2144-2725) was cut from pACT2-FLNCC plasmid. cDNAs were subcloned into pGADT7 (Clontech) for yeast expression, pET28a (Novagen, EMD Chemicals, Gibbstown, NJ) for bacterial expression, pcDNA3.1 for mammalian expression, and pCHGF for *Xenopus* oocyte expression. cDNAs encoding Human α-ENaC N terminus (α-ENaCN, aa 1-82), α-ENaC C terminus (α-ENaCC, aa 588-669), β-ENaC N terminus (β-ENaCN, aa 1-14), β-ENaC C terminus (β-ENaCC, aa 559-640), γ-ENaC N terminus (γ-ENaCN, aa 1-76), and γ-ENaC C terminus (γ-ENaCC, aa 568-649) were subcoloned into pGBKT7 (Clontech) for yeast expression. cDNAs encoding α-ENaCC and β-ENaCC were constructed into vector pGEX5X (Pharmacia, Piscataway, NJ) for GST pull-down assay. Human α-ENaC and β-ENaC were subcloned into vectors pcDNA3.1 and pEGFPC2, in which GFP is fused to the N terminus for mammalian expression. Rabbit α, β, and γ subunits of ENaC in pSD series vector for oocyte expression were generous gifts of Dr. L. Schild from University of Lausanne. All plasmid constructs were confirmed by sequencing.

Yeast two-hybrid analysis

A yeast two-hybrid screen was performed in the yeast strain AH109 containing *Ade2*, *His3* and *LacZ* reporter genes under the control of the GAL4 upstream-activating sequences as described before (45)(22). Briefly, the cDNAs encoding ENaC fragments were subcloned in frame into the GAL4 DNA binding domain of vector pGBKT7 by a PCR-based approach. Both C- and N- termini of ENaC subunits were used as baits to screen human kidney and heart cDNA libraries (Clontech) constructed in vector pGADT7 containing the GAL4 activation domain. Transformants were grown on the minimal synthetic dropout medium lacking leucine, tryptophan, adenine and histidine. Colonies survived were further screened for activation of a *Lac*Z reporter gene by a filter lift assay (Clontech). Plasmid cDNAs were isolated from the positive colonies and individually tested against the bait and empty vector.

GST pull-down

Pre-cleared bacterial protein extract (250 µl) containing GST-α-ENaCC, GST-β-ENaCC or GST alone was incubated with 2 µg of purified His-FLNAC in the binding buffer (50 mM Tris, 150 mM NaCl, and 1 mM $CaCl_2$, pH 7.5). The mixture was incubated at RT for 1 hr with gentle shaking, followed by another hour of incubation after addition of 100 µl glutathione–agarose beads (Sigma). The beads were then washed 4-5 times with 140 mM NaCl, 10 mM Na_2HPO_4, and 1.8 mM KH_2PO_4, pH 7.5 and the remaining proteins were eluted using 10 mM glutathione, and 50 mM Tris, pH 8.0. The protein samples were prepared for WB.

Co-immunoprecipitation (Co-IP)

Co-IP was performed using lysate of native IMCD and LLC-PK1, ENaC-transfected HEK293 and HeLa cells, and α-ENaC stably expressed A7 cell line. A cell monolayer in 100

mm dishes was washed twice with phosphate-buffered saline (PBS) and solubilized in ice-cold CellLytic-M lysis buffer and proteinase inhibitor mixture (Sigma). Supernatant was collected following centrifugation at 16,000 × *g* for 15 min. Equal amounts of total protein from postnuclear supernatants were pre-cleared for 1 hr with protein G-Sepharose (GE Healthcare) and then incubated for 4 hr in a cold room with antibody against ENaC or FLNA. After the addition of 100 μl of 50% protein G-Sepharose, the mixtures were incubated overnight with gentle shaking. The immune complexes absorbed to protein G-Sepharose were washed five times with the NP40 lysis buffer (50 mM Tris, 150 mM NaCl, and 1% Nonidet P-40, pH 7.5) with proteinase inhibitor. The precipitated proteins were analyzed by WB using antibodies against FLNA or ENaC.

Preparation of mRNAs and microinjection into oocytes

Capped synthetic rabbit α, β, and γ subunits of *ENaC* mRNAs were synthesized by in vitro transcription from a linearized template in the pSD series vector using the mMESSAGE mMACHINE1 kit (Ambion, Austin, TX). FLNAC and FLNBC in the pCHGF vector were used to synthesize their mRNAs in a similar way. α- and γ-ENaC were linearized by PvuII and β-ENaC by BgIII; FLNAC and FLNBC were linearized by MluI. Stage V–VI oocytes were prepared as previously described (240). Each oocyte was injected with 50 nl of water containing mRNA of ENaC subunits (10 ng each) alone or together with 20 ng of FLNAC mRNA 5 hr following defolliculation. An equal volume of RNase-free water was injected into each control oocyte. Injected oocytes were incubated at 16–18°C in the Barth solution supplemented with penicillin/streptomycin and 2 μm amiloride for 2–3 days (to reduce Na^+ loading via ENaC) prior to experiments.

Two-electrode voltage clamp

Two-electrode voltage clamp was performed as described previously (240). Briefly, the two electrodes (capillary pipettes, Warner Instruments, Hamden, CT) impaling *Xenopus* oocytes were filled with 3 M KCl to form a tip resistance of 0.3–2 megohms. Oocyte whole-cell currents were recorded using a Geneclamp 500B amplifier and Digidata 1322A AD/DA converter (Molecular Devices, Union City, CA). Gap-free and voltage ramp protocols, as described previously (285), were used in experiments, with current/voltage signals sampled at intervals of 100 ms and 100 μs, respectively. The standard sodium solution contained 100 mM NaCl, 2 mM KCl, 1 mM $CaCl_2$, 1 mM $MgCl_2$, and 10 mM HEPES, pH 7.5. *N*-Methyl-D-glucamine (NMDG, Acros Organics, Monroeville, NJ) was used to replace Na^+ to generate the NMDG-containing solution.

Protein preparation and lipid bilayer electrophysiology

Human α-, β-, and γ-ENaC proteins were purified from MDCK cell lines stably transfected with pGTAP3F-ENaCs. TAP-ENaC was prepared and reconstituted in a lipid bilayer system as described previously (217) to assess the channel activity. Briefly, PC-ONE amplifier (Dagan Corp., Minneapolis, MN) in combination with Clampex 9 program (Molecular Devices) was used in these experiments. The *cis* (or *trans*) compartment contained 150 (or 15) mM NaCl, and 15 μM Ca^{2+}, pH 7.4 (adjusted by MOPS-KOH). TAP-α-ENaC protein was added to the *cis* chamber in proximity of the membrane or used to directly 'paint' the membrane. To examine the effect of *Escherichia coli* purified FLNAC on α-ENaC, single channel activity of α-ENaC was recorded for 20–40 min before and after the addition of FLNAC.

Biotinylation

Xenopus oocytes and HeLa or M2 cells were washed three times with Barth solution/PBS before incubation with 5 or 1 mg/ml Sulfo-NHS-SS-Biotin (Pierce) for 30 min at RT. After adding 1 M NH_4Cl to quench the nonreacted biotinylation reagent, oocytes/cells were washed with Barth solution/PBS and then harvested in ice-cold CellLytic-M lysis buffer and proteinase inhibitor mixture. Oocyte/cell lysates were incubated at RT for 3 hr with gentle shaking upon addition of 100 μl of streptavidin (Pierce). The surface protein absorbed by streptavidin was resuspended in SDS and subjected to SDS-PAGE.

Immunohistochemistry

Immunohistochemistry was used to determine the surface expression of ENaC with or without FLNAC co-expression in *Xenopus* oocytes. Oocytes were washed with PBS and then fixed in 3% paraformaldehyde for 15 min at RT. After washing three times with 50 mM NH_4Cl in PBS, oocytes were permeabilized with 0.1% Triton X-100 for 4 min. After rinsing in PBS, oocytes were blocked in 2% bovine serum albumin for 30 min before incubating with anti-α-ENaC PA1–920A (1:100) in blocking buffer for 1 hr at RT. Oocytes were then washed three times with PBS and incubated with a secondary FITC-conjugated anti-rabbit antibody (1:200) for 30 min at RT. After washing, oocytes were mounted in VECTASHIELD (Vector Laboratories, Burlingame, CA) on slides with secure-seal spacers (Grace Bio-Labs, Inc., Bend, OR) for fluorescence detection with a Zeiss 510 confocal laser-scanning microscope. Signals were quantified by ImageJ (National Institutes of Health, Bethesda).

Data analysis and statistics

Data were analyzed and plotted by Sigmaplot 11 or 12, and expressed as means ± S.E. (*n*), where *n* indicates the number of independent measurements. Comparisons between two sets of data were analyzed by *t*-test. A probability value (*p*) of less than 0.05 and 0.01 was considered significant and very significant, respectively.

5.4 RESULTS

5.4.1 Physical interaction between ENaC and filamins

We employed a yeast two-hybrid system to screen proteins that associate with the C terminus of human α-ENaC (α-ENaCC, aa 588–669). α-ENaCC was constructed into the pGBKT7 vector, as a bait, to screen human kidney and heart cDNA libraries. We found that the C terminus of human filamin A (FLNAC, aa 2150–2647) from the heart library binds α-ENaCC. We then performed one-to-one yeast two-hybrid assays and found that the C termini of three human filamins (FLNAC, aa 2150–2647; FLNBC, aa 2105–2602; FLNCC, aa 2144–2725) bind α-ENaCC and the C terminus of human β-ENaC (β-ENaCC, aa 559–640) (Figure 5-1 A), despite the fact that there is no significant sequence similarity among the C termini of α and β subunits of ENaC. To confirm the results obtained from our yeast two-hybrid experiments, we performed *in vitro* GST fusion protein affinity binding assays. For this, α- and β-ENaCC were constructed in the pGEX-5X vector in-frame with a GST epitope and expressed in the bacterial strain BL21, and then cell lysate was collected (Figure 5-1 B). His-tagged FLNAC was similarly expressed and purified. Both α- and β-ENaCC overexpressed in *E. coli* were able to interact with purified FLNAC (Figure 5-1 B).

A

prey (PGADT7) / bait (PGBKT7)	FLNAC (2150-2647)	FLNBC (2105-2602)	FLNCC (2144-2725)	Vector (Control)
□-ENaCN (1-82)	-	-	-	-
□-ENaCC (588-669)	++	++	++	-
β-ENaCN (1-47)	-	-	-	-
β-ENaCC (559-640)	++	++	++	-
γ-ENaCN (1-76)	-	-	-	-
γ-ENaCC (568-649)	Self-activation, not tested for binding			
Vector (Control)	-	-	-	-

B

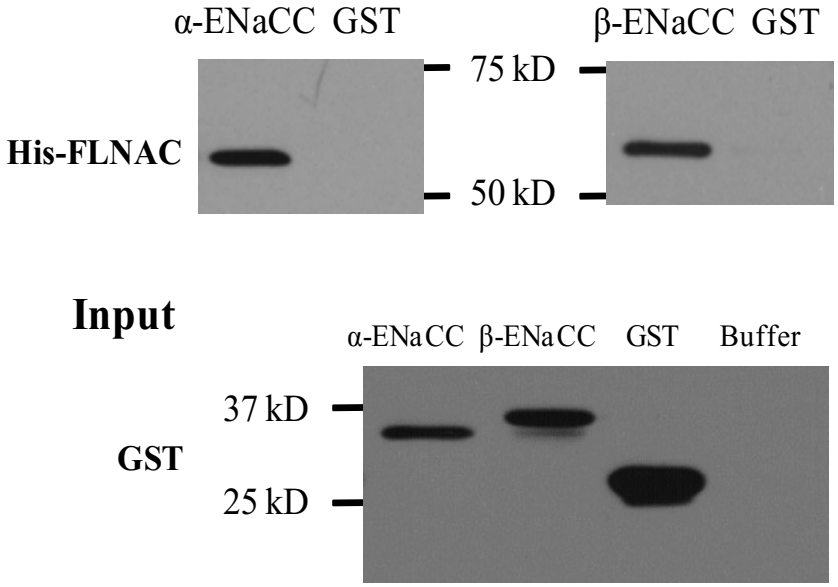

Figure 5-1. Physical interaction between ENaC and filamins. A, yeast two-hybrid assays for the ENaC-filamin interaction. ++ and − indicate the presence of a strong interaction and the absence of the interaction, respectively. B, interaction between ENaC and FLNA C termini by *in vitro* GST pull-down assays. *E.coli* lysates containing GST-α-ENaCC, GST-β-ENaCC, or GST alone were incubated with purified His-FLNAC. The expression of GST-tagged α-/β-ENaCC and GST is shown as Input (*lower panel*) by IB with GST B-14 antibody. Buffer served as a nonprotein control (n = 3).

To determine whether ENaC subunits bind FLNA *in vivo*, we overexpressed α-ENaC and β-ENaC in the HEK293 cell line and performed co-IP. Both α-ENaC and β-ENaC were found to interact with native FLNA (Figure 5-2 A). In HeLa cells transfected with GFP-α-ENaC, anti-FLNA E-3 antibody was able to precipitate GFP-α-ENaC (Figure 5-2 B), indicating that the two proteins are in the same complex. Moreover, in the A7 α-ENaC stably expressing cell line, FLNA was found to interact with GFP-α-ENaC (Figure 5-2 C). Furthermore, the presence of FLNAC through overexpression reduced the interaction of α-ENaC with full-length FLNA (Figure 5-2 C), presumably through competitive binding.

The endogenous ENaC-FLNA interaction was confirmed using native IMCD and LLC-PK1 cell lines. FLNA protein was detected in the precipitates of LLC-PK1 and IMCD cells using an anti-α-ENaC antibody but not in the precipitates using nonimmune IgG (Figure 5-3 A and B). Reciprocally, α-ENaC signal was observed in the precipitates of LLC-PK1 using an antibody against FLNA for IP. These data demonstrated that α-ENaC and FLNA are in the same complex *in vivo*. Thus, ENaC interacts with filamins *in vitro* and *in vivo*.

Because ENaC channels mainly exhibit their channel function on the plasma membrane, we wondered whether surface ENaC interacts with filamins. For this we first isolated surface membrane proteins by biotinylation assays using HeLa cells with or without overexpression of HA-tagged α-ENaC. Both streptavidin-absorbed and flow-through lysates were immunoblotted with antibody against α-ENaC, FLNA, or Na^+/K^+-ATPase. We found that overexpression of ENaC results in increased biotinylated ENaC and FLNA but not Na^+/K^+-ATPase (Figure 5-3 C), suggesting that more FLNA molecules are specifically recruited to complex with an increased population of the surface membrane ENaC. We then performed co-IP assays using biotinylated lysates to directly examine their interaction on the surface membrane. For this

purpose we utilized the monomeric avidin kit (Pierce) that allows biotinylated lysates to dissociate from streptavidin without disrupting protein complexing in the lysates. Indeed, our experiments using HeLa and M2 cells demonstrated that ENaC channels located on the plasma membrane interact with FLNA (Figure 5-3 D).

Of note, when we employed both kidney and heart libraries in parallel for screening interacting partners of α-ENaCC, FLNAC came out as one of the interacting partners from the heart library but not the kidney library. The exact reasons for this outcome remain to be determined, but it may be due in part to the low reproducibility nature of this screen method. Nevertheless, it is important to note that filamin is widely distributed and that we confirmed its interaction with ENaC by one-to-one yeast two-hybrid (Figure 5-1 A), GST pull-down (Figure 5-1 B), and by co-IP in renal and nonrenal cell lines (Figures 5-2 and 5-3).

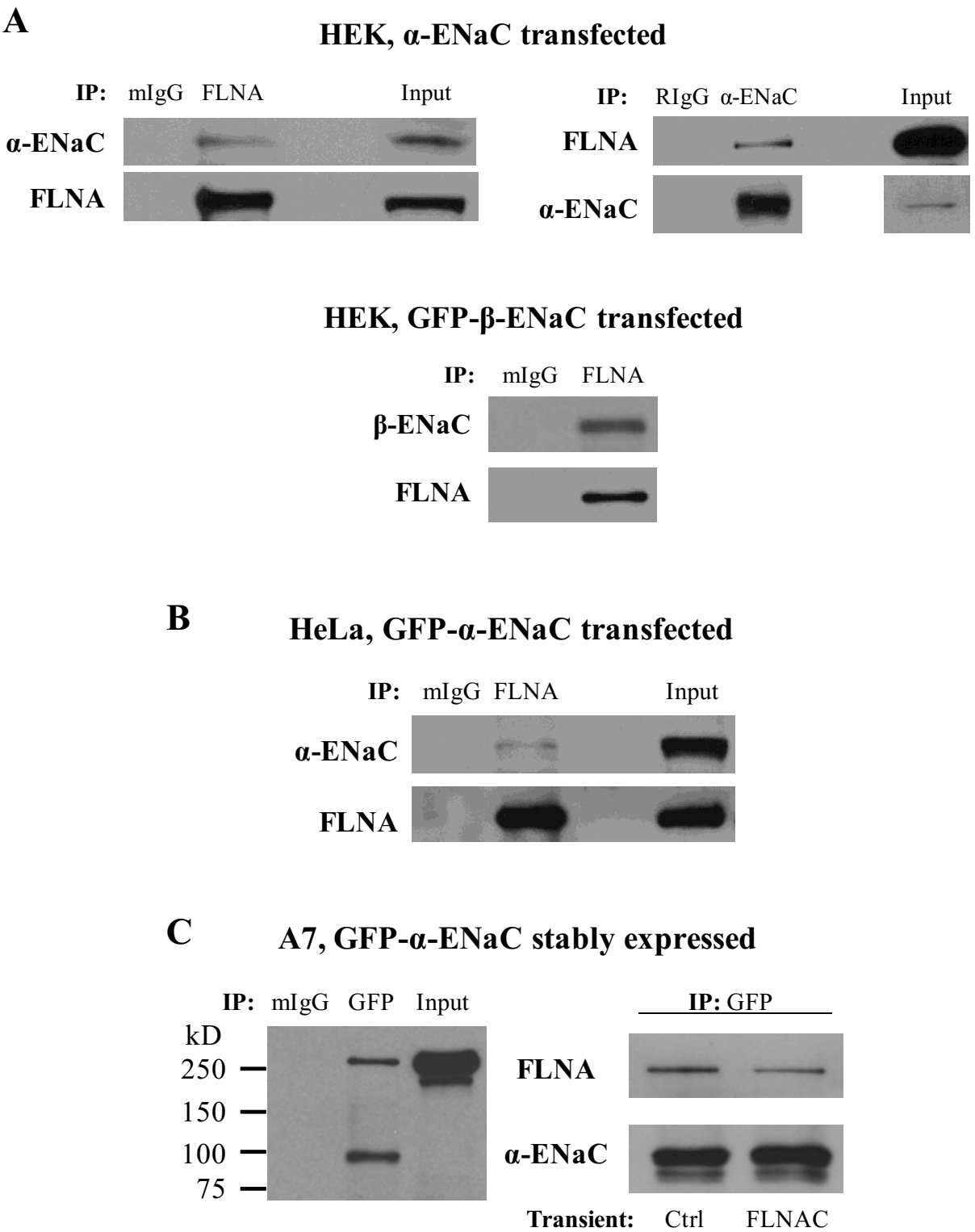
A
HEK, α-ENaC transfected
IP: mIgG FLNA Input
α-ENaC
FLNA
IP: RIgG α-ENaC Input
FLNA
α-ENaC
HEK, GFP-β-ENaC transfected
IP: mIgG FLNA
β-ENaC
FLNA
B
HeLa, GFP-α-ENaC transfected
IP: mIgG FLNA Input
α-ENaC
FLNA
C
A7, GFP-α-ENaC stably expressed
IP: mIgG GFP Input
kD
250
150
100
75
IP: GFP
FLNA
α-ENaC
Transient: Ctrl FLNAC

Figure 5-2. Interaction between ENaC and FLNA by co-IP. Data shown here are representative of those from three to five independent experiments. A, *upper panels*, HEK293 cells overexpressing α-ENaC. Cell lysates were used for reciprocal co-IP assays, using anti-FLNA E-3 or anti-α-ENaC (Calbiochem) antibody for IP or IB, as indicated. Non-immune serum mouse IgG (mIgG) and rabbit IgG (RIgG) were used as controls. *Lower panels*, cell lysates from HEK293 cells overexpressing GFP-α-ENaC were precipitated with anti-FLNA E-3 or mIgG (control). Immunoprecipitated proteins were analyzed by WB using anti-FLNA E-3 or anti-GFP (Santa Cruz Biotechnology) antibody. B*,* lysates from HeLa cells overexpressing GFP-α-ENaC were precipitated with anti-FLNA E-3 or mIgG (control). Immunoprecipitated proteins were analyzed by WB using anti-FLNA E-3 or anti-GFP. C*,* A7 cells stably expressing GFP-α-ENaC were used for IP using GFP or mIgG (control). Immunoprecipitated proteins were detected with anti-FLNA E-3 or anti-GFP (*left panels*). *Right panels*, A7 cells stably expressing GFP-α-ENaC were transiently transfected with empty vector (Ctrl*)* or the FLNAC fragment. GFP antibody was used for IP, and anti-FLNA E-3 and anti-GFP were used for IB.

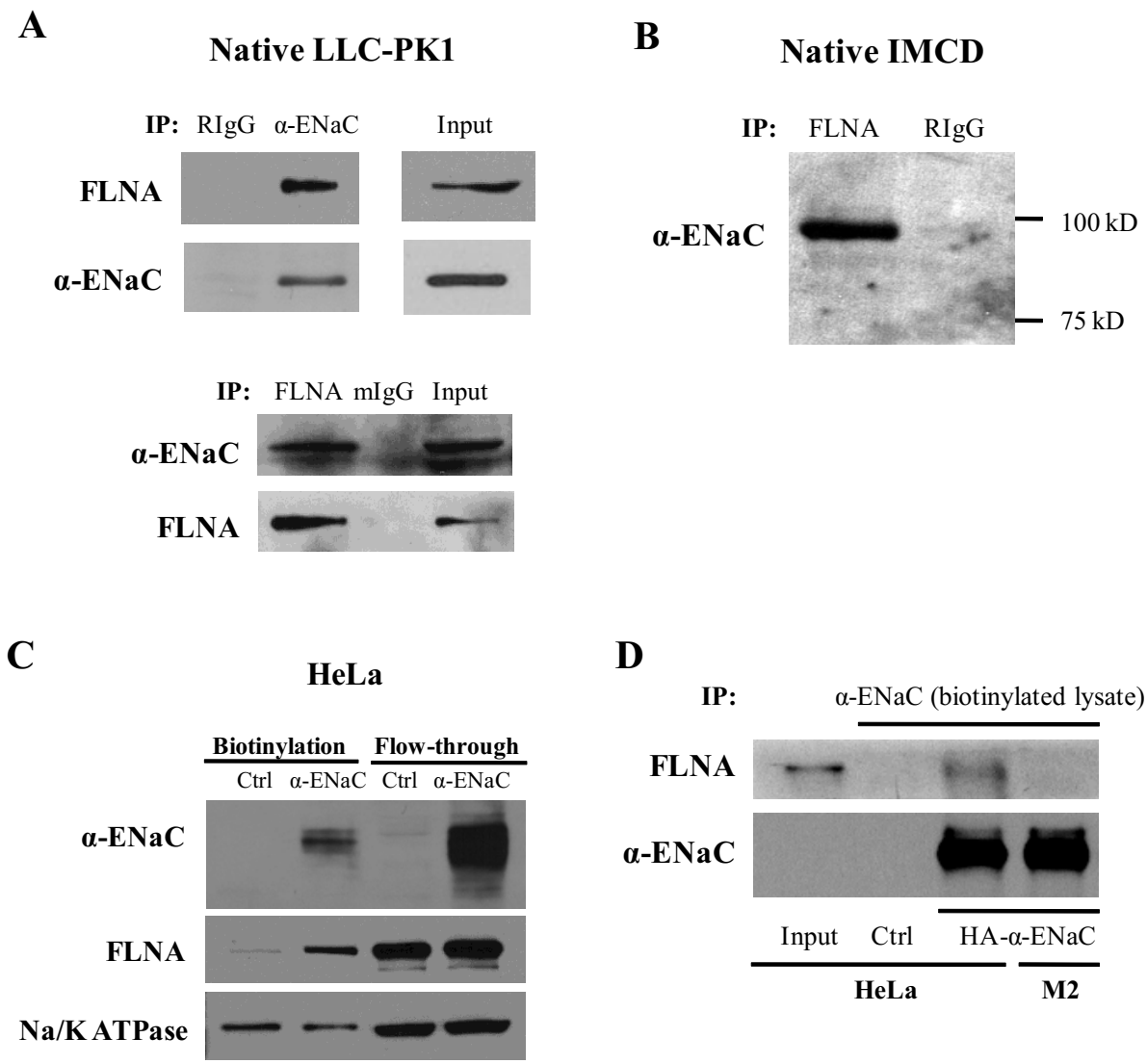
A
Native LLC-PK1
IP: RIgG α-ENaC Input
FLNA
α-ENaC
IP: FLNA mIgG Input
α-ENaC
FLNA
B
Native IMCD
IP: FLNA RIgG
α-ENaC
100 kD
75 kD
C
HeLa
Biotinylation
Flow-through
Ctrl α-ENaC Ctrl α-ENaC
α-ENaC
FLNA
Na/K ATPase
D
IP: α-ENaC (biotinylated lysate)
FLNA
α-ENaC
Input Ctrl HA-α-ENaC
HeLa
M2

Figure 5-3. Interaction between endogenous ENaC and FLNA by co-IP. Data shown here are representative of those from three to four independent experiments. A, LLC-PK1 cell lysates were used for reciprocal co-IP using anti-α-ENaC (Calbiochem) and anti-FLNA E-3 for IP and IB as indicated. Non-immune serum RIgG and mIgG were used as controls. *B*, cell lysates from IMCD cells were precipitated with anti-FLNA H-300 and RIgG as control. Immunoprecipitated proteins were analyzed by WB using anti-α-ENaC antibody (Calbiochem). *C,* biotinylation was performed on HeLa cells transfected with either human α-ENaC or empty pcDNA3.1 plasmid (Ctrl). Biotinylated proteins were subjected to SDS-PAGE and detected by antibody against ENaC, FLNA, or Na^+/K^+-ATPase (as a control).*D,* biotinylation was performed on HeLa and M2 cells transfected with human α-ENaC or empty pcDNA3.1 plasmid (HeLa only, Ctrl). Biotinylated proteins were collected using the monomeric avidin kit (Pierce) and proceeded to co-IP assays with α-ENaC antibody. Precipitated proteins were immunoblotted with FLNA H-300 or α-ENaC antibody.

5.4.2 Modulation of ENaC channel function by FLNA in *Xenopus* oocytes

We co-injected *α-, β-,* and *γ-ENaC* mRNAs into oocytes with a concentration ratio of 2:1:1. The average Na^+ current, equals to the total current in the presence of 100 mM Na^+ minus the one when Na^+ was replaced by the equimolar *N*-methyl-D-glucamine, was 2.7 ± 0.3 μA (n = 30) at −50 mV in oocytes expressing ENaC. This Na^+ current was reversibly inhibited by 10 μM amiloride present in the extracellular solution, with the amiloride-sensitive currents averaging 2.42 ± 0.39 μA (n = 17) (Figure 5-4), accounting for 90% of the Na^+ current. Co-expression of FLNAC substantially reduced the Na^+ current as well as the amiloride-sensitive current (Figure 5-4). In the presence of FLNAC, the amiloride-sensitive current was 0.47 ± 0.21 μA (n = 15), which represents only 19% of the corresponding currents in the absence of FLNAC. The inhibition effect of FLNBC was similar to that of FLNAC (Figure 5-4 B). FLNA also substantially reduced amiloride-sensitive currents in other membrane potentials ranging from −120 mV to +80 mV, as revealed by use of a voltage ramp protocol (Figure 5-4 C). Although it was reported that efficient trafficking of ENaC to the surface membrane requires assembly of all three subunits (286), individual ENaC subunits are still capable of trafficking to the surface membrane (287). We thus examined the effect of filamin on α-ENaC channel function. When only α-ENaC was expressed in oocytes, significant amiloride-inhibitable currents were observed, although they were much smaller (Figure 5-4 D) than those in the presence of α, β, and γ subunits (Figure 5-4). On average, the amiloride-sensitive currents were 181 ± 5 nA (n = 11). Similarly, the co-expression of FLNAC reduced the currents to 71 ± 6 nA (n = 21) (Figure 5-4 D), a 61% reduction. By using a voltage ramp protocol, we found that FLNAC is able to suppress the α-ENaC activity in the tested voltage range of −120 mV to +80 mV (Figure 5-4 E).

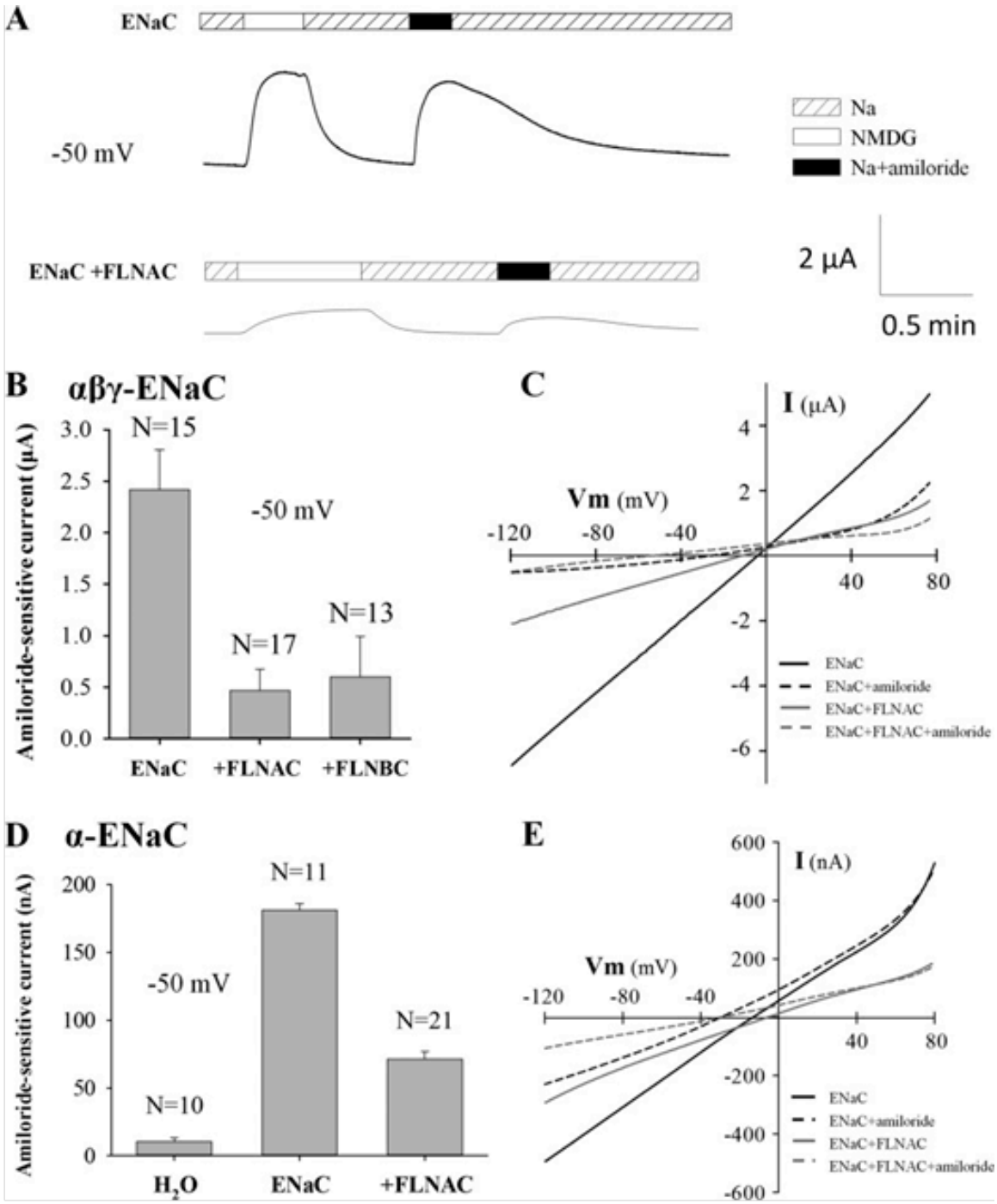
A
ENaC
-50 mV
Na
NMDG
Na+amiloride
ENaC +FLNAC
2 µA
0.5 min
B
αβγ-ENaC
Amiloride-sensitive current (µA)
N=15
N=17
N=13
-50 mV
ENaC
+FLNAC
+FLNBC
C
I (µA)
Vm (mV)
ENaC
ENaC+amiloride
ENaC+FLNAC
ENaC+FLNAC+amiloride
D
α-ENaC
Amiloride-sensitive current (nA)
N=11
N=10
N=21
-50 mV
H2O
ENaC
+FLNAC
E
I (nA)
Vm (mV)
ENaC
ENaC+amiloride
ENaC+FLNAC
ENaC+FLNAC+amiloride

Figure 5-4. Effect of filamin on whole-cell transport mediated by overexpressed αβγ-ENaC or α-ENaC in *Xenopus* oocytes. A, representative ENaC-mediated whole-cell currents recorded at −50 mV with the two-microelectrode voltage clamp in the presence of the standard Na^+- or NMDG-containing solution, ± amiloride (10 μM), as indicated in an oocyte injected with *αβγ-ENaC* mRNA together with (*lower panel*) or without (*upper panel*) *FLNAC* mRNA. B, averaged amiloride-sensitive Na^+ currents measured at −50 mV, from oocytes expressing αβγ-ENaC, αβγ-ENaC+FLNAC, or αβγ-ENaC+FLNBC. C, representative current-voltage (*I-V*) relationships obtained using a voltage ramp protocol with other conditions similar to A and B. D, effect of FLNAC on α-ENaC function, assessed by amiloride-sensitive Na^+ currents. Shown are averages obtained from oocytes expressing α-ENaC with or without FLNAC ($p < 0.001$, between ± FLNAC, by unpaired *t* test), or water-injected oocytes. E, representative I-V curves obtained using a voltage ramp protocol with other conditions similar to C.

5.4.3 Modulation of ENaC expression and distribution by FLNA

To determine whether the reduced whole-cell channel function of ENaC by filamins is due to reduced ENaC expression and surface membrane targeting or reduced single channel activity, we performed WB and biotinylation assays to examine the effect of filamins on the total and PM expression of α-ENaC. FLNAC modestly reduced α-ENaC total expression (Figure 5-5 A) as assessed by WB but had no significant effect on its plasma membrane targeting assessed by biotinylation (Figure 5-5 B). In average, the α-ENaC total expression was reduced to 83 ± 6% by FLNAC (n = 3; p = 0.005, by paired t-test). Furthermore, we performed immunohistochemistry (IHC) experiments to illustrate the effect of filamin on the subcellular distribution of α-ENaC on oocytes that were first tested for amiloride-inhibited currents. We found that, in the presence of FLNAC, the α-ENaC plasma membrane density assessed by IHC in average only reduced to 78% (Figure 5-5 C), which is similar to the reduction in the total ENaC expression. We next calculated the ratio of the α-ENaC amiloride-sensitive current to the plasma membrane density for each tested individual oocyte as a normalized current to assess the channel activity of each α-ENaC protein. We found that in the presence of FLNAC, α-ENaC activity dropped to 52% (n = 4; p = 0.01, by unpaired t-test) (Figure 5-5 D). Taken together, our data from using oocytes indicate that filamin inhibits α-ENaC channel activity, in addition to modestly reducing its overall expression.

We also employed filamin-deficient M2 cells and FLNA-replete A7 cells stably expressing α-ENaC to examine the effect of FLNA on the α-ENaC expression. Our WB analysis revealed that the expression of α-ENaC is reduced with FLNAC co-transfection in M2 cells and is lower in A7 than in M2 cells (Figure 5-5 E), possibly because filamin down-regulates the ENaC expression. Interestingly, endogenous FLNA in A7 cells was significantly reduced by the

expression of FLNAC (Figure 5-5 E), suggesting a competitive expression between FLNAC and full-length FLNA. Because the process of selection of stably expressing M2 and A7 cells may have picked up this A7 cell line with lower ENaC expression than the M2 cell line, we next performed transient transfection of α-ENaC to eliminate this potential factor. Furthermore, to avoid/reduce the potential influence of limited protein synthesis capability of cells on the simultaneous expression of two exogenous proteins, we performed transient transfection with α-ENaC plasmid in M2 cells on day 1, followed by an equal split into two wells on day 2 for transient transfection with an empty or FLNAC plasmid. We found that FLNAC significantly reduces the expression of α-ENaC (Figure 5-5 F), in agreement with the results obtained using stable M2 cells (Figure 5-5 E). Averaging from three independent experiments found a reduction to 74 ± 8% (p = 0.003, by paired t-test). These data using mammalian melanoma M2 and A7 cells are in agreement with our results obtained using *Xenopus* oocytes that filamin modestly reduces the ENaC expression.

Taken together, we found that there is a modest reduction in the ENaC total (by WB) and PM (by IHC) expression, which is insufficient to account for the substantial decrease in the whole-cell current in the presence of filamin (Figure 5-4). Normalizing the amiloride-sensitive current by the surface membrane density, we found that ENaC channel activity drops to half in the presence of FLNA.

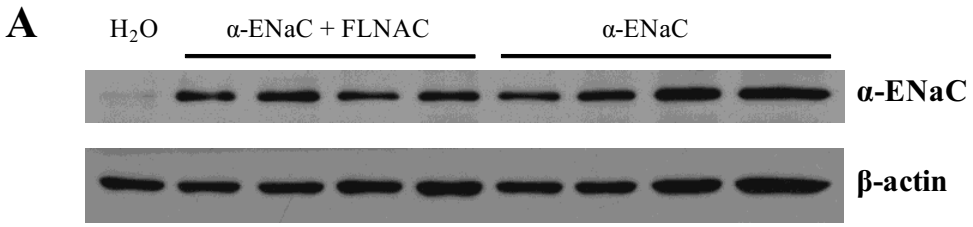
A
H2O
α-ENaC + FLNAC
α-ENaC
α-ENaC
β-actin

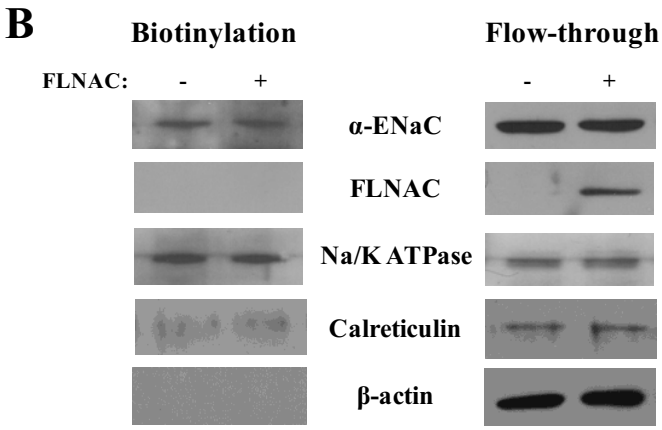
B
Biotinylation
Flow-through
FLNAC:
-
+
-
+
α-ENaC
FLNAC
Na/K ATPase
Calreticulin
β-actin

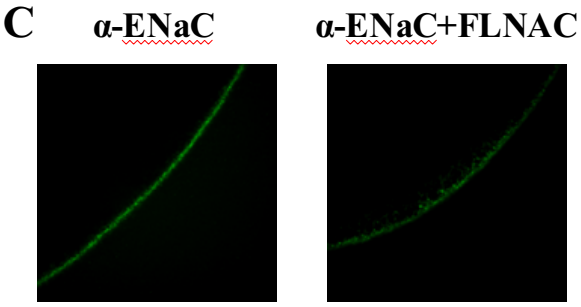
C
α-ENaC
α-ENaC+FLNAC

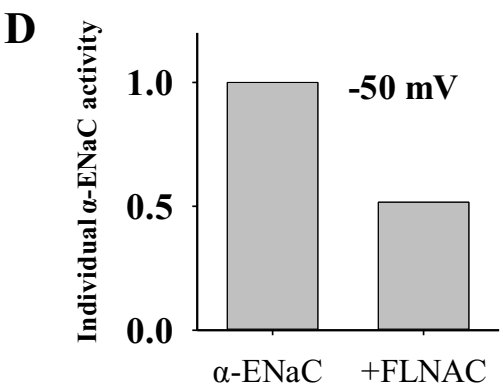
D
Individual α-ENaC activity
1.0
0.5
0.0
-50 mV
α-ENaC
+FLNAC

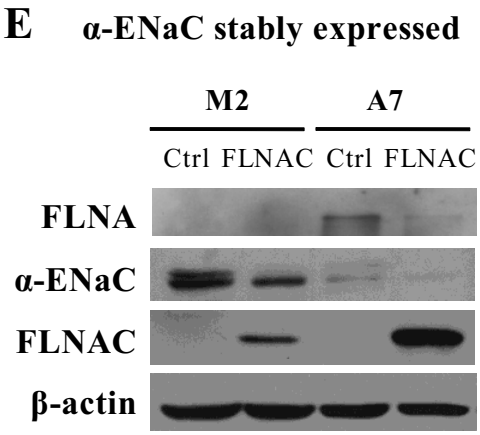
E
α-ENaC stably expressed
M2
A7
Ctrl
FLNAC
Ctrl
FLNAC
FLNA
α-ENaC
FLNAC
β-actin

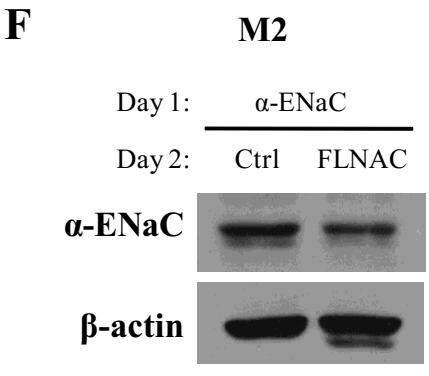
F
M2
Day 1:
α-ENaC
Day 2:
Ctrl
FLNAC
α-ENaC
β-actin

Figure 5-5. **Effect of FLNAC on the expression and subcellular distribution of α-ENaC.** A, effect of FLNAC on the total expression of α-ENaC. Representative data showing the expression of α-ENaC in each individual oocyte assessed by WB. B, representative data showing the effect of FLNAC on the plasma membrane expression of α-ENaC by biotinylation assay (n = 3). Expressions of Na^+/K^+-ATPase, calreticulin, and β-actin serve as controls. C, representative IHC data, using anti-α-ENaC antibody PA1–920A, showing the staining of α-ENaC with or without FLNAC co-expression (n = 3). D, effect of FLNAC on the amiloride-sensitive currents (at −50 mV) normalized by the surface membrane density of α-ENaC assessed by IHC (n = 4). E and F, regulation of α-ENaC expression by FLNAC in M2 and A7 cells. E, M2 and A7 cells stably expressing α-ENaC were transfected with FLNAC for 48 hr. WB was performed to check the expression level with anti-FLNA E-3, anti-α-ENaC 324870, anti-FLNA H-300, and β-actin C-4 for normalization. F, M2 cells were transiently transfected with α-ENaC, following by transfection the next day with FLNAC or an empty vector pcDNA3.1 (negative control *(*Ctrl*)*. Cell lysates were collected after 48 hr. α-ENaC expression was detected by WB using anti-α-ENaC 324870 antibody and controlled by β-actin C-4.

5.4.4 Modulation of α-ENaC channel function by FLNAC in planar lipid bilayer

Our data obtained from *Xenopus* oocytes indicated that FLNA inhibits ENaC single channel activity, in addition to modestly reducing its expression. To verify the inhibition of channel activity, we utilized planar lipid bilayer electrophysiology in combination with tandem affinity purification to purify full-length α-ENaC proteins from the MDCK stable cell line and with *E. coli* purification of FLNAC. We have previously modified and improved the vector construct and affinity purification protocol for use with TRPP2 and TRPP3 channels (217). Indeed, purified α, β, and γ subunits were detectable by Coomassie Blue staining and WB (Figure 5-6 A). After α-ENaC was reconstituted into lipid membrane, single channel openings were observed and showed single channel conductance value compatible with the activities of α-ENaC channels (Figure 5-6 B). In fact, in the presence of 150 mM *cis*-NaCl, single channel conductance was in the 18–21 picosiemens range, larger than when all α, β, and γ subunits are co-expressed, which is consistent with previous reports (288,289). We then introduced purified FLNAC proteins into the *cis* chamber of the lipid bilayer system to examine whether/how FLNAC affects ENaC single channel activity. We found that addition of FLNAC, but not of control solution containing denatured (boiled for 5–10 min) FLNAC, substantially inhibits the open probability (NP_o) and mean current, but not the mean open time, of α-ENaC channels (Figure 5-7). The corresponding NP_o and mean current values at +40 mV decreased from 2.0 ± 0.4 to 0.5 ± 0.2 ($n = 4$; $p = 0.005$, by paired *t*-test) and from 4.1 ± 1.2 to 1.1 ± 0.4 pA ($n = 4$; $p = 0.01$), respectively (Figure 5-7 C). These experiments demonstrate that FLNAC suppresses ENaC single channel activities, presumably through direct binding. Of note, based on our immunofluorescence experiments (Figure 5-5 C), co-expression of FLNA modestly decreased the plasma membrane expression of ENaC (to 78%), presumably through regulating

the half-life of ENaC on the plasma membrane. In contrast, because artificial lipid bilayer has no intracellular systems and FLNA proteins were present during experiments only for short time, we can presume that FLNA reduces the P_o value and has no effect on the number of ENaC channels on the bilayer.

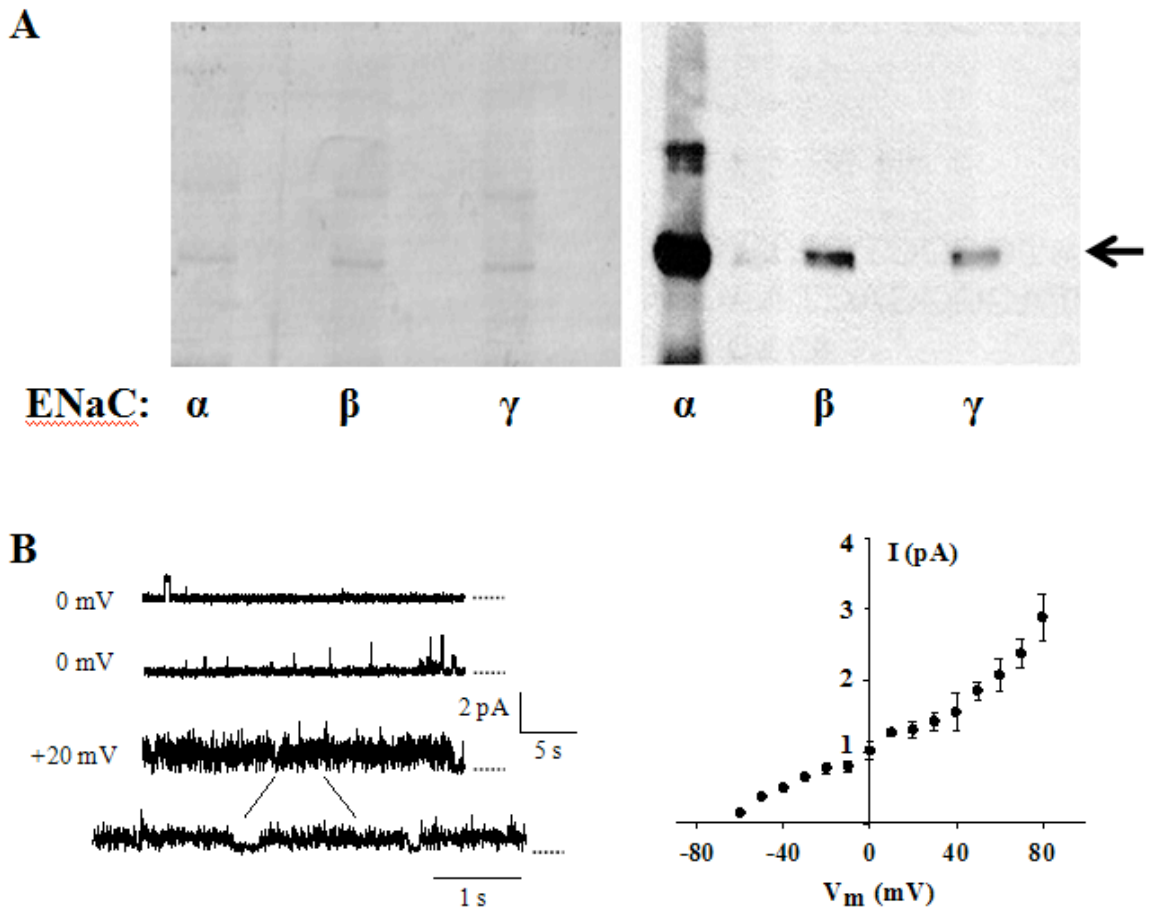

Figure 5-6. Tandem affinity purification of human α-, β-, and γ-ENaC from MDCK stable cell lines and channel function of α-ENaC reconstituted in lipid bilayer. A, purified human α-, β-, and γ-ENaC proteins visualized by Coomassie blue staining (*left panel*) and WB (*right panel*), as indicated by the arrow. All proteins were purified from MDCK cell lines stably transfected with α-, β- and γ-ENaC cDNAs in the pGTAP3F vector. Antibodies against α-, β- and γ-ENaC (Santa Cruz) were used for WB**. B,** representative tracings obtained using purified α-ENaC channels reconstituted in the lipid bilayer system (*left panel*) and current-voltage relationship (*right panel*). Single channel activities were recorded under an asymmetrical condition (150/15 mM NaCl on *cis/trans*). Dotted lines indicate closed states.

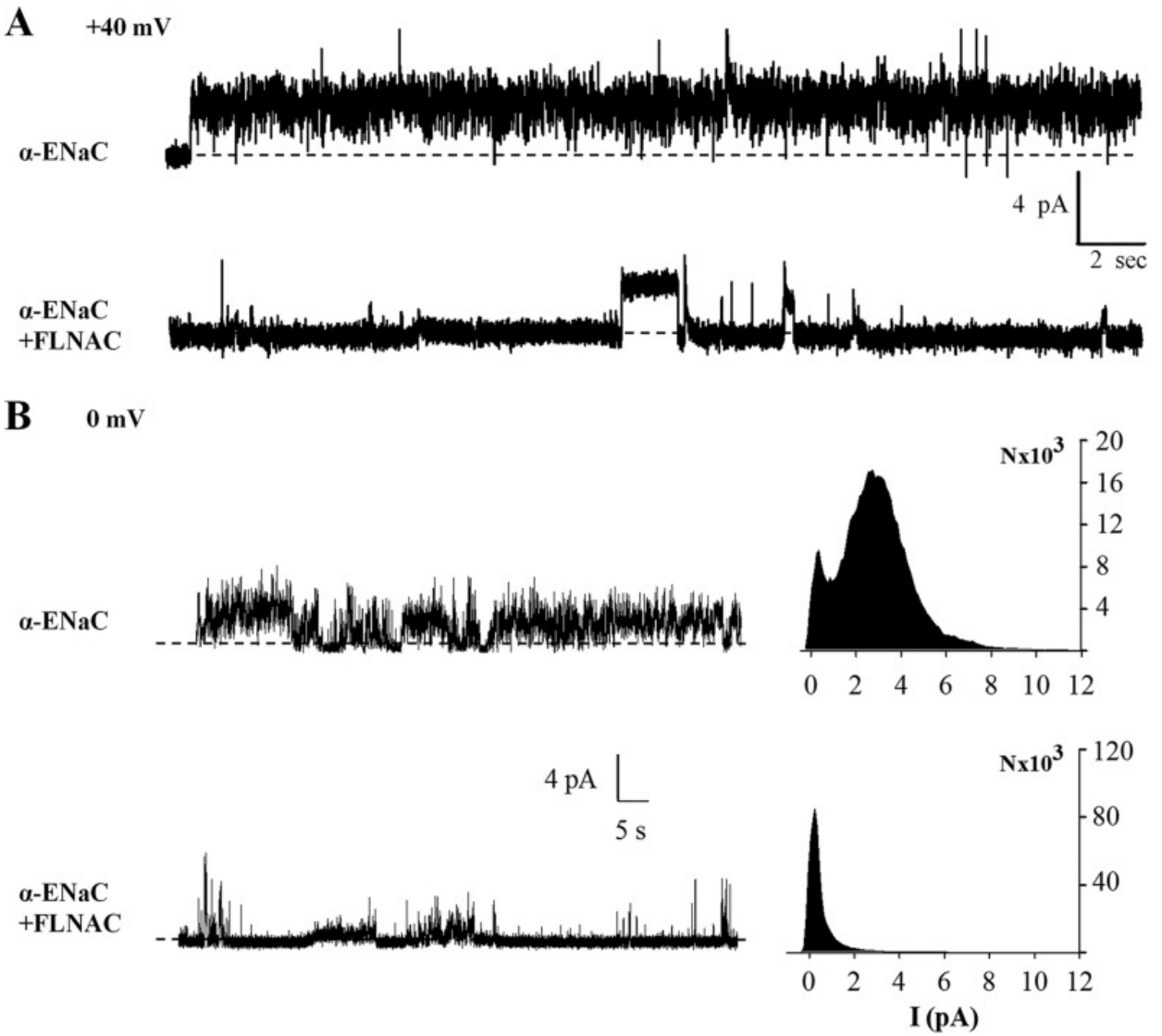
A
+40 mV
α-ENaC
4 pA
2 sec
α-ENaC
+FLNAC
B
0 mV
α-ENaC
Nx10³
20
16
12
8
4
0 2 4 6 8 10 12
4 pA
5 s
α-ENaC
+FLNAC
Nx10³
120
80
40
0 2 4 6 8 10 12
I (pA)

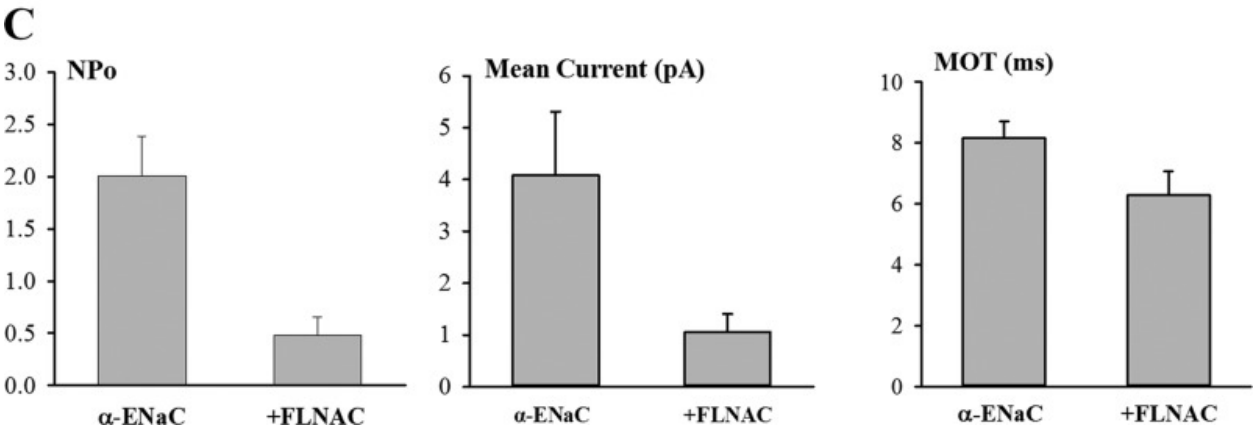
C
NPo
3.0
2.5
2.0
1.5
1.0
0.5
0.0
α-ENaC
+FLNAC
Mean Current (pA)
6
5
4
3
2
1
0
α-ENaC
+FLNAC
MOT (ms)
10
8
6
4
2
0
α-ENaC
+FLNAC

Figure 5-7. Regulation of α-ENaC channels by FLNAC in a lipid bilayer system. A, representative tracings of reconstituted α-ENaC at +40 mV before and after adding FLNAC to the *cis* chamber. *cis* chamber, 150 mM NaCl; *trans* chamber, 15 mM NaCl. B, representative tracings recorded at +0 mV before and after adding FLNAC to the *cis* chamber, and density plots. Dashed lines in A and B indicate closed states. C, open probability (NP_o) was calculated and averaged from different patches recorded at +40 mV in the absence and presence of FLNAC (n = 4; p = 0.005, by paired t test). Mean current and mean open time (*MOT*) were also calculated from the same patches and similarly compared (p = 0.01 and 0.07, respectively).

5.5 DISCUSSION

In this study, we firmly characterized the physical interaction between ENaC and filamin by various *in vitro* and *in vivo* protein-protein binding approaches. Yeast two-hybrid and *E. coli* GST pull-down assays showed interaction between soluble parts of an ENaC subunit and a filamin isoform, presumably through direct binding. In comparison, mammalian cells are more *in vivo* models, and co-IP assays allowed us to show that two full-length proteins interact with each other, although this technique does not tell whether they bind each other directly. Also, when a partner protein is overexpressed, the exhibited interaction may be nonspecific or of an artifactual nature. It was thus important to verify the interaction using native mammalian cells. The fact that the two proteins are in the same complex *in vivo* leads to the question as to what is the functional role of the physical interaction.

Using *Xenopus* oocyte expression model for IHC assays, we showed that the presence of filamin C terminus modestly reduces the surface membrane targeting of α-ENaC. Because similar reductions in the ENaC total expression and surface membrane targeting are insufficient to account for substantially reduced ENaC currents, we concluded that filamin reduces the activity of each individual ENaC channel complex located on the plasma membrane. This was in fact directly demonstrated when comparing normalized amiloride-sensitive currents in the presence and absence of FLNA co-expression (Figure 5-5 D). Of note, it is still possible that the inhibition of ENaC by filamin is indirect, e.g. by an intermediate protein. In a recent study, we utilized blocking peptides to disrupt the physical binding between the TRPP3 channel and the RACK1 protein, which abolished the inhibitory effect of RACK1 on TRPP3, demonstrating that the inhibition is mediated by direct physical binding (240). In the present study we performed lipid bilayer experiments using purified

ENaC and filamin C terminus for several purposes. First, it confirmed the inhibitory effect of filamin observed in oocytes. Second, it showed that channel inhibition is through direct binding between filamin and α-ENaC. Third, it allowed characterizing ENaC single channel parameters, including NP_o, single channel conductance, and MOT. In particular, we found that NP_o but not single channel conductance is inhibited by filamin, indicating that filamin gates channel opening through binding to a site in ENaC outside the channel pore.

Given that ENaC is highly selective to Na^+ and the specific effect of amiloride blockade in oocytes, the predicted reversal potential for an amiloride-sensitive I-V curve should be about 70 mV in the presence of 100 mM extracellular Na^+, assuming 6.2 or 6.6 mM intracellular Na^+ (290,291). However, our observed a reversal potential averaged 1.0 ± 0.6 mV (n = 6) and 7.1 ± 4.5 mV (n = 3) in the absence and presence of FLNAC, respectively (also see Figure 5-4 C). Our results are in agreement with previously reported shift in the reversal potential or resting potential (290,291). This should be, at least in part, due to loading of Na^+ through overexpressed ENaC channels during incubation for which Na^+/K^+-ATPases are unable to counterbalance. Indeed, we observed that oocytes expressing αβγ-ENaC have depolarized resting membrane potentials averaging −2.1 ± 1.3 mV (n = 6). This indicates that Na^+ permeability (via ENaC), in addition to K^+ and Cl^- permeabilities (via native K^+ and Cl^- channels), plays an important role in defining the oocyte resting potential and results in significant intracellular Na^+ accumulation. Of note, intracellular concentrations of K^+ and Cl^-, in addition to that of Na^+, also significantly changed in oocytes overexpressing ENaC (291), indicating that K^+ and Cl^- permeabilities remain important for the resting potential. The resting potential became more negative and oocytes appeared healthier when 2 μM amiloride was added to the incubation medium, FLNAC was co-expressed (−10.2 ± 1.6 mV, n = 3), and/or

only the α subunit was expressed, presumably because intracellular Na^+ concentration was much lower than extracellular Na^+ concentration under these conditions, as a consequence of much reduced Na^+ loading via ENaC. Consistently, under these conditions, the reversal potential for the amiloride-sensitive I-V became more positive (7.1 mV, with FLNA co-expression; also see e.g. Figure 5-4, C and E).

The mammalian cytoskeleton is composed of three major protein families as follows: microfilaments, microtubules, and intermediate filaments, as well as numerous cytoskeleton-associated proteins (292). They are implicated in cell shape, motility, signal transduction, vesicular trafficking and function of ion channel/transporter/receptor. The actin-based cytoskeleton has been shown to interact indirectly and directly with ion channels and membrane transport proteins (293-295). The hypothesis that actin cytoskeleton is directly involved in regulation of ENaC was first supported by a immunocolocalization study showing ENaC channels always present in close proximity to actin filaments and further demonstrated by characterizing the modulatory role of actin filament organization on ENaC channel activity in A6 epithelial cells (152). In this study, Cantiello *et al.* also revealed a potential functional regulation of ENaC by full-length filamin protein in A6 cells. However, whether there is a physical interaction between ENaC and filamin, which domains are involved in the interaction, and whether the functional regulation is through the physical interaction remained unclear. This study specifically answered these questions by various *in vitro* and *in vivo* protein-protein interaction approaches and by electrophysiological analyses.

It was reported that dimerization of filamin is mediated by a C terminal domain and that the majority of filamin interacting partners bind its C terminus as well (257). Filamin N terminus binds actin thereby cross-linking cortical actin into a dynamic three-dimensional

structure. Our data suggest that the binding of FLNAC to ENaC C terminus is enough to inhibit the channel function. Thus, it is possible that the filamin N terminus serves to stabilize ENaC via cross-linking with the actin network. Future studies would examine whether and how the filamin-ENaC interaction is critical to the physiological functions currently known to be associated with ENaC or filamins.

CHAPTER 6

GENERAL DISCUSSION

6.1 Transient Receptor Potential Polycystins (TRPPs) and diseases

6.1.1 Polycystins and ADPKD

Polycystin-1 and Polycystin-2

Transient Receptor Potential Polycystins (TRPPs) form a subfamily of the TRP superfamily of ion channels, which function in the sensory system and activated by a variety of stimuli such as heat/cold, light, sound, chemicals, hormones and mechanical forces (296). TRPPs have been found in association with autosomal dominant polycystic kidney disease (ADPKD), which is characterized by the formation of fluid-filled cysts in the kidney. About 95% cases of ADPKD result from mutations of either *PKD1* or *PKD2* gene, which encode polycystin-1 (PC1, also called TRPP1) and polycystin-2 (PC2, also called TRPP2), respectively (297). However, the mechanism of how polycystins cause ADPKD remains unknown. It was reported in 2003 that PC1 and PC2 co-localize in the primary cilia of kidney epithelium and contribute to mechanosensation (25). And cilia dysfunction caused by either PC1 or PC2 deficiency results in abnormal kidney development and cyst formation (297). Whereas, another study showed that PC2 alone is targeted to the plasma membrane (PM) of renal epithelium (200) and functions as a Ca^{2+} permeable cation channel that contributes to the transport of cation entry in renal segments (57), suggesting a role of PM PC2 in the development and progression of ADPKD. In addition, ER resident PC2 is involved in the regulation of cellular Ca^{2+} homeostasis (59,67), which has been found to be disrupted in ADPKD cases (298). Thus, it is controversial that which subcellular compartment/s of PC2 is involved in ADPKD pathogenesis. Cilia PC2 is more likely to mediate the kidney phenotype of ADPKD, as a number of cilia genes have been shown to be related to cysts formation (272). Even though, it is still valuable to study the roles of PC2 in different organs and compartments,

because 1) ADPKD is not limited to kidney phenotypes but with abnormalities in other organs such as the liver, pancreas, brain, heart and reproductive systems. Notably, cardiovascular abnormality is one of the two leading causes of death in patients with ADPKD (4). The cardiovascular phenotype caused by PC2 is possibly due to its function in regulating intracellular Ca^{2+} homeostasis in smooth muscle cells (299); 2) PC2 is also expressed in non-epithelial cells, such as muscle cells (smooth, skeletal and cardiac), endothelial cells, nucleated red cells, and neurons (207), where the function is largely unknown; 3) In addition of the cation channel property, PC2 has been shown to have other functions, e.g., to regulate other receptors and kinases such as IP3R (66), RyR (31), pancreatic ER-resident eIF2α kinase (PERK) (211), and to participate in handling cellular stress conditions (300).

Polycystin-2-like-1 (TRPP3)

Polycystin-2-like-1 (PCL), also called TRPP3, is another member of the TRPP subfamily and next to TRPP2 in the phylogenetic tree (296). However, it has not been found to be linked to ADPKD. This is interesting because PC2 and PCL (TRPP2 and TRPP3) share many similarities in terms of amino acid sequence, structural topology, tissue distribution, and channel properties. One of the possibilities that result in the physiological difference is their cell type specific localization in the tissues. E.g., in the kidney, PC2 is widely distributed in all renal segments including the proximal tubule, distal tubule, and collecting duct (72,301). And cysts have been found to be formed in all the renal tubules. Whereas, PCL is restricted in the apical membrane of the inner medullary collecting duct, but not in the proximal tubule, descending limb, ascending thick limb, or the distal convoluted tubule (302). Therefore PCL deficiency could be easily compensated by PC2, leading to no disease phenotype, but not verse

vice. Another possibility is their distinct Ca^{2+} regulatory properties though both can be activated by intracellular Ca^{2+} (38,285). PC2 is tightly regulated by intracellular Ca^{2+} that low range of Ca^{2+} permeation induces Ca^{2+} inactivation (self-inactivation) (26). However as to PCL, regardless of intracellular Ca^{2+}, after each Ca^{2+} activation the channel undergoes desensitization which needs a recovery time of 5-10 min. This difference is probably due to the function of their EF hand domains, that the EF hand of PC2 enables channel activation (62), while of PCL prevents the channel from over activation (39). Physiologically, this Ca^{2+}-regulated channel property enables PC2 to rapidly respond to Ca^{2+} oscillations while weakens the role of PCL in sensing fluctuated Ca^{2+}, especially in the myocytes of heart, the defect of which is one of the major deaths causing reason of ADPKD (4).

6.1.2 Polycystins and cancer

PKD cystic cells display characteristics of fetal, dividing, or cancerous cells, such as intense canonical (β-catenin) Wnt signaling activity and high expression of cellular factors such as c-Myc, TNFα, and TGF-β1 (303-305). Though cystic cells share many cellular features with cancer cells, the functional implication of polycystins in cancer is rarely reported and the current two reports seem to be controversial in terms of whether polycystins are 'tumor suppressor' or 'oncoprotein'.

Zhen *et al* firstly found in 2008 that PC1 induces apoptosis of cancer cells and arrests cells in the G0/G1 phase, which thus suppress tumor growth (306). However, in the non-cancerous MDCK cells, PC1 was found to induce resistance to apoptosis (80), indicating that the function of polycystins in cancer cells maybe different with non-cancerous kidney cells. In early 2015, Gargalionis *et al* reported that polycystins, especially PC1, increase cancer cell proliferation and migration and thus is proposed as an oncoprotein (307). This is in controversy with previous finding that PC1/PC2 overexpression inhibits cell proliferation in MDCK cells (80,211). Even though the function of polycystins in non-cancerous and cancer cell lines may be different, the use of PC1 anti-loop antibody to 'knockdown' PC1 in Gargalionis' study is less convincing because of lacking of proper control. PBS, rather than the non-immune IgG containing solution, was used as a control treatment, which makes it hard to assess the specificity of anti-PC1 antibody.

The implication of polycystins in cancer is a new notion and very exciting. However, clinical analysis of the samples from colorectal cancer (CRC) patients reveals that there is no regular expression pattern of polycystins in cancer tissues compared with the adjacent

non-cancerous tissues. However, the expression of polycystins was found to correlate with CRC severity and the patients' survival rate. (307).

Taken together, *PKD* gene/polycystins may not function to induce cancer as the well-known oncogenes/proteins such as c-myc, Ras and Wnt do. However, they may be downstream molecules of the cancer signaling pathways and function to regulate cancer development given polycystins are involved in cell proliferation and apoptosis pathways (235). Thus polycystins are possible to serve as potential biomarkers to indicate cancer stages.

6.2 Regulation of PC2 by FLNA

The major part of this thesis is focusing on the regulation of PC2 by its binding partner, an actin-binding cytoskeleton protein FLNA, in terms of three aspects, expression, localization and channel function. We have found that FLNA regulates PC2 mRNA level that determines protein synthesis, protein degradation, PM stability and single channel activity. This is interesting but also puzzling that FLNA appears to affect several aspects of PC2. One of the controversies is that on one hand FLNA stabilizes PC2 total and plasma membrane expression (Chapter 3), however, on the other hand inhibits PC2 single channel activity (Chapter 2). It remains hard to interpret the physiological significance until we discovered a Ca-dependent physical interaction and functional regulation of PC2 and FLNA, indicating that in live cells, PC2-filamin interaction and regulation is a dynamic process that responds to intracellular Ca^{2+} fluctuation.

6.2.1 Expression

The steady-state level of PC2 equals protein synthesis minus degradation. In this thesis, FLNA was found to be associated with lower mRNA level (data not shown), which results in decreased protein synthesis of PC2 (Chapter 3). The mechanism of how FLNA regulates the mRNA level of *PKD2* remains to be determined in future studies. However, it was previously reported that cytoplasmic FLNA regulates gene transcription through binding with transcription factor PEBP2/CBF in the cytoplasm and preventing it from entering the nucleus where it would interact with transcription factor Runx1 to induce transcription of a number of genes (174,257), e.g., interleukin-3 (257,308). It was also known that FLNA sequesters transcription factor p73α in the cytoplasm, which results in transcriptional repression of

cell-cycle inhibitor p21Waf1/Cip1 (175). FLNA also represses the transcriptional regulatory activity of FOXC1 (309). Further, a recent report found that FLNA is present in the nucleolus where it associates with the RNA polymerase transcription machinery to suppress the transcription of ribosomal RNA (180). Therefore, it is possible that *PKD2* gene is a downstream target of FLNA-regulated transcription factors.

On the other hand, FLNA was found to slow down PC2 degradation by anchoring it to the actin filament and forming PC2-filamin-actin triplex. This is not a novel mechanism as previous reports have indicated that filamin links several membrane proteins to the actin cytoskeleton, such as dopamine receptors and platelet glycoprotein Ibα (244,251). However there has never been any direct and firm demonstration about how filamin mediates the link. In this thesis, I demonstrated for the first time the presence of the membrane protein-filamin-actin triplex in live cells and confirmed the central role of filamin in mediating an interaction of PC2 with the actin network.

6.2.2 Localization

We have found that FLNA stabilizes the PM localization of PC2, and this is through the same mechanism by anchoring to the actin filaments that prevents membrane protein retrieval/degradation. It was reported that FLNA stabilizes the surface membrane localization and/or inhibit retrieval/degradation of several PM localized proteins such as the calcitonin receptor (229), chloride channel CFTR (242), and Ca-sensing receptor (247).

Previous studies have shown that endogenous PC2 is present on the PM and cilia of native tissues and some cell lines (25,57,301), while overexpressed form is localized almost entirely in the ER (60,310). In this thesis, we have demonstrated that hetero-expressed PC2 is targeted to the PM, though in small proportion, and is anchored to actin filaments by FLNA. Overall, our studies added PC2 to the list of protein targets of FLNA, in terms of PM localization and stabilization.

6.2.3 Functional regulation

We have demonstrated that filamin regulates PC2 channel function in a Ca^{2+}-dependent manner, i.e. filamin shows an inhibitory effect on PC2 single channel activity only in the presence of high Ca^{2+}. A previous paper has shown that PC2 extracted from human placenta membranes, but not the *in vitro* translated PC2, can be regulated by intracellular Ca^{2+}, suggesting that it is not PC2 but a partner protein/s which attaches to it, that is responsive to the regulation of Ca^{2+} (270). In this case, filamin is one of the possible partner proteins that are responsible for the Ca^{2+} regulated PC2 channel funtion. Of note, it is possible that other linker proteins such as α-actinin and tropomyosin are also involved in the Ca^{2+} sensation and activation of PC2.

This Ca^{2+}-dependent regulation of PC2 by filamin is likely achieved by Ca^{2+}-dependent physical binding. High Ca^{2+} enhances the binding strength of PC2 and filamin. Thus, this physical binding is not only for the purpose of membrane protein stabilization as stated in Chapter 2.2, but also for the purpose of channel functional regulation. In the presence of low cytosolic Ca^{2+}, filamin mainly functions to anchor PC2 on the membrane. While once the cytosolic Ca^{2+} increases, filamin inhibits PC2 channel activity by enhancing their physical binding. Both PC2 N- and C- termini bind FLNA, but the binding strength changed oppositely in response to Ca^{2+}. It is possible that the binding of FLNA with one terminus is for the purpose of stabilization and with another one for the purpose of functional regulation. Future study can be conducted to narrow down the domains on PC2 N- and C- tails that bind FLNA and to investigate their specific function. Briefly, cDNAs encoding PC2 N-/C- termini will be divided into several fragments, amplified by PCR, and then constructed into proper vector for expression. The expressed protein fragments will be used in co-IP experiemens to

narrow down the binding domain on PC2 N-/C- tails with FLNA and to identify the Ca^{2+} responding motifs. This will help better understand how FLNA regulates PC2 activity and its sensitivity to intracellular Ca^{2+}.

6.2.4 Physiological importance of PC2-FLNA interaction

The physiological relevance of PC2-FLNA interaction largely depends on the net effect of this complex. By live cell Ca^{2+} imaging, we observed disrupted Ca^{2+} homeostasis in intact cells with either component of the complex deficient. Although, no direct evidence has been found to indicate the significance of PC2-FLNA complex in animal models. In zebrafish, embryos with *pkd2* morpholino (MO) KD or those with alterations in other genes that lead to decreased PC2 level develop renal cysts and tail dorsal curvature phenotype after 2-3 dpf (98,99). However, KD of *flna* results in more severe phenotype with developmental deficiency (311), possibly becasue FLNA affects a number of other significant protein partners other than PC2. Thus in order to study the role of PC2-FLNA complex, a strategy specifically targeting to their interaction is more reliable. In the mouse model, homozygous *Pkd2*$^{-/-}$ (101) and *Flna*$^{-/-}$ (192) mice are embryonic lethal due to severe cardiac structure defect but heterozygous mice show normal development. *Pkd2*$^{+/-}$ mice develop cysts in the kidney and liver from 3-4 months old (101) and *Flna*$^{+/-}$ mice die in the first 3-4 months with many anomalies including heart dilation (312). Thus, *Pkd2*$^{+/-}$/*Flna*$^{+/-}$ mice are not a good model to study the physiological significance of PC2-FLNA complex in terms of the kidney phenotype. Tissue specific conditional knockout mice will probably help in this case. Additionally, the heart phenotype seems interesting to study PC2-FLNA complex given both have been linked to cardiovascular abnormalities.

6.3 Regulation of PC2 by the cytoskeleton

A number of PC2 interacting partners have been identified so far, among which half are cytoskeletal proteins (213). Interaction with the cytoskeleton has been found to be important for the regulation of PC2 expression, localization and channel function (213). Actin filaments, one of the predominant form of the cytoskeleton, have been shown to be necessary for PC2 channel activity and disruption of the actin filament totally abolishes PC2 channel activation caused by different simulators (214). This indicates that it is not PC2 alone, but the PC2-actin filament complex, that confers PC2 sensitivity to the stimuli. There is no evidence pointing to direct interaction between PC2 and actin, but an intermediate protein α-actinin (45) was previously suggested to mediate the effect of actin filament on PC2 regulation. In this thesis, we discovered that filamin, acts as another intermediate protein between PC2 and the actin filament and provided direct evidence that filamin mediates the interaction of PC2 and actin, and regulates PC2 channel function. Even though both filamin and α-actinin are actin-binding proteins, they have opposite effect in terms of regulating PC2 channel function, with filamin as an inhibitor (237) while alpha-actinin as a stimulator (45). Interestingly, in the absence of Ca^{2+}, filamin losses its inhibitory effect on PC2 with weakened physical binding, while α-actinin enhances its binding strength. We reasoned that physical binding should be for the purpose of (channel) functional regulation. Thus, it is reasonable to predict that α-actinin should gain its stimulatory effect on PC2 channel function under the condition of no Ca^{2+} or low Ca^{2+}. Taken together, a working model was proposed that these two actin-binding proteins (possibly more), may function synergistically and compensatorily to regulate the channel function of PC2. PC2 functions as either PM non-selective cation channel or ER Ca^{2+} release/leak channel. Both filamin and α-actinin bind PC2 for structural purpose, but regulate PC2 channel activity

oppositely. In the presence of low cytosolic Ca^{2+}, filamin binds PC2 weakly with no inhibitory effect, while α-actinin binds stronger with PC2 and activates the channel; In case that the cytosolic Ca^{2+} increased, filamin enhances its binding with PC2 to replace actinin, and inhibits PC2 channel activity to avoid Ca^{2+} overloading to the cytosol. The Ca^{2+}-dependent binding of PC2-FLNA and PC2-α-actinin was previously stated, that Ca^{2+} enhances PC2-FLNA binding (313) while weakens PC2-α-actinin interaction (45), but from separate reports. Thus, it would be great if the two Ca^{2+}-regulated Co-IP can be revealed in one competitive Co-IP experiment, to demonstrate that filamin and α-actinin compete for PC2 binding and different Ca^{2+} conditions favours the binding of PC2 with one cytoskeleton. As well, the functional effect of the two actin-binding proteins under different Ca^{2+} condition can be tested in one lipid bilayer system.

6.4 ENaC channel function and regulation by filamin

The current known ENaC caused human disease such as Liddle Sydrome and pseudohypoaldosteronism type-1 are believed due to dysfunction of kidney ENaC. However a significant physiological role of ENaC in other organs has been clearly demonstrated. E.g., in the lung, ENaC-mediated Na^+ transport is important to maintain the airway surface fluid. In fetal mouse lung, the ENaC expression was sharply increased in the late fetal and early postnatal life (314) and αENaC knock out mice die soon after birth from respiratory failure due to severe defect of lung liquid clearance (126). In contrast to the kidney, Na^+ transport in the fetal lung can be maintained efficiently by only two functional subunits, i.e. the pairs of α-β (315) or α-γ (316). This heterogeneity of the subunit compositions in different organs could explain the phenotype of ENaC gene related disease.

In addition, ENaC is indirectly involved in the autosomal recessive polycystic kidney disease (ARPKD), which is also characterized by cystogenesis in the renal collecting ducts, but mostly in infants and children (317). ENaC was found to be regulated by the ARPKD disease causing protein fibrocystin, and increased expression/function of ENaC is believed to contribute to the abnormal cystic fluid transport and ARPKD pathophysiology (318).

In this thesis, we have reported a physical interaction and functional regulation of ENaC by actin binding protein filamin. As α-ENaC was found to co-localize with PC2 on the primary cilia of renal epithelial cells (319) and PC2 also directly binds filamin (Chapter 2), these results together suggest a link of ENaC with ADPKD through the cytoskeleton. It is possible that filamin mediates PC2-ENaC interaction through PC2-filamin-ENaC triplex, or PC2 and ENaC compete for the binding with filamin for channel stabilization and functional regulation purpose. In any case, ENaC is likely one of the downstream targets of PKD proteins. Thus,

mutations of ENaC are not cystogenesis but ENaC has been found to be modulated in PKD cases.

6.5 REFERENCES

1. (1988) A standard nomenclature for structures of the kidney. The Renal Commission of the International Union of Physiological Sciences (IUPS). *Pflugers Arch* **411**, 113-120
2. Torres, V. E., Harris, P. C., and Pirson, Y. (2007) Autosomal dominant polycystic kidney disease. *Lancet* **369**, 1287-1301
3. Harris, P. C., and Torres, V. E. (2009) Polycystic kidney disease. *Annu Rev Med* **60**, 321-337
4. Fick, G. M., Johnson, A. M., Hammond, W. S., and Gabow, P. A. (1995) Causes of death in autosomal dominant polycystic kidney disease. *J Am Soc Nephrol* **5**, 2048-2056
5. Hateboer, N., v Dijk, M. A., Bogdanova, N., Coto, E., Saggar-Malik, A. K., San Millan, J. L., Torra, R., Breuning, M., and Ravine, D. (1999) Comparison of phenotypes of polycystic kidney disease types 1 and 2. European PKD1-PKD2 Study Group. *Lancet* **353**, 103-107
6. Rossetti, S., Burton, S., Strmecki, L., Pond, G. R., San Millan, J. L., Zerres, K., Barratt, T. M., Ozen, S., Torres, V. E., Bergstralh, E. J., Winearls, C. G., and Harris, P. C. (2002) The position of the polycystic kidney disease 1 (PKD1) gene mutation correlates with the severity of renal disease. *J Am Soc Nephrol* **13**, 1230-1237
7. Magistroni, R., He, N., Wang, K., Andrew, R., Johnson, A., Gabow, P., Dicks, E., Parfrey, P., Torra, R., San-Millan, J. L., Coto, E., Van Dijk, M., Breuning, M., Peters, D., Bogdanova, N., Ligabue, G., Albertazzi, A., Hateboer, N., Demetriou, K., Pierides, A., Deltas, C., St George-Hyslop, P., Ravine, D., and Pei, Y. (2003) Genotype-renal function correlation in type 2 autosomal dominant polycystic kidney disease. *J Am Soc Nephrol* **14**, 1164-1174
8. Paterson, A. D., Magistroni, R., He, N., Wang, K., Johnson, A., Fain, P. R., Dicks, E., Parfrey, P., St George-Hyslop, P., and Pei, Y. (2005) Progressive loss of renal function is an age-dependent heritable trait in type 1 autosomal dominant polycystic kidney disease. *J Am Soc Nephrol* **16**, 755-762
9. Persu, A., Duyme, M., Pirson, Y., Lens, X. M., Messiaen, T., Breuning, M. H., Chauveau, D., Levy, M., Grunfeld, J. P., and Devuyst, O. (2004) Comparison between siblings and twins supports a role for modifier genes in ADPKD. *Kidney Int* **66**, 2132-2136
10. Qian, F., Watnick, T. J., Onuchic, L. F., and Germino, G. G. (1996) The molecular basis of focal cyst formation in human autosomal dominant polycystic kidney disease type I. *Cell* **87**, 979-987
11. Pei, Y., Watnick, T., He, N., Wang, K., Liang, Y., Parfrey, P., Germino, G., and St George-Hyslop, P. (1999) Somatic PKD2 mutations in individual kidney and liver cysts support a "two-hit" model of cystogenesis in type 2 autosomal dominant polycystic kidney disease. *J Am Soc Nephrol* **10**, 1524-1529
12. Lantinga-van Leeuwen, I. S., Dauwerse, J. G., Baelde, H. J., Leonhard, W. N., van de Wal, A., Ward, C. J., Verbeek, S., Deruiter, M. C., Breuning, M. H., de Heer, E., and Peters, D. J. (2004) Lowering of Pkd1 expression is sufficient to cause polycystic kidney disease. *Hum Mol Genet* **13**, 3069-3077
13. Kurbegovic, A., Cote, O., Couillard, M., Ward, C. J., Harris, P. C., and Trudel, M. (2010) Pkd1 transgenic mice: adult model of polycystic kidney disease with extrarenal and renal phenotypes. *Hum Mol Genet* **19**, 1174-1189

14. Hopp, K., Ward, C. J., Hommerding, C. J., Nasr, S. H., Tuan, H. F., Gainullin, V. G., Rossetti, S., Torres, V. E., and Harris, P. C. (2012) Functional polycystin-1 dosage governs autosomal dominant polycystic kidney disease severity. *J Clin Invest* **122**, 4257-4273
15. Park, E. Y., Sung, Y. H., Yang, M. H., Noh, J. Y., Park, S. Y., Lee, T. Y., Yook, Y. J., Yoo, K. H., Roh, K. J., Kim, I., Hwang, Y. H., Oh, G. T., Seong, J. K., Ahn, C., Lee, H. W., and Park, J. H. (2009) Cyst formation in kidney via B-Raf signaling in the PKD2 transgenic mice. *J Biol Chem* **284**, 7214-7222
16. Torres, V. E., and Harris, P. C. (2009) Autosomal dominant polycystic kidney disease: the last 3 years. *Kidney Int* **76**, 149-168
17. Chapin, H. C., Rajendran, V., and Caplan, M. J. (2010) Polycystin-1 surface localization is stimulated by polycystin-2 and cleavage at the G protein-coupled receptor proteolytic site. *Mol Biol Cell* **21**, 4338-4348
18. Qian, F., Boletta, A., Bhunia, A. K., Xu, H., Liu, L., Ahrabi, A. K., Watnick, T. J., Zhou, F., and Germino, G. G. (2002) Cleavage of polycystin-1 requires the receptor for egg jelly domain and is disrupted by human autosomal-dominant polycystic kidney disease 1-associated mutations. *Proc Natl Acad Sci U S A* **99**, 16981-16986
19. Yu, S., Hackmann, K., Gao, J., He, X., Piontek, K., Garcia-Gonzalez, M. A., Menezes, L. F., Xu, H., Germino, G. G., Zuo, J., and Qian, F. (2007) Essential role of cleavage of Polycystin-1 at G protein-coupled receptor proteolytic site for kidney tubular structure. *Proc Natl Acad Sci U S A* **104**, 18688-18693
20. Chauvet, V., Tian, X., Husson, H., Grimm, D. H., Wang, T., Hiesberger, T., Igarashi, P., Bennett, A. M., Ibraghimov-Beskrovnaya, O., Somlo, S., and Caplan, M. J. (2004) Mechanical stimuli induce cleavage and nuclear translocation of the polycystin-1 C terminus. *J Clin Invest* **114**, 1433-1443
21. Qian, F., Germino, F. J., Cai, Y., Zhang, X., Somlo, S., and Germino, G. G. (1997) PKD1 interacts with PKD2 through a probable coiled-coil domain. *Nat Genet* **16**, 179-183
22. Peters, D. J., van de Wal, A., Spruit, L., Saris, J. J., Breuning, M. H., Bruijn, J. A., and de Heer, E. (1999) Cellular localization and tissue distribution of polycystin-1. *J Pathol* **188**, 439-446
23. Geng, L., Segal, Y., Peissel, B., Deng, N., Pei, Y., Carone, F., Rennke, H. G., Glucksmann-Kuis, A. M., Schneider, M. C., Ericsson, M., Reeders, S. T., and Zhou, J. (1996) Identification and localization of polycystin, the PKD1 gene product. *J Clin Invest* **98**, 2674-2682
24. Boletta, A., Qian, F., Onuchic, L. F., Bragonzi, A., Cortese, M., Deen, P. M., Courtoy, P. J., Soria, M. R., Devuyst, O., Monaco, L., and Germino, G. G. (2001) Biochemical characterization of bona fide polycystin-1 in vitro and in vivo. *Am J Kidney Dis* **38**, 1421-1429
25. Nauli, S. M., Alenghat, F. J., Luo, Y., Williams, E., Vassilev, P., Li, X., Elia, A. E., Lu, W., Brown, E. M., Quinn, S. J., Ingber, D. E., and Zhou, J. (2003) Polycystins 1 and 2 mediate mechanosensation in the primary cilium of kidney cells. *Nat Genet* **33**, 129-137
26. Gonzalez-Perrett, S., Kim, K., Ibarra, C., Damiano, A. E., Zotta, E., Batelli, M., Harris, P. C., Reisin, I. L., Arnaout, M. A., and Cantiello, H. F. (2001) Polycystin-2, the protein mutated in autosomal dominant polycystic kidney disease (ADPKD), is a

Ca2+-permeable nonselective cation channel. *Proc Natl Acad Sci U S A* **98**, 1182-1187
27. Mochizuki, T., Wu, G., Hayashi, T., Xenophontos, S. L., Veldhuisen, B., Saris, J. J., Reynolds, D. M., Cai, Y., Gabow, P. A., Pierides, A., Kimberling, W. J., Breuning, M. H., Deltas, C. C., Peters, D. J., and Somlo, S. (1996) PKD2, a gene for polycystic kidney disease that encodes an integral membrane protein. *Science* **272**, 1339-1342
28. Geng, L., Okuhara, D., Yu, Z., Tian, X., Cai, Y., Shibazaki, S., and Somlo, S. (2006) Polycystin-2 traffics to cilia independently of polycystin-1 by using an N-terminal RVxP motif. *J Cell Sci* **119**, 1383-1395
29. Streets, A. J., Moon, D. J., Kane, M. E., Obara, T., and Ong, A. C. (2006) Identification of an N-terminal glycogen synthase kinase 3 phosphorylation site which regulates the functional localization of polycystin-2 in vivo and in vitro. *Hum Mol Genet* **15**, 1465-1473
30. Feng, S., Okenka, G. M., Bai, C. X., Streets, A. J., Newby, L. J., DeChant, B. T., Tsiokas, L., Obara, T., and Ong, A. C. (2008) Identification and functional characterization of an N-terminal oligomerization domain for polycystin-2. *J Biol Chem* **283**, 28471-28479
31. Anyatonwu, G. I., Estrada, M., Tian, X., Somlo, S., and Ehrlich, B. E. (2007) Regulation of ryanodine receptor-dependent calcium signaling by polycystin-2. *Proc Natl Acad Sci U S A* **104**, 6454-6459
32. Celic, A., Petri, E. T., Demeler, B., Ehrlich, B. E., and Boggon, T. J. (2008) Domain mapping of the polycystin-2 C-terminal tail using de novo molecular modeling and biophysical analysis. *J Biol Chem* **283**, 28305-28312
33. Petri, E. T., Celic, A., Kennedy, S. D., Ehrlich, B. E., Boggon, T. J., and Hodsdon, M. E. (2010) Structure of the EF-hand domain of polycystin-2 suggests a mechanism for Ca2+-dependent regulation of polycystin-2 channel activity. *Proc Natl Acad Sci U S A* **107**, 9176-9181
34. Kuo, I. Y., Keeler, C., Corbin, R., Celic, A., Petri, E. T., Hodsdon, M. E., and Ehrlich, B. E. (2014) The number and location of EF hand motifs dictates the calcium dependence of polycystin-2 function. *FASEB J* **28**, 2332-2346
35. Yang, Y., Keeler, C., Kuo, I. Y., Lolis, E. J., Ehrlich, B. E., and Hodsdon, M. E. (2015) Oligomerization of the polycystin-2 C-terminal tail and effects on its Ca2+-binding properties. *J Biol Chem* **290**, 10544-10554
36. Schumann, F., Hoffmeister, H., Bader, R., Schmidt, M., Witzgall, R., and Kalbitzer, H. R. (2009) Ca2+-dependent conformational changes in a C-terminal cytosolic domain of polycystin-2. *J Biol Chem* **284**, 24372-24383
37. Celic, A. S., Petri, E. T., Benbow, J., Hodsdon, M. E., Ehrlich, B. E., and Boggon, T. J. (2012) Calcium-induced conformational changes in C-terminal tail of polycystin-2 are necessary for channel gating. *J Biol Chem* **287**, 17232-17240
38. Cai, Y., Anyatonwu, G., Okuhara, D., Lee, K. B., Yu, Z., Onoe, T., Mei, C. L., Qian, Q., Geng, L., Wiztgall, R., Ehrlich, B. E., and Somlo, S. (2004) Calcium dependence of polycystin-2 channel activity is modulated by phosphorylation at Ser812. *J Biol Chem* **279**, 19987-19995
39. Li, Q., Liu, Y., Zhao, W., and Chen, X. Z. (2002) The calcium-binding EF-hand in polycystin-L is not a domain for channel activation and ensuing inactivation. *FEBS Lett* **516**, 270-278
40. Kottgen, M., Benzing, T., Simmen, T., Tauber, R., Buchholz, B., Feliciangeli, S.,

Huber, T. B., Schermer, B., Kramer-Zucker, A., Hopker, K., Simmen, K. C., Tschucke, C. C., Sandford, R., Kim, E., Thomas, G., and Walz, G. (2005) Trafficking of TRPP2 by PACS proteins represents a novel mechanism of ion channel regulation. *EMBO J* **24**, 705-716

41. Giamarchi, A., Feng, S., Rodat-Despoix, L., Xu, Y., Bubenshchikova, E., Newby, L. J., Hao, J., Gaudioso, C., Crest, M., Lupas, A. N., Honore, E., Williamson, M. P., Obara, T., Ong, A. C., and Delmas, P. (2010) A polycystin-2 (TRPP2) dimerization domain essential for the function of heteromeric polycystin complexes. *EMBO J* **29**, 1176-1191
42. Yu, Y., Ulbrich, M. H., Li, M. H., Buraei, Z., Chen, X. Z., Ong, A. C., Tong, L., Isacoff, E. Y., and Yang, J. (2009) Structural and molecular basis of the assembly of the TRPP2/PKD1 complex. *Proc Natl Acad Sci U S A* **106**, 11558-11563
43. Tsiokas, L., Arnould, T., Zhu, C., Kim, E., Walz, G., and Sukhatme, V. P. (1999) Specific association of the gene product of PKD2 with the TRPC1 channel. *Proc Natl Acad Sci U S A* **96**, 3934-3939
44. Wu, Y., Dai, X. Q., Li, Q., Chen, C. X., Mai, W., Hussain, Z., Long, W., Montalbetti, N., Li, G., Glynne, R., Wang, S., Cantiello, H. F., Wu, G., and Chen, X. Z. (2006) Kinesin-2 mediates physical and functional interactions between polycystin-2 and fibrocystin. *Hum Mol Genet* **15**, 3280-3292
45. Li, Q., Montalbetti, N., Shen, P. Y., Dai, X. Q., Cheeseman, C. I., Karpinski, E., Wu, G., Cantiello, H. F., and Chen, X. Z. (2005) Alpha-actinin associates with polycystin-2 and regulates its channel activity. *Hum Mol Genet* **14**, 1587-1603
46. Li, Q., Shen, P. Y., Wu, G., and Chen, X. Z. (2003) Polycystin-2 interacts with troponin I, an angiogenesis inhibitor. *Biochemistry* **42**, 450-457
47. MacKinnon, R. (1991) Determination of the subunit stoichiometry of a voltage-activated potassium channel. *Nature* **350**, 232-235
48. Barrera, N. P., Shaifta, Y., McFadzean, I., Ward, J. P., Henderson, R. M., and Edwardson, J. M. (2007) AFM imaging reveals the tetrameric structure of the TRPC1 channel. *Biochem Biophys Res Commun* **358**, 1086-1090
49. Kedei, N., Szabo, T., Lile, J. D., Treanor, J. J., Olah, Z., Iadarola, M. J., and Blumberg, P. M. (2001) Analysis of the native quaternary structure of vanilloid receptor 1. *J Biol Chem* **276**, 28613-28619
50. Hoenderop, J. G., Voets, T., Hoefs, S., Weidema, F., Prenen, J., Nilius, B., and Bindels, R. J. (2003) Homo- and heterotetrameric architecture of the epithelial Ca2+ channels TRPV5 and TRPV6. *EMBO J* **22**, 776-785
51. Maruyama, Y., Ogura, T., Mio, K., Kiyonaka, S., Kato, K., Mori, Y., and Sato, C. (2007) Three-dimensional reconstruction using transmission electron microscopy reveals a swollen, bell-shaped structure of transient receptor potential melastatin type 2 cation channel. *J Biol Chem* **282**, 36961-36970
52. Tsuruda, P. R., Julius, D., and Minor, D. L., Jr. (2006) Coiled coils direct assembly of a cold-activated TRP channel. *Neuron* **51**, 201-212
53. Garcia-Sanz, N., Fernandez-Carvajal, A., Morenilla-Palao, C., Planells-Cases, R., Fajardo-Sanchez, E., Fernandez-Ballester, G., and Ferrer-Montiel, A. (2004) Identification of a tetramerization domain in the C terminus of the vanilloid receptor. *J Neurosci* **24**, 5307-5314
54. Bai, C. X., Giamarchi, A., Rodat-Despoix, L., Padilla, F., Downs, T., Tsiokas, L., and Delmas, P. (2008) Formation of a new receptor-operated channel by heteromeric

assembly of TRPP2 and TRPC1 subunits. *EMBO Rep* **9**, 472-479
55. Zhang, P., Luo, Y., Chasan, B., Gonzalez-Perrett, S., Montalbetti, N., Timpanaro, G. A., Cantero Mdel, R., Ramos, A. J., Goldmann, W. H., Zhou, J., and Cantiello, H. F. (2009) The multimeric structure of polycystin-2 (TRPP2): structural-functional correlates of homo- and hetero-multimers with TRPC1. *Hum Mol Genet* **18**, 1238-1251
56. Kobori, T., Smith, G. D., Sandford, R., and Edwardson, J. M. (2009) The transient receptor potential channels TRPP2 and TRPC1 form a heterotetramer with a 2:2 stoichiometry and an alternating subunit arrangement. *J Biol Chem* **284**, 35507-35513
57. Luo, Y., Vassilev, P. M., Li, X., Kawanabe, Y., and Zhou, J. (2003) Native polycystin 2 functions as a plasma membrane Ca2+-permeable cation channel in renal epithelia. *Mol Cell Biol* **23**, 2600-2607
58. Vassilev, P. M., Guo, L., Chen, X. Z., Segal, Y., Peng, J. B., Basora, N., Babakhanlou, H., Cruger, G., Kanazirska, M., Ye, C., Brown, E. M., Hediger, M. A., and Zhou, J. (2001) Polycystin-2 is a novel cation channel implicated in defective intracellular Ca(2+) homeostasis in polycystic kidney disease. *Biochem Biophys Res Commun* **282**, 341-350
59. Koulen, P., Cai, Y., Geng, L., Maeda, Y., Nishimura, S., Witzgall, R., Ehrlich, B. E., and Somlo, S. (2002) Polycystin-2 is an intracellular calcium release channel. *Nat Cell Biol* **4**, 191-197
60. Cai, Y., Maeda, Y., Cedzich, A., Torres, V. E., Wu, G., Hayashi, T., Mochizuki, T., Park, J. H., Witzgall, R., and Somlo, S. (1999) Identification and characterization of polycystin-2, the PKD2 gene product. *J Biol Chem* **274**, 28557-28565
61. Hanaoka, K., Qian, F., Boletta, A., Bhunia, A. K., Piontek, K., Tsiokas, L., Sukhatme, V. P., Guggino, W. B., and Germino, G. G. (2000) Co-assembly of polycystin-1 and -2 produces unique cation-permeable currents. *Nature* **408**, 990-994
62. Chen, X. Z., Segal, Y., Basora, N., Guo, L., Peng, J. B., Babakhanlou, H., Vassilev, P. M., Brown, E. M., Hediger, M. A., and Zhou, J. (2001) Transport function of the naturally occurring pathogenic polycystin-2 mutant, R742X. *Biochem Biophys Res Commun* **282**, 1251-1256
63. Scheffers, M. S., Le, H., van der Bent, P., Leonhard, W., Prins, F., Spruit, L., Breuning, M. H., de Heer, E., and Peters, D. J. (2002) Distinct subcellular expression of endogenous polycystin-2 in the plasma membrane and Golgi apparatus of MDCK cells. *Hum Mol Genet* **11**, 59-67
64. Yoder, B. K., Hou, X., and Guay-Woodford, L. M. (2002) The polycystic kidney disease proteins, polycystin-1, polycystin-2, polaris, and cystin, are co-localized in renal cilia. *J Am Soc Nephrol* **13**, 2508-2516
65. Pazour, G. J., San Agustin, J. T., Follit, J. A., Rosenbaum, J. L., and Witman, G. B. (2002) Polycystin-2 localizes to kidney cilia and the ciliary level is elevated in orpk mice with polycystic kidney disease. *Curr Biol* **12**, R378-380
66. Li, Y., Wright, J. M., Qian, F., Germino, G. G., and Guggino, W. B. (2005) Polycystin 2 interacts with type I inositol 1,4,5-trisphosphate receptor to modulate intracellular Ca2+ signaling. *J Biol Chem* **280**, 41298-41306
67. Wegierski, T., Steffl, D., Kopp, C., Tauber, R., Buchholz, B., Nitschke, R., Kuehn, E. W., Walz, G., and Kottgen, M. (2009) TRPP2 channels regulate apoptosis through the Ca2+ concentration in the endoplasmic reticulum. *EMBO J* **28**, 490-499
68. Miyakawa, A., Ibarra, C., Malmersjo, S., Aperia, A., Wiklund, P., and Uhlen, P. (2013)

Intracellular calcium release modulates polycystin-2 trafficking. *BMC Nephrol* **14**, 34
69. Hackmann, K., Markoff, A., Qian, F., Bogdanova, N., Germino, G. G., Pennekamp, P., Dworniczak, B., Horst, J., and Gerke, V. (2005) A splice form of polycystin-2, lacking exon 7, does not interact with polycystin-1. *Hum Mol Genet* **14**, 3249-3262
70. Hoffmeister, H., Babinger, K., Gurster, S., Cedzich, A., Meese, C., Schadendorf, K., Osten, L., de Vries, U., Rascle, A., and Witzgall, R. (2011) Polycystin-2 takes different routes to the somatic and ciliary plasma membrane. *J Cell Biol* **192**, 631-645
71. Karcher, C., Fischer, A., Schweickert, A., Bitzer, E., Horie, S., Witzgall, R., and Blum, M. (2005) Lack of a laterality phenotype in Pkd1 knock-out embryos correlates with absence of polycystin-1 in nodal cilia. *Differentiation* **73**, 425-432
72. Markowitz, G. S., Cai, Y., Li, L., Wu, G., Ward, L. C., Somlo, S., and D'Agati, V. D. (1999) Polycystin-2 expression is developmentally regulated. *Am J Physiol* **277**, F17-25
73. Wu, G., Markowitz, G. S., Li, L., D'Agati, V. D., Factor, S. M., Geng, L., Tibara, S., Tuchman, J., Cai, Y., Park, J. H., van Adelsberg, J., Hou, H., Jr., Kucherlapati, R., Edelmann, W., and Somlo, S. (2000) Cardiac defects and renal failure in mice with targeted mutations in Pkd2. *Nat Genet* **24**, 75-78
74. Kuo, I. Y., Kwaczala, A. T., Nguyen, L., Russell, K. S., Campbell, S. G., and Ehrlich, B. E. (2014) Decreased polycystin 2 expression alters calcium-contraction coupling and changes beta-adrenergic signaling pathways. *Proc Natl Acad Sci U S A* **111**, 16604-16609
75. Paavola, J., Schliffke, S., Rossetti, S., Kuo, I. Y., Yuan, S., Sun, Z., Harris, P. C., Torres, V. E., and Ehrlich, B. E. (2013) Polycystin-2 mutations lead to impaired calcium cycling in the heart and predispose to dilated cardiomyopathy. *J Mol Cell Cardiol* **58**, 199-208
76. Hu, Q., Wu, Y., Tang, J., Zheng, W., Wang, Q., Nahirney, D., Duszyk, M., Wang, S., Tu, J. C., and Chen, X. Z. (2014) Expression of polycystins and fibrocystin on primary cilia of lung cells. *Biochem Cell Biol* **92**, 547-554
77. Aben, J. A., Hoogervorst, D. A., Paul, L. C., Borrias, M. C., Noble, N. A., Border, W. A., Bruijn, J. A., and de Heer, E. (2003) Genes expressed by the kidney, but not by bone marrow-derived cells, underlie the genetic predisposition to progressive glomerulosclerosis after mesangial injury. *J Am Soc Nephrol* **14**, 2264-2270
78. Chang, M. Y., and Ong, A. C. (2008) Autosomal dominant polycystic kidney disease: recent advances in pathogenesis and treatment. *Nephron Physiol* **108**, p1-7
79. Calvet, J. P. (1998) Molecular genetics of polycystic kidney disease. *J Nephrol* **11**, 24-34
80. Boletta, A., Qian, F., Onuchic, L. F., Bhunia, A. K., Phakdeekitcharoen, B., Hanaoka, K., Guggino, W., Monaco, L., and Germino, G. G. (2000) Polycystin-1, the gene product of PKD1, induces resistance to apoptosis and spontaneous tubulogenesis in MDCK cells. *Mol Cell* **6**, 1267-1273
81. Davidow, C. J., Maser, R. L., Rome, L. A., Calvet, J. P., and Grantham, J. J. (1996) The cystic fibrosis transmembrane conductance regulator mediates transepithelial fluid secretion by human autosomal dominant polycystic kidney disease epithelium in vitro. *Kidney Int* **50**, 208-218
82. Wilson, P. D., Sherwood, A. C., Palla, K., Du, J., Watson, R., and Norman, J. T. (1991) Reversed polarity of Na(+) -K(+) -ATPase: mislocation to apical plasma membranes in polycystic kidney disease epithelia. *Am J Physiol* **260**, F420-430

83. Charron, A. J., Nakamura, S., Bacallao, R., and Wandinger-Ness, A. (2000) Compromised cytoarchitecture and polarized trafficking in autosomal dominant polycystic kidney disease cells. *J Cell Biol* **149**, 111-124
84. Scherer, W. F., Syverton, J. T., and Gey, G. O. (1953) Studies on the propagation in vitro of poliomyelitis viruses. IV. Viral multiplication in a stable strain of human malignant epithelial cells (strain HeLa) derived from an epidermoid carcinoma of the cervix. *J Exp Med* **97**, 695-710
85. Landry, J. J., Pyl, P. T., Rausch, T., Zichner, T., Tekkedil, M. M., Stutz, A. M., Jauch, A., Aiyar, R. S., Pau, G., Delhomme, N., Gagneur, J., Korbel, J. O., Huber, W., and Steinmetz, L. M. (2013) The genomic and transcriptomic landscape of a HeLa cell line. *G3 (Bethesda)* **3**, 1213-1224
86. Lin, Y. C., Boone, M., Meuris, L., Lemmens, I., Van Roy, N., Soete, A., Reumers, J., Moisse, M., Plaisance, S., Drmanac, R., Chen, J., Speleman, F., Lambrechts, D., Van de Peer, Y., Tavernier, J., and Callewaert, N. (2014) Genome dynamics of the human embryonic kidney 293 lineage in response to cell biology manipulations. *Nat Commun* **5**, 4767
87. Shaw, G., Morse, S., Ararat, M., and Graham, F. L. (2002) Preferential transformation of human neuronal cells by human adenoviruses and the origin of HEK 293 cells. *FASEB J* **16**, 869-871
88. Dautzenberg, F. M., Higelin, J., and Teichert, U. (2000) Functional characterization of corticotropin-releasing factor type 1 receptor endogenously expressed in human embryonic kidney 293 cells. *Eur J Pharmacol* **390**, 51-59
89. Valentich, J. D. (1981) Morphological similarities between the dog kidney cell line MDCK and the mammalian cortical collecting tubule. *Ann N Y Acad Sci* **372**, 384-405
90. Wunsch, S., Gekle, M., Kersting, U., Schuricht, B., and Oberleithner, H. (1995) Phenotypically and karyotypically distinct Madin-Darby canine kidney cell clones respond differently to alkaline stress. *J Cell Physiol* **164**, 164-171
91. Hull, R. N., Cherry, W. R., and Weaver, G. W. (1976) The origin and characteristics of a pig kidney cell strain, LLC-PK. *In Vitro* **12**, 670-677
92. Rabito, C. A. (1986) Occluding junctions in a renal cell line (LLC-PK1) with characteristics of proximal tubular cells. *Am J Physiol* **250**, F734-743
93. Rauchman, M. I., Nigam, S. K., Delpire, E., and Gullans, S. R. (1993) An osmotically tolerant inner medullary collecting duct cell line from an SV40 transgenic mouse. *Am J Physiol* **265**, F416-424
94. Battini, L., Macip, S., Fedorova, E., Dikman, S., Somlo, S., Montagna, C., and Gusella, G. L. (2008) Loss of polycystin-1 causes centrosome amplification and genomic instability. *Hum Mol Genet* **17**, 2819-2833
95. Kim, I., Ding, T., Fu, Y., Li, C., Cui, L., Li, A., Lian, P., Liang, D., Wang, D. W., Guo, C., Ma, J., Zhao, P., Coffey, R. J., Zhan, Q., and Wu, G. (2009) Conditional mutation of Pkd2 causes cystogenesis and upregulates beta-catenin. *J Am Soc Nephrol* **20**, 2556-2569
96. Xu, C., Rossetti, S., Jiang, L., Harris, P. C., Brown-Glaberman, U., Wandinger-Ness, A., Bacallao, R., and Alper, S. L. (2007) Human ADPKD primary cyst epithelial cells with a novel, single codon deletion in the PKD1 gene exhibit defective ciliary polycystin localization and loss of flow-induced Ca2+ signaling. *Am J Physiol Renal Physiol* **292**, F930-945

97. Yamaguchi, T., Pelling, J. C., Ramaswamy, N. T., Eppler, J. W., Wallace, D. P., Nagao, S., Rome, L. A., Sullivan, L. P., and Grantham, J. J. (2000) cAMP stimulates the in vitro proliferation of renal cyst epithelial cells by activating the extracellular signal-regulated kinase pathway. *Kidney Int* **57**, 1460-1471
98. Obara, T., Mangos, S., Liu, Y., Zhao, J., Wiessner, S., Kramer-Zucker, A. G., Olale, F., Schier, A. F., and Drummond, I. A. (2006) Polycystin-2 immunolocalization and function in zebrafish. *J Am Soc Nephrol* **17**, 2706-2718
99. Tran, U., Zakin, L., Schweickert, A., Agrawal, R., Doger, R., Blum, M., De Robertis, E. M., and Wessely, O. (2010) The RNA-binding protein bicaudal C regulates polycystin 2 in the kidney by antagonizing miR-17 activity. *Development* **137**, 1107-1116
100. Lu, W., Fan, X., Basora, N., Babakhanlou, H., Law, T., Rifai, N., Harris, P. C., Perez-Atayde, A. R., Rennke, H. G., and Zhou, J. (1999) Late onset of renal and hepatic cysts in Pkd1-targeted heterozygotes. *Nat Genet* **21**, 160-161
101. Wu, G., D'Agati, V., Cai, Y., Markowitz, G., Park, J. H., Reynolds, D. M., Maeda, Y., Le, T. C., Hou, H., Jr., Kucherlapati, R., Edelmann, W., and Somlo, S. (1998) Somatic inactivation of Pkd2 results in polycystic kidney disease. *Cell* **93**, 177-188
102. Wu, G., Tian, X., Nishimura, S., Markowitz, G. S., D'Agati, V., Park, J. H., Yao, L., Li, L., Geng, L., Zhao, H., Edelmann, W., and Somlo, S. (2002) Trans-heterozygous Pkd1 and Pkd2 mutations modify expression of polycystic kidney disease. *Hum Mol Genet* **11**, 1845-1854
103. Gainullin, V. G., Hopp, K., Ward, C. J., Hommerding, C. J., and Harris, P. C. (2015) Polycystin-1 maturation requires polycystin-2 in a dose-dependent manner. *J Clin Invest* **125**, 607-620
104. Lu, W., Peissel, B., Babakhanlou, H., Pavlova, A., Geng, L., Fan, X., Larson, C., Brent, G., and Zhou, J. (1997) Perinatal lethality with kidney and pancreas defects in mice with a targetted Pkd1 mutation. *Nat Genet* **17**, 179-181
105. Canessa, C. M., Horisberger, J. D., and Rossier, B. C. (1993) Epithelial sodium channel related to proteins involved in neurodegeneration. *Nature* **361**, 467-470
106. Canessa, C. M., Schild, L., Buell, G., Thorens, B., Gautschi, I., Horisberger, J. D., and Rossier, B. C. (1994) Amiloride-sensitive epithelial Na+ channel is made of three homologous subunits. *Nature* **367**, 463-467
107. Jasti, J., Furukawa, H., Gonzales, E. B., and Gouaux, E. (2007) Structure of acid-sensing ion channel 1 at 1.9 A resolution and low pH. *Nature* **449**, 316-323
108. Stockand, J. D., Staruschenko, A., Pochynyuk, O., Booth, R. E., and Silverthorn, D. U. (2008) Insight toward epithelial Na+ channel mechanism revealed by the acid-sensing ion channel 1 structure. *IUBMB Life* **60**, 620-628
109. Kosari, F., Sheng, S., Li, J., Mak, D. O., Foskett, J. K., and Kleyman, T. R. (1998) Subunit stoichiometry of the epithelial sodium channel. *J Biol Chem* **273**, 13469-13474
110. Firsov, D., Gautschi, I., Merillat, A. M., Rossier, B. C., and Schild, L. (1998) The heterotetrameric architecture of the epithelial sodium channel (ENaC). *EMBO J* **17**, 344-352
111. Eskandari, S., Snyder, P. M., Kreman, M., Zampighi, G. A., Welsh, M. J., and Wright, E. M. (1999) Number of subunits comprising the epithelial sodium channel. *J Biol Chem* **274**, 27281-27286
112. Stewart, A. P., Haerteis, S., Diakov, A., Korbmacher, C., and Edwardson, J. M. (2011) Atomic force microscopy reveals the architecture of the epithelial sodium channel

(ENaC). *J Biol Chem* **286**, 31944-31952
113. Kleyman, T. R., and Cragoe, E. J., Jr. (1988) Amiloride and its analogs as tools in the study of ion transport. *J Membr Biol* **105**, 1-21
114. Bentley, P. J. (1968) Amiloride: a potent inhibitor of sodium transport across the toad bladder. *J Physiol* **195**, 317-330
115. Schild, L., Schneeberger, E., Gautschi, I., and Firsov, D. (1997) Identification of amino acid residues in the alpha, beta, and gamma subunits of the epithelial sodium channel (ENaC) involved in amiloride block and ion permeation. *J Gen Physiol* **109**, 15-26
116. Li, X. J., Xu, R. H., Guggino, W. B., and Snyder, S. H. (1995) Alternatively spliced forms of the alpha subunit of the epithelial sodium channel: distinct sites for amiloride binding and channel pore. *Mol Pharmacol* **47**, 1133-1140
117. Kieber-Emmons, T., Lin, C., Foster, M. H., and Kleyman, T. R. (1999) Antiidiotypic antibody recognizes an amiloride binding domain within the alpha subunit of the epithelial Na+ channel. *J Biol Chem* **274**, 9648-9655
118. Kashlan, O. B., Sheng, S., and Kleyman, T. R. (2005) On the interaction between amiloride and its putative alpha-subunit epithelial Na+ channel binding site. *J Biol Chem* **280**, 26206-26215
119. Kellenberger, S., Gautschi, I., and Schild, L. (2003) Mutations in the epithelial Na+ channel ENaC outer pore disrupt amiloride block by increasing its dissociation rate. *Mol Pharmacol* **64**, 848-856
120. Kellenberger, S., Auberson, M., Gautschi, I., Schneeberger, E., and Schild, L. (2001) Permeability properties of ENaC selectivity filter mutants. *J Gen Physiol* **118**, 679-692
121. Sheng, S., Li, J., McNulty, K. A., Avery, D., and Kleyman, T. R. (2000) Characterization of the selectivity filter of the epithelial sodium channel. *J Biol Chem* **275**, 8572-8581
122. Baconguis, I., Bohlen, C. J., Goehring, A., Julius, D., and Gouaux, E. (2014) X-ray structure of acid-sensing ion channel 1-snake toxin complex reveals open state of a Na(+)-selective channel. *Cell* **156**, 717-729
123. Kellenberger, S., and Schild, L. (2002) Epithelial sodium channel/degenerin family of ion channels: a variety of functions for a shared structure. *Physiol Rev* **82**, 735-767
124. Hansson, J. H., Schild, L., Lu, Y., Wilson, T. A., Gautschi, I., Shimkets, R., Nelson-Williams, C., Rossier, B. C., and Lifton, R. P. (1995) A de novo missense mutation of the beta subunit of the epithelial sodium channel causes hypertension and Liddle syndrome, identifying a proline-rich segment critical for regulation of channel activity. *Proc Natl Acad Sci U S A* **92**, 11495-11499
125. Chang, S. S., Grunder, S., Hanukoglu, A., Rosler, A., Mathew, P. M., Hanukoglu, I., Schild, L., Lu, Y., Shimkets, R. A., Nelson-Williams, C., Rossier, B. C., and Lifton, R. P. (1996) Mutations in subunits of the epithelial sodium channel cause salt wasting with hyperkalaemic acidosis, pseudohypoaldosteronism type 1. *Nat Genet* **12**, 248-253
126. Hummler, E., Barker, P., Gatzy, J., Beermann, F., Verdumo, C., Schmidt, A., Boucher, R., and Rossier, B. C. (1996) Early death due to defective neonatal lung liquid clearance in alpha-ENaC-deficient mice. *Nat Genet* **12**, 325-328
127. Smith, J. J., Travis, S. M., Greenberg, E. P., and Welsh, M. J. (1996) Cystic fibrosis airway epithelia fail to kill bacteria because of abnormal airway surface fluid. *Cell* **85**, 229-236
128. Boucher, R. C., Stutts, M. J., Knowles, M. R., Cantley, L., and Gatzy, J. T. (1986) Na+

transport in cystic fibrosis respiratory epithelia. Abnormal basal rate and response to adenylate cyclase activation. *J Clin Invest* **78**, 1245-1252
129. Boughter, J. D., Jr., and Gilbertson, T. A. (1999) From channels to behavior: an integrative model of NaCl taste. *Neuron* **22**, 213-215
130. Chandrashekar, J., Kuhn, C., Oka, Y., Yarmolinsky, D. A., Hummler, E., Ryba, N. J., and Zuker, C. S. (2010) The cells and peripheral representation of sodium taste in mice. *Nature* **464**, 297-301
131. Drummond, H. A., Abboud, F. M., and Welsh, M. J. (2000) Localization of beta and gamma subunits of ENaC in sensory nerve endings in the rat foot pad. *Brain Res* **884**, 1-12
132. Garty, H., and Palmer, L. G. (1997) Epithelial sodium channels: function, structure, and regulation. *Physiol Rev* **77**, 359-396
133. Kemendy, A. E., Kleyman, T. R., and Eaton, D. C. (1992) Aldosterone alters the open probability of amiloride-blockable sodium channels in A6 epithelia. *Am J Physiol* **263**, C825-837
134. Chen, S. Y., Bhargava, A., Mastroberardino, L., Meijer, O. C., Wang, J., Buse, P., Firestone, G. L., Verrey, F., and Pearce, D. (1999) Epithelial sodium channel regulated by aldosterone-induced protein sgk. *Proc Natl Acad Sci U S A* **96**, 2514-2519
135. Spindler, B., and Verrey, F. (1999) Aldosterone action: induction of p21(ras) and fra-2 and transcription-independent decrease in myc, jun, and fos. *Am J Physiol* **276**, C1154-1161
136. Yu, Z., Kong, Q., and Kone, B. C. (2013) Aldosterone reprograms promoter methylation to regulate alphaENaC transcription in the collecting duct. *Am J Physiol Renal Physiol* **305**, F1006-1013
137. Snyder, P. M. (2000) Liddle's syndrome mutations disrupt cAMP-mediated translocation of the epithelial Na(+) channel to the cell surface. *J Clin Invest* **105**, 45-53
138. Marunaka, Y., and Eaton, D. C. (1991) Effects of vasopressin and cAMP on single amiloride-blockable Na channels. *Am J Physiol* **260**, C1071-1084
139. Hughey, R. P., Bruns, J. B., Kinlough, C. L., Harkleroad, K. L., Tong, Q., Carattino, M. D., Johnson, J. P., Stockand, J. D., and Kleyman, T. R. (2004) Epithelial sodium channels are activated by furin-dependent proteolysis. *J Biol Chem* **279**, 18111-18114
140. Bruns, J. B., Carattino, M. D., Sheng, S., Maarouf, A. B., Weisz, O. A., Pilewski, J. M., Hughey, R. P., and Kleyman, T. R. (2007) Epithelial Na+ channels are fully activated by furin- and prostasin-dependent release of an inhibitory peptide from the gamma-subunit. *J Biol Chem* **282**, 6153-6160
141. Goulet, C. C., Volk, K. A., Adams, C. M., Prince, L. S., Stokes, J. B., and Snyder, P. M. (1998) Inhibition of the epithelial Na+ channel by interaction of Nedd4 with a PY motif deleted in Liddle's syndrome. *J Biol Chem* **273**, 30012-30017
142. Peters, D. M., Vadasz, I., Wujak, L., Wygrecka, M., Olschewski, A., Becker, C., Herold, S., Papp, R., Mayer, K., Rummel, S., Brandes, R. P., Gunther, A., Waldegger, S., Eickelberg, O., Seeger, W., and Morty, R. E. (2014) TGF-beta directs trafficking of the epithelial sodium channel ENaC which has implications for ion and fluid transport in acute lung injury. *Proc Natl Acad Sci U S A* **111**, E374-383
143. Turnheim, K. (1991) Intrinsic regulation of apical sodium entry in epithelia. *Physiol Rev* **71**, 429-445
144. Sheng, S., Bruns, J. B., and Kleyman, T. R. (2004) Extracellular histidine residues

crucial for Na+ self-inhibition of epithelial Na+ channels. *J Biol Chem* **279**, 9743-9749
145. Sheng, S., Maarouf, A. B., Bruns, J. B., Hughey, R. P., and Kleyman, T. R. (2007) Functional role of extracellular loop cysteine residues of the epithelial Na+ channel in Na+ self-inhibition. *J Biol Chem* **282**, 20180-20190
146. Snyder, P. M. (2002) The epithelial Na+ channel: cell surface insertion and retrieval in Na+ homeostasis and hypertension. *Endocr Rev* **23**, 258-275
147. Awayda, M. S., Tousson, A., and Benos, D. J. (1997) Regulation of a cloned epithelial Na+ channel by its beta- and gamma-subunits. *Am J Physiol* **273**, C1889-1899
148. Mazzochi, C., Bubien, J. K., Smith, P. R., and Benos, D. J. (2006) The carboxyl terminus of the alpha-subunit of the amiloride-sensitive epithelial sodium channel binds to F-actin. *J Biol Chem* **281**, 6528-6538
149. Berdiev, B. K., Latorre, R., Benos, D. J., and Ismailov, II. (2001) Actin modifies Ca2+ block of epithelial Na+ channels in planar lipid bilayers. *Biophys J* **80**, 2176-2186
150. Sudarikova, A. V., Tsaplina, O. A., Chubinskiy-Nadezhdin, V. I., Morachevskaya, E. A., and Negulyaev, Y. A. (2015) Amiloride-insensitive sodium channels are directly regulated by actin cytoskeleton dynamics in human lymphoma cells. *Biochem Biophys Res Commun* **461**, 54-58
151. Rotin, D., Bar-Sagi, D., O'Brodovich, H., Merilainen, J., Lehto, V. P., Canessa, C. M., Rossier, B. C., and Downey, G. P. (1994) An SH3 binding region in the epithelial Na+ channel (alpha rENaC) mediates its localization at the apical membrane. *EMBO J* **13**, 4440-4450
152. Cantiello, H. F., Stow, J. L., Prat, A. G., and Ausiello, D. A. (1991) Actin filaments regulate epithelial Na+ channel activity. *Am J Physiol* **261**, C882-888
153. Els, W. J., and Chou, K. Y. (1993) Sodium-dependent regulation of epithelial sodium channel densities in frog skin; a role for the cytoskeleton. *J Physiol* **462**, 447-464
154. Compeau, C. G., Rotstein, O. D., Tohda, H., Marunaka, Y., Rafii, B., Slutsky, A. S., and O'Brodovich, H. (1994) Endotoxin-stimulated alveolar macrophages impair lung epithelial Na+ transport by an L-Arg-dependent mechanism. *Am J Physiol* **266**, C1330-1341
155. Broderick, M. J., and Winder, S. J. (2005) Spectrin, alpha-actinin, and dystrophin. *Adv Protein Chem* **70**, 203-246
156. Nakamura, F., Stossel, T. P., and Hartwig, J. H. (2011) The filamins: organizers of cell structure and function. *Cell Adh Migr* **5**, 160-169
157. Castresana, J., and Saraste, M. (1995) Does Vav bind to F-actin through a CH domain? *FEBS Lett* **374**, 149-151
158. Kolakowski, J., Makuch, R., Stepkowski, D., and Dabrowska, R. (1995) Interaction of calponin with actin and its functional implications. *Biochem J* **306 (Pt 1)**, 199-204
159. Uribe, R., and Jay, D. (2009) A review of actin binding proteins: new perspectives. *Mol Biol Rep* **36**, 121-125
160. Nakamura, F., Hartwig, J. H., Stossel, T. P., and Szymanski, P. T. (2005) Ca2+ and calmodulin regulate the binding of filamin A to actin filaments. *J Biol Chem* **280**, 32426-32433
161. Kesner, B. A., Milgram, S. L., Temple, B. R., and Dokholyan, N. V. (2010) Isoform divergence of the filamin family of proteins. *Mol Biol Evol* **27**, 283-295
162. Franzot, G., Sjoblom, B., Gautel, M., and Djinovic Carugo, K. (2005) The crystal structure of the actin binding domain from alpha-actinin in its closed conformation:

structural insight into phospholipid regulation of alpha-actinin. *J Mol Biol* **348**, 151-165
163. Garcia-Alvarez, B., Bobkov, A., Sonnenberg, A., and de Pereda, J. M. (2003) Structural and functional analysis of the actin binding domain of plectin suggests alternative mechanisms for binding to F-actin and integrin beta4. *Structure* **11**, 615-625
164. Goldsmith, S. C., Pokala, N., Shen, W., Fedorov, A. A., Matsudaira, P., and Almo, S. C. (1997) The structure of an actin-crosslinking domain from human fimbrin. *Nat Struct Biol* **4**, 708-712
165. Fucini, P., Renner, C., Herberhold, C., Noegel, A. A., and Holak, T. A. (1997) The repeating segments of the F-actin cross-linking gelation factor (ABP-120) have an immunoglobulin-like fold. *Nat Struct Biol* **4**, 223-230
166. Nakamura, F., Osborn, T. M., Hartemink, C. A., Hartwig, J. H., and Stossel, T. P. (2007) Structural basis of filamin A functions. *J Cell Biol* **179**, 1011-1025
167. van Kogelenberg, M., Clark, A. R., Jenkins, Z., Morgan, T., Anandan, A., Sawyer, G. M., Edwards, M., Dudding, T., Homfray, T., Castle, B., Tolmie, J., Stewart, F., Kivuva, E., Pilz, D. T., Gabbett, M., Sutherland-Smith, A. J., and Robertson, S. P. (2015) Diverse phenotypic consequences of mutations affecting the C-terminus of FLNA. *J Mol Med (Berl)* **93**, 773-782
168. Gorlin, J. B., Yamin, R., Egan, S., Stewart, M., Stossel, T. P., Kwiatkowski, D. J., and Hartwig, J. H. (1990) Human endothelial actin-binding protein (ABP-280, nonmuscle filamin): a molecular leaf spring. *J Cell Biol* **111**, 1089-1105
169. van der Flier, A., and Sonnenberg, A. (2001) Structural and functional aspects of filamins. *Biochim Biophys Acta* **1538**, 99-117
170. Liu, G., Thomas, L., Warren, R. A., Enns, C. A., Cunningham, C. C., Hartwig, J. H., and Thomas, G. (1997) Cytoskeletal protein ABP-280 directs the intracellular trafficking of furin and modulates proprotein processing in the endocytic pathway. *J Cell Biol* **139**, 1719-1733
171. Feng, S., Lu, X., and Kroll, M. H. (2005) Filamin A binding stabilizes nascent glycoprotein Ibalpha trafficking and thereby enhances its surface expression. *J Biol Chem* **280**, 6709-6715
172. Ohta, Y., Suzuki, N., Nakamura, S., Hartwig, J. H., and Stossel, T. P. (1999) The small GTPase RalA targets filamin to induce filopodia. *Proc Natl Acad Sci U S A* **96**, 2122-2128
173. Edwards, D. N., Towb, P., and Wasserman, S. A. (1997) An activity-dependent network of interactions links the Rel protein Dorsal with its cytoplasmic regulators. *Development* **124**, 3855-3864
174. Yoshida, N., Ogata, T., Tanabe, K., Li, S., Nakazato, M., Kohu, K., Takafuta, T., Shapiro, S., Ohta, Y., Satake, M., and Watanabe, T. (2005) Filamin A-bound PEBP2beta/CBFbeta is retained in the cytoplasm and prevented from functioning as a partner of the Runx1 transcription factor. *Mol Cell Biol* **25**, 1003-1012
175. Kim, E. J., Park, J. S., and Um, S. J. (2007) Filamin A negatively regulates the transcriptional activity of p73alpha in the cytoplasm. *Biochem Biophys Res Commun* **362**, 1101-1106
176. Ozanne, D. M., Brady, M. E., Cook, S., Gaughan, L., Neal, D. E., and Robson, C. N. (2000) Androgen receptor nuclear translocation is facilitated by the f-actin cross-linking protein filamin. *Mol Endocrinol* **14**, 1618-1626
177. Loy, C. J., Sim, K. S., and Yong, E. L. (2003) Filamin-A fragment localizes to the

nucleus to regulate androgen receptor and coactivator functions. *Proc Natl Acad Sci U S A* **100**, 4562-4567
178. Savoy, R. M., Chen, L., Siddiqui, S., Melgoza, F. U., Durbin-Johnson, B., Drake, C., Jathal, M. K., Bose, S., Steele, T. M., Mooso, B. A., D'Abronzo, L. S., Fry, W. H., Carraway, K. L., 3rd, Mudryj, M., and Ghosh, P. M. (2015) Transcription of Nrdp1 by the androgen receptor is regulated by nuclear filamin A in prostate cancer. *Endocr Relat Cancer* **22**, 369-386
179. Wang, Y., Kreisberg, J. I., Bedolla, R. G., Mikhailova, M., deVere White, R. W., and Ghosh, P. M. (2007) A 90 kDa fragment of filamin A promotes Casodex-induced growth inhibition in Casodex-resistant androgen receptor positive C4-2 prostate cancer cells. *Oncogene* **26**, 6061-6070
180. Deng, W., Lopez-Camacho, C., Tang, J. Y., Mendoza-Villanueva, D., Maya-Mendoza, A., Jackson, D. A., and Shore, P. (2012) Cytoskeletal protein filamin A is a nucleolar protein that suppresses ribosomal RNA gene transcription. *Proc Natl Acad Sci U S A* **109**, 1524-1529
181. Velkova, A., Carvalho, M. A., Johnson, J. O., Tavtigian, S. V., and Monteiro, A. N. (2010) Identification of Filamin A as a BRCA1-interacting protein required for efficient DNA repair. *Cell Cycle* **9**, 1421-1433
182. Yuan, Y., and Shen, Z. (2001) Interaction with BRCA2 suggests a role for filamin-1 (hsFLNa) in DNA damage response. *J Biol Chem* **276**, 48318-48324
183. Browne, K. A., Johnstone, R. W., Jans, D. A., and Trapani, J. A. (2000) Filamin (280-kDa actin-binding protein) is a caspase substrate and is also cleaved directly by the cytotoxic T lymphocyte protease granzyme B during apoptosis. *J Biol Chem* **275**, 39262-39266
184. Szeto, S. G., Williams, E. C., Rudner, A. D., and Lee, J. M. (2015) Phosphorylation of filamin A by Cdk1 regulates filamin A localization and daughter cell separation. *Exp Cell Res* **330**, 248-266
185. Vadlamudi, R. K., Li, F., Adam, L., Nguyen, D., Ohta, Y., Stossel, T. P., and Kumar, R. (2002) Filamin is essential in actin cytoskeletal assembly mediated by p21-activated kinase 1. *Nat Cell Biol* **4**, 681-690
186. Woo, M. S., Ohta, Y., Rabinovitz, I., Stossel, T. P., and Blenis, J. (2004) Ribosomal S6 kinase (RSK) regulates phosphorylation of filamin A on an important regulatory site. *Mol Cell Biol* **24**, 3025-3035
187. Jay, D., Garcia, E. J., Lara, J. E., Medina, M. A., and de la Luz Ibarra, M. (2000) Determination of a cAMP-dependent protein kinase phosphorylation site in the C-terminal region of human endothelial actin-binding protein. *Arch Biochem Biophys* **377**, 80-84
188. Yada, Y., Okano, Y., and Nozawa, Y. (1990) Enhancement of GTP gamma S-binding activity by cAMP-dependent phosphorylation of a filamin-like 250 kDa membrane protein in human platelets. *Biochem Biophys Res Commun* **172**, 256-261
189. Ohta, Y., and Hartwig, J. H. (1995) Actin filament cross-linking by chicken gizzard filamin is regulated by phosphorylation in vitro. *Biochemistry* **34**, 6745-6754
190. Chen, M., and Stracher, A. (1989) In situ phosphorylation of platelet actin-binding protein by cAMP-dependent protein kinase stabilizes it against proteolysis by calpain. *J Biol Chem* **264**, 14282-14289
191. Jay, D., Garcia, E. J., and de la Luz Ibarra, M. (2004) In situ determination of a PKA

phosphorylation site in the C-terminal region of filamin. *Mol Cell Biochem* **260**, 49-53
192. Feng, Y., Chen, M. H., Moskowitz, I. P., Mendonza, A. M., Vidali, L., Nakamura, F., Kwiatkowski, D. J., and Walsh, C. A. (2006) Filamin A (FLNA) is required for cell-cell contact in vascular development and cardiac morphogenesis. *Proc Natl Acad Sci U S A* **103**, 19836-19841
193. Kyndt, F., Gueffet, J. P., Probst, V., Jaafar, P., Legendre, A., Le Bouffant, F., Toquet, C., Roy, E., McGregor, L., Lynch, S. A., Newbury-Ecob, R., Tran, V., Young, I., Trochu, J. N., Le Marec, H., and Schott, J. J. (2007) Mutations in the gene encoding filamin A as a cause for familial cardiac valvular dystrophy. *Circulation* **115**, 40-49
194. Hart, A. W., Morgan, J. E., Schneider, J., West, K., McKie, L., Bhattacharya, S., Jackson, I. J., and Cross, S. H. (2006) Cardiac malformations and midline skeletal defects in mice lacking filamin A. *Hum Mol Genet* **15**, 2457-2467
195. Fox, J. W., Lamperti, E. D., Eksioglu, Y. Z., Hong, S. E., Feng, Y., Graham, D. A., Scheffer, I. E., Dobyns, W. B., Hirsch, B. A., Radtke, R. A., Berkovic, S. F., Huttenlocher, P. R., and Walsh, C. A. (1998) Mutations in filamin 1 prevent migration of cerebral cortical neurons in human periventricular heterotopia. *Neuron* **21**, 1315-1325
196. Sjoblom, T., Jones, S., Wood, L. D., Parsons, D. W., Lin, J., Barber, T. D., Mandelker, D., Leary, R. J., Ptak, J., Silliman, N., Szabo, S., Buckhaults, P., Farrell, C., Meeh, P., Markowitz, S. D., Willis, J., Dawson, D., Willson, J. K., Gazdar, A. F., Hartigan, J., Wu, L., Liu, C., Parmigiani, G., Park, B. H., Bachman, K. E., Papadopoulos, N., Vogelstein, B., Kinzler, K. W., and Velculescu, V. E. (2006) The consensus coding sequences of human breast and colorectal cancers. *Science* **314**, 268-274
197. Tian, Z. Q., Shi, J. W., Wang, X. R., Li, Z., and Wang, G. Y. (2015) New cancer suppressor gene for colorectal adenocarcinoma: filamin A. *World J Gastroenterol* **21**, 2199-2205
198. Hogan, M. C., Masyuk, T. V., Page, L. J., Kubly, V. J., Bergstralh, E. J., Li, X., Kim, B., King, B. F., Glockner, J., Holmes, D. R., 3rd, Rossetti, S., Harris, P. C., LaRusso, N. F., and Torres, V. E. (2010) Randomized clinical trial of long-acting somatostatin for autosomal dominant polycystic kidney and liver disease. *J Am Soc Nephrol* **21**, 1052-1061
199. Stallone, G., Infante, B., Grandaliano, G., Bristogiannis, C., Macarini, L., Mezzopane, D., Bruno, F., Montemurno, E., Schirinzi, A., Sabbatini, M., Pisani, A., Tataranni, T., Schena, F. P., and Gesualdo, L. (2012) Rapamycin for treatment of type I autosomal dominant polycystic kidney disease (RAPYD-study): a randomized, controlled study. *Nephrol Dial Transplant* **27**, 3560-3567
200. Torres, V. E., Chapman, A. B., Devuyst, O., Gansevoort, R. T., Grantham, J. J., Higashihara, E., Perrone, R. D., Krasa, H. B., Ouyang, J., Czerwiec, F. S., and Investigators, T. T. (2012) Tolvaptan in patients with autosomal dominant polycystic kidney disease. *N Engl J Med* **367**, 2407-2418
201. Hartwig, J. H., and Stossel, T. P. (1975) Isolation and properties of actin, myosin, and a new actinbinding protein in rabbit alveolar macrophages. *J Biol Chem* **250**, 5696-5705
202. Stossel, T. P., Condeelis, J., Cooley, L., Hartwig, J. H., Noegel, A., Schleicher, M., and Shapiro, S. S. (2001) Filamins as integrators of cell mechanics and signalling. *Nat Rev Mol Cell Biol* **2**, 138-145
203. de Wit, M. C., Kros, J. M., Halley, D. J., de Coo, I. F., Verdijk, R., Jacobs, B. C., and

Mancini, G. M. (2009) Filamin A mutation, a common cause for periventricular heterotopia, aneurysms and cardiac defects. *J Neurol Neurosurg Psychiatry* **80**, 426-428
204. Feng, Y., and Walsh, C. A. (2004) The many faces of filamin: a versatile molecular scaffold for cell motility and signalling. *Nat Cell Biol* **6**, 1034-1038
205. Pilop, C., Aregger, F., Gorman, R. C., Brunisholz, R., Gerrits, B., Schaffner, T., Gorman, J. H., 3rd, Matyas, G., Carrel, T., and Frey, B. M. (2009) Proteomic analysis in aortic media of patients with Marfan syndrome reveals increased activity of calpain 2 in aortic aneurysms. *Circulation* **120**, 983-991
206. Barr, M. M., DeModena, J., Braun, D., Nguyen, C. Q., Hall, D. H., and Sternberg, P. W. (2001) The Caenorhabditis elegans autosomal dominant polycystic kidney disease gene homologs lov-1 and pkd-2 act in the same pathway. *Curr Biol* **11**, 1341-1346
207. Ong, A. C., Ward, C. J., Butler, R. J., Biddolph, S., Bowker, C., Torra, R., Pei, Y., and Harris, P. C. (1999) Coordinate expression of the autosomal dominant polycystic kidney disease proteins, polycystin-2 and polycystin-1, in normal and cystic tissue. *Am J Pathol* **154**, 1721-1729
208. (1995) Polycystic kidney disease: the complete structure of the PKD1 gene and its protein. The International Polycystic Kidney Disease Consortium. *Cell* **81**, 289-298
209. Harris, P. C., and Torres, V. E. (1993) Polycystic Kidney Disease, Autosomal Dominant. in *GeneReviews(R)* (Pagon, R. A., Adam, M. P., Ardinger, H. H., Wallace, S. E., Amemiya, A., Bean, L. J. H., Bird, T. D., Fong, C. T., Mefford, H. C., Smith, R. J. H., and Stephens, K. eds.), Seattle (WA). pp
210. Pirson, Y. (2010) Extrarenal manifestations of autosomal dominant polycystic kidney disease. *Adv Chronic Kidney Dis* **17**, 173-180
211. Liang, G., Yang, J., Wang, Z., Li, Q., Tang, Y., and Chen, X. Z. (2008) Polycystin-2 down-regulates cell proliferation via promoting PERK-dependent phosphorylation of eIF2alpha. *Hum Mol Genet* **17**, 3254-3262
212. Liang, G., Li, Q., Tang, Y., Kokame, K., Kikuchi, T., Wu, G., and Chen, X. Z. (2008) Polycystin-2 is regulated by endoplasmic reticulum-associated degradation. *Hum Mol Genet* **17**, 1109-1119
213. Chen, X. Z., Li, Q., Wu, Y., Liang, G., Lara, C. J., and Cantiello, H. F. (2008) Submembraneous microtubule cytoskeleton: interaction of TRPP2 with the cell cytoskeleton. *FEBS J* **275**, 4675-4683
214. Montalbetti, N., Li, Q., Timpanaro, G. A., Gonzalez-Perrett, S., Dai, X. Q., Chen, X. Z., and Cantiello, H. F. (2005) Cytoskeletal regulation of calcium-permeable cation channels in the human syncytiotrophoblast: role of gelsolin. *J Physiol* **566**, 309-325
215. Montalbetti, N., Li, Q., Gonzalez-Perrett, S., Semprine, J., Chen, X. Z., and Cantiello, H. F. (2005) Effect of hydro-osmotic pressure on polycystin-2 channel function in the human syncytiotrophoblast. *Pflugers Arch* **451**, 294-303
216. Cunningham, C. C., Gorlin, J. B., Kwiatkowski, D. J., Hartwig, J. H., Janmey, P. A., Byers, H. R., and Stossel, T. P. (1992) Actin-binding protein requirement for cortical stability and efficient locomotion. *Science* **255**, 325-327
217. Li, Q., Dai, X. Q., Shen, P. Y., Cantiello, H. F., Karpinski, E., and Chen, X. Z. (2004) A modified mammalian tandem affinity purification procedure to prepare functional polycystin-2 channel. *FEBS Lett* **576**, 231-236
218. Li, Q., Dai, X. Q., Shen, P. Y., Wu, Y., Long, W., Chen, C. X., Hussain, Z., Wang, S.,

and Chen, X. Z. (2007) Direct binding of alpha-actinin enhances TRPP3 channel activity. *J Neurochem* **103**, 2391-2400
219. Li, Q., Dai, Y., Guo, L., Liu, Y., Hao, C., Wu, G., Basora, N., Michalak, M., and Chen, X. Z. (2003) Polycystin-2 associates with tropomyosin-1, an actin microfilament component. *J Mol Biol* **325**, 949-962
220. Gallagher, A. R., Cedzich, A., Gretz, N., Somlo, S., and Witzgall, R. (2000) The polycystic kidney disease protein PKD2 interacts with Hax-1, a protein associated with the actin cytoskeleton. *Proc Natl Acad Sci U S A* **97**, 4017-4022
221. Lehtonen, S., Ora, A., Olkkonen, V. M., Geng, L., Zerial, M., Somlo, S., and Lehtonen, E. (2000) In vivo interaction of the adapter protein CD2-associated protein with the type 2 polycystic kidney disease protein, polycystin-2. *J Biol Chem* **275**, 32888-32893
222. Lehtonen, S., Zhao, F., and Lehtonen, E. (2002) CD2-associated protein directly interacts with the actin cytoskeleton. *Am J Physiol Renal Physiol* **283**, F734-743
223. Li, Q., Montalbetti, N., Wu, Y., Ramos, A., Raychowdhury, M. K., Chen, X. Z., and Cantiello, H. F. (2006) Polycystin-2 cation channel function is under the control of microtubular structures in primary cilia of renal epithelial cells. *J Biol Chem* **281**, 37566-37575
224. Maruoka, N. D., Steele, D. F., Au, B. P., Dan, P., Zhang, X., Moore, E. D., and Fedida, D. (2000) alpha-actinin-2 couples to cardiac Kv1.5 channels, regulating current density and channel localization in HEK cells. *FEBS Lett* **473**, 188-194
225. Sadeghi, A., Doyle, A. D., and Johnson, B. D. (2002) Regulation of the cardiac L-type Ca2+ channel by the actin-binding proteins alpha-actinin and dystrophin. *Am J Physiol Cell Physiol* **282**, C1502-1511
226. Rycroft, B. K., and Gibb, A. J. (2004) Regulation of single NMDA receptor channel activity by alpha-actinin and calmodulin in rat hippocampal granule cells. *J Physiol* **557**, 795-808
227. Wyszynski, M., Lin, J., Rao, A., Nigh, E., Beggs, A. H., Craig, A. M., and Sheng, M. (1997) Competitive binding of alpha-actinin and calmodulin to the NMDA receptor. *Nature* **385**, 439-442
228. Sharif-Naeini, R., Folgering, J. H., Bichet, D., Duprat, F., Lauritzen, I., Arhatte, M., Jodar, M., Dedman, A., Chatelain, F. C., Schulte, U., Retailleau, K., Loufrani, L., Patel, A., Sachs, F., Delmas, P., Peters, D. J., and Honore, E. (2009) Polycystin-1 and -2 dosage regulates pressure sensing. *Cell* **139**, 587-596
229. Seck, T., Baron, R., and Horne, W. C. (2003) Binding of filamin to the C-terminal tail of the calcitonin receptor controls recycling. *J Biol Chem* **278**, 10408-10416
230. Beekman, J. M., van der Poel, C. E., van der Linden, J. A., van den Berg, D. L., van den Berghe, P. V., van de Winkel, J. G., and Leusen, J. H. (2008) Filamin A stabilizes Fc gamma RI surface expression and prevents its lysosomal routing. *J Immunol* **180**, 3938-3945
231. Fiori, J. L., Zhu, T. N., O'Connell, M. P., Hoek, K. S., Indig, F. E., Frank, B. P., Morris, C., Kole, S., Hasskamp, J., Elias, G., Weeraratna, A. T., and Bernier, M. (2009) Filamin A modulates kinase activation and intracellular trafficking of epidermal growth factor receptors in human melanoma cells. *Endocrinology* **150**, 2551-2560
232. Anilkumar, G., Rajasekaran, S. A., Wang, S., Hankinson, O., Bander, N. H., and Rajasekaran, A. K. (2003) Prostate-specific membrane antigen association with filamin A modulates its internalization and NAALADase activity. *Cancer Res* **63**, 2645-2648

233. Rundle, D. R., Gorbsky, G., and Tsiokas, L. (2004) PKD2 interacts and co-localizes with mDia1 to mitotic spindles of dividing cells: role of mDia1 IN PKD2 localization to mitotic spindles. *J Biol Chem* **279**, 29728-29739
234. Wilson, P. D., Schrier, R. W., Breckon, R. D., and Gabow, P. A. (1986) A new method for studying human polycystic kidney disease epithelia in culture. *Kidney Int* **30**, 371-378
235. Lanoix, J., D'Agati, V., Szabolcs, M., and Trudel, M. (1996) Dysregulation of cellular proliferation and apoptosis mediates human autosomal dominant polycystic kidney disease (ADPKD). *Oncogene* **13**, 1153-1160
236. Ibraghimov-Beskrovnaya, O., and Bukanov, N. O. (2006) In vitro cystogenesis: the search for drugs antagonizing cyst development. *Nephrol Ther* **2 Suppl 2**, S109-114
237. Wang, Q., Dai, X. Q., Li, Q., Wang, Z., Cantero Mdel, R., Li, S., Shen, J., Tu, J. C., Cantiello, H., and Chen, X. Z. (2012) Structural interaction and functional regulation of polycystin-2 by filamin. *PLoS One* **7**, e40448
238. Wu, Y., Li, Q., and Chen, X. Z. (2007) Detecting protein-protein interactions by Far western blotting. *Nat Protoc* **2**, 3278-3284
239. Tian, Y., Kolb, R., Hong, J. H., Carroll, J., Li, D., You, J., Bronson, R., Yaffe, M. B., Zhou, J., and Benjamin, T. (2007) TAZ promotes PC2 degradation through a SCFbeta-Trcp E3 ligase complex. *Mol Cell Biol* **27**, 6383-6395
240. Yang, J., Wang, Q., Zheng, W., Tuli, J., Li, Q., Wu, Y., Hussein, S., Dai, X. Q., Shafiei, S., Li, X. G., Shen, P. Y., Tu, J. C., and Chen, X. Z. (2012) Receptor for activated C kinase 1 (RACK1) inhibits function of transient receptor potential (TRP)-type channel Pkd2L1 through physical interaction. *J Biol Chem* **287**, 6551-6561
241. Popowicz, G. M., Schleicher, M., Noegel, A. A., and Holak, T. A. (2006) Filamins: promiscuous organizers of the cytoskeleton. *Trends Biochem Sci* **31**, 411-419
242. Thelin, W. R., Chen, Y., Gentzsch, M., Kreda, S. M., Sallee, J. L., Scarlett, C. O., Borchers, C. H., Jacobson, K., Stutts, M. J., and Milgram, S. L. (2007) Direct interaction with filamins modulates the stability and plasma membrane expression of CFTR. *J Clin Invest* **117**, 364-374
243. Gravante, B., Barbuti, A., Milanesi, R., Zappi, I., Viscomi, C., and DiFrancesco, D. (2004) Interaction of the pacemaker channel HCN1 with filamin A. *J Biol Chem* **279**, 43847-43853
244. Lin, R., Karpa, K., Kabbani, N., Goldman-Rakic, P., and Levenson, R. (2001) Dopamine D2 and D3 receptors are linked to the actin cytoskeleton via interaction with filamin A. *Proc Natl Acad Sci U S A* **98**, 5258-5263
245. Sampson, L. J., Leyland, M. L., and Dart, C. (2003) Direct interaction between the actin-binding protein filamin-A and the inwardly rectifying potassium channel, Kir2.1. *J Biol Chem* **278**, 41988-41997
246. Wang, Q., Dai, X. Q., Li, Q., Tuli, J., Liang, G., Li, S. S., and Chen, X. Z. (2013) Filamin interacts with epithelial sodium channel and inhibits its channel function. *J Biol Chem* **288**, 264-273
247. Zhang, M., and Breitwieser, G. E. (2005) High affinity interaction with filamin A protects against calcium-sensing receptor degradation. *J Biol Chem* **280**, 11140-11146
248. Guiet, R., Verollet, C., Lamsoul, I., Cougoule, C., Poincloux, R., Labrousse, A., Calderwood, D. A., Glogauer, M., Lutz, P. G., and Maridonneau-Parini, I. (2012) Macrophage mesenchymal migration requires podosome stabilization by filamin A. *J*

Biol Chem **287**, 13051-13062
249. Kley, R. A., van der Ven, P. F., Olive, M., Hohfeld, J., Goldfarb, L. G., Furst, D. O., and Vorgerd, M. (2013) Impairment of protein degradation in myofibrillar myopathy caused by FLNC/filamin C mutations. *Autophagy* **9**, 422-423
250. Calderwood, D. A., Huttenlocher, A., Kiosses, W. B., Rose, D. M., Woodside, D. G., Schwartz, M. A., and Ginsberg, M. H. (2001) Increased filamin binding to beta-integrin cytoplasmic domains inhibits cell migration. *Nat Cell Biol* **3**, 1060-1068
251. Yuan, Y., Zhang, W., Yan, R., Liao, Y., Zhao, L., Ruan, C., Du, X., and Dai, K. (2009) Identification of a novel 14-3-3zeta binding site within the cytoplasmic domain of platelet glycoprotein Ibalpha that plays a key role in regulating the von Willebrand factor binding function of glycoprotein Ib-IX. *Circ Res* **105**, 1177-1185
252. Prasad, S., McDaid, J. P., Tam, F. W., Haylor, J. L., and Ong, A. C. (2009) Pkd2 dosage influences cellular repair responses following ischemia-reperfusion injury. *Am J Pathol* **175**, 1493-1503
253. Zhao, Y., Haylor, J. L., and Ong, A. C. (2002) Polycystin-2 expression is increased following experimental ischaemic renal injury. *Nephrol Dial Transplant* **17**, 2138-2144
254. Obermuller, N., Cai, Y., Kranzlin, B., Thomson, R. B., Gretz, N., Kriz, W., Somlo, S., and Witzgall, R. (2002) Altered expression pattern of polycystin-2 in acute and chronic renal tubular diseases. *J Am Soc Nephrol* **13**, 1855-1864
255. Lantinga-van Leeuwen, I. S., Leonhard, W. N., Dauwerse, H., Baelde, H. J., van Oost, B. A., Breuning, M. H., and Peters, D. J. (2005) Common regulatory elements in the polycystic kidney disease 1 and 2 promoter regions. *Eur J Hum Genet* **13**, 649-659
256. Sun, H., Li, Q. W., Lv, X. Y., Ai, J. Z., Yang, Q. T., Duan, J. J., Bian, G. H., Xiao, Y., Wang, Y. D., Zhang, Z., Liu, Y. H., Tan, R. Z., Yang, Y., Wei, Y. Q., and Zhou, Q. (2010) MicroRNA-17 post-transcriptionally regulates polycystic kidney disease-2 gene and promotes cell proliferation. *Mol Biol Rep* **37**, 2951-2958
257. Zhou, A. X., Hartwig, J. H., and Akyurek, L. M. (2010) Filamins in cell signaling, transcription and organ development. *Trends Cell Biol* **20**, 113-123
258. Perrone, R. D. (1985) In vitro function of cyst epithelium from human polycystic kidney. *J Clin Invest* **76**, 1688-1691
259. Berridge, M. J., Lipp, P., and Bootman, M. D. (2000) The versatility and universality of calcium signalling. *Nature reviews. Molecular cell biology* **1**, 11-21
260. Smith, P. M., and Gallacher, D. V. (1994) Thapsigargin-induced Ca2+ mobilization in acutely isolated mouse lacrimal acinar cells is dependent on a basal level of Ins(1,4,5)P3 and is inhibited by heparin. *The Biochemical journal* **299 (Pt 1)**, 37-40
261. Camello, C., Lomax, R., Petersen, O. H., and Tepikin, A. V. (2002) Calcium leak from intracellular stores--the enigma of calcium signalling. *Cell calcium* **32**, 355-361
262. Hofer, A. M., Curci, S., Machen, T. E., and Schulz, I. (1996) ATP regulates calcium leak from agonist-sensitive internal calcium stores. *FASEB journal : official publication of the Federation of American Societies for Experimental Biology* **10**, 302-308
263. Missiaen, L., De Smedt, H., Parys, J. B., Raeymaekers, L., Droogmans, G., Van Den Bosch, L., and Casteels, R. (1996) Kinetics of the non-specific calcium leak from non-mitochondrial calcium stores in permeabilized A7r5 cells. *The Biochemical journal* **317 (Pt 3)**, 849-853
264. Beecroft, M. D., and Taylor, C. W. (1998) Luminal Ca2+ regulates passive Ca2+ efflux from the intracellular stores of hepatocytes. *The Biochemical journal* **334 (Pt 2)**,

431-435
265. Van Coppenolle, F., Vanden Abeele, F., Slomianny, C., Flourakis, M., Hesketh, J., Dewailly, E., and Prevarskaya, N. (2004) Ribosome-translocon complex mediates calcium leakage from endoplasmic reticulum stores. *Journal of cell science* **117**, 4135-4142
266. Pinton, P., Ferrari, D., Magalhaes, P., Schulze-Osthoff, K., Di Virgilio, F., Pozzan, T., and Rizzuto, R. (2000) Reduced loading of intracellular Ca(2+) stores and downregulation of capacitative Ca(2+) influx in Bcl-2-overexpressing cells. *The Journal of cell biology* **148**, 857-862
267. Tu, H., Nelson, O., Bezprozvanny, A., Wang, Z., Lee, S. F., Hao, Y. H., Serneels, L., De Strooper, B., Yu, G., and Bezprozvanny, I. (2006) Presenilins form ER Ca2+ leak channels, a function disrupted by familial Alzheimer's disease-linked mutations. *Cell* **126**, 981-993
268. Lang, S., Schauble, N., Cavalie, A., and Zimmermann, R. (2011) Live cell calcium imaging combined with siRNA mediated gene silencing identifies Ca(2)(+) leak channels in the ER membrane and their regulatory mechanisms. *Journal of visualized experiments : JoVE*, e2730
269. Grynkiewicz, G., Poenie, M., and Tsien, R. Y. (1985) A new generation of Ca2+ indicators with greatly improved fluorescence properties. *The Journal of biological chemistry* **260**, 3440-3450
270. Cantero Mdel, R., and Cantiello, H. F. (2013) Calcium transport and local pool regulate polycystin-2 (TRPP2) function in human syncytiotrophoblast. *Biophys J* **105**, 365-375
271. Mekahli, D., Sammels, E., Luyten, T., Welkenhuyzen, K., van den Heuvel, L. P., Levtchenko, E. N., Gijsbers, R., Bultynck, G., Parys, J. B., De Smedt, H., and Missiaen, L. (2012) Polycystin-1 and polycystin-2 are both required to amplify inositol-trisphosphate-induced Ca2+ release. *Cell calcium* **51**, 452-458
272. Sun, Z., Amsterdam, A., Pazour, G. J., Cole, D. G., Miller, M. S., and Hopkins, N. (2004) A genetic screen in zebrafish identifies cilia genes as a principal cause of cystic kidney. *Development* **131**, 4085-4093
273. Barbry, P., and Hofman, P. (1997) Molecular biology of Na+ absorption. *Am J Physiol* **273**, G571-585
274. Mano, I., and Driscoll, M. (1999) DEG/ENaC channels: a touchy superfamily that watches its salt. *Bioessays* **21**, 568-578
275. Lingueglia, E., Deval, E., and Lazdunski, M. (2006) FMRFamide-gated sodium channel and ASIC channels: a new class of ionotropic receptors for FMRFamide and related peptides. *Peptides* **27**, 1138-1152
276. Zuckerman, J. B., Chen, X., Jacobs, J. D., Hu, B., Kleyman, T. R., and Smith, P. R. (1999) Association of the epithelial sodium channel with Apx and alpha-spectrin in A6 renal epithelial cells. *J Biol Chem* **274**, 23286-23295
277. Awayda, M. S., and Subramanyam, M. (1998) Regulation of the epithelial Na+ channel by membrane tension. *J Gen Physiol* **112**, 97-111
278. Satlin, L. M., Sheng, S., Woda, C. B., and Kleyman, T. R. (2001) Epithelial Na(+) channels are regulated by flow. *Am J Physiol Renal Physiol* **280**, F1010-1018
279. Rossier, B. C., Pradervand, S., Schild, L., and Hummler, E. (2002) Epithelial sodium channel and the control of sodium balance: interaction between genetic and environmental factors. *Annu Rev Physiol* **64**, 877-897

280. Schild, L. (2004) The epithelial sodium channel: from molecule to disease. *Rev Physiol Biochem Pharmacol* **151**, 93-107
281. Gormley, K., Dong, Y., and Sagnella, G. A. (2003) Regulation of the epithelial sodium channel by accessory proteins. *Biochem J* **371**, 1-14
282. Takafuta, T., Saeki, M., Fujimoto, T. T., Fujimura, K., and Shapiro, S. S. (2003) A new member of the LIM protein family binds to filamin B and localizes at stress fibers. *J Biol Chem* **278**, 12175-12181
283. Cantiello, H. F., Prat, A. G., Bonventre, J. V., Cunningham, C. C., Hartwig, J. H., and Ausiello, D. A. (1993) Actin-binding protein contributes to cell volume regulatory ion channel activation in melanoma cells. *J Biol Chem* **268**, 4596-4599
284. Jovov, B., Tousson, A., Ji, H. L., Keeton, D., Shlyonsky, V., Ripoll, P. J., Fuller, C. M., and Benos, D. J. (1999) Regulation of epithelial Na(+) channels by actin in planar lipid bilayers and in the Xenopus oocyte expression system. *J Biol Chem* **274**, 37845-37854
285. Chen, X. Z., Vassilev, P. M., Basora, N., Peng, J. B., Nomura, H., Segal, Y., Brown, E. M., Reeders, S. T., Hediger, M. A., and Zhou, J. (1999) Polycystin-L is a calcium-regulated cation channel permeable to calcium ions. *Nature* **401**, 383-386
286. Snyder, P. M. (2005) Minireview: regulation of epithelial Na+ channel trafficking. *Endocrinology* **146**, 5079-5085
287. Weisz, O. A., Wang, J. M., Edinger, R. S., and Johnson, J. P. (2000) Non-coordinate regulation of endogenous epithelial sodium channel (ENaC) subunit expression at the apical membrane of A6 cells in response to various transporting conditions. *J Biol Chem* **275**, 39886-39893
288. Kizer, N., Guo, X. L., and Hruska, K. (1997) Reconstitution of stretch-activated cation channels by expression of the alpha-subunit of the epithelial sodium channel cloned from osteoblasts. *Proc Natl Acad Sci U S A* **94**, 1013-1018
289. Ismailov, II, Awayda, M. S., Berdiev, B. K., Bubien, J. K., Lucas, J. E., Fuller, C. M., and Benos, D. J. (1996) Triple-barrel organization of ENaC, a cloned epithelial Na+ channel. *J Biol Chem* **271**, 807-816
290. McDonald, F. J., Snyder, P. M., McCray, P. B., Jr., and Welsh, M. J. (1994) Cloning, expression, and tissue distribution of a human amiloride-sensitive Na+ channel. *Am J Physiol* **266**, L728-734
291. Nakhoul, N. L., Hering-Smith, K. S., Abdulnour-Nakhoul, S. M., and Hamm, L. L. (2001) Ammonium interaction with the epithelial sodium channel. *Am J Physiol Renal Physiol* **281**, F493-502
292. Khurana, S. (2000) Role of actin cytoskeleton in regulation of ion transport: examples from epithelial cells. *J Membr Biol* **178**, 73-87
293. Noda, Y., Horikawa, S., Katayama, Y., and Sasaki, S. (2004) Water channel aquaporin-2 directly binds to actin. *Biochem Biophys Res Commun* **322**, 740-745
294. Chasan, B., Geisse, N. A., Pedatella, K., Wooster, D. G., Teintze, M., Carattino, M. D., Goldmann, W. H., and Cantiello, H. F. (2002) Evidence for direct interaction between actin and the cystic fibrosis transmembrane conductance regulator. *Eur Biophys J* **30**, 617-624
295. Cantiello, H. F. (1997) Role of actin filament organization in cell volume and ion channel regulation. *J Exp Zool* **279**, 425-435
296. Nilius, B. (2007) Transient receptor potential (TRP) cation channels: rewarding unique proteins. *Bull Mem Acad R Med Belg* **162**, 244-253

297. Calvet, J. P., and Grantham, J. J. (2001) The genetics and physiology of polycystic kidney disease. *Semin Nephrol* **21**, 107-123
298. Chebib, F. T., Sussman, C. R., Wang, X., Harris, P. C., and Torres, V. E. (2015) Vasopressin and disruption of calcium signalling in polycystic kidney disease. *Nat Rev Nephrol* **11**, 451-464
299. Qian, Q., Hunter, L. W., Li, M., Marin-Padilla, M., Prakash, Y. S., Somlo, S., Harris, P. C., Torres, V. E., and Sieck, G. C. (2003) Pkd2 haploinsufficiency alters intracellular calcium regulation in vascular smooth muscle cells. *Hum Mol Genet* **12**, 1875-1880
300. Yang, J., Zheng, W., Wang, Q., Lara, C., Hussein, S., and Chen, X. Z. (2013) Translational up-regulation of polycystic kidney disease protein PKD2 by endoplasmic reticulum stress. *FASEB J* **27**, 4998-5009
301. Foggensteiner, L., Bevan, A. P., Thomas, R., Coleman, N., Boulter, C., Bradley, J., Ibraghimov-Beskrovnaya, O., Klinger, K., and Sandford, R. (2000) Cellular and subcellular distribution of polycystin-2, the protein product of the PKD2 gene. *J Am Soc Nephrol* **11**, 814-827
302. Basora, N., Nomura, H., Berger, U. V., Stayner, C., Guo, L., Shen, X., and Zhou, J. (2002) Tissue and cellular localization of a novel polycystic kidney disease-like gene product, polycystin-L. *J Am Soc Nephrol* **13**, 293-301
303. Cowley, B. D., Jr., Smardo, F. L., Jr., Grantham, J. J., and Calvet, J. P. (1987) Elevated c-myc protooncogene expression in autosomal recessive polycystic kidney disease. *Proc Natl Acad Sci U S A* **84**, 8394-8398
304. Li, X., Magenheimer, B. S., Xia, S., Johnson, T., Wallace, D. P., Calvet, J. P., and Li, R. (2008) A tumor necrosis factor-alpha-mediated pathway promoting autosomal dominant polycystic kidney disease. *Nat Med* **14**, 863-868
305. Liu, Y., Dai, B., Xu, C., Fu, L., Hua, Z., and Mei, C. (2011) Rosiglitazone inhibits transforming growth factor-beta1 mediated fibrogenesis in ADPKD cyst-lining epithelial cells. *PLoS One* **6**, e28915
306. Zheng, R., Zhang, Z., Lv, X., Fan, J., Chen, Y., Wang, Y., Tan, R., Liu, Y., and Zhou, Q. (2008) Polycystin-1 induced apoptosis and cell cycle arrest in G0/G1 phase in cancer cells. *Cell Biol Int* **32**, 427-435
307. Gargalionis, A. N., Korkolopoulou, P., Farmaki, E., Piperi, C., Dalagiorgou, G., Adamopoulos, C., Levidou, G., Saetta, A., Fragkou, P., Tsioli, P., Kiaris, H., Zizi-Serbetzoglou, A., Karavokyros, I., Papavassiliou, K. A., Tsavaris, N., Patsouris, E., Basdra, E. K., and Papavassiliou, A. G. (2015) Polycystin-1 and polycystin-2 are involved in the acquisition of aggressive phenotypes in colorectal cancer. *Int J Cancer* **136**, 1515-1527
308. Nimer, S., Zhang, J., Avraham, H., and Miyazaki, Y. (1996) Transcriptional regulation of interleukin-3 expression in megakaryocytes. *Blood* **88**, 66-74
309. Berry, F. B., O'Neill, M. A., Coca-Prados, M., and Walter, M. A. (2005) FOXC1 transcriptional regulatory activity is impaired by PBX1 in a filamin A-mediated manner. *Mol Cell Biol* **25**, 1415-1424
310. Kottgen, M., and Walz, G. (2005) Subcellular localization and trafficking of polycystins. *Pflugers Arch* **451**, 286-293
311. Adams, M., Simms, R. J., Abdelhamed, Z., Dawe, H. R., Szymanska, K., Logan, C. V., Wheway, G., Pitt, E., Gull, K., Knowles, M. A., Blair, E., Cross, S. H., Sayer, J. A., and Johnson, C. A. (2012) A meckelin-filamin A interaction mediates ciliogenesis. *Hum*

Mol Genet **21**, 1272-1286
312. Zhao, B., Zeng, H., Tian, Y., and Israelachvili, J. (2006) Adhesion and detachment mechanisms of sugar surfaces from the solid (glassy) to liquid (viscous) states. *Proc Natl Acad Sci U S A* **103**, 19624-19629
313. Wang, Q., Zheng, W., Wang, Z., Yang, J., Hussein, S., Tang, J., and Chen, X. Z. (2015) Filamin-a increases the stability and plasma membrane expression of polycystin-2. *PLoS One* **10**, e0123018
314. Talbot, C. L., Bosworth, D. G., Briley, E. L., Fenstermacher, D. A., Boucher, R. C., Gabriel, S. E., and Barker, P. M. (1999) Quantitation and localization of ENaC subunit expression in fetal, newborn, and adult mouse lung. *Am J Respir Cell Mol Biol* **20**, 398-406
315. Barker, P. M., Nguyen, M. S., Gatzy, J. T., Grubb, B., Norman, H., Hummler, E., Rossier, B., Boucher, R. C., and Koller, B. (1998) Role of gammaENaC subunit in lung liquid clearance and electrolyte balance in newborn mice. Insights into perinatal adaptation and pseudohypoaldosteronism. *J Clin Invest* **102**, 1634-1640
316. McDonald, F. J., Yang, B., Hrstka, R. F., Drummond, H. A., Tarr, D. E., McCray, P. B., Jr., Stokes, J. B., Welsh, M. J., and Williamson, R. A. (1999) Disruption of the beta subunit of the epithelial Na+ channel in mice: hyperkalemia and neonatal death associated with a pseudohypoaldosteronism phenotype. *Proc Natl Acad Sci U S A* **96**, 1727-1731
317. Zerres, K., Rudnik-Schoneborn, S., Senderek, J., Eggermann, T., and Bergmann, C. (2003) Autosomal recessive polycystic kidney disease (ARPKD). *J Nephrol* **16**, 453-458
318. Veizis, I. E., and Cotton, C. U. (2005) Abnormal EGF-dependent regulation of sodium absorption in ARPKD collecting duct cells. *Am J Physiol Renal Physiol* **288**, F474-482
319. Raychowdhury, M. K., McLaughlin, M., Ramos, A. J., Montalbetti, N., Bouley, R., Ausiello, D. A., and Cantiello, H. F. (2005) Characterization of single channel currents from primary cilia of renal epithelial cells. *J Biol Chem* **280**, 34718-34722